Step-Growth Polymerization Towards the Design of Polymers: Assembly and Disassembly of Macromolecules

Stephen M. June

Dissertation submitted to the faculty of the Virginia Polytechnic Institute and State University in partial fulfillment of the requirements for the degree of

Doctor of Philosophy
in
Chemistry

Timothy E. Long, Chair
Richey M. Davis
Robert B. Moore
S. Richard Turner

March 22nd, 2012

Blacksburg, VA

Keywords: Step-Growth Polymers; Polyaddition; Polycondensation; Microbial Fuel Cells: Photo-active Polymers; Poly(siloxane imides); Polyesters; "Click" Chemistry; Stimuli Responsive Polymers; Bisphenol-A; BPA; Epoxy Networks

Step-Growth Polymerization Towards the Design of Polymers: Assembly and Disassembly of Macromolecules

Stephen M. June

Abstract

Step-growth polymerization provided an effective method for the preparation of several high performance polymers. Step-growth polymerization was used for syntheses of poly(siloxane imides), polyesters, poly(triazole esters), poly(triazole ether esters), and epoxy networks. Each of these polymeric systems exhibited novel structures, and either photoreactive capabilities, or high performance properties.

There is an increasing trend towards the development of photoactive adhesives. In particular these polymers are often used in flip bonding, lithography, stimuli responsive polymers, drug delivery, and reversible adhesives. The ability to tailor polymer properties carefully with exposure to light allows for very unique stimuli responsive properties for many applications. This dissertation primarily investigates photoreactive polymers for reversible adhesion for use in the fabrication of microelectronic devices. In particular cyclobutane diimide functionality within polyimides and poly(siloxane imides) and *o*-nitro benzyl ester functionality within polyesters acted effectively as chromophores to this end.

Thermal solution imidization allowed for the effective synthesis of polyimides and poly(siloxane imides). 1,2,3,4-Cyclobutane tetracarboxylic dianhydride acted as the chromophore within the polymer backbone. The polyimides obtained exhibited dispersibility only in dipolar, aprotic, high boiling solvents such as DMAc or NMP. The obtained poly(siloxane imides) demonstrated enhanced dispersibility in lower boiling organic solvents such as THF and $CHCl_3$. Dynamic mechanical analysis and tensile testing effectively measure

the mechanical properties of the photoactive poly(siloxane imides) and confirmed elastomeric properties. Atomic force microscopy confirmed microphase separation of the photoactive poly(siloxane imides). ^{1}H NMR spectroscopy confirmed formation of maleimide peaks upon exposure to narrow band UV light with a wavelength of 254 nm. This suggested photo-cleavage of the cyclobutane diimide units within the polymer backbone.

Melt transesterification offered a facile method for the synthesis of *o*-nitro benzyl ester-containing polyesters. ^{1}H NMR spectroscopy confirmed the structures of the photoactive polyesters and size exclusion chromatography confirmed reasonable molecular weights and polydispersities of the obtained samples. ^{1}H NMR spectroscopy also demonstrated a decrease in the integration of the resonance corresponding to the *o*-nitro benzyl ester functionality relative to the photo-stable *m*-nitro benzyl ester functionality upon exposure to high-intensity UV light, suggesting photo-degradation of the adhesive. ASTM wedge testing verified a decrease in fracture energy of the adhesive upon UV exposure, comparable to the decrease in fracture energy of a commercial hot-melt adhesive upon an increase in temperature.

Click chemistry was used to synthesize polyesters and segmented block copolyesters. Triazole-containing homopolyesters exhibited a marked increase (~40 °C) in T_g, relative to structurally analogous classical polyesters synthesized in the melt. However, the triazole-containing homopolyesters exhibited insignificant dispersibility in many organic solvents and melt-pressed films exhibited poor flexibility. Incorporation of azide-functionalized poly(propylene glycol) difunctional oligomers in the synthesis of triazole-containing polyesters resulted in segmented block copolyesters which exhibited enhanced dispersibility and film robustness relative to the triazole-containing homopolyesters. The segmented triazole-containing polyesters all demonstrated a soft segment T_g near -62 °C, indicating microphase separation.

Dynamic mechanical analysis confirmed the presence of a rubbery plateau, with increasing plateau moduli as a function of hard segment content, as well as increasing flow temperatures as a function of hard segment content. Tensile testing revealed increasing tensile strength as a function of hard segment, approaching 10 MPa for the 50 wt % HS sample. Atomic force microscopy confirmed the presence of microphase separated domains, as well as semicrystalline domains. These results indicated the effectiveness of click chemistry towards the synthesis of polyesters and segmented block copolyesters.

Click chemistry was also used for the synthesis of photoactive polyesters and segmented block polyesters. The preparation of 2-nitro-*p*-xylylene glycol bispropiolate allowed for the synthesis of triazole-containing polyesters, which exhibited poor dispersibility and flexibility of melt-pressed films. The synthesis of segmented photoactive polyesters afforded photoactive polyesters with improved dispersibility and film robustness. ^{1}H NMR spectroscopy confirmed the photodegradation of the *o*-nitro benzyl functional groups within the triazole-containing polyesters, which indicated the potential utility of these polyesters for reversible adhesion.

Synthesis of the glycidyl ether of 2,2,4,4-tetramethyl-1,3-cyclobutane diol (CBDOGE) allowed for the subsequent preparation of epoxy networks which did not contain bisphenol-A or bisphenol-A derivatives. Preparation of analogous epoxy networks from the glycidyl ether of bisphenol-A (BPA-GE) provided a method for control experiments. Tensile testing demonstrated that, dependent on network T_g, the epoxy networks prepared from CBDOGE exhibited similar Young's moduli and tensile strain at break as epoxy networks prepared from BPAGE. Dynamic mechanical analysis demonstrated similar glassy moduli for the epoxy networks, regardless of the glycidyl ether utilized. T_g and rubbery plateau moduli varied as a function of diamine molecular weight. Melt rheology demonstrated a gel time of 150 minutes

for the preparation of epoxy networks from CBDO-GE and 78 minutes for the preparation of epoxy networks from BPA-GE, with the difference attributed to increased sterics surrounding CBDO-GE. These results indicated the suitability of CBDO-GE as a replacement for BPA-GE in many applications.

Acknowledgments

I would like to thank my Ph.D. advisor, Professor Timothy Long, for his guidance and support throughout my time at Virginia Tech. I appreciate that he gave me the opportunity to join his research group, and pursue my academic interests. In particular, I appreciate the freedom in the last several years to explore areas that I find particularly interesting, even when those areas may have strayed a little from the overall topic of my research. I would like to thank my research committee for their advice and guidance as I pursued my Ph.D. In particular, I'd like to thank Professor Richard Turner for agreeing to replace committee members who have since departed Virginia Tech. I'd also be remiss if I didn't thank Professor Bob Howell, at Central Michigan University, for giving me my first opportunity and experience working in a research lab, and introducing me to polymer chemistry.

I would like to thank Brewer Science, especially Dr. Rama Puligadda and Dr. Qin Lin, and the National Science Foundation's MILES IGERT program for financial support and research collaborations, and the Army Research Laboratories for providing me a summer internship during my tenure at Virginia Tech. I'd like to thank Laurie Good, Tammy Jo Hiner, Mary Jane Smith, Angie Miller, and Valerie Owens and Naya Sou in particular for administrative support and guidance, and for having Tim's schedule available so I would know when and where to find him. I would like to thank my collaborators on the Brewer Science work, Dr. David Dillard and Lei Yan, for their insightful discussions and research efforts.

I'd like to thank my colleagues in the Long research group, both past and present. Your assistance, advice, and friendship have been instrumental in my success. In particular I'd like to thank my friend Ashley Nelson for always letting me know when she thought I wasn't meeting my potential, and pushing me to do my best, as well as for her continued friendship and support.

I'd like to thank Dr. Matt Green, Mike Allen, Dr. Erin Murphy, and Eva van der Aa for making our time at the Corporate Research Labs interesting, to say the least. Thanks to Mana Tamami, Tianyu Wu, Shijing Cheng, and Renlong Gao for your support during the time I spent working in Hahn Hall South 3007. I know that there are many others who I haven't mentioned from our group over the years, and I'd like to thank the entire Long group for your friendship. I'd also like to thank some of my friends in the Department of Chemistry who are not Long group members: Kyle and Amanda Wilmsmeyer, for always letting me invite myself over to watch Hokie away games, David Bryson, for usually being willing to let me beat him at golf when I needed an afternoon away from graduate school, Josh Layfield, Tim Fuhrer, and so many others who I've had the good fortune to spend time with over the last 5 years.

I owe so much to my parents, Matt and Cindy June, for their constant love, support and insightful guidance throughout my life. Without so many rides to all of my activities, their cheers in the stands as I performed abysmally in sports, words of encouragement during hard times and praise during my successes, I would not be the man I am today. They inspired me to accomplish all that I could, and never accepted anything less than what I was capable of, but never asked for more. This achievement is as much because of what they did, as it is my own effort. I owe a big thank you to all of my siblings and their spouses: Jen and Brad, Cate and Gabe, Gary and Allie, and Emily, for all of their love, support, and encouragement as I pursued graduate studies. Without all of my family, I could not have survived this process, and I thank you all from the bottom of my heart.

Dedication

This dissertation is dedicated in loving memory to my grandmother, Helen Mae Oakley. She and my grandfather always had a passion for education, and an insistence on well-educated children that really was the starting point of a 50 year process that ultimately led to this achievement. She always had a sharp, thoughtful, and scientific mind, and I'm certain that I inherited some of my abilities from her. Words cannot describe how much she is missed.

Table of Contents

List of Figures

List of Schemes

List of Tables

Chapter 1: Design of Charged Polymers for Microbial Fuel Cells

Stephen M. June and Timothy E. Long

Department of Chemistry,
Virginia Polytechnic Institute and State University,
Blacksburg, Virginia 24061

(From: Chem. 5904 Literature Review Course)

1.1 Abstract

The current energy crisis is making the need for renewable sources of energy increasingly obvious. There is a considerable amount of research in a variety of energy sources, including non-petroleum carbon based fuels, hydrogen power, nuclear power, solar energy, and many others. Emerging in the last several years as a potential energy source are microbial fuel cells (MFC's). MFC's provide the ability to harvest energy from organic biomass, such as waste streams, or marine sediment as well as provide an environmentally friendly approach to wastewater purification and hydrogen production. Using these renewable fuels, MFC's provide a possible future source for "green" energy, but many difficulties remain. These challenges often result from a limited understanding and design of the polymeric materials used in the construction. Polymeric materials are used in nearly every component of the MFC, in many cases either enhancing the effectiveness, or decreasing the cost when compared to some of the more standard fuel cell materials. However, in many cases, the materials used are commercially available polymers, and there are currently very few systematic studies on the effects of some of the fundamental physical properties, such as molecular weight, morphology, and topology of these polymers. It is clear that microbial fuel cells are a technology that has great potential for a

vast array of applications, but there is a significant amount of research necessary in order to fully harness the capabilities of this technology.

1.2 Introduction

It is clear that in today's energy consuming society demand for power will soon far outreach supply.[1] Also, as climate change and environmental pressures take the spotlight, it will become increasingly important to utilize "green" energy.[1,2] We can continue to tap new oil sources, and burn other non-petroleum organic fuels, but this does little to stop the spread of global warming, and it is not a long term solution.[1] Ultimately, it is essential to begin to utilize renewable energy resources such as wind, solar, geothermal, hydroelectricity, and biomass.[1]

Microbial fuel cells may fill some of the renewable energy gap. MFC's utilize natural electrochemical oxidative processes to generate electrons in order to convert biochemical energy into electrical energy. The electrons are then transferred to an anode, where they are subsequently transferred through a load, and to a cathode, generating current. It is estimated that if large scale reactors are designed such that they are able to generate 1 kW/m^3, at projected system costs and current energy costs, a factory that produces 7500 kg/day of biowaste would have a 10 year payback period for an MFC electricity generation system.[3,4] However, there are a number of challenges that require addressing before utilization of MFC's on a large scale and creation of usable amounts of renewable energy is possible.[1]

1.2.1 Operation of a Microbial Fuel Cell

The concept of using biomass to generate electrical energy via an interception of electrons generated in bacterial digestion is not novel.[4,5] In fact, theories for the conversion of the energies

contained in chemical bonds to electrical energy have existed since the mid 19th century.[6] Preliminary experiments were performed as early as the 1960's to generate electricity from microbial digestion of hydrocarbons.[5] In the early 1990's, Habermann and Pommer were able to use microbial fuel cells to obtain electricity from the treatment of domestic wastewater .[6] However, only in the last decade has it become possible to produce sufficient power generations for practical uses (as high as ~300 W/m^3 for single batch systems).[1]

MFC's are not only used for the direct formation of electricity. Using the same design concept, it is also possible to cleanse wastewater.[1-3,7-16], power small scale implantable devices[17-19] or small scale sensors[20], harvest marine sediment to power submergible underwater devices[2,18,19,21-26], and to generate biohydrogen using electrohydrogenesis.[27-36] Also, similar designs are currently used in enzymatic fuel cells, which differ from microbial fuel cells due to the fact that particular enzymes are added to the microbe/fuel mixture to catalyze the oxidative processes[18,37-47]. These have the advantage of creating higher power densities than standard microbial fuel cells, but have lifetimes limited to 7-10 days, compared to lifetimes of up to several years for microbial fuel cells.[41]

Furthermore, Minteer et. al recently demonstrated the first organelle biofuel cell, where mitochondria were used to oxidize the pyruvate fuel, and convert the chemical energy into electrical energy. The power density obtained of 0.203 ± 0.014 mW/cm^2 is lower than that of a typical enzymatic fuel cell, but has better efficiencies, and higher than that of a standard microbial fuel cell, with comparable efficiencies. [48]

It is important to distinguish between a microbial fuel cell and a biobattery. A battery differs from a fuel cell because fuel cells requires refueling, whereas batteries are a self-contained system.[3]

1.2.2 Biology of a Microbial Fuel Cell

Microbial fuel cells work via allowing a bacterium to interact with a fuel, such as biowaste, or loading with a renewable fuel, such as cellulose, or acetic acid. Bacteria digest the fuel and release electrons via cellular chemical reactions. Bacteria utilize biological processes to produce and store adenosine triphosphate (ATP). The reduced form of nicotinamide adenine dinucleotide (NAD), NADH, then transports the electrons formed from oxidation of the biofuel into the respiratory cycles. Electrons move down the respiratory chain, creating a proton gradient. The electrons can, with the aid of the ATPase enzyme, flow back into the cell, and create one molecule of ATP per molecule of adenosine diphosphate (ADP) with the assistance of 3-4 protons. Eventually the electrons are transported to a soluble electron accepter such as dissolved oxygen in a biological system. Utilizing this process, bacteria can create as many as 38 molecules of ATP utilizing one molecule of glucose. In some cases, bacteria can transfer electrons to a non-soluble electron acceptor. When this occurs, less ATP is produced in the cell. Therefore, there is a difference in electric potential between the ATP produced, and the theoretical ATP produced. This potential is then harvested for electricity generation in a MFC. The maximum theoretical voltage produced is -1.2 V, based on the difference in potential between NADH and the typical soluble electron acceptor, oxygen.[1] **Figure 1.1** below demonstrates the operating theory of a microbial fuel cell.[4]

Microbial fuel cells can utilize a wide range of bacteria. The only requirement for the bacteria is that they are capable of electron transfer to the anode, otherwise known as anodophilic electron transfer.[3] Studies have shown in several cases that cultures of mixed bacteria can

produce higher power outputs than pure cultures[3,49,50], but high power outputs are obtainable using pure cultures[3,51].

1.2.3 Design of a Microbial Fuel Cell

There are three major components of a MFC; the anode, the cathode, and the electrolyte. Also important in many types of MFC's, or niche variants thereof, is the membrane that separates the anode chamber and the cathode chamber. The anode is typically formed from some form of carbon. It is typically in the form of a graphite plate, rod, or granule, or as a graphitic fiber, sheet, felt, form, or paper. Other anode materials include some metals, such as a stainless steel mesh,[52] but copper, which is a common anode for non-microbial systems, is toxic even in small doses to most bacteria, which prevents its use in MFCs. Biocompatibility of the anode material, as well as conductivity and chemical stability in the electrolyte solution is crucial for MFCs.[3] Utilization of metal blends to mediate electron transfer may also increase anode performance.[53] The use of an electrocatalyst also can increase anode potential.[54-56] Studies have also shown that water flow in the direction of the anode can increase power densities.[3,57]

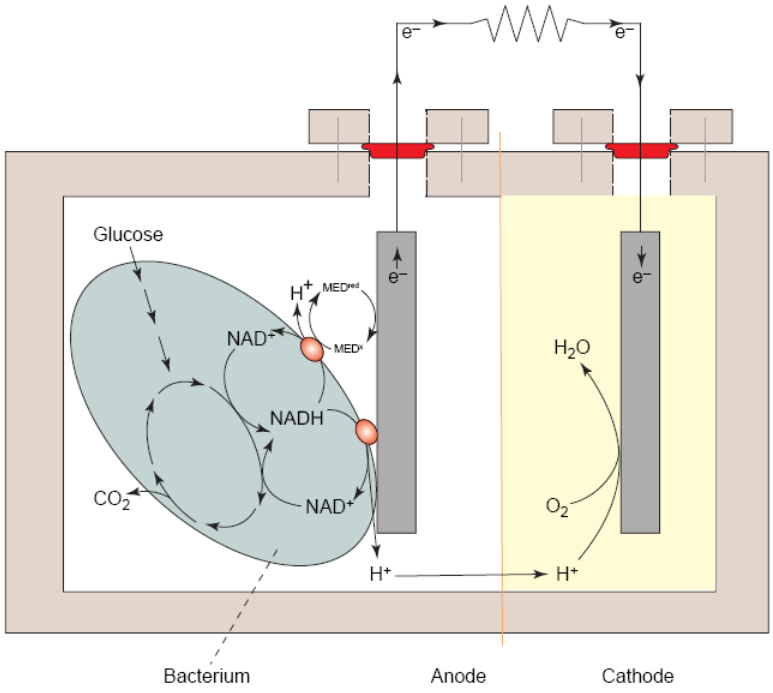

Figure 1.1 Operation of a microbial fuel cell. Fuel substrate is metabolized via the bacteria, which is then transported to the anode, and subsequently transported to the cathode, generating current.[4] (Reprinted from Rabaey, K.; Verstraete, W. *Trends in Biotechnology* **2005**, 23, (6), 291-298., with permission from Elsevier.)

Cathode solution materials must readily accept electrons, and should have a low over-potential relative to a carbon cathode, which allows an actual overall potential relatively close to an open circuit. It should also reoxidize relatively easily with exposure to oxygen, so that it is not necessary to replace the catholyte often. It should also not diffuse across the cation exchange membrane that separates the anode chamber from the cathode chamber.[3] The most commonly used electron accepter is ferricyanide, and it fits well with the former requirement[53], but not well with the two latter.[3,58] Oxygen is an excellent electron accepter, due to its high oxidative potential. Furthermore, oxygen is readily available, inexpensive, and forms no hazardous byproducts.[3] Unfortunately, with a plain carbon cathode, the reduction of oxygen is relatively slow, and typically requires a catalyst such as platinum.[22,59-61] It is possible to use relatively low loadings of platinum, but on large scale, this is still expensive.[62] Catalysts based off of non-

noble inexpensive metals were recently developed, although the long term stabilities of either these less inexpensive catalysts or the platinum catalysts are not known.[62,63] The choice of cathode material and form of that material greatly affect fuel cell efficiency.[3]

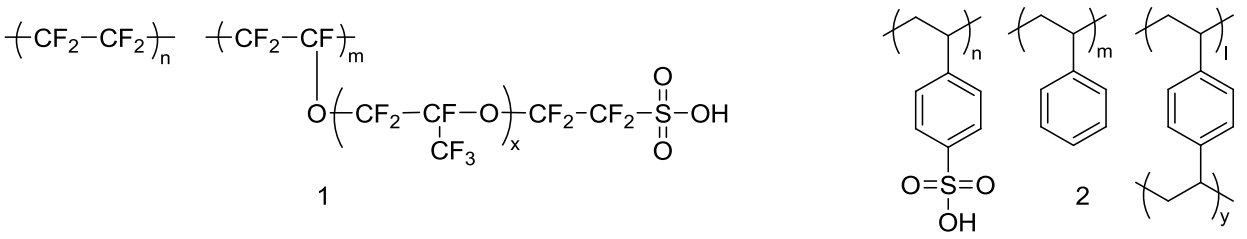

Figure 1.2 1) Nafion®, and 2) Ultrex® (CMI 7000 – Membranes International Inc.) are common PEM's used for MFC's.

The majority of MFC designs require an ion exchange membrane to separate the cathode chamber from the anode chamber. Typically the membrane used is some version of Nafion®[3] or the less expensive Ultrex®[49]. With a polymeric membrane, it is important to consider that the membranes are likely slightly permeable to oxygen in solution, the electron acceptor, or, perhaps most detrimentally, given the type of solutions used in the anode chamber, cations other than hydrogen[3,64]. The requirements for an acceptable ion exchange membrane include chemical stability over extended periods of time, and high conductivity.[3] The ion exchange membrane is perhaps the least understood portion of the design of a MFC, and systematic studies are necessary to evaluate the requirements for the best type of membrane for these systems.[64]

There are several types of MFC that do not require an ion exchange membrane. In particular, in some cases, salt bridges are used instead of membranes to separate the anode and the cathode chambers. However, salt bridges tend to have high resistance, and therefore have considerably lower power outputs compared to systems with ion exchange membranes.[65] There are also some systems that do not require artificial separation between the electrodes. For

example, some sediment microbial fuel cells have a naturally occurring separation, where one electrode is buried in sea sediment, and the other is exposed to the seawater.[21,22] Furthermore, there are a few samples of fuel cells that are specifically designed such that the components are non-separated. These are referred to as single-compartment MFCs or membraneless MFCs.[66-70] These examples are the exception rather than the rule. Most systems require an ion exchange membrane, and for the purposes of this review, we will focus primarily on these systems.

The physical design of microbial fuel cells is relatively simple. For many practical experimental MFCs, a simple "H" design works well. In this design, the anode and cathode chambers are essentially two jars, each with an electrode placed inside, and they are connected via a tube containing a salt bridge or a cation exchange membrane (CEM).[3] This design works well to test power output, or new materials, but it is not practical for long term studies. Also, power densities are typically low due to low surface areas of the anode in reference to the cathode surface area, as well as a low surface area of the CEM.[59,71,72]

Immersion of the cathode into a solution is not necessary. If oxygen is used as the electron acceptor, placement of the cathode directly in air is possible.[61] In fact, it is possible to obtain higher power densities when the cathode is placed in an air system, as opposed to an aqueous system, when oxygen is the electron acceptor in both cases.[61]

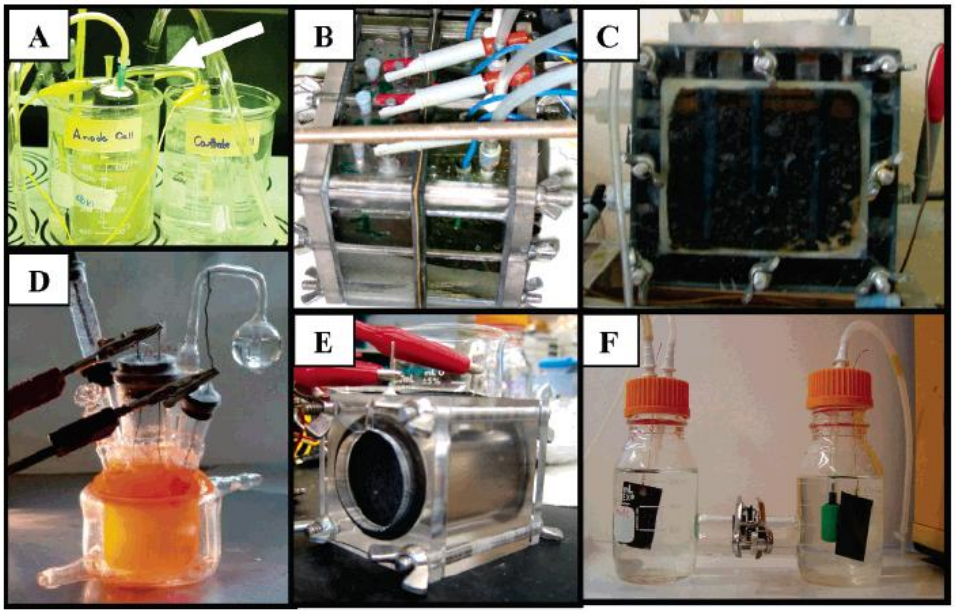

Figure 1.3 Several designs of MFCs. A is a standard H type system separated with a tube containing a salt bridge. B is a multi batch system where the anode and cathode chambers are separated directly with a CEM clamped between the two chambers. C is a similar design to B, but one that allows direct flow through the anode chamber. D is a membraneless single compartment MFC. E is a single compartment system where the cathode is exposed to air instead of a catholyte solution. F is an H type two jar system that is set up to allow purging with gases.[3] (Reprinted with permission from Logan, B. E.; Hamelers, B.; Rozendal, R.; Schroder, U.; Keller, J.; Freguia, S.; Aelterman, P.; Verstraete, W.; Rabaey, K. *Environ. Sci. Technol.* **2006**, 40, (17), 5181-5192. Copyright(2006) American Chemical Society.)

The above mentioned systems were both single batch systems. For applications in renewable power generation, batch systems are not practical. Instead, the fuel solution should flow continuously through the anode chamber.[73] There are MFC designs with an outer reaction tube that is the anode chamber, allowing flow of the microbe solution, and an inner concentric cylinder that is the cathode.[6,59] Conversely, there are also designs with an outer cathode tube, and an inner tube that contains the anode and laminar flow of the microbe solution.[58] It is also possible to increase output via stacking multiple individual cells in series.[74] Also, in order to increase anode surface area, systems were developed where the microbe solution was allowed to flow through porous anodes toward the membrane separating the cathode chamber.[75] Some

MFC's are designed similarly to a hydrogen fuel cell, where a CEM directly separates the anode and cathode chamber.[3] **Figure 1.3** above shows several types of MFC designs.[3]

1.2.4 Applications of Microbial Fuel Cells

Although the obvious rationale of the investigation of microbial fuel cells is to produce inexpensive energy from a renewable source, the challenges in technology and power output that these systems face may keep them from becoming practical for such large scale power generation for a number of years. These challenges become especially difficult to overcome when the many competing types of fuel cell are taken into consideration. Hydrogen fuel cell technology is becoming increasingly available, and increasingly less expensive. Direct methanol fuel cells are also approaching the forefront of energy research. Given the competition, MFC research could easily subside. However, it is important to bear in mind that hydrogen production is typically performed via a process that either directly consumes fossil fuels, or via a process that requires a substantial amount of energy to function.[76]

Given some of the constraints of MFC's, in particular due to the competition with other renewable energy sources, there is a wealth of current research attempting to utilize this same technology and applying it to a number of smaller, more "niche" like uses. The research involved in commercializing some of these small scale uses may well provide some of the technology necessary for the future large scale power generation and commercialization of these MFCs. In particular, many studies have evaluated the possibility of MFCs for use as a method for wastewater treatment[1-3,10,15,59], for powering submergible underwater devices[1,3,21,22,54], small scale implantable medical devices[18], and for utilizing electrohydrogenesis to produce hydrogen for more "standard" hydrogen fuel cells[1,3,29,30,76]. It is quite possible that some of these smaller

target applications for MFCs will become commercialized well before large scale power generation is practically feasible.[1]

Perhaps the most immediately usable application of MFCs is for wastewater treatment. Over 2 billion people worldwide lack clean, potable water.[1] The United States spends approximately 25 billion dollars every year on water purification and wastewater treatment. In the next several decades, it is estimated that the costs of operating, maintaining, and replacing water purification and treatment infrastructure will approach 2 trillion dollars.[1] With every increasing energy costs it is perhaps more alarming that nearly 5% of the total energy produced in the United States goes towards the water and water purification process.[1] It is estimated that there is nearly 10 times the energy contained in wastewater as it takes to treat the water.[1,77] It is easy to see how the use of MFCs to both clean water and to create energy in the process can aid in some of the most serious issues facing society today. Now, potentially instead of expending energy and money to treat water, we can in fact not only produce enough energy to treat the water, but yield an excess of energy.[1] Even if the net energy produced is negligible, at least we could save some of the money and energy currently put into water treatment. The challenges that are faced in using MFCs to treat wastewater are primarily economics and the ability to scale up the reactors.[1,3,4] As mentioned previously, many of the systems require expensive catalysts and fragile materials. If solutions to these challenges are found, it is likely that this method will find use as a large-scale wastewater treatment in the near future.

Another promising application of the technology utilized for microbial fuel cells are what are known as sediment fuel cells.[21,22,54] These harvest the energy contained in the organic matter of marine sediment. A convenient nature of these sediment fuel cells is that they do not need an artificial separation such as a CEM. Instead, the sediment-seawater interface acts as a natural

separation. These devices are particularly useful for powering underwater devices such as current and temperature detectors used to monitor sea conditions as these draw low voltage and replacing batteries in these detectors is inconvenient and expensive.[21,22,54]

One of obvious logical applications of a fuel cell powered from organic biomaterials is for implantable microscale devices. There are many implantable medical devices currently on the market for drug delivery, as well as the common cardiac pacemaker. These types of devices are typically powered with modern battery technology, and the batteries typically replacing after several years. The electrical draw of one of these implantable devices is typically well within the reach of the standard power outputs experimentally obtained from microbial fuel cells.[18] It is not a stretch to imagine the convenience of an implantable device receives its power from the body's energy. However, there are some challenges to consider. Many of the challenges with the previous applications discussed hold true here, but in a different manner. Scaling remains an issue, but in this case, it's making the MFCs in a small enough scale for feasible use alongside an implantable device. Also, some of the catalysts and materials used in the cathode chamber of MFCs may prove toxic over long time periods in physiological conditions.

One of the most intriguing and potentially useful applications of MFCs for transportation purposes is technically not an application of MFCs at all. However, it utilizes some of the same technology, and is worth discussing here. Many studies have investigated hydrogen gas as a potential environmentally friendly fuel for automobiles, as complete combustion of hydrogen yields only water as a byproduct. Unfortunately, the most commonly practiced production of hydrogen requires significant amounts of energy, which is, of course, currently primarily obtained from burning fossil fuels. This makes hydrogen production expensive and some of the environmentally friendly benefits of hydrogen fuel cells are lost.

Studies have shown that if a small voltage is applied to the MFC, and oxygen at the cathode is removed, it is possible to produce hydrogen in a sustainable and efficient matter via a process called electrohydrogenesis.[1,3,29,30] The bacteria at the anode produce a potential in much the same way as they do in MFCs. The electrons and protons produced in this process can combine under relatively low applied voltage to produce hydrogen. The amount of hydrogen produced per mole of glucose is currently very close to the estimated required moles of hydrogen per mole of glucose to make this process economically viable when compared to the costs of electrolysis.[29] Glucose is not the only fuel that is possible to convert to hydrogen. In fact, some studies have shown that conversion of wastewater to hydrogen is achievable, but a high concentration of waste in the water is essential. Electricity generation from a typical MFC technology is a much more feasible use for low strength wastewater.[30]

1.3 Charged Polymers for Microbial Fuel Cells

As discussed above, it is clear that polymers can play an important role in the design of microbial fuel cells. In particular, in many cases the design of a fuel cell requires separation of the two electrode chambers with an ion exchange membrane. Typically Nafion® is used as the cation exchange membrane for a number of reasons. It is readily available commercially and a significant amount of research on its structure and morphology exists.[78-81] It is thermally stable and relatively chemically inert, and operates relatively well for the purpose. However, it is expensive, and it does have a number of factors that limit its usefulness for microbial fuel cells.[3,4,52,64,65]

Although the primary use of polymers in a typical microbial fuel cell is the membrane between the electrode chambers, polymers are used in other locations as well. Ion exchange

membranes are occasionally used as a less expensive cathode material as an alternative to the graphite sheets or cloths currently used as a cathode.[62] Polymeric coatings are sometimes used in the anode to prevent expensive noble catalysts such as platinum from fouling effects of the microbial anolyte.[55] Many of these applications for polymers in MFCs are discussed herein.

1.3.1 Ion exchange membranes as proton conductors for MFCs

As discussed in the sections above, many designs of MFCs require a CEM to separate the cathode and anode chambers, and to transfer protons across the proton gradient, in order to provide balance to the movement of electrons between the anode and the cathode. Cation exchange membranes for MFCs require chemical, biological, oxidative, and thermal stablility at relatively neutral pH, ambient temperatures, in the presence of dissolved or ambient oxygen, and under microbial and enzymatic stress, as well has highly proton conductive. It is well known that morphology of the membranes is important.[78-86] Ion exchange membranes typically are necessarily micro-phase separated block copolymers, where one of the blocks is charged and the other is not. In this case, the microscale phase separation distinguishes the uncharged section from the charged section, which allows for well-defined channels through which ion transport can occur. These channels are on the order of approximately 10-100 nm wide, for good conductivities.[87] Typically, in polymeric membranes for fuel cell applications, the ion exchange group is the sulfonic acid group, and the backbone polymers are thermally stable polymers such as perfluoronated polymers, poly(arylene ether sulfones) or poly(arylene thioether sulfones).[83]

Nafion® is the most commonly used material for experimental MFCs, due to its high proton conductivity and the fact that it is readily available for purchase, but it does have a number of disadvantages. First, although it is readily available due to its high

commercialization, it is also expensive due to its perfluoronated structure. Secondly, it is susceptible to bio-fouling, particularly from ammonia.[64]

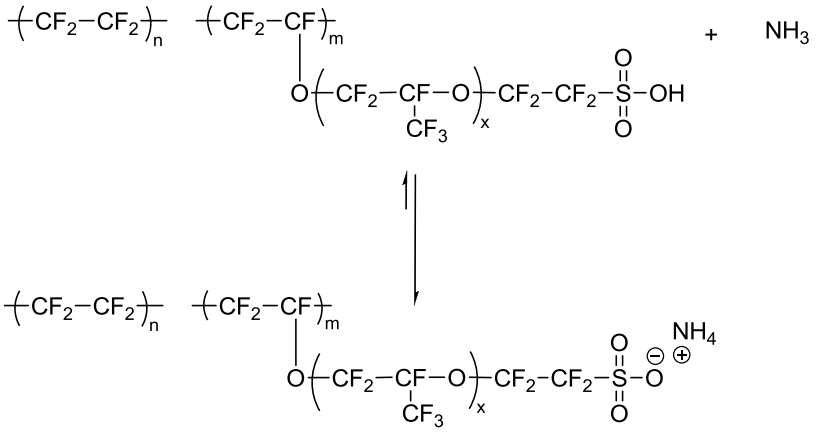

Figure 1.4 Scheme for the bio-fouling of Nafion® with ammonia.

Studies have shown that although MFCs that utilize Nafion® as a CEM between the electrode compartments can initially provide a high power density; over time the power outputs of these experimental MFCs decrease. Many of these longevity issues are due in part to fouling of Nafion® membranes from the variety of cations in the biological systems used in MFCs.[64]

Requirements for the Ion-Exchange Membrane

- Biocompatable
- Chemically stable at moderate pH
- Conductive to charge transfer species
- Impermeable to anolyte, catholyte, and oxygen
- Resistant to bio-film formation
- Resistant to bio-fouling
- Thermally stable at slightly elevated temperatures (below 100 °C)

In general, tests have shown that some of the operational issues found with Nafion® are due to the fact that it readily transports cations other than protons, for example K^+, Na^+, Ca^{2+}, NH_4^+, and Mg^{2+}.[64] Rozendal, et al. demonstrated that over time in a typical MFC, the pH in the cathode chamber increased, and decreased in the anode chamber. Furthermore, they showed that

over time, a strong increase in the concentration of non-protic cations in the cathode chamber was observed. This is due to transport of these cations from the anode fuel solution to the cathode chamber across the CEM. **Figure 1.5** outlines the changes in concentration of the various cations as a function of time.[64] In the types of solutions that are typically used in experimental microbial fuel cells, and the eventual types of fuel solutions utilized in a full scale MFC, these other cations are likely found in concentrations on the order of 10^5 times higher than the concentrations of protons. The competitive binding of these other cations disallows proton transfer through the CEM, which does not allow for the proton gradient to equilibrate over time. Therefore, a lower pH builds on the anode side of the MFC, and a higher pH on the cathode side. Without balance of protons being transported across the CEM at the same rate as electrons are transported from the anode to the cathode, it is not possible to sustain current levels.[64] The list above highlights some of the requirements for an ion-exchange membrane.

Experimental MFC's have utilized other CEM membranes which are not as cost prohibitive, and production of good power densities are obtainable, in some cases even better than Nafion® MFCs. One example of such a CEM is Ultrex®. Although there are no systematic studies judging the effect of pH and cation concentration on MFCs utilizing an Ultrex® membrane, it is intuitively follows that similar results would occur.[1,3,64]

In order for CEMs to maintain efficiency over a long period of time, they should not just transport cations, but should distinguish between protons and other cations, and allow only transport of the smaller protons. Highly selective proton exchange membranes do exist, but they are not currently commercially available. Kim, Cheng, Oh and Logan were able to demonstrate that when using an anion exchange membrane instead of a cation exchange membrane, it is possible to obtain higher power generation than when using Nafion® CEMs, so long as addition

of the AEM did not affect the overall internal resistance. Successful charge balance is maintained via transport of protons across the AEM from utilization of phosphate anions as a proton carrier.[88] It is clear that there is much more research necessary on the types of CEMs which will optimize MFC power densities and outputs on a scale and time period such that they will produce useful amounts of energy.

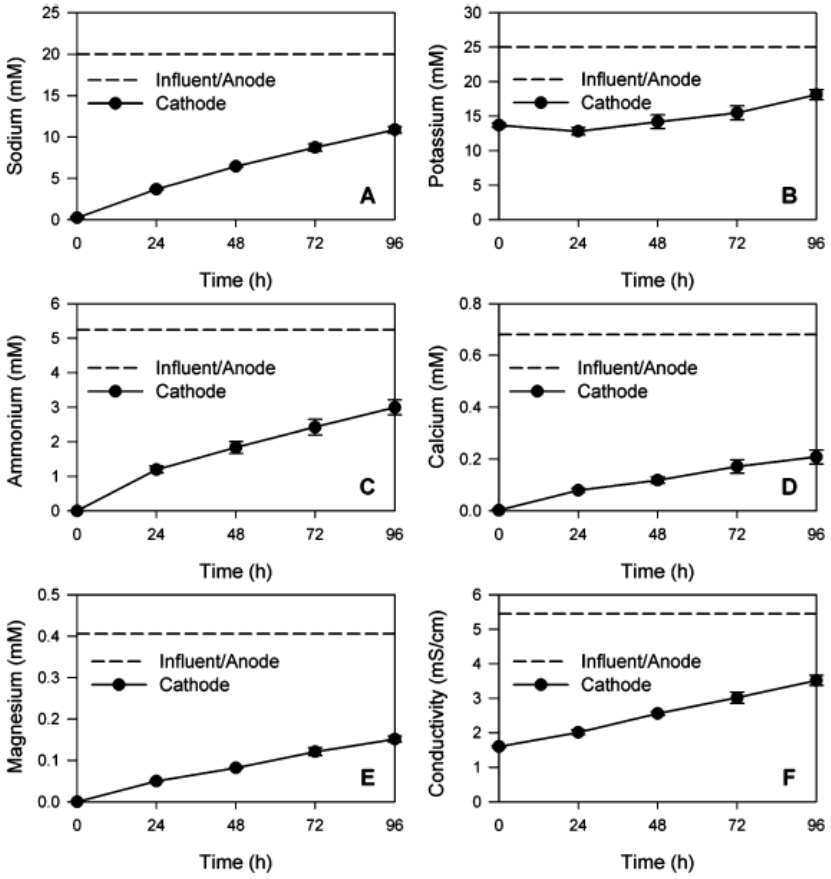

Figure 1.5 Increase of Na+, K+, NH4+, Ca2+,and Mg2+ concentrations as a function of time in the catholyte solution of a MFC. Also shown is an increase in conductivity of the catholyte as a function of time due to an increase in ionic strength.[64] (Reprinted with permission from Rozendal, R. A.; Hamelers, H. V. M.; Buisman, C. J. N. *Environ. Sci. Technol.* **2006,** 40, (17), 5206-5211. Copyright(2006) American Chemical Society.)

1.3.2 Charged polymers at the cathode of MFCs

Although cathode materials are typically some form of carbon, such as sheets, granules, cloths, or rods, plain carbon electrodes are not as effective as when noble catalysts such as platinum are used in conjunction with carbon based cathode materials.[3] In this case, it is necessary to bind the catalyst to the carbon electrode. Tests have shown that a proton conducting polymer such as Nafion® is required to obtain maximum power densities. Cheng, Liu, and Logan demonstrated when comparing a Nafion® binder to a poly(tetrafluoroethylene) (PTFE) binder that charge densities and coulombic efficiencies were higher approximately 33% with a Nafion® binder for a given catalyst loading level. The evaluation of performance, however, does not take into consideration the significant cost difference between Nafion® and PTFE. PTFE can cost as much as 500 times less than Nafion®.[62]

Expense of the materials used to build MFCs is one of the primary difficulties complicating the use of MFCs in large scale devices. Many of the materials used for MFCs are prohibitively expensive on a larger scale. For example, Zuo, Cheng, and Logan demonstrated that the cost of a carbon cathode with a platinum catalyst is approximately 1700 dollars/m^2. Since the surface area of the electrodes is crucial in developing high power outputs, it is easy to see how these values are a deterrent to the eventual production of large scale MFCs for power output or wastewater purification.[89]

In light of these costs, Zuo, Cheng, and Logan demonstrated that with utilization of a non-conductive anion exchange membranes as conductive anode materials via coating the non-conductive materials with carbon and a catalyst that is not composed of a precious metal, they

were able to create power generation comparable with carbon electrodes of the same surface area, at significantly lower costs. The materials utilized for these cathodes were approximately 14% of the costs of a carbon cathode with standard loadings of a platinum catalyst. Although there is further work necessary to reduce the internal resistances of these systems, it appears that this technology could become exceptionally instrumental in the eventual production of large scale MFCs for power generation and wastewater treatment.[89] However, it is important to note, that as is the case in the CEMs for separation of the electrode chambers, the membranes used in this case are commercial membranes and the effect of the choice of the membrane is not well understood. Future studies will determine if choice of AEM can increase the productivity of these cathodes.

1.3.3 Charged polymers at the anode of MFCs

In the anode materials of a MFC, biocompatibility, resistance to fouling from the fuel mixture, thermally stability and chemical resistance are crucial.[3] It is possible to construct anodes relatively inexpensively from graphite plates or rods. Carbon felts or brushes are occasionally used to provide higher anode surface areas.[3] Some research exists in using polymers as mediators for electron transfer from bacteria to the anode. In particular, Adachi, et al. were able to show that with the use of a poly(ethylene imine) backbone functionalized with 9,10-anthraquinone-2,6-disulfonyl chloride (AQDS chloride), that enhanced anode performance is obtainable, and that extended stability of the system in an MFC was possible.[90]

Acknowledging the economic constraints of platinum catalysts, they are regardless essentially unmatched in their ability to facilitate the oxidation of hydrogen in an MFC. Unfortunately, without protection, platinum is susceptible to poisoning from the analyte in an

MFC. MFC analytes contain biological waste consisting of many charged species, bacteria, organic fuels, and byproducts from bacterial metabolism. These species, left unchecked, can easily decrease the efficiency of platinum catalysts in anodes.[55,56]

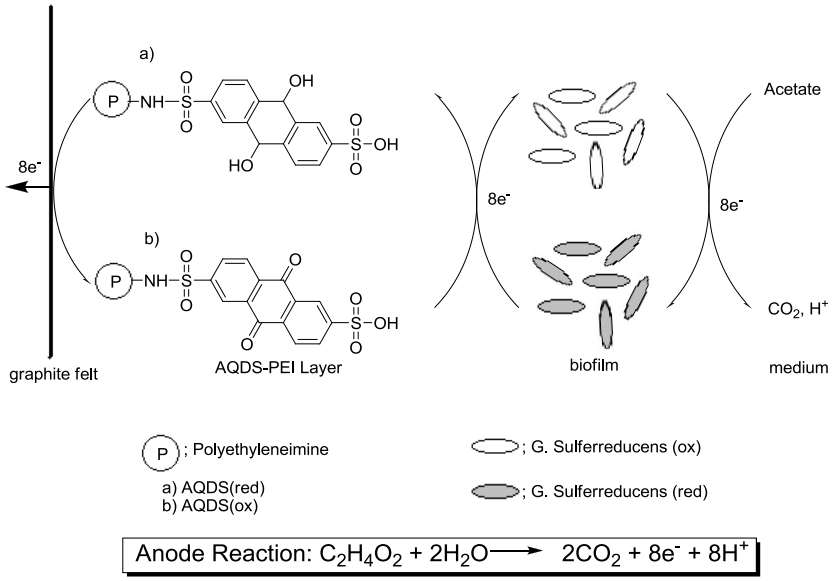

Figure 1.6 Scheme for the electron transfer to the anode via AQDS and G. Sulferreducens[90] (Fair use)

For this reason, Schröder, Niessen, and coworkers developed electrocatalytic anodes that are created from coating platinum in fluorinated polyanilines. These coatings not only were demonstrated to protect the platinum from analyte poisoning, but were also found to enhance the catalytic performance of the platinum. These polymers were found to possess high thermal stability and may prove themselves as an excellent coating for platinum in the eventual application of MFCs to treat potentially biologically degrading fuel systems such as wastewater or sewage.[55,56]

Figure 1.7 a) poly(2-fluoroaniline) and poly(2,3,5,6-tetrafluoroaniline) have demonstrated themselves as efficient electrocatalytic anodes for MFCs.[55,56]

1.4 Outlook

It is clear that MFCs have great potential for wastewater treatment, power generation, implantable devices, and biohydrogen production. MFCs are capable of producing modest but reasonable power outputs, and potential exists for moderately cost-effective large scale systems. However, a number of limitations still exist, and need addressing. Many of the materials used are still cost-prohibitive, and even the "low cost" materials may fail to compete economically with fossil fuels for power production, even with the recent relatively high costs of oil. Also, the durability and longevity of MFCs are still in question for industrial applications. Further studies on the materials and fuel cell designs need performing.

In particular, in reference to polymeric materials for MFCs, many of the materials used are simply purchased from a commercial source and used as received. In many cases, there is an incomplete understanding of how the structures and morphological properties of these membranes affect the performance of MFCs. Systematic studies require performing on both anionic and cationic exchange membranes to attempt to determine if it is possible to tailor the molecular structure to enhance performance and durability.

It is clear that a significant body of work needs performing before MFCs become viable for large scale production, both on electrode components, and on the membranes used for ion transport. If this is accomplishable, MFCs should become a viable and environmentally friendly technology for renewable power generation and wastewater purification.

1.5 References

(1) Logan, B. E.; Regan, J. M. *Environmental Science & Technology* **2006,** 40, (17), 5172-5180.
(2) Schubert, C. *Nature* **2006,** 441, (7091), 277-279.
(3) Logan, B. E.; Hamelers, B.; Rozendal, R.; Schroder, U.; Keller, J.; Freguia, S.; Aelterman, P.; Verstraete, W.; Rabaey, K. *Environ. Sci. Technol.* **2006,** 40, (17), 5181-5192.
(4) Rabaey, K.; Verstraete, W. *Trends in Biotechnology* **2005,** 23, (6), 291-298.
(5) Davis, J. B.; Yarbrough, H. F., Jr. *Science* **1962,** 137, (3530), 615-616.
(6) Habermann, W.; Pommer, E. H. *Applied Microbiology and Biotechnology* **1991,** 35, (1), 128-133.
(7) Kim, J. R.; Zuo, Y.; Regan, J. M.; Logan, B. E. *Biotechnology and Bioengineering* **2008,** 99, (5), 1120-1127.
(8) Feng, Y.; Wang, X.; Logan, B. E.; Lee, H. *Applied Microbiology and Biotechnology* **2008,** 78, (5), 873-880.
(9) Wang, X.; Feng, Y. J.; Lee, H. *Water Science and Technology* **2008,** 57, (7), 1117-1121.
(10) Min, B.; Kim, J. R.; Oh, S. E.; Regan, J. M.; Logan, B. E. *Water Research* **2005,** 39, (20), 4961-4968.
(11) Logan, B. E. In *Simultaneous wastewater treatment and biological electricity generation*, 10th IWA International Congress on Anaerobic Digestion, Montreal, CANADA, Aug 29-Sep 02, 2004; I W a Publishing: Montreal, CANADA, 2004; pp 31-37.
(12) Huang, L. P.; Logan, B. E. *Applied Microbiology and Biotechnology* **2008,** 80, (2), 349-355.
(13) Kim, J. R.; Dec, J.; Bruns, M. A.; Logan, B. E. *Appl. Environ. Microbiol.* **2008,** 74, (8), 2540-2543.
(14) Du, Z.; Li, H.; Gu, T. *Biotechnology Advances* **2007,** 25, (5), 464-482.
(15) Zuo, Y.; Cheng, S.; Call, D.; Logan, B. E. *Environmental Science & Technology* **2007,** 41, (9), 3347-3353.
(16) Aelterman, P.; Rabaey, K.; Clauwaert, P.; Verstraete, W. In *Microbial fuel cells for wastewater treatment*, 5th World Water Congress of the International-Water-Association, Beijing, Peoples R. China, Sep 10-14, 2006; Beijing, Peoples R. China, 2006; pp 9-15.
(17) Scott, K.; Cotlarciuc, I.; Head, I.; Katuri, K. P.; Hall, D.; Lakeman, J. B.; Browning, D. *Journal of Chemical Technology & Biotechnology* **2008,** 83, (9), 1244-1254.
(18) Barton, S. C.; Gallaway, J.; Atanassov, P. *Chem. Rev.* **2004,** 104, (10), 4867-4886.
(19) Liu, Z.; Li, H.; Liu, J.; Su, Z. *Journal of Applied Microbiology* **2008,** 104, (4), 1163-1170.
(20) Germain, M. N.; Arechederra, R. L.; Minteer, S. D. *Journal of the American Chemical Society* **2008,** 130, (46), 15272-15273.
(21) Bond, D. R.; Holmes, D. E.; Tender, L. M.; Lovley, D. R. *Science* **2002,** 295, (5554), 483.
(22) Reimers, C. E.; Tender, L. M.; Fertig, S.; Wang, W. *Environ. Sci. Technol.* **2001,** 35, (1), 192-195.
(23) Rezaei, F.; Richard, T. L.; Brennan, R. A.; Logan, B. E. *Environ. Sci. Technol.* **2007,** 41, (11), 4053-4058.

(24) Donovan, C.; Dewan, A.; Heo, D.; Beyenal, H. *Environmental Science & Technology* **2008,** 42, (22), 8591-8596.
(25) Tender, L. M.; Gray, S. A.; Groveman, E.; Lowy, D. A.; Kauffman, P.; Melhado, J.; Tyce, R. C.; Flynn, D.; Petrecca, R.; Dobarro, J. *Journal of Power Sources* **2008,** 179, (2), 571-575.
(26) He, Z.; Shao, H.; Angenent, L. T. *Biosensors and Bioelectronics* **2007,** 22, (12), 3252-3255.
(27) Tartakovsky, B.; Manuel, M. F.; Neburchilov, V.; Wang, H.; Guiot, S. R. *Journal of Power Sources* **2008,** 182, (1), 291-297.
(28) Clauwaert, P.; Toledo, R.; Van der Ha, D.; Crab, R.; Verstraete, W.; Hu, H.; Udert, K. M.; Rabaey, K. *Water Science and Technology* **2008,** 57, (4), 575-579.
(29) Cheng, S.; Logan, B. E. *Proceedings of the National Academy of Sciences of the United States of America* **2007,** 104, (47), 18871-18873.
(30) Logan, B. E. *Environmental Science & Technology* **2004,** 38, (9), 160A-167A.
(31) Uwe, S. *ChemSusChem* **2008,** 1, (4), 281-282.
(32) Oh, S.; Logan, B. E. *Water Research* **2005,** 39, (19), 4673-4682.
(33) Chae, K.-J.; Choi, M.-J.; Lee, J.; Ajayi, F. F.; Kim, I. S. *International Journal of Hydrogen Energy* **2008,** 33, (19), 5184-5192.
(34) Cheng, S. A.; Logan, B. E. *Water Science and Technology* **2008,** 58, (4), 853-857.
(35) Sun, M.; Sheng, G.-P.; Zhang, L.; Xia, C.-R.; Mu, Z.-X.; Liu, X.-W.; Wang, H.-L.; Yu, H.-Q.; Qi, R.; Yu, T.; Yang, M. *Environmental Science & Technology* **2008,** 42, (21), 8095-8100.
(36) Liu, W.-z.; Wang, A.-j.; Ren, N.-q.; Zhao, X.-y.; Liu, L.-h.; Yu, Z.-g.; Lee, D.-J. *Energy & Fuels* **2008,** 22, (1), 159-163.
(37) Cracknell, J. A.; Vincent, K. A.; Armstrong, F. A. *Chem. Rev.* **2008,** 108, (7), 2439-2461.
(38) Cracknell, J. A.; Vincent, K. A.; Armstrong, F. A. *Chemical Reviews* **2008,** 108, (7), 2439-2461.
(39) Ramanavicius, A.; Kausaite, A.; Ramanaviciene, A. *Biosensors and Bioelectronics* **2008,** 24, (4), 767-772.
(40) Jeon, S. W.; Lee, J. Y.; Lee, J. H.; Kang, S. W.; Park, C. H.; Kim, S. W. *Journal of Industrial and Engineering Chemistry* **2008,** 14, (3), 338-343.
(41) Minteer, S. D.; Liaw, B. Y.; Cooney, M. J. *Current Opinion in Biotechnology* **2007,** 18, (3), 228-234.
(42) Gao, F.; Yan, Y.; Su, L.; Wang, L.; Mao, L. *Electrochemistry Communications* **2007,** 9, (5), 989-996.
(43) Akers, N. L.; Moore, C. M.; Minteer, S. D. *Electrochimica Acta* **2005,** 50, (12), 2521-2525.
(44) Moore, C. M.; Akers, N. L.; Hill, A. D.; Johnson, Z. C.; Minteer, S. D. *Biomacromolecules* **2004,** 5, (4), 1241-1247.
(45) Klotzbach, T. L.; Watt, M.; Ansari, Y.; Minteer, S. D. *Journal of Membrane Science* **2008,** 311, (1-2), 81-88.
(46) Moehlenbrock, M. J.; Minteer, S. D. *Chem. Soc. Rev.* **2008,** 37, (6), 1188-1196.
(47) Rezaei, F.; Richard, T. L.; Logan, B. E. *Biotechnology and Bioengineering* **2008,** 101, (6), 1163-1169.
(48) Arechederra, R.; Minteer, S. D. *Electrochimica Acta* **2008,** 53, (23), 6698-6703.

(49) Rabaey, K.; Boon, N.; Siciliano, S. D.; Verhaege, M.; Verstraete, W. *Applied and Environmental Microbiology* **2004,** 70, (9), 5373-5382.
(50) Rabaey, K.; Boon, N.; Hofte, M.; Verstraete, W. *Environmental Science & Technology* **2005,** 39, (9), 3401-3408.
(51) Ringeisen, B. R.; Henderson, E.; Wu, P. K.; Pietron, J.; Ray, R.; Little, B.; Biffinger, J. C.; Jones-Meehan, J. M. *Environmental Science & Technology* **2006,** 40, (8), 2629-2634.
(52) Tanisho, S.; Kamiya, N.; Wakao, N. *Bioelectrochemistry and Bioenergetics* **1989,** 21, (1), 25-32.
(53) Park, D. H.; Zeikus, J. G. *Biotechnology and Bioengineering* **2003,** 81, (3), 348-355.
(54) Lowy, D. A.; Tender, L. M.; Zeikus, J. G.; Park, D. H.; Lovley, D. R. *Biosensors & Bioelectronics* **2006,** 21, (11), 2058-2063.
(55) Niessen, J.; Schröder, U.; Rosenbaum, M.; Scholz, F. *Electrochemistry Communications* **2004,** 6, (6), 571-575.
(56) Schroder, U.; Niessen, J.; Scholz, F. *Angewandte Chemie-International Edition* **2003,** 42, (25), 2880-2883.
(57) Cheng, S.; Liu, H.; Logan, B. E. *Environmental Science & Technology* **2006,** 40, (7), 2426-2432.
(58) Rabaey, K.; Clauwaert, P.; Aelterman, P.; Verstraete, W. *Environmental Science & Technology* **2005,** 39, (20), 8077-8082.
(59) Liu, H.; Ramnarayanan, R.; Logan, B. E. *Environmental Science & Technology* **2004,** 38, (7), 2281-2285.
(60) Sell, D.; Kramer, P.; Kreysa, G. *Applied Microbiology and Biotechnology* **1989,** 31, (2), 211-213.
(61) Liu, H.; Logan, B. E. *Environ. Sci. Technol.* **2004,** 38, (14), 4040-4046.
(62) Cheng, S.; Liu, H.; Logan, B. E. *Environ. Sci. Technol.* **2006,** 40, (1), 364-369.
(63) Zhao, F.; Harnisch, F.; Schroder, U.; Scholz, F.; Bogdanoff, P.; Herrmann, I. *Electrochemistry Communications* **2005,** 7, (12), 1405-1410.
(64) Rozendal, R. A.; Hamelers, H. V. M.; Buisman, C. J. N. *Environ. Sci. Technol.* **2006,** 40, (17), 5206-5211.
(65) Min, B.; Cheng, S.; Logan, B. E. *Water Research* **2005,** 39, (9), 1675-1686.
(66) Liu, H.; Ramnarayanan, R.; Logan, B. E. *Environ. Sci. Technol.* **2004,** 38, (7), 2281-2285.
(67) Cheng, S.; Liu, H.; Logan, B. E. *Electrochemistry Communications* **2006,** 8, (3), 489-494.
(68) Topcagic, S.; Minteer, S. D. *Electrochimica Acta* **2006,** 51, (11), 2168-2172.
(69) Coman, V.; Vaz-Dominguez, C.; Ludwig, R.; Herreither, W.; Haltrich, D.; De Lacey, A. L.; Ruzgas, T.; Gorton, L.; Shleev, S. *Phys. Chem. Chem. Phys.* **2008,** 10, (40), 6093-6096.
(70) Yang, S.; Jia, B.; Liu, H. *Bioresource Technology* **2009,** 100, (3), 1197-1202.
(71) Oh, S.; Min, B.; Logan, B. E. *Environmental Science & Technology* **2004,** 38, (18), 4900-4904.
(72) Oh, S. E.; Logan, B. E. *Applied Microbiology and Biotechnology* **2006,** 70, (2), 162-169.
(73) Huang, L. P.; Logan, B. E. *Applied Microbiology and Biotechnology* **2008,** 80, (4), 655-664.
(74) Aelterman, P.; Rabaey, K.; Pham, H. T.; Boon, N.; Verstraete, W. *Environmental Science & Technology* **2006,** 40, (10), 3388-3394.

(75) He, Z.; Minteer, S. D.; Angenent, L. T. *Environmental Science & Technology* **2005,** 39, (14), 5262-5267.
(76) Logan, B. E.; Call, D.; Cheng, S.; Hamelers, H. V. M.; Sleutels, T. H. J. A.; Jeremiasse, A. W.; Rozendal, R. A. *Environmental Science & Technology* **2008,** 42, (23), 8630-8640.
(77) Shizas, I.; Bagley, D. M. *Journal of Energy Engineering* **2004,** 130, (2), 45-53.
(78) Moore, R. B.; Martin, C. R. *Macromolecules* **1988,** 21, (5), 1334-1339.
(79) Greso, A. J.; Moore, R. B.; Cable, K. M.; Jarrett, W. L.; Mauritz, K. A. *Polymer* **1997,** 38, (6), 1345-1356.
(80) Landis, F. A.; Moore, R. B. *Macromolecules* **2000,** 33, (16), 6031-6041.
(81) Mauritz, K. A.; Moore, R. B. *Chem. Rev.* **2004,** 104, (10), 4535-4586.
(82) Ghassemi, H.; McGrath, J. E.; Zawodzinski, J. T. A. *Polymer* **2006,** 47, (11), 4132-4139.
(83) Harrison, W. L.; Wang, F.; Mecham, J. B.; Bhanu, V. A.; Hill, M.; Kim, Y. S.; McGrath, J. E. *Journal of Polymer Science Part a-Polymer Chemistry* **2003,** 41, (14), 2264-2276.
(84) Hickner, M. A.; Ghassemi, H.; Kim, Y. S.; Einsla, B. R.; McGrath, J. E. *Chem. Rev.* **2004,** 104, (10), 4587-4612.
(85) Kim, Y. S.; Hickner, M. A.; Dong, L.; Pivovar, B. S.; McGrath, J. E. *Journal of Membrane Science* **2004,** 243, (1-2), 317-326.
(86) W. L. Harrison; Hickner, M. A.; Kim, Y. S.; McGrath, J. E. *Fuel Cells* **2005,** 5, (2), 201-212.
(87) Einsla, M. L.; Kim, Y. S.; Hawley, M.; Lee, H.-S.; McGrath, J. E.; Liu, B.; Guiver, M. D.; Pivovar, B. S. *Chemistry of Materials* **2008,** 20, (17), 5636-5642.
(88) Kim, J. R.; Cheng, S.; Oh, S. E.; Logan, B. E. *Environmental Science & Technology* **2007,** 41, (3), 1004-1009.
(89) Zuo, Y.; Cheng, S.; Logan, B. E. *Environ. Sci. Technol.* **2008**.
(90) Adachi, M.; Shimomura, T.; Komatsu, M.; Yakuwa, H.; Miya, A. *Chemical Communications* **2008**, (17), 2055-2057.

Chapter 2: Introduction to Step-Growth Polymerization and New Methods in Step-Growth

Stephen M. June, Musan Zhang, and Timothy E. Long
Department of Chemistry,
Virginia Polytechnic Institute and State University,
Blacksburg, Virginia 24061

(From portions of: Manuscript in Press – Comprehensive Polymer Science 3rd Ed. Chapter 5: Polycondensations and Polyadditions – Musan Zhang, Stephen M. June, and Timothy E. Long)

2.1 Structure-Property Relationships in Step-Growth Polymers

One of the fundamental problems facing polymer chemists today and throughout history is attempting to understand and predict how structural changes may impact the physical, mechanical, chemical, and thermal properties of the polymers that are being synthesized. One of the many jobs of a polymer chemist is to attempt to understand this phenomenon and apply this understanding towards understanding and predicting structure-property relationships. This is no simple task, as there are a plethora of different aspects of a polymer's structure which play a significant role in deciding the ultimate properties of that material. For example, even when keeping the structure of the repeating unit in a polymer the same, dramatic differences in properties may be observed due to molecular weight, topology, morphology, and thermal history. Furthermore, differences in chemical structure can determine huge differences in polymer properties. For example, Nylon-6,6 exhibits dramatically different properties than the polyester formed from reacting 1,6-hexane diol with adipic acid. The only structural difference is that the linkages between the monomers are amides in the case of Nylon and esters in the case of the polyester. This minor structural difference contributes to a great deal of difference in the mechanical, morphological, and thermal properties of the two materials. Understanding these differences and intelligently utilizing these molecular properties to design polymers with

tailorable bulk properties is a challenge that the polymer chemistry community has still not completely solved. Many of the recent advances in understanding of structure-property relationships, specifically within step-growth polymers, will be discussed herein, but there is still a significant amount of progress yet to be made in this area.

2.1.1 Molecular weight control

Molecular weight is likely the single most important polymer parameter. Low molecular weight polymers typically have lower tensile strength, flexibility, impact strength, toughness, and mechanical strength than their high molecular weight (> 5,000 – 10,000 g/mol) counterparts. As such, an understanding and control of molecular weight is crucial towards the synthesis and development of step growth polymers. Fortunately, for high-yielding step-growth reactions at similarly high conversions, a theoretical approach towards understanding and predicting molecular weight is possible.[1]

Initially, it is important to consider the extent of conversion at some time t within the reaction. At this given time, for a 1:1 stoichiometric ratio of two difunctional monomers A-A and B-B, there should be on average one unreacted A functionality and one unreacted B functionality per oligomer (or polymer) molecule.[1-4] The reaction product of one A functional group reacting with one B functional group would consist of one repeat unit within the polymer mainchain. Thus, a polymer formed of the monomers A-A and B-B would have a repeat unit of -(-A-A-B-B-)-.[1-4] The total number of repeat units within a polymer is equal to one half the total number of monomer units (assuming 1:1 stoichiometry), because there are two monomer residues per repeat unit. The degree of conversion or $\bar{X}_n$ of a polymer is equal to one half the number of repeat units per polymer molecule. This value is one half the number of repeat units

because each repeat unit contains two structural units, one corresponding to the A-A monomer, and one to the B-B monomer. Restated, $\bar{X}_n$ is equal to the number of structural units per polymer chain. $\bar{X}_n$ is often also signified as $\bar{P}$ or $\overline{DP}$.[1-4]

In order to understand $\bar{X}_n$, one should first examine the mechanism through which step-growth polymerization proceed. Unlike chain-growth polymerization, step-growth reactions do not proceed in a linear manner, but rather two monomers react to form a dimer, which may react with another monomer to form a trimer, or another dimer to form a tetramer. Ultimately, any length of monomer or polymer molecule may react with any other length monomer or polymer molecule. Comparatively, in chain-growth polymerization, the reactive polymer chain always reacts with another single monomer, until the propagating reactive center is terminated. Therefore, the degree of polymerization of a given step-growth reaction is directly related to monomer conversion. In order to calculate$\bar{X}_n$e at a given time during the reaction, the concentration of polymer or oligomer molecules and the initial monomer concentration must be known. The concentration of unreacted monomer M is

$$[M] = [M]_0 - [M]_0 p = [M]_0(1 - p) \qquad \text{Equation 2.1.1}$$

where [M] is the concentration of polymer or oligomer molecules, $[M]_0$ is the initial concentration of monomer, and p is the fraction of functional group conversion, or extent of reaction. Since the number of molecules in the system is directly proportional to the concentration of molecules (concentration is equal to moles of molecules/liters of solution) then one can write the degree of polymerization as

$$\bar{X}_n = \frac{N_0}{N} = \frac{[M]_0}{[M]} \qquad \text{Equation 2.1.2}$$

where N_0 is the initial number of monomer molecules and N is the number of polymer of oligomer or polymer molecules present in the system.[1-4] Rearrangement of Equation 5.2-1 yields "Carothers' Equation"[1] or

$$\bar{X}_n = \frac{1}{(1-p)} \qquad \text{Equation 2.1.3}$$

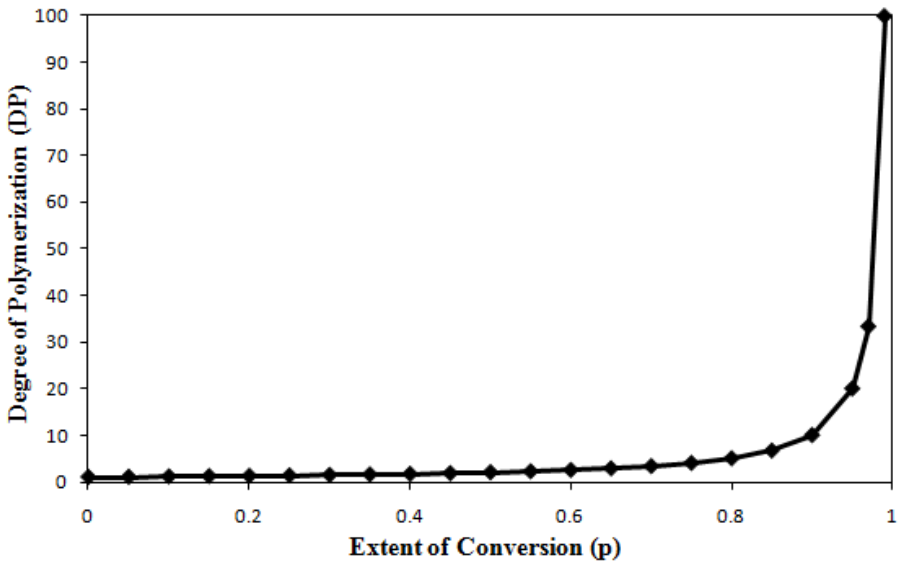

Figure 2.1 Degree of polymerization (*DP*) as a function of extent of conversion (*p*) or monomer consumption, assuming1:1 stoichiometry of functional groups.[4]

A careful examination of Equation 5.2-3 demonstrates the importance of high conversion in step-growth polymerization. Without extremely high conversion, high degrees of polymerization, and subsequently high molecular weight, are impossible to obtain. In the synthesis of small organic molecules, a reaction conversion of 90% is considered excellent. However, 90% conversion (p = 0.9) in a step-growth polymerization limits the degree of polymerization of the final product to a staggeringly low 10 repeat units per polymer chain. As mentioned previously, a polymer's physical and mechanical properties are directly related to molecular weight, and therefore a polymer with only 10 repeat units is extremely unlikely to possess desirable mechanical properties. **Figure 2.1** shows *DP* as a function of *p*. From this

plot, it is evident that only as conversion reaches ca. 98% or higher do the resulting products begin to exhibit high degrees of polymerization.[1-4]

Although knowledge of the degree of polymerization is helpful, $\bar{X}_n$ itself does not tell the whole story. Different polymer structures may have identical degrees of polymerization, and very different molecular weights. This is based on the fact that the repeat units have differing molecular weights. Therefore, the number average molecular weight (M_n) of a polymer may be calculated as

$$\bar{M}_n = M_0\bar{X}_n + M_e = \frac{M_0}{(1-p)} + M_e \qquad \text{Equation 2.1.4}$$

where $\bar{X}_n$ is the degree of polymerization, M_0 is the average molecular weight of the monomer residues (or the molecular weight of the repeat unit divided by 2) and M_e is the molecular weight of the end groups.[1-4] For sufficiently high molecular weight polymers, M_e is considered negligible, and thus M_n is equal to

$$\bar{M}_n = M_0\bar{X}_n = \frac{M_0}{(1-p)} \qquad \text{Equation 2.1.5}$$

Utilizing equation 5, it is possible to reliably predict, based on the percent conversion of monomer functionality and the molecular weight of the repeating unit, and assuming 1:1 stoichiometry, the molecular weight of a synthesized polymer. However, there is some experimental error in weighing and measuring monomers, so a thorough understanding of the effects of imperfect stoichiometric ratios should be evaluated.[1-4]

As in equation 2, if it is assumed that a polymer is being synthesized of two difunctional monomers, A-A and B-B, then the degree of polymerization should be equal to the initial number of monomer molecules, divided by the oligomer or polymer molecules present in the system. However, in equation 2, it is assumed that there are an equal number of A-A molecules as B-B molecules, and thus, an equal number of A functional groups as B functional groups.

Therefore, if the stoichiometry is not 1:1, then we need to focus on the number of available reactive functional groups. Thus, N_0 is the average number of A-A monomers and B-B monomers, and therefore;

$$N_0 = \frac{N_A+N_B}{2} = \frac{N_A}{2}\left(1+\frac{1}{r}\right) = \frac{N_A}{2}\left(\frac{1+r}{r}\right) \qquad \text{Equation 2.1.6}$$

where N_A and N_B are equal to the number of A-A monomers and B-B monomers, respectively. Also, *r* is equal to $\frac{N_A}{N_B}$. It is assumed that the B-B monomer is always the monomer in excess. Therefore, r will always be less than 1. After the fraction p (extent of reaction) monomers have reacted, the number of unreacted chain ends left is equal to

$$N_A(1-p) + (N_B - pN_A) \qquad \text{Equation 2.1.7}$$

Substituting in *r* and calculating for N in equation 7 (the total number of molecules after reaction) yields

$$N = \frac{1}{2}[N_A(1-p) + N_B(1-rp)] = \frac{N_A}{2}\left[(1-p) + \frac{(1-rp)}{r}\right] \qquad \text{Equation 2.1.8}$$

Rearrange equation 8 and substitute into equation 2 to get the number-average chain length (degree of polymerization).

$$\bar{X}_n = \frac{N_0}{N} = \frac{1+r}{1+r-2rp} \qquad \text{Equation 2.1.9}$$

If you assume 100% conversion, this simplifies to

$$\bar{X}_n = \frac{1+r}{1-r} \qquad \text{Equation 2.1.10}$$

As with conversion, assuring a 1:1 stoichiometry is crucial in obtaining a high molecular weight material. A 10% deficiency in monomer A-A would result in a maximum degree of polymerization of 19. Figure 2 demonstrates degree of conversion as a function of *r*. It is shown that only when the stoichiometric deficiency of A-A is less than ca. 2% are high degrees of polymerization, and as such, high molecular weights obtained.[1-4]

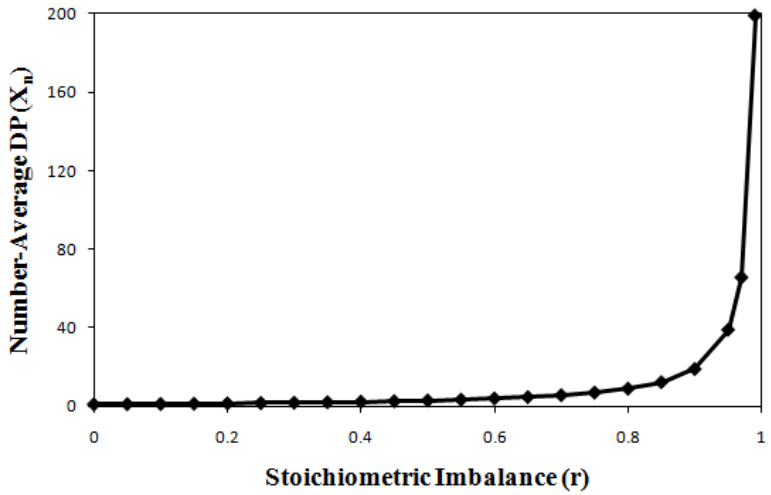

Figure 2.2 Number-average degree of polymerization (X_n) as a function of stoichiometric imbalance, *r*.

Although extreme care must be taken when performing a step-growth synthesis in order to obtain high molecular weight polymers, the statistical effect of stoichiometry on molecular weight does provide for one major advantage; control over molecular weight. As discussed previously, obtaining a high molecular weight polymer is crucial towards obtaining good mechanical, impact, and viscoelastic properties. However, high molecular weight can be a double-edged sword. Along with mechanical properties such as modulus and elasticity, melt viscosity dramatically increases with increasing molecular weight. Above a certain molecular weight, the melt viscosity actually increases exponentially with molecular weight, which can make processing of the polymers and fabrication of materials from the polymers virtually impossible. Furthermore, solubility is also linked closely with molecular weight. As a general rule, for a given solvent, polymer solubility is inversely related to molecular weight. Restated, as the molecular weight of a polymer increases, the solubility decreases. Therefore, the ability to control and limit molecular weight proves exceptionally useful when trying to tailor mechanical properties.[1-4]

Another advantage to limiting the molecular weight arises during the synthesis of segmented block copolymers. These copolymers will be discussed at length later in this chapter, but many times the synthesis of segmented block copolymers by step-growth chemistry requires the initial synthesis of a lower molecular weight oligomer. These lower molecular weight oligomers may be referred to as macromonomers or prepolymers. Utilizing a controlled excess of monomer A-A with monomer B-B allows for the ability to accurately target and predict the molecular weight of the synthesized polymer, and ensure that the obtained polymer has reactive end-groups containing "A" type functionality. Then, the synthesized "A"-functionalized prepolymer may subsequently be reacted with complementary B-B monomer and perhaps a different A'-A' functionalized polymer to obtain segmented block copolymers. This synthetic route is commonly used in polyurethanes and polysulfones, but finds utilization in a wide variety of step-growth techniques.[1-4]

As mentioned previously, molecular weight may be the single most important variable when attempting to understand structure-property relationships within polymers. Thus, the ability to control molecular weight within a step-growth polymer is critical. Utilizing the techniques discussed herein, a reasonable amount of control of molecular weight in step-growth polymerization is possible either by stoichiometric control, or monitoring the extent of conversion of a polymerization reaction. With these controls, the beginning of polymer property control has been established.[1-4]

2.1.2 Polymer architecture

After molecular weight, perhaps the second most important parameter of a polymer in regards to mechanical, thermal, rheological, and impact properties is the architecture of the

polymer. Architecture, sometimes also referred to as topology, can have a significant impact on the physical properties of a polymer.[2-4] For a polymer with a given molecular weight, and a constant repeat unit, the properties will be extremely different if this polymer is linear than if it is branched or hyperbranched. Furthermore, a cyclic polysulfone will have considerably different qualities than a linear one of the same molecular weight. Within this chapter, we will review seven different types of major polymer architectures: linear homopolymer, block copolymers, radial or star-shaped copolymers, graft copolymers, dendrimers, branched and hyperbranched copolymers, and cyclic polymers.

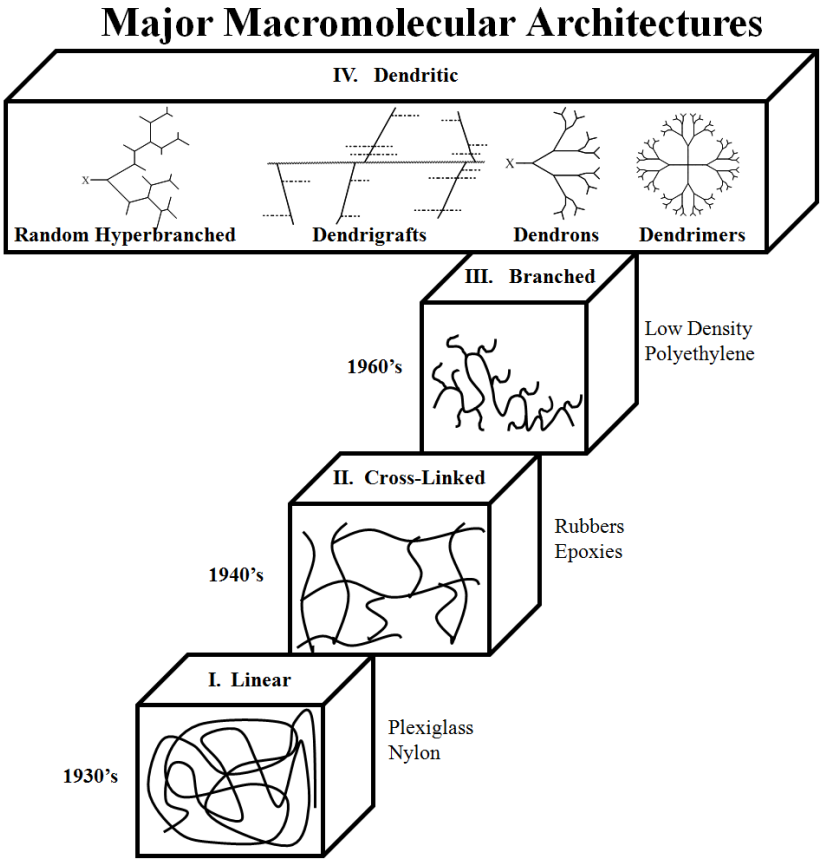

Figure 2.3 Cartoon demonstrating a chronological representation of major macromolecular architectures including linear polymers, cross-linked networks, branched polymers, and dendritic structures. [5] (Reprinted with permission from Tomalia, D. A.; Fréchet, J. M. J. *J. Polym. Sci. Part A: Polym. Chem.* **2002**, *40*, 2719.)

2.1.2.1 Linear homopolymers

Most of the original step-growth polymers such as simple polyesters or polyamides were linear polymers. A polymer is considered to be linear if there are two end-groups, and no branch points.[2-4] In the absence of a undesired side reaction, such as cyclic formation, the reaction products of stoichiometric ratios of two difunctional monomers A-A and B-B will produce a linear polymer. The majority of polymers produced by step-growth methods are linear polymers, as typically other topologies result from the intentional incorporation of branch or graft points, or undesirable side reactions such as cyclicizations. Although linear polymers do not posses cross-link or branch points, linear polymers may still exhibit good mechanical properties for several reasons.

Above a certain molecular weight of a polymer, polymer chains may become entangled just like a large pile of yarn or spaghetti. Below this molecular weight, the chains are not long enough that they entangle. This molecular weight is called the critical entanglement molecular weight or C_e. Above C_e, entanglements result in what may be considered "physical" cross-links (as opposed to covalent cross-links). Unlike covalent cross-links, these physical cross-links due to entanglements are transient, and may unentangle, allowing for movement of the polymer chain. This is particularly aided when the polymer chains have increased mobility, which can be obtained at elevated temperatures.[2-4]

Other methods by which linear polymers may exhibit good mechanical properties are non-covalent interactions. These interactions include crystallinity, hydrogen bonding, and ionic aggregation. For example, when comparing the linear polyamide nylon-6,6 with the analogous linear polyester formed from 1,6-hexane diol and adipic acid, the polyamide exhibits significantly higher tensile strength and Young's modulus than the polyester. This is due to the

large amount of crystallites formed within nylon-6,6. These crystallites act as temporary cross-links in much the same way that entanglements do, leading to enhanced mechanical properties. In Nylon-6,6, these crystallites are formed due, in part, to the extremely regular placement of amide functional groups, where there is one amide N-H between every 6 carbons. The N-H of the amide hydrogen bonds with a carbonyl on an adjacent chain, allowing adjacent chains to pack very tightly together. Like entanglements, but unlike covalent cross-links, this temporary cross-link formed by the hydrogen bonded crystallites is reversible at elevated temperatures, allowing for melt processing of polyamides, but still yielding high mechanical strength.[2-4]

2.1.2.2 Block copolymers

Block copolymers are copolymers where, given two repeat units A and B, the repeat units A are adjacent primarily to other repeat units A, and vice versa. For example, a block copolymer of A and B may have the structure AAAAAAAAAAA-BBBBBBBBBBBBB. This type of block copolymer is typically referred to as a "diblock" copolymer. However, there are many different topologies which are considered block copolymers. Triblock copolymers are those where there are three blocks, either two blocks of one repeat unit surrounding a third block of a different repeat unit; for example, AAAAAAAAAABBBBBBBBBBBBAAAAAAAAAA. A segmented block copolymer has many alternating small blocks of two or more different types of repeat unit. Graft or brush block copolymers are those where there is one long chain of one type, and branching off of those are several smaller blocks of a second type. In general, any copolymer when repeat unit type A is typically segregated from repeat unit B is considered a block copolymer.[2-4] **Figure 2.4** demonstrates several of these different major block copolymer architectures.

In step growth polymerization with difunctional monomers, typically block copolymers are synthesized using one B-B monomer, and two monomers with "A" functionality; A-A and A'-A'. Due to the difunctional nature of A-A and B-B step-growth polymerizations, it is difficult to synthesize a true diblock copolymer with difunctional monomers. In order to synthesize diblock copolymers by step-growth chemistry, there are a few synthetic techniques utilized. One method involves the utilization of an A-B type monomer such as 6-amino hexanoic acid. After reaching a desired % conversion for a targeted molecular weight (using Carothers' equation to target a molecular weight), a selective end-capping agent must be utilized to remove one of the functionalities (A or B). At this point, each oligomer or polymer chain would only contain one functionality (B or A, respectively). Then, a second A-B type monomer may be added to couple with the initial oligomer, to yield the diblock copolymer.

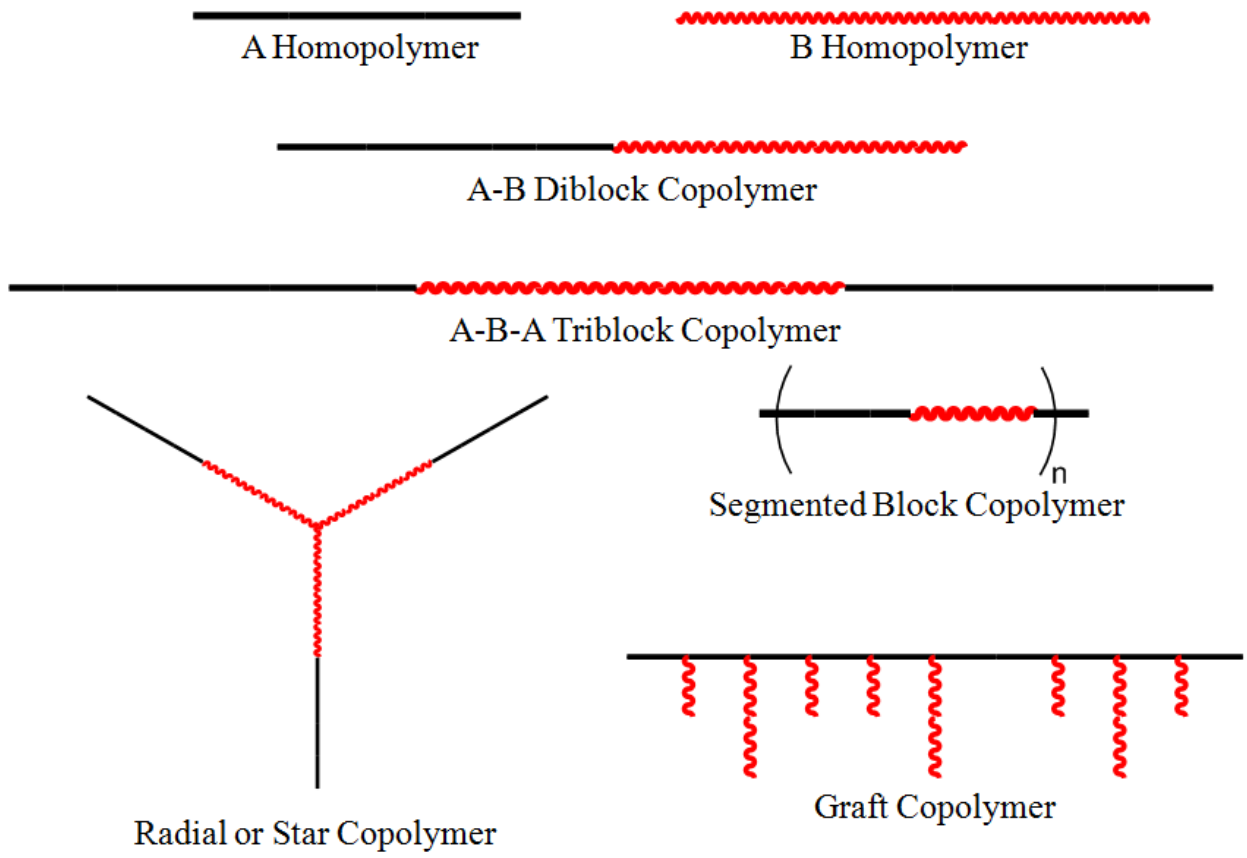

Figure 2.4 Various architectures for block copolymers.

A triblock copolymer may be synthesized by a similar method, except initially you would use an excess of one difunctional monomer A-A with another difunctional monomer B-B. This would leave each chain capped by functionality A on either side. Then, A-B type monomers would be added to produce the two outside blocks. Both of these methods are tedious, and involve several steps, so typically linear block copolymers produced by step-growth polymerization are "segmented" block copolymers. Segmented block copolymers are typically synthesized utilizing difunctional macromonomers. For example, in order to synthesize a segmented poly(siloxane imide) one would use a poly(dimethyl siloxane) macromonomer which is end-capped on both sides with aminopropyl functionality. This macromonomer would be reacted with another diamine and a dianhydride. The portions of the polymer that resulted from

the reaction of the other diamine and the dianhydride would be considered the "polyimide block" whereas the siloxane segment would be the "siloxane block". Another example is the utilization of polyether diols such as PEG or PPG in polyurethane synthesis. In this case, PEG or PPG diols are reacted with an excess of diisocyanate to form a "prepolymer" which is then subsequently reacted with a "chain extender" such as hexane diol or butane diol to form high molecular weight polymer.

One of the primary advantages of multi-block copolymers is their ability to micro-phase separate. In much the same way that a blend of poly(dimethyl siloxane) homopolymer and polyimide homopolymer would not remain stable, and would eventually phase separate, blocks of poly(dimethyl siloxane) and blocks of polyimide within the same polymer chain do not prefer to associate with each other, and thus will phase separate to as much of an extent as their block length allows. Therefore, below the glass transition temperature (T_g) of the higher T_g block, but above the T_g of the lower T_g block, there is a region where the phase segments of the higher T_g block act as temporary cross-links, allowing for elastomeric properties. Due to the temporary nature of these cross-links, at temperatures above the higher T_g, these materials will melt and thus are melt processable. Therefore, these materials are known as thermoplastic elastomers.[2-4]

In a measurement technique that measures modulus as a function of temperature, such as dynamic mechanical analysis (DMA), a noticeable drop in the storage modulus of the material is observed at both glass transitions. The region between the transitions where the modulus does not change significantly with increased temperature is the "rubbery plateau". This is comparable to the region after the glass transition of a cross-linked or thermoset material where the modulus does not drop. The difference lies in the fact that the thermoset does not exhibit a second drop in

modulus. However, as mentioned above, thermoplastic elastomers exhibit a second drop in modulus following the glass transition of the higher T_g segment. [2-4]

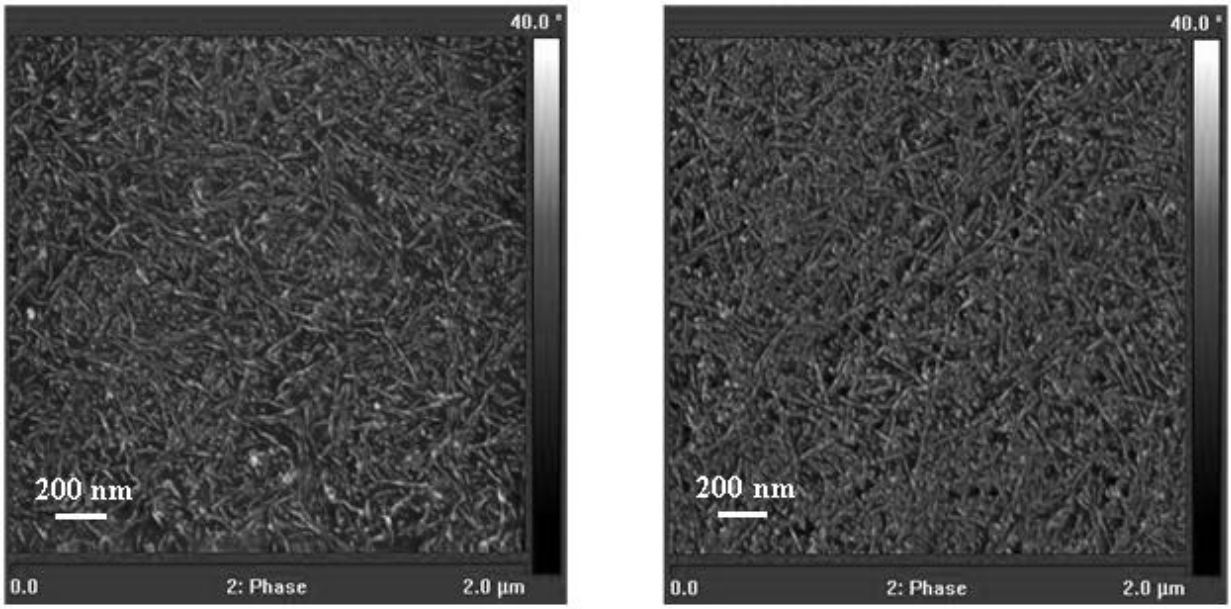

Figure 2.5 AFM phase images of a segmented block poly(siloxane imide) containing different ratios of two different anhydrides demonstrating significant microphase separation. [6] (Reprinted from "June, S. M.; Suga, T.; Heath, W. H.; Long, T. E.; Lin, Q.; Puligadda, R. *The Journal of Adhesion* **2010,** 86, (10), 1012 – 1028" with permission from Taylor and Francis publishing company.)

Typically the higher T_g block is referred to as the "hard segment" and the lower T_g block is referred to as the "soft segment". Atomic force microscopy (AFM) is an efficient method for viewing this type of phase separation, as well as other surface morphologies. Standard tapping mode AFM measures the phase of a material by tapping a nanometer sized piezo-driven gold tip on the surface of the material with a specific amplitude and frequency. The instrument measures deviations in amplitude and frequency of the tip as it taps the surface. The deviations occur because different materials with different moduli affect the tip vibration differently. **Figure 2.5** is an AFM phase image of a phase-separated poly(siloxane imide) that exhibits elastomeric

properties. The lighter portion is the "hard" polyimide segment and the darker section is the "soft" poly(dimethyl siloxane) segment.

2.1.2.3 Radial or star-shaped copolymers

To this point, the discussion of polymers by step-growth methods has primarily revolved around polymers with two chain-ends, or linear polymers. However, there is a wealth of research in the literature dealing with the synthesis and characterization of polymers containing one or more branch points. Some of the more prominent examples of branched polymers are radial or star-shaped copolymers. Star-shaped polymers are typically one central branch point from which three or more arms extend. Typically in step-growth polymerization this is accomplished utilizing a small amount of three or more functionalized molecule, and two difunctional monomers. Usually 1:1 stoichiometry of the functional groups is not utilized, because high molecular weight stars are not as desirable as controlled molecular weight stars. As always, utilization of Carothers' equation and control of stoichiometry and conversion will lead to a controlled molecular weight. It is also important to carefully control the reaction conditions, especially the concentration of monomers in order to avoid cross-linking or cyclicizations. Utilization of A-B type monomers along with a central molecule with three or more functional groups may allow for the ability to avoid such concerns as cross-linking or cyclicizations.

2.1.2.4 Graft copolymers

Graft or "brush" copolymers are copolymers where there is a long polymer mainchain with many shorter chains stemming from the long backbone. It is important to distinguish graft copolymers from other types of branched copolymers in that the branch points only occur off of

the main backbone chain, and the graft blocks do not branch separately. In many cases these are synthesized in a two-step process. Typically, a difunctional monomer A-A is reacted with a complementary difunctional B-B. One or both of the monomers also contains a third functionality C, which is either protected or non-reactive with functional groups A and B. Once the backbone polymer is synthesized, an oligomer which has one end group that is reactive with functionality C is added, which forms the brush polymer. Alternatively, two more difunctional monomers C-C and D-D (neither of which should react with the end-groups of the backbone polymer) are added in stoichiometric ratios such that the brush blocks are the desired molecular weight (using Carothers' equation).

An alternative and less-utilized method is to synthesize the "brush" section first. After synthesis of the brush, the brush block is end-capped on one end with a difunctional monomer. This difunctional monomer is reacted with a complementary difunctional monomer to form the backbone chain. This method is rarely utilized because conversion of the difunctional end-capped brush block is typically low. Conversion is low due to steric hindrance. The difunctional monomers have trouble reacting with other difunctional monomers, due to the bulky side chains of the graft chain. This problem is further enhanced when the reaction proceeds past the initial dimer and trimer phase into coupling of oligomers to form high order polymers. At this point the steric hindrance slows the rate of reaction to essentially zero. This makes this method extremely rare.

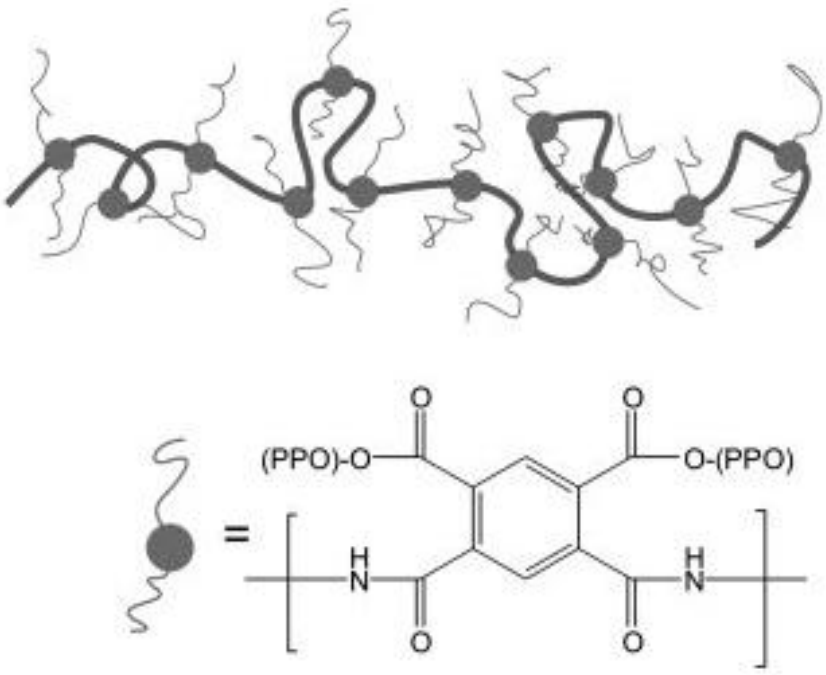

Figure 2.6 Poly(amic ester)-graft-propylene oxide. Condensation of the amic ester into the imide releases the PPO block.[7] (Reprinted with permission from Lebedeva, E.; Kesler, B. S.; Carter, K. R. *J. Polym. Sci. Part A: Polym. Chem.* **2005**, *43*, 2266.)

Figure 2.6 shows a cartoon and a chemical structure for a graft block copolymer. This polymer is a poly(amic ester) backbone with poly(propylene oxide) (PPO) grafts. This polymer is one of the few examples in the literature of the second synthetic route. In this case, two mono-hydroxy end-capped PPO macromonomers were reacted with a dianhydride to form the corresponding bis-isopthalic acid ester. This acid ester was then converted to the corresponding acid chloride and subsequently reacted with an aromatic diamine to form the poly(amic acid) backbone containing PPO grafts. This reaction was successful in spite of the steric hindrance due in part to the flexibility of PPO, and perhaps more importantly, the high reaction rate of amines with acid chlorides. As an aside, this particular graft polymer has an advantage. Upon

heating, the PPO blocks may be condensed off to form the polyimide and regenerating the macromonomer. This may be useful towards forming nanoporous polyimide films, as the PPO blocks and the PAE backbone will be phase separated in film form.

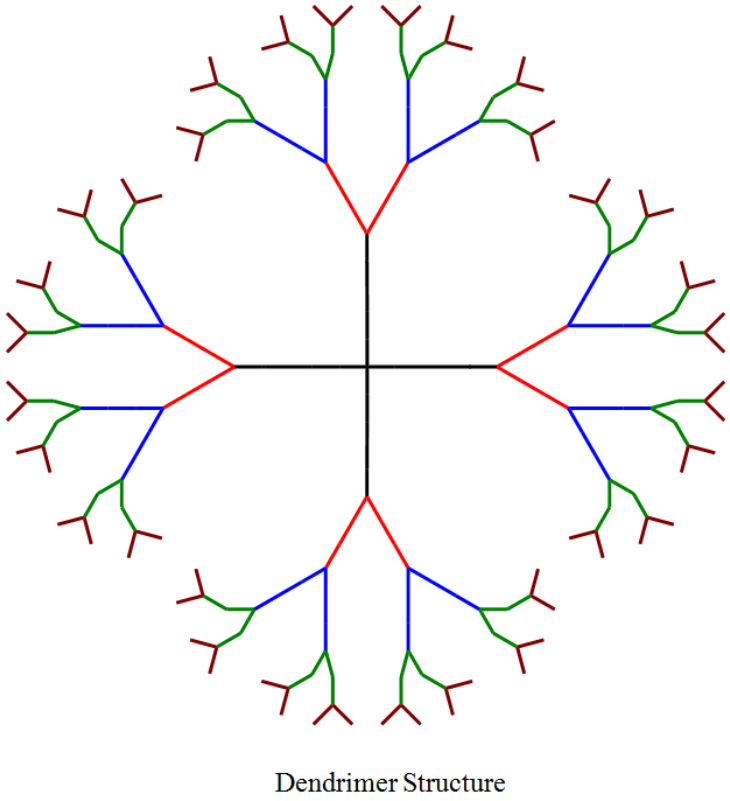

Figure 2.7 Cartoon demonstrating dendrimer structures where black is the core, red is the 1st generation, blue is the 2nd generation, green is the 3rd generation, and brown is the 4th generation

2.1.2.5 Dendrimers

Another form of branched polymers that have obtained significant prominence in the scientific community in the last few decades is dendrimers. Dendrimers are highly branched monodisperse polymers. There are two major methodologies for the synthesis of dendrimers; divergent and convergent. Dendrimers are centered around a core. In a divergent synthesis, this core is a di-, tri-, or more functional monomer (which we will refer to as A_2, A_3, etc. From this

point, another monomer, typically difunctional with the core functionality and monofunctional with a complementary functionality, such as A_2B is reacted with the core. Oftentimes, to limit conversion and maintain monodispersity, the A functionalities are protected. This would be referred to as a generation 1, or G1 dendrimer. Another generation is attached by adding yet more A_2B monomer (after deprotection of G1). After each subsequent generation, very rigorous separations and purifications are necessary to ensure monodispersity and complete conversion of the previous generation. This can lead to structure defects, which make this method disadvantageous. However, this method does allow for a high degree of control of dendrimer growth, and therefore the addition of more and more generations until steric hindrance prevents conversion.

In a typical convergent synthesis, the separate dendrons, or arms of the dendrimer are synthesized separately then combined with the inner core to make the final dendrimer. In this case, the dendrons can be functionalized and the core linker can be protected and then subsequently deprotected and reacted with the core, or the dendron ends can be functionalized and protected, then deprotected after final dendrimer assembly. This method is advantageous because dendrons are smaller than dendrimers, and thus much easier to isolate and purify, leading to a more facile synthesis of higher order dendrimers. However, steric constraints can make it difficult for the focal points to react with the core, which is often overcome by using a large excess of the high generation dendrons. This is synthetically wasteful and therefore can be very expensive.

A cartoon structure of a dendritic polymer is shown as **Figure 2.7**. This cartoon outlines the core (black), G_1 (red), G_2 (blue), G_3 (green), and G_4 (brown). The cartoon also demonstrates the fractal or repeating nature of dendrimers. Each end-point of each generation splits into two

subsequent endpoints in the next generation. The number of end-groups of a dendrimer can be expressed as:

$$EG = x2^n \qquad \text{Equation 2.1.11}$$

In this equation, EG is the number of end-groups, x is the number of branches off the core, and n is the generation. Therefore for a G_1 dendrimer with four branch points (like above), there are 8 end groups. The corresponding G_4 dendrimer would have 64 end groups. When considering the number of end groups of a dendrimer, it is clear to see that the higher generation dendrimer or dendron synthesized by the divergent method or convergent method, respectively, the more tedious the synthesis. As mentioned previously, it is important to ensure that all end-groups of the generation prior have successfully deprotected and subsequently undergo reaction to 100% conversion. Often, chemists will use a large excess of the A_2B monomer to drive the previous generation to good conversion. However, the method presents its own difficulties as after synthesis of every generation, rigorous purification and deprotection is required.

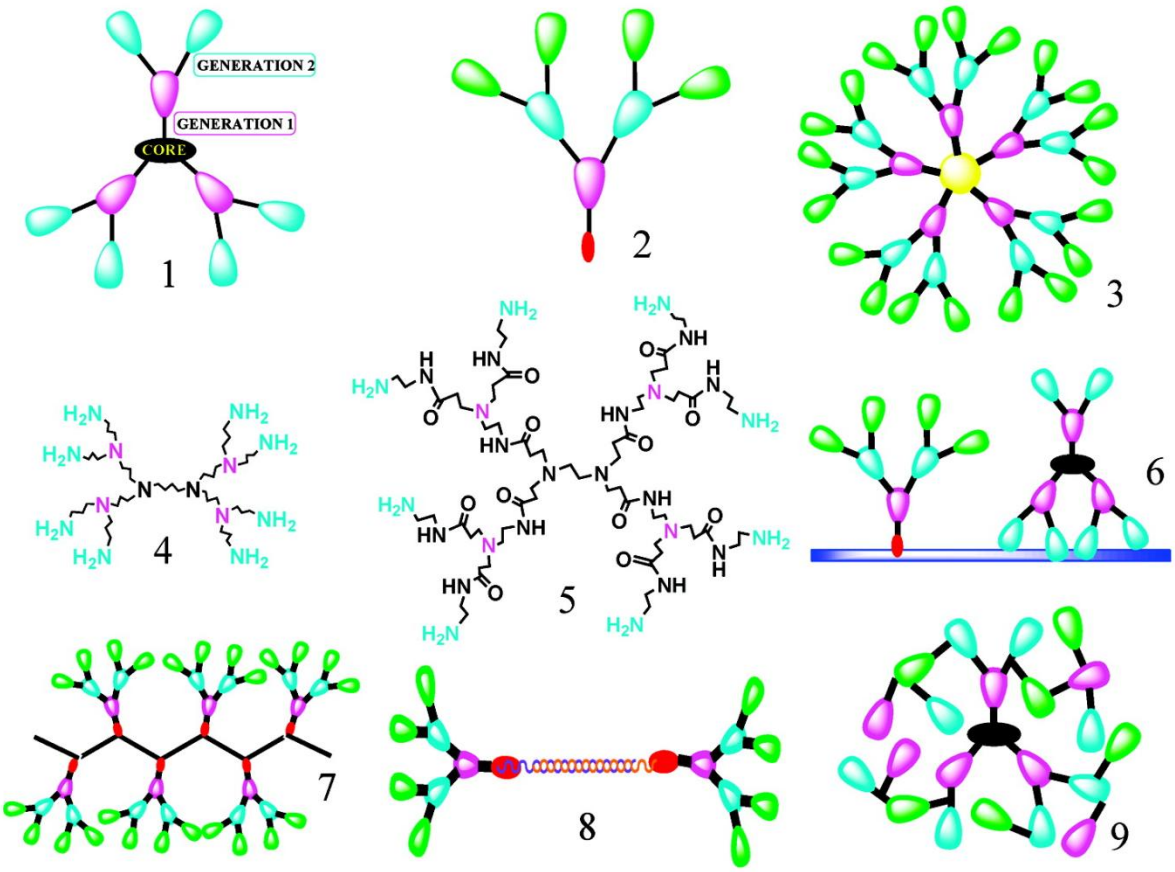

Figure 2.8: Cartoon representing several dendritic structures including: 1) Dendrimer, 2) Dendron, 3) Dendritic nanoparticle, 4) PPI dendrimer, 5) PAMAM dendrimer, 6) Dendronic and dendritic surface, 7) Dendronized polymer, 8) Dendriplex, and 9) Dendrigraft.[8] (Reprinted with permission from Astruc, D.; Boisselier, E.; Ornelas, C. T. *Chem. Rev.* **2010**, *110*, 1857. Copyright(2010) American Chemical Society.)

As mentioned previously, dendrimers and dendritic structures have seen a wide amount of exposure in the literature. There are several different types of dendritic structure, such as dendrimers, dendrons, dendronic surfaces, dendriplex's, dendrigrafts, and more. **Figure 2.8** shows cartoon representations of these dendritic structures as well as others. Dendrimers were discovered in the late 1970's independently by two groups Buhlier et al.[9] in Germany and Tomalia et al.[10] at Dow Chemical in Midland, MI. Tomalia et al. coined the term "dendrimer" in 1985 in an article outlining in a very comprehensive manner the synthesis of the PAMAM

(poly(amidoamine)) series of dendrimers.[10] By the mid-nineties, dendrimers had garnered a significant amount of attention in the literature, with literally tens of thousands of papers, patents, and lectures given on the topic since their inception less than 3 decades ago.[5]

Dendrimers are used for a plethora of applications.[5,8,11] The functions of dendrimers have been well reviewed elsewhere and thus will only be discussed briefly herein. They have been used in blends with polymers and as gels of dendrimers to obtain different mechanical properties than their non-dendritic counterparts, such as fast cure coatings and highly gelled surfaces. They have been utilized in photochemistry for light-harvesting and subsequent energy transfer, modifying the wavelength of absorbed light and retransmitting it, effectively converting UV light into IR or visible light, and charge separation. Functionalized dendrimers have been utilized in supramolecular assembly. Dendrimers have been involved in hydrogen bonding, electrostatic binding, ionic binding, metal ion coordination, liquid crystalline, and many other types of self-assembled microstructures. Dendrimers have also been widely used in catalysis. In particular, they have seen use as catalysts for separation and recycling and organocatalysis. Some of the most prominent and promising applications of dendrimers are those for biomedical applications. In particular dendrimers have seen significant use in drug delivery. For example, they have seen utilization for drug encapsulation, dendrimer-drug conjugates, drug nanocarriers, anticancer agents, and gene delivery agents. Other biomedical applications include photodynamic therapy, medical diagnostics, and biosensors. With this wide array of applications, it seems that perhaps some of the synthetic complexities of dendrimers are overshadowed by their usefulness, and it is expected that dendrimers and dendritic structures will continue to play a significant role in materials and biomaterials science.[5,8,11]

2.1.2.6 Branching and hyperbranching

Dendrimers may well be the best known type of polymer with multiple branch points, but other branched polymers have also obtained significant amounts of notoriety in the literature.[5,12-17] There are a plethora of branched polymers that are not as well controlled or monodisperse as dendrimers, but still have significant applications. These polymers are known as branched or hyperbranched polymers, depending on the number of branch points. Unlike dendrimers, these can be synthesized in a one-pot reaction, without any need for stepwise synthesis and purification. These reactions are typically not exceptionally well controlled, either in molar mass, or polydispersity. In fact, the products are often rather polydisperse, and often the products do not have a homogenous extent of branching per unit. However compared to dendrimers, these branched polymers are more typical step-growth polymers, and obey step-growth kinetics and Carothers' equations. **Figure 2.9** demonstrates a cartoon stick representation of a hyperbranched polymer.

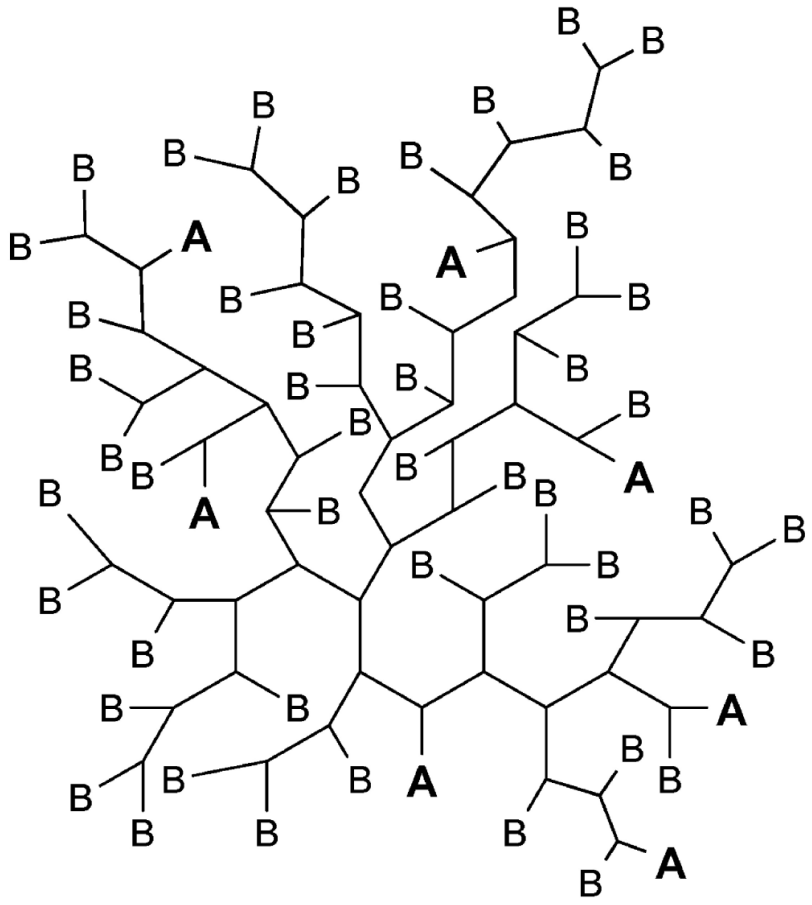

Figure 2.9 Cartoon depicting a polymer hyperbranched structure.[16] (Reprinted with permission from Voit, B. I.; Lederer, A. *Chem. Rev.* **2009**, *109*, 5924 Copyright(2009) American Chemical Society.)

Because hyperbranched polymers are not as controlled or symmetric as dendrimers, they have not seen quite as much utility as dendrimers in nanotechnology or medicine. However, they do have many of the same advantages in that they have very interesting properties relative to their linear counterparts, and may poses a large number of functional end-groups per polymer chain. This makes them very useful for applications like coatings and resins, and synthetically simple and cheap enough to be utilized in large scale applications. In many of these applications, it is much less important that the structure be "perfect" like that of a dendrimer, and much more important that the synthetic process be simple and inexpensive.

Typically, hyperbranched polymers are synthesized using monomers that have two or more of one functional group, and one of the second functional group (ex. AB_2). However, a similar method can be utilized to form branched polymers utilizing a combination of A-A difunctional, B-B difunctional, and a small amount of AB_x functionalized monomers. Caution is required in this method, as too much of the AB_x branching agent is likely to lead to cyclizications and eventual cross-linking. Also, AB_x monomers are often difficult to isolate due undesired self-reactions, so it is not uncommon to utilize one A_2 monomer and one B_3 monomer for the synthesis of hyperbranched polymers. Even more caution is required in this method, and reaction conditions much be carefully controlled, as this reaction may easily lead to cross-linking and cyclizications. To prevent this, many times the A_2 monomer is added slowly to the reaction vessel which already contains the B_3 monomer, thereby making it statistically less likely, especially at first, that the A_2 monomer will react to form a cycle.[15,16]

Figure 2.10 displays a cartoon scheme of synthesis of hyperbranched polymers by two routes. In particular, the route on the left is designed so as to leave behind one focal point, or type A functionality per hyperbranched polymer molecule. The route on the right is designed such that there is no residual unreacted A functionality. This is accomplished by utilizing a small amount of B_3 monomer such that all focal points react with that monomer. This could also be accomplished using any di-, tri- or higher order functionalized B monomer, B_x. Both of the synthetic schemes below have no potential for cyclization or cross-linking, as no A functionality is ever present more than once per monomer unit.[15,16]

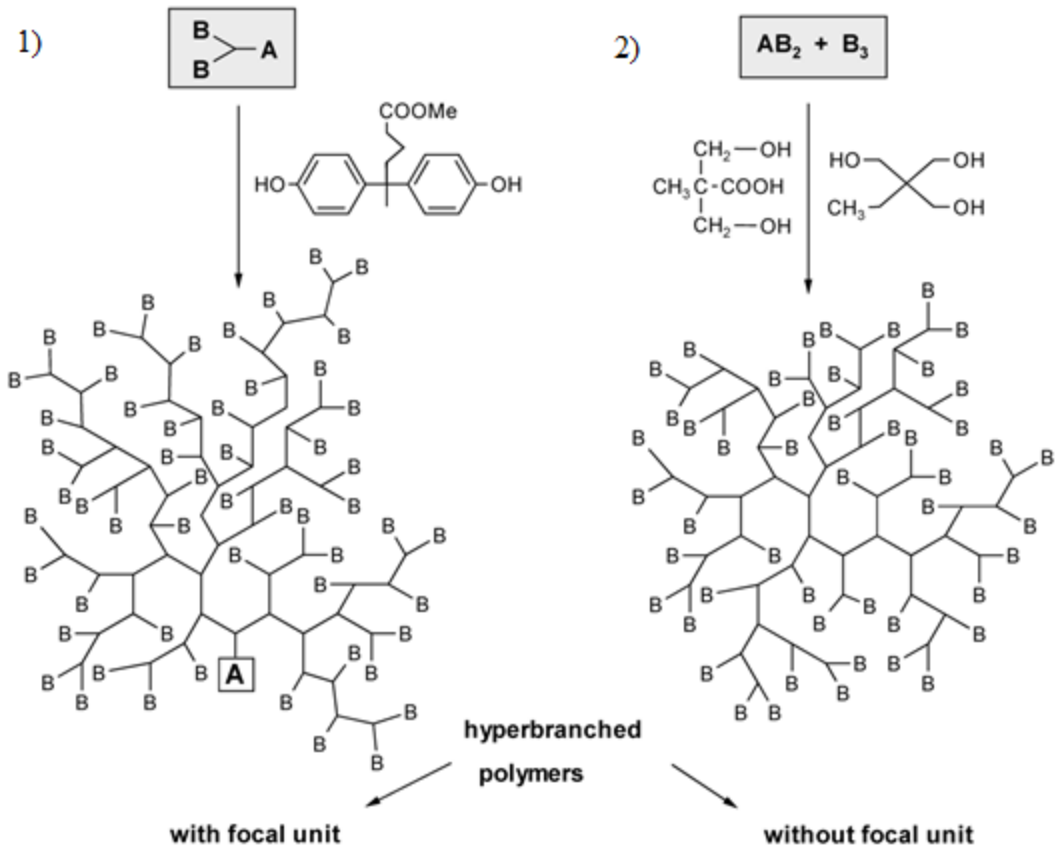

Figure 2.10 Synthesis of hyperbranched polymers using two methods: 1) Utilization of an AB_2 monomer; this approach will always leave one unreacted "A" functionality, or "focal point" per macromolecule and 2) Utilization of an AB_2 monomer with a B_3 monomer (no unreacted "A" functionality or "focal point".)[16] (Reprinted with permission from Voit, B. I.; Lederer, A. *Chem. Rev.* **2009**, *109*, 5924 Copyright(2009) American Chemical Society.)

As mentioned above, the primary applications for hyperbranched polymers include large-scale applications such as resins or coatings. For these applications, the ability to have a large number of functional end-groups per polymer molecule is exceptionally useful. For example, if every B functionality in **Figure 2.10** was an epoxy, and that hyperbranched polymer was utilized in an epoxy resin, the rate of gelation of that epoxy resin would be very fast, making this a very useful additive in a "quick cure" epoxy resin. Hyperbranched polymers have also found some utilization as additives in linear polymers in order to improve the rheological and flow properties of these polymers. Furthermore, they have demonstrated utility as additives to modify the

thermal properties and modulus properties of polymers. Hyperbranched polymers demonstrate a significantly lower solution and melt viscosity than linear polymers of similar molecular weight. Also, hyperbranched polymers tend to be exceptionally soluble. In spite of these advantages, hyperbranched polymers do show limited utility for some of the standard linear high-performance step-growth polymer applications. For example, hyperbranched polymers typically do not form free-standing films. This is due to the fact that hyperbranched polymers do not entangle, and therefore films of hyperbranched polymers tend to be brittle and fragile. In spite of this disadvantage, it is clear that hyperbranched polymers do have some significant uses in materials science.[15,16]

2.1.2.7 Cyclic polymers

So far throughout this chapter, the need for caution has arisen with many synthetic techniques involving step-growth polymerization to avoid cyclicization and cross-linking. However, a fair amount of literature exists on an understanding of synthesis of cyclic polymers, and their presence in virtually all step-growth polymerization reactions.[18-20] Even standard difunctional A_2 + B_2 linear polycondensations all at some point reach a molecular weight at which it is possible for the remaining A functionality on one end-group to bend around and react with the unreacted B functionality on the other end-group of the polymer. When this happens a cyclic polymer is formed and the chain is effectively terminated, resulting in a lowered polydispersity and lowered molecular weight. At some times this may be desirable, but often it is an un-desired reaction.[18-20]

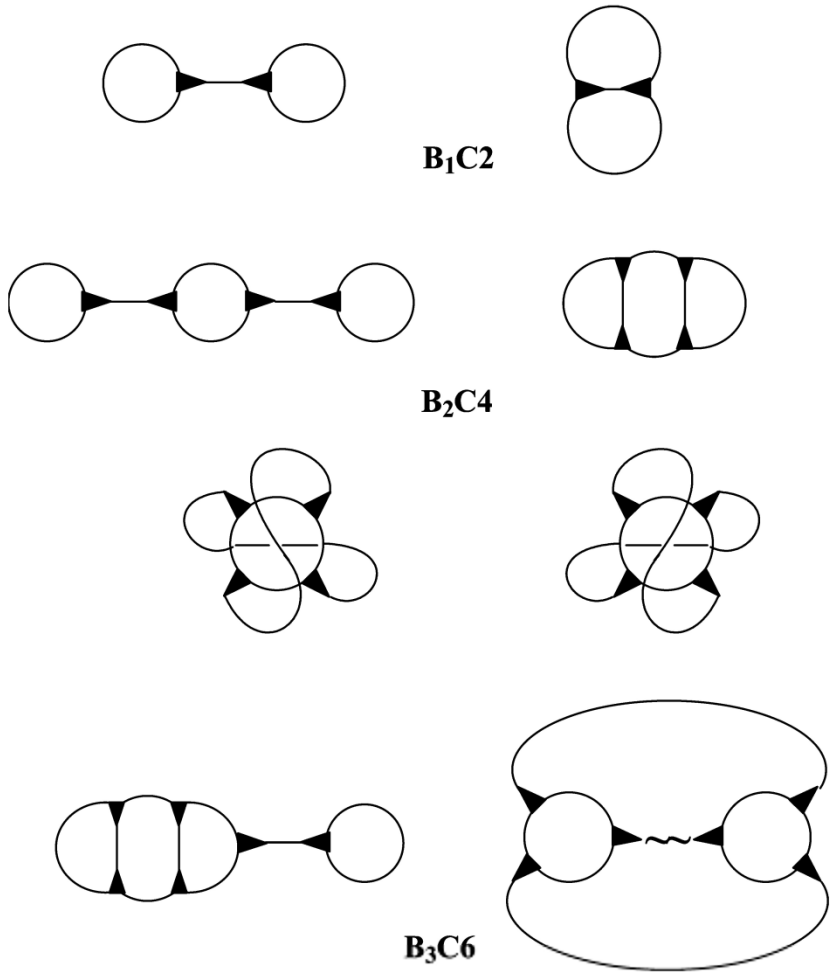

Figure 2.11: Cartoon demonstrating cyclic polymer structures based on monomer functionality, where B stands for "bridge" units and C stands for "cyclic structures".[20] (Reprinted with permission from Kricheldorf, H. R. *Acc. Chem. Res.* **2009**, *42*, 981. Copyright(2009) American Chemical Society.)

Cyclicization is especially prevalent at lower concentrations. At low concentrations, an oligomer chain's end group is statistically less likely to encounter a complementary end-group from another growing oligomer and increasingly likely to simply encounter its own tail and form the macrocycle. However, this reaction is increasingly likely with AB_2, $A_2 + B_3$, and other standard monomer schemes for making branched and hyperbranched polymers. In fact, hyperbranched polymers at high conversions often have a cyclic or multicyclic core, and a

hyperbranched exterior. The intentional synthesis and study of cycles and multicycles within polymers in branched, hyperbranched, and linear step-growth polymerizations has been well studied and reviewed elsewhere, particularly by Kricheldorf et al.[18-20] A complete understanding of cyclic polymers and their presence within linear and branched polymer syntheses has yet to be finalized, and thus the practical applications thus far of cyclic polymers and cyclic residues within linear polymerizations have not been established. However, as all step-growth polymerizations have the potential for cyclicization, it is certain that research in this area will continue, and that interest in cyclic polymers will continue to grow.

Based on the discussion of polymer architecture included herein, it is evident that polymer architecture and topology are both extremely important factors to consider when attempting to understand and subsequently control properties of a given polymer. For a given type of step-growth polymer (polyester, polyamide, etc.) it is clear that drastically different properties may be obtained simply by modifying the architecture of the polymer. Whether it be comparing a segmented block copolymer to a non-block copolymer of the same composition, or comparing a linear polymer with its branched or hyperbranched counterpart, small changes in architecture dramatically alter the properties of the polymer. A good understanding of the effects of topology and architecture on polymer properties may lead to dramatically enhanced property control.

2.2 New Strategies for Step-Growth Polymers

In the previous several sections, the discussion has primarily revolved around many of the "classical" step-growth polymers and synthetic techniques. However, some of the most exciting work performed in the last decade on polycondensations and polyadditions has been in

non-traditional step growth polymers. These non-traditional step growth polymers are primarily synthesized in similar manners to those previously discussed herein. However, these methods utilize functional groups that are not typically considered to be standard step-growth functional groups. Although an understanding of "standard" step-growth methodologies is important, the authors feel that a detailed discussion on several of these non-traditional methods is important towards a complete understanding of step-growth polymerization.

2.2.1 Click chemistry

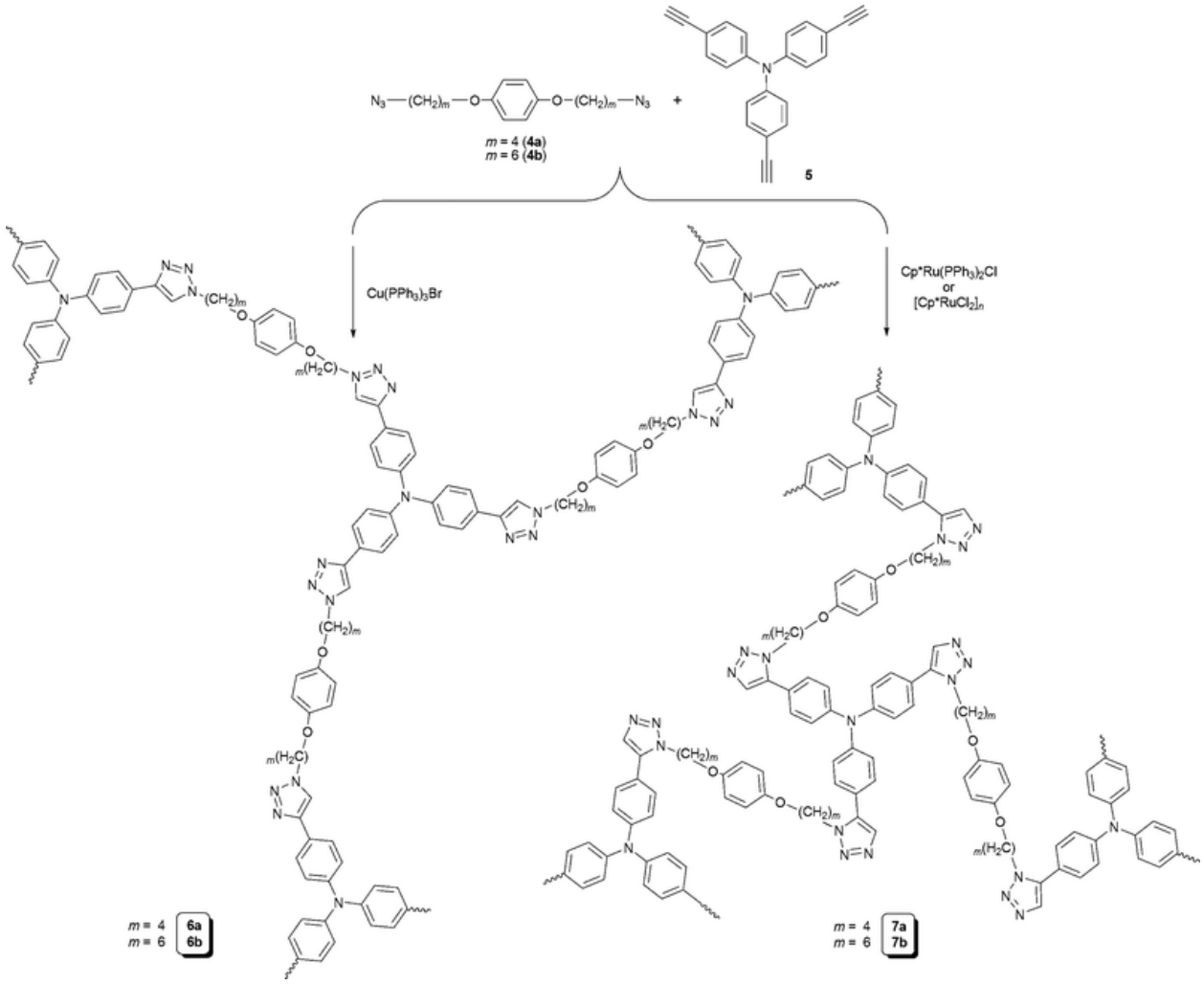

Figure 2.12 Hyperbranched polytriazole synthesized by $A_2 + B_3$ step growth polymerization[21] (Fair Use)

Since its discovery by Huisgen in the 1950's and, much later, the development by Sharpless, et al.[22-24], "click" chemistry has seen a huge surge in utilization in synthetic chemistry. The Huisgen "click" cycloaddition reaction is the reaction of a terminal alkyne with a terminal azide to form a 1,2,3-triazole unit. There are many other reactions referred to in the literature as "click" reactions[21,23,25-38], but the copper catalyzed alkyne-azide cycloaddition is the most prevalent, and will be the primary method discussed. Within this chapter, when "click" chemistry is referred to, it may be assumed that the version of "click" being referenced is the aklyne-azide cycloaddition. One of the reasons that the Huisgen "click" reaction has come to such prominence in synthetic chemistry is the extremely efficient nature of the "click" reaction. Also, the Huisgen "click" reaction is atom efficient, and produces no byproducts, making it an environmentally friendly reaction. Copper catalyzed "click" chemistry, as discovered by Sharpless[22-24], et al. is a remarkably stereochemically regular reaction, leading almost exclusively to the 1,2,3-triazole product. The predictability and regularity of this reaction is exceptionally convenient towards high-yield synthesis of compounds which are stereoregular, leading to a 1,4 cycloaddition. Ruthenium-catalyzed click chemistry is also prevalent in the literature, albeit not to the extent of the Sharpless method, and yields the stereoregular 1,5 cycloaddition.[21] Another important aspect of the "click" reaction is that it is typically very tolerant to other functional groups present in the system, allowing for easy synthesis of functionalized compounds, or coupling of two functionalized compounds without protecting or disturbing their functionality. Furthermore, the "click" reaction can occur in virtually any solvent, including aqueous solvent systems. Perhaps most importantly, the "click" reaction proceeds quickly with high conversions and typically at low temperatures. These combined advantages make "click" reactions

particularly well suited for step-growth polymerizations of all varieties; from linear polymers to graft block copolymers to hyperbranched polymers and dendrimers. Step-growth polymers synthesized by "click" chemistry are referred to as polytriazoles.[21]

Almost since the inception of the Cu catalyzed "click" chemistry discovered by Sharpless and coworkers[22-24], "click" has been utilized in a number of ways in polymer science. Researchers have utilized "click" chemistry to synthesize pendant functional polymers as well as end-group functional polymers. This allows for the facile post-polymerization addition of subsequent functionality that may not be compatible with the polymerization reaction. Also, when synthesizing pendant functionalized polymers, this allows for the simple addition of terminally functionalized blocks for synthesis of graft block copolymers.[26] Utilization of end-functionalized polymers makes it possible possible to use "click" chemistry to couple together oligomers to make di-, tri-, or segmented block copolymers.[26,37] Star copolymers have also been synthesized via "click" chemistry by utilizing a multifunctional core molecule, and mono-functionalized oligomeric arms. Also, "click" chemistry has been used extensively to conjugate polymers to surfaces, fullerenes, nanotubes, and other nanomaterials.[26]

Despite the clear advantages of "click" chemistry for organic and polymer synthesis, only recently has "click" been utilized as the direct polymerization mechanism for step-growth polymers. The first attempt at synthesis of a hyperbranched polymer via "click" chemistry was performed in 2004 by Voit, et al., but unfortunately the only product was a rubbery, insoluble precipate from the reaction.[39] The first linear polytriazole was reported in 2004 as a fluorene ring containing polytriazole.[40] Because polyfluorenes are well known to be conjugated light-emitting polymers, and the triazole ring is electron deficient, these fluorene containing polytriazoles were expected to have unique optoelectronic properties.[21]

The first successful synthesis of a soluble hyperbranched polytriazole was performed in 2008 by Shi, et al.[41,42] Almost simultaneously, Tang and coworkers were also able to obtain soluble hyperbranched polytriazoles.[43] Instead of an AB_2 monomer, a system of $A_2 + B_3$ was utilized. This method was advantageous due to the inclination of AB_2 monomers to autopolymerize in storage, or even immediately upon synthesis. This inclination is particularly strong when the reactions proceed as efficiently and at as low temperatures as the formation of triazole in the "click" reaction.[21]

"Click" chemistry has been utilized somewhat extensively towards the synthesis of dendrimers and dendritic materials.[8,11,27,30,44] The first report of a copper catalyzed "click" reaction towards the synthesis of a dendrimer was published in 2004 by Sharpless and coworkers,[44] and featured a two-step and convergent method for the synthesis of a triazole based dendrimer. Not long after this publication, a divergent triazole based dendrimer was synthesized and reported, as well as an example of how "click" can be utilized to create functional end groups.[45]

As outlined above, one of the advantages of "click" polymerization is the high reaction rates at relatively low temperatures. This is especially advantageous for the synthesis of polyesters. Some of the disadvantages of classical polyester synthesis are the extremely high reaction temperatures, long times, high vacuums, and precious metal catalysts required to get high molecular weight. Takasu and coworkers recently published a manuscript detailing the synthesis of a series of polyesters by "click" chemistry.[35,46] Necessarily, these polyesters are triazole containing polyesters, but they demonstrate high molecular weight and relatively good solubility. In contrast to polyesters synthesized by conventional methods, these polyesters were

synthesized under relatively benign conditions; in dimethyl formamide (DMF) at 50 °C with ppm amounts of CuBr.

Some of the major disadvantages associated with copper catalyzed "click" chemistry as a mechanism for step-growth polymerization include poor solubility of the final product, necessity of a metal catalyst, and difficulty removing the catalyst upon polymerization. However, many of these disadvantages are more than outweighed by the convenience of this reaction, the high reaction efficiency, the lack of byproduct, and the ability to include heteroatoms within the backbone of a polymer mainchain. Although "click" chemistry's role in polymer science has been primarily as a pendant or terminal functional group for which to perform post-polymerization reactions, polytriazoles synthesized directly by step-growth polymerization of bisalkynes and bisazides are reaching higher and higher levels of prominence in the literature and will continue to be investigated in the years to come.

2.2.2 Ionene synthesis

Ion containing polymers have received a lot of attention in the literature due to their potential applications in many emerging technologies. Ion containing polymers play a crucial role in many recent developments for energy storage, transport, and generation.[47-55] Also, they have found significant usage in water purification systems, anti-microbial membranes[56], and other biomaterials. They have been utilized as biomaterials for drug delivery and gene delivery agents. [57-60] However, the vast majority of ion containing polymers are synthesized with the ionic site pendant to the polymer mainchain. Very few examples exist where the polymer backbone itself is ion containing and charged.[61]

Ionenes[56,58-65] are ion containing polymers where the charge is located in the backbone of the polymer. In particular, the charge is contained in a quaternized nitrogen within the polymer mainchain. Ionenes are typically synthesized as the step-growth reaction of ditertiary amines with alkyl dihalides via an S_N2 reaction process. This reaction process is named after Nikolai Menshutkin, and was first utilized to synthesize ionenes in 1933.[66] One of the major advantages of ionenes is that precise synthetic control over the charge placement and density within the polymer backbone is readily achievable. Most ion-containing polymers, such as sulfonated polysulfones or polystyrenes or Nafion® type polymers do not have regular charge placement due to the non-controlled nature in which they are synthesized.[67] **Figure 2.13** demonstrates several possible highly controlled polymer architectures that are available when synthesizing ionenes. Careful selection of monomer allows for this precise control.

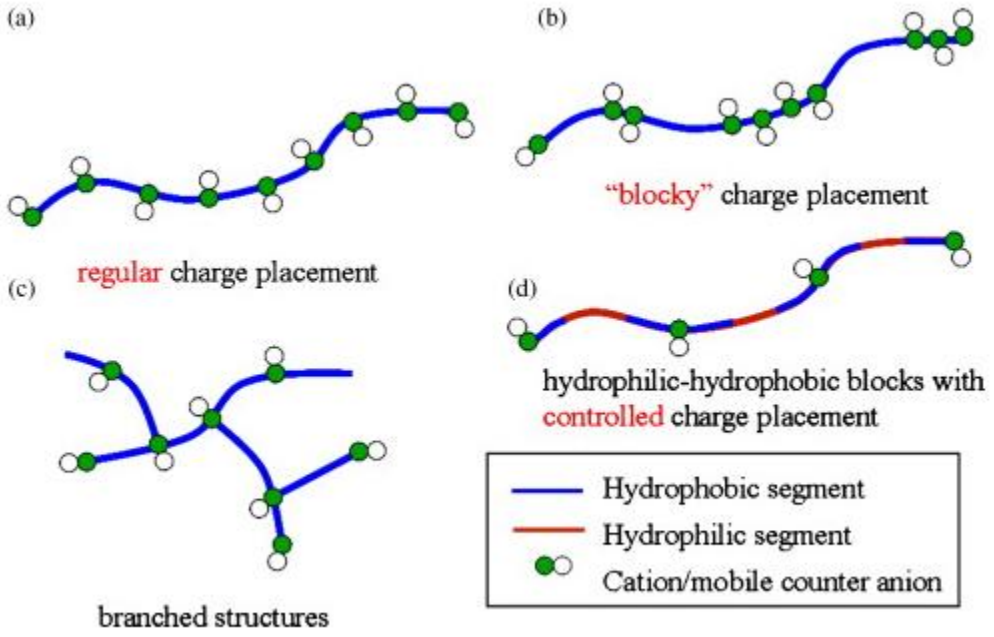

Figure 2.13 Various ionene morphology and structure through precise placement of charge. In particular, the ability to vary the charge density and structure type may dramatically modify the polymer properties.[61] (Reprinted with permission from Williams, S. R.; Long, T. E. *Prog. Polym. Sci.* **2009**, *34*, 762. Copyright(2009) American Chemical Society.)

In order carefully control the architecture and charge density of an ammonium ionene, careful selection of monomers must be utilized. To obtain regular charge placement, researchers have simply utilized a ditertiary amine with an alkyl dihalide of the same length. For example, N,N,N',N'-tetramethylhexane-1,6-diamine polymerized with 1,6-dibromohexane produces a polyionene containing exactly one quaternized nitrogen per 6 carbons in the backbone. To obtain more "blocky" charge placement, simply varying the lengths of the ditertiary amine and the alkyl dihalide yields the desired charge placement.[61] For example, the polymerization of N,N,N',N'-tetramethyldodecane-1,12-diamine with 1,2-dibromoethane produces a much more "blocky" charge placement.[62-64] Extending this even further, researchers have functionalized long PEG segment with alkyl halide end-groups, and then polymerizing this with 1,6-hexane diamine to yield ionenes with very blocky charge placements.[65] In order to obtain segmented block ionenes that also contain hydrophobic segments and hydrophilic segments, utilization of blocky polyether diols, such as pluronic diols, or incorporate multiple diols, with varying hydrophobicities, such as PEG diols and PTMO diols have also been synthesized.[61] Some interest does exist in branched and cross-linked ammonium ionenes, and although the typical A_2+B_3 monomer system could be utilized, most of the work in branched and cross-linked ionenes has revolved around functionalizing them with acrylate and allyl cross-linking residues and subsequently cross-linking using free-radical techniques.[61]

In order to have an effective discussion of ionenes, the nomenclature should be well understood. The nomenclature of non-segmented ionenes with simple aliphatic monomer structures without double bonds, or aromatic groups in between is conventionally x,y-ammonium

ionene where x is the number of methylene units in the diamine and y is the number of methylene units in the dihalide.[61]

The choice of the dihalide is particularly important when considering polymer properties. More basic, smaller halides will typically result in lower thermal stability. This is because the primary degradation mechanisms of ionenes are the reverse Menshutkin reaction and the Hoffman elimination reaction. The Hoffman elimination reaction, in particular, is much faster with a more basic anion. Therefore, the larger, less basic anions, such as Br- and I- are much more likely to result in higher thermal stability polymers.[61]

As with all polymers, one of the most important property characteristics of ammonium ionenes is molecular weight. However, due to the high charge ratio in ammonium ionenes, coupled with the propensity of charged polymers to aggregate in solution, obtaining reliable molecular weight values can be complicated. It is crucial that for measurement techniques such as SEC, light scattering, and intrinsic viscosity that the polymer chains in solution be free of each other and non-aggregated. Therefore, the choice of solvent for these techniques can be very taxing, and tedious. In 2008, Long and coworkers were able to perform absolute molecular weight characterization of 6,12- and 12,12-ammonium ionenes in 54/23/23 (v/v/v %) H_2O/MeOH/AcOH with 0.54 M NaOAc at a pH of 4.0. Many different solvent compositions were attempted, but this was the only solvent system that offered complete screening of charges and demonstrated no aggregation. Dynamic light scattering (DLS) was utilized to confirm the lack of polymer aggregates in solution.[61,62]

Although the primary discussion of this section has pertained to linear aliphatic ammonium ionenes and polyether segmented ammonium ionenes, many other ionene structures have been synthesized. Ammonium ionenes with one or more of the monomers being short

ether, ketone, and aromatic diols have been synthesized. Furthermore, ionenes have been synthesized with bicyclic DABCO and with imidazoliums. Also, segmented ionenes have not only been synthesized with polyethers, but also with PDMS segments. Finally, not all ionenes synthesized have been ammonium ionenes. Our research group has also synthesized ionenes based on phosphorous, or phosphonium ionenes.[61]

Ion containing polymers have shown significant promise in many applications, and the controllable charge placement in ionenes gives them high potential both as model compounds for understanding the effects of charge placement in ion containing polymers, but also for real life applications such as gene transfer agents, antimicrobials, and cancer thereputics. Care should be taken with monomer choice, and careful selection of solvent system is necessary for accurate SEC results.

2.2.3 Michael addition

Another common organic chemistry mechanism that has been known for many years but is only recently garnering attention for step-growth polymerization is the Michael addition (conjugate addition) reaction.[13,68-74] This reaction is an easy and relatively fast reaction between a nucleophile (Michael donor) and an activated olefin or alkyne (michael acceptor); for example, an acrylate. In this case, the nucleophile adds across the double bond of the olefin to form the product. This reaction does not require harsh reaction conditions, it is relatively fast, and does not produce byproducts. Also, this reaction may be performed in the absence of environmentally harmful solvents. Furthermore, it is relatively tolerant to other functional groups. Although this definition could apply broadly to virtually any nucleophile and activated alkene or alkyne, the most typical and most widely discussed Michael addition is the base-catalyzed addition of an

enolate to an acrylate. One of the advantages of this particular reaction is that the enolate has the potential to react twice, under the right conditions. **Scheme 2.1** outlines this reaction.[13]

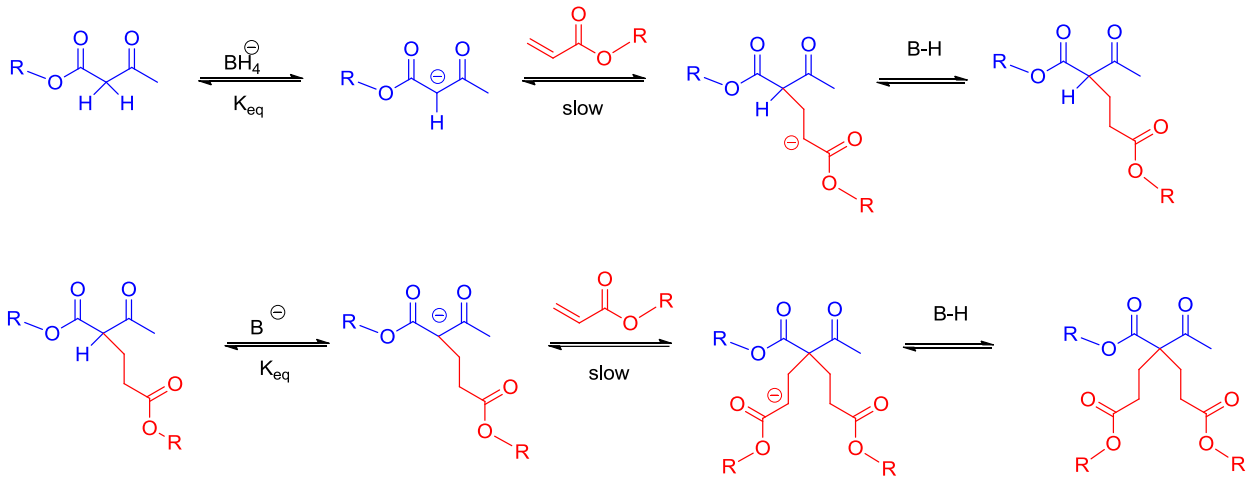

Scheme 2.1 Michael addition as an efficient and byproduct-free method towards novel polymers and networks.[13] (Reprinted with permission from Mather, B. D.; Viswanathan, K.; Miller, K. M.; Long, T. E. *Prog. Polym. Sci.* **2006**, *31*, 487. Copyright(2006) American Chemical Society.)

As one may expect, based on the reaction scheme, there is a large effect of the base strength on the rate of reaction. The rate of addition across the double bond is strongly dependant on the concentration of enolate anion, and thus the base strength. Additionally, the basicity/conjugate acid acidity of the Michael donor is important as well. The selection of the base catalyst should strongly depend on the pK_a of the Michael donor, and the extent of reaction desired. For example, the pK_{a1} of an acetoacetate group is 12, and the pK_{a2} is 13.6. Therefore, in order to react at both hydrogens in the acetoacetate, the pK_a of the base catalyst should be above 13.6. If it is only desirable to react once per acetoacetate, then the pK_a should be much closer to 12 than 13.6, but still above 12.[13]

Although the enolate-acrylate coupling Michael addition is the most prevalent, there are several other types of Michael nucleophiles utilized in the literature. In particular, amines and thiols have both been shown to act as Michael donors. Amines are particularly useful as they can

act both as the base catalyst and the Michael donor. Primary amines are advantageous because the nitrogen can act as a Michael donor twice, and thus react with two Michael acceptors. However, secondary amines are more basic, and thus react faster in Michael additions. Given the amount of amines present in biological systems, this reaction has been utilized extensively in biomaterials applications.[13]

Thiols have also been used extensively in Michael addition reactions for biological applications. The utilization of thiols is a little more specific, as the primary source of thiols in biological systems is within a cysteine residue. Thiols are also convenient because they are typically more nucleophilic than amines. Unfortunately, thiols are also prone to formation of disulfide bonds, which can inhibit their utility in Michael reactions without protecting group chemistry.[13]

Without exceptional care in base selection, acetoacetates are not considered effective Michael donors for the formation of linear step-growth polymers, due to the propensity of the acetoacetate group to react twice, making the functionality of a bis-acetoacetate greater than two. However, thiols and amines have both been utilized to produce linear polymers, as well as hyperbranched polymer and dendrimers, by step-growth polymerization. Furthermore, utilization of molecules containing one acrylate functionality and one acetoacetate functionality has lead to hyperbranched polymers. Perhaps the most common utilization of Michael chemistry for the formation of polymer materials, however, is the formation of a polymer network by Michael addition of an enolate to an acrylate, as depicted in **Scheme 2.1**.[13]

Elastomeric networks are some of the most industrially important polymeric materials as they are insoluble, robust, and have excellent mechanical properties. Reaction of a bis-acetoacetate with a bis-acrylate catalyzed by a small amount of base leads to highly cross-linked

polymer networks. These networks show significant potential in applications such as coatings, adhesives, and laminates. One of the interesting elements of these networks is the tailorability of the mechanical properties based on the selection of the monomers, as well as the base. By tailoring the length of the monomers, a significant amount of control over cross-link density is possible. Also, by careful selection of the chemical structure of the monomers, it is possible to control the properties of the material. Significant work has been done in the synthesis of novel Michael networks containing PPG,[68] PEG,[71] and polycaprolactone[70] "soft" segments in order to obtain unique mechanical properties. Also, there have been papers outlining the synthesis of Michael networks containing urethane linkages.[72] These linkages incorporate the interesting aspect of hydrogen bonding interactions with a Michael network. The hydrogen bonding networks demonstrated higher tensile strengths and elongations at break than non-hydrogen bonding analogues.[72]

Some interest has also developed in the formation of reversible networks via Michael addition. In 2007, Long and coworkers published a paper detailing the synthesis of acid-labile Michael networks.[69] A novel diacrylate was reacted with a bis-acetoacetate functionalized PEG in the presence of base to form insoluble networks. However, upon addition of catalytic amounts of acid, the cross-links were cleaved to form soluble polymer products.[69] Furthermore, recent work in the Long group has yielded the synthesis of a novel bis-acetoacetate which contains an *o*-nitro benzyl ester photo-degradable site. This acetoacetate was reacted with PEG bis-acrylates to form insoluble cross-linked networks with the potential to undergo photo-cleavage and form soluble polymeric products upon exposure to UV light. **Figure 2.14** details the structure of this *o*-nitro benzyl ester-containing bis-acetoacetate and the subsequent network formation.[75]

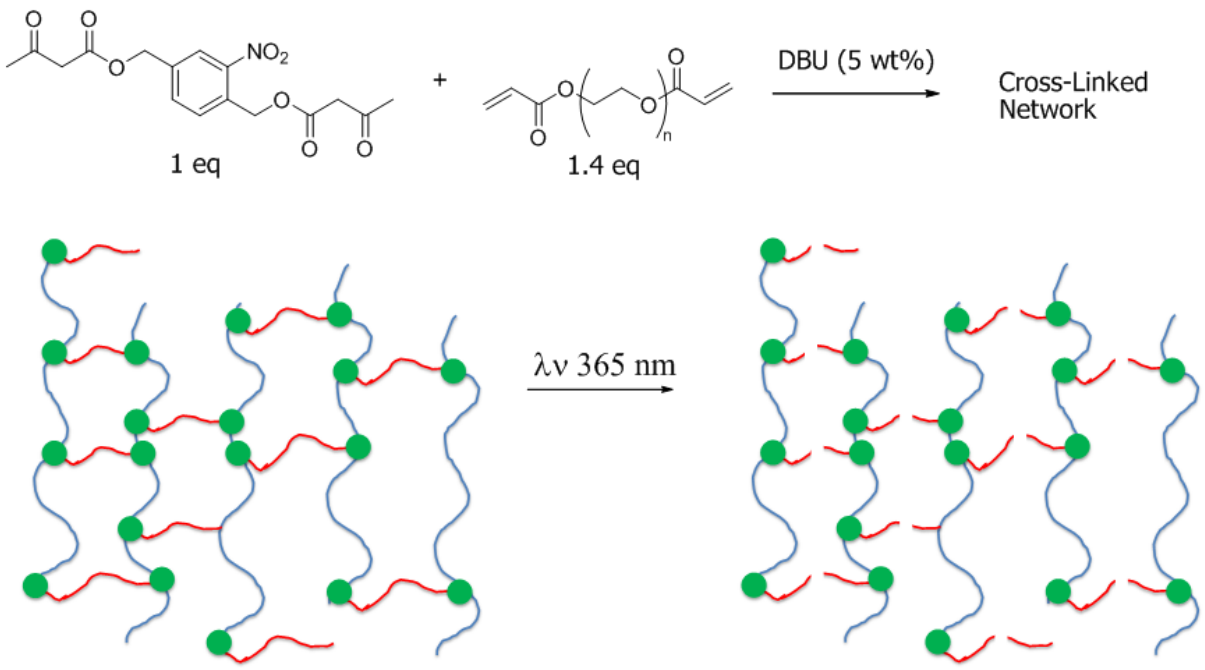

Figure 2.14 Michael addition networks containing a novel chromophore-containing bis-acetoacetate for a potentially photo-reversible network.[75]

Michael addition is a relatively simple, byproduct free and efficient reaction for the formation of linear, branched, and dendritic polymers and polymeric networks. With careful selection of monomers and base catalysts, a variety of architectures and topologies are available. Although this reaction has been known for some time, only recently has Michael addition reached any level of prominence within the polymer science community.

2.2.4 Diels Alder polymerizations

As mentioned previously, Huisgen "click" chemistry has reached a fairly high level of prominence in polymer science. However, there are many other types of reactions that are considered "click" reactions. One of these is the well-known Diels-Alder [4+2] cycloaddition.[27-29,36,37,76-79] Diels Alder is well-studied in organic chemistry, and well taught in organic

chemistry textbooks as a unique and convenient method for the synthesis of 6-membered rings, and especially for the synthesis of bridged 6-membered rings. It is a convenient reaction because it proceeds nearly quantitatively, with good stereoregularity, and does not produce any byproducts. Much like the azide-alkyne "click" coupling, Diels Alder reactions have found significant use in polymers for side chain coupling, star formation, or brush polymers, but limited use as a polymerization mechanism itself. Unlike Huisgen cycloaddition, however, Diels Alder can undergo the reverse "retro-Diels Alder" reaction.[28,29,78,79]

There have been some reports of Diels Alder as a polymerization mechanism for step growth polymerization in the literature. In fact, one of the first known reactions of cyclopentadiene was by the "father of polymer science" H. Staudinger.[78,79] He was able to synthesize poly(cyclobutadiene) by the [2+4] cycloaddition reaction, but in fact was not aware that this was the reaction mechanism under which the reaction was proceeding, because this was prior to the work by Alder and Stein. Only in the last few years have researchers attempted to repeat their work. Wudl and coworkers were able to successfully synthesize Diels Alder cyclopentadiene and mass spectrometry of the resulting polymer revealed that it was at least 18 repeat units long.[78,79]

Other groups have also successfully utilized Diels Alder reactions to make step-growth polymers. In particular, significant effort has been devoted to the furan-maleimide coupling. In this case, the bulk of the work that has been performed utilizes an A-B type monomer. These compounds are relatively stable, because the Diels Alder reaction does not occur until approximately 80 °C or hotter. [36,76,77]

One of the unique features of Diels Alder reactions are their inherent reversibility. Above a certain temperature (which varies depending on the substituents), compounds

synthesized by Diels Alder will undergo the reverse or retro-Diels Alder reaction to yield the initial conjugated diene and alkene starting materials. The majority of the work that has been done in Diels Alder polymerizations considers this a disadvantage, as it limits the thermal stability of the material. However, Wudl and coworkers have utilized this property, as well as the understanding of the polymerization mechanisms of cyclopentadiene obtained by revisiting Staudinger's work, to synthesize polymers that are thermally remendable. In fact, their initial monomer starts in the form that would normally be produced by Diels Alder. Above 120 °C, their monomer undergoes the retro-Diels Alder to form a bis-cyclopentadiene monomer, which then undergoes the Diels alder reaction to form the step-growth polymer. The residual double bond remaining after the Diels Alder reaction may then couple with one of the cyclopentadiene units in a growing polymer chain to form the cross-linked network. As with most cross-linked networks, these materials are mechanically durable and resistant to solvents.[78]

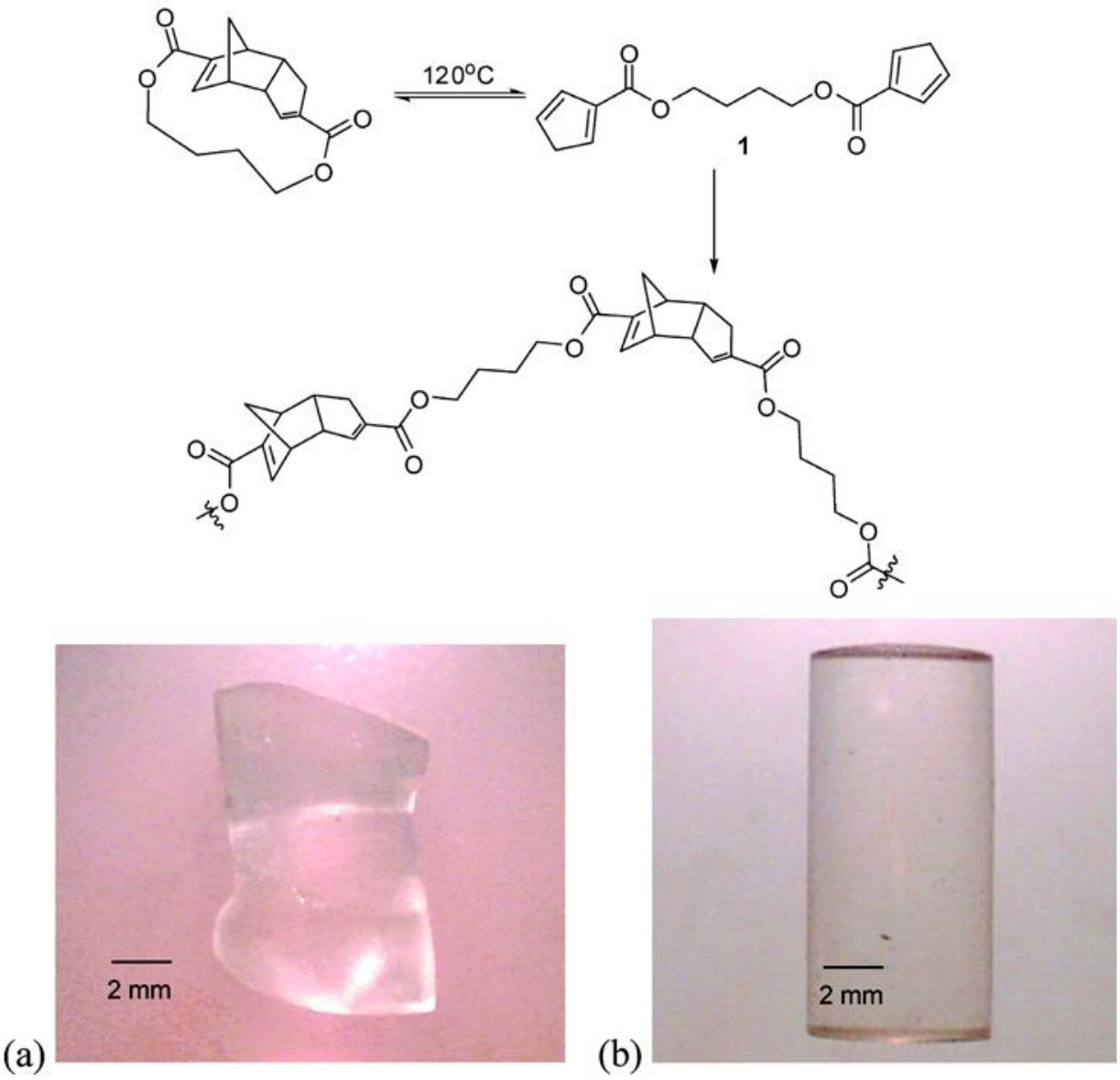

Scheme 2.2 Diels-alder as a synthetic method for the synthesis of healable materials and photographs of (a) polymer after compression testing and (b) the same sample after thermal remending, demonstrating shape memory.[78] (Reprinted with permission from Murphy, E. B.; Bolanos, E.; Schaffner-Hamann, C.; Wudl, F.; Nutt, S. R.; Auad, M. L. *Macromolecules* **2008**, 41, 5203. Copyright(2008) American Chemical Society.)

More importantly, when these compounds are subject to a stress or a fracture, the chemical bonds that fracture are typically those bonds that are the most strained, or in this case, the Diels Alder bonds. Therefore, upon heating, the Diels Alder reaction may reoccur, making

these polymers thermally remendable. **Scheme 2.2** shows the synthesis of Wudl's Diels Alder based polymer, and an image of a sample after compression testing. The sample after compression testing was then heated to above 120 °C, and demonstrated excellent shape memory. Also, when performing fracture testing and subsequent heating, the point of fracture was almost completely removed, and the sample recovered a significant amount (as much as 60%) of its initial strength.[78]

Although there is not an extensive supply of research on Diels Alder as a polymerization technique, the [4+2] cycloaddition is clearly a versatile tool for polymer science. In particular, the advantage of the reversibility of Diels Alder under thermal stress makes it a particularly useful technique for thermally remendable polymer systems.

2.2.5 Polybenzimidazoles

Polybenzimidazoles (PBIs) are a class of polymers that are reasonably well known in the literature. They have been well reviewed elsewhere and so only will be briefly mentioned here.[49,80] However, these compounds have only recently reached any level of commercial significance. They are typically very thermally stable and flame resistant, and have found utilization in firefighter coats, space suits, and metalworking gloves. Commercially PBIs are synthesized in a two-step melt-solid state polymerization from 3,3',4,4'-tetraaminobiphenyl and diphenyl isophthalate. This process produces only moderate molecular weights and the polymers are typically only soluble in dipolar aprotic solvents with a salt under high pressure.[49]

Recently, PBIs as a class of polymers (as opposed to the commercially available PBI discussed above) have garnered some interest in the fuel cell industries as potential proton exchange membranes. The tertiary nitrogen in the five membered imidazole ring is susceptible

to protonation in acidic conditions, and thus may be utilized for proton transfer. In order for this to occur, the polymer must first be doped with phosphoric acid, in order to create an acidic enough media to protonate the PBI and thus allow for transfer of protons. This method does have some advantages.[49]

One of the primary disadvantages of typical proton exchange membranes such as Nafion® is that they need to be hydrated in order to present high proton conductivity. Unfortunately, this eliminates their utility at temperatures above ca. 80 °C. This is because above this temperature, the membranes tend to try out and therefore display low conductivity. Phosphoric acid's boiling point is significantly higher than that of water, which allows for PBI proton exchange membranes to operate at significantly higher temperatures. This is advantageous because PEM fuel cell kinetics are enhanced at elevated temperatures, increasing the efficiency.[49,54,55]

Unfortunately, PBIs can only be doped in phosphoric acid to relatively low loadings before mechanical properties start to significantly diminish. Furthermore, the methods used to load PBI membranes with high amounts of phosphoric acid are tedious and have several steps. These complications eliminate the usage of highly phosphoric acid doped PBI membranes. However, in 2005, Benicewicz and coworkers developed the synthesis of PBIs in polyphosphoric acid via a sol-gel process. After film casting, the polyphosphoric acid (PPA) was hydrolyzed to phosphoric acid. These membranes contain high amounts of phosphoric acid, and retain extremely good mechanical properties, even at elevated temperatures. They are also highly conductive. These membranes operate efficiently in high-temperature proton exchange membrane fuel cells.[54,55]

The Benicewicz group is currently working on synthesizing functionalized PBIs by this method and recently published the synthesis of hydroxy-functionalized PBI membranes in PPA. The hydroxy functionalization allows for reversible cross-linking when exposed to phosphoric acid, which leads to extremely durable films and membranes. In fact, flexible, free-standing, tough films suitable for proton exchange membrane fuel cells were cast with loadings as low as 2.5% PBI in PPA. **Scheme 2.3** demonstrates the synthesis of these samples in PPA.[54,55]

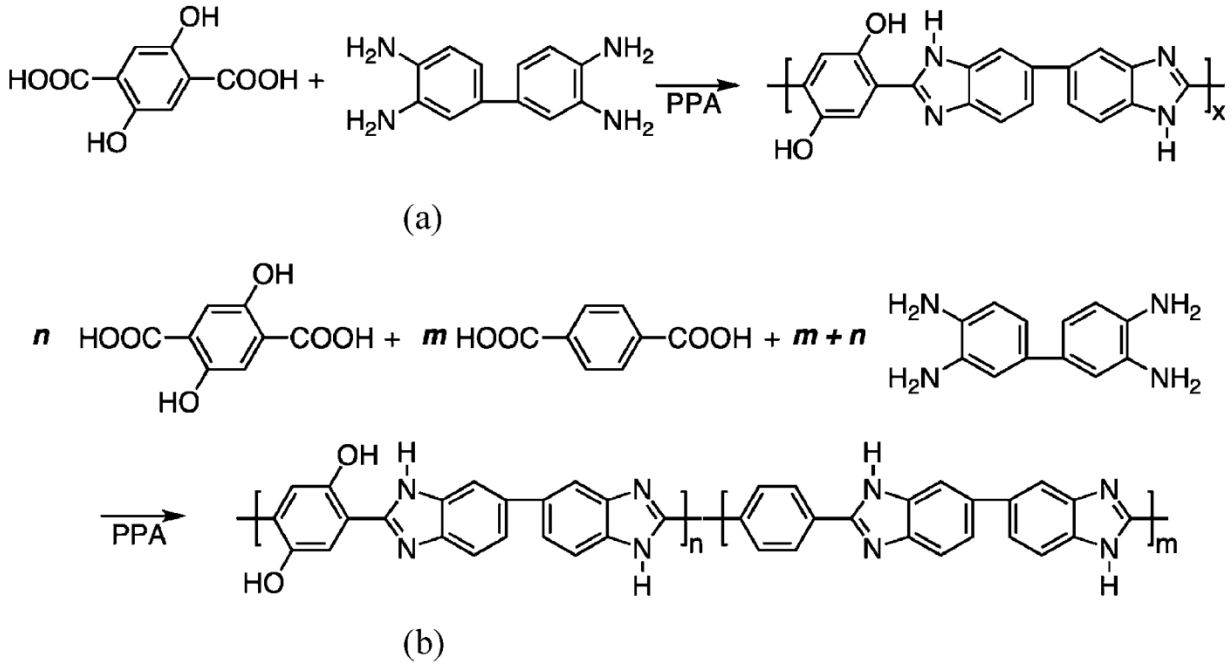

Scheme 2.3 Synthesis of a functionalized polybenzimidazole in poly(phosphoric acid) (PPA) for high-temperature proton exchange membrane fuel cell application.[55] (Reprinted with permission from Yu, S.; Benicewicz, B. C. *Macromolecules* **2009**, *42*, 8640. Copyright(2009) American Chemical Society.)

Although for many years PBI was only used in select niche applications, they are beginning to find significant utilization as proton exchange membranes. By utilizing new synthetic techniques, these materials may find increased prominence commercially in the years to come. Synthesis of these materials in poly(phosphoric acid) allows for flexible membranes

even at high loading levels. These membranes demonstrate extremely good conductivity for utilization in proton exchange membranes.[54,55]

Although the bulk of this chapter focused on some of the more "standard" step-growth polymers, it is clear to see that there is significant interest in finding novel monomers, functionalities, and methods towards synthesizing the step growth polymers of the future. As polymer scientists, we have come a long way since the first industrial step-growth polymers by Carothers. However, there is still a large amount of work to be done in the area of step-growth monomers. As materials needs become increasingly complex, the chemical structures of the polymers required will have to change and evolve to meet those needs.

2.3 References

(1) Carothers, W. H. *Transactions of the Faraday Society* **1936**, *32*, 39.
(2) Coleman, M. M.; Painter, P. C. *Fundamentals of Polymer Science, 2nd Ed.*, 1997.
(3) Odian, G. *Principles of Polymerization, 4th Ed.*, 2004.
(4) Rogers, M. E.; Long, T. E. *Synthetic Methods in Step-Growth Polymers*, 2003.
(5) Tomalia, D. A.; Fréchet, J. M. J. *J. Polym. Sci. Part A: Polym. Chem.* **2002**, *40*, 2719.
(6) June, S. M.; Suga, T.; Heath, W. H.; Lin, Q.; Puligadda, R.; Long, T. E. *J. Adhes.* **2010**, *In Press*.
(7) Lebedeva, E.; Kesler, B. S.; Carter, K. R. *J. Polym. Sci. Part A: Polym. Chem.* **2005**, *43*, 2266.
(8) Astruc, D.; Boisselier, E.; Ornelas, C. T. *Chem. Rev.* **2010**, *110*, 1857.
(9) Buhleier, E.; Wehner, W.; Voegtle, F. *Synthesis* **1978**, 155.
(10) Tomalia, D. A.; Baker, H.; Dewald, J.; Hall, M.; Kallos, G.; Martin, S.; Roeck, J.; Ryder, J.; Smith, P. *Polym. J.* **1985**, *17*, 117.
(11) Hourani, R.; Kakkar, A. *Macromol. Rapid Commun.* **2010**, *31*, 947.
(12) Hunley, M. T.; Harber, A.; Orlicki, J. A.; Rawlett, A. M.; Long, T. E. *Langmuir* **2008**, *24*, 654.
(13) Mather, B. D.; Viswanathan, K.; Miller, K. M.; Long, T. E. *Prog. Polym. Sci.***2006**, *31*, 487.
(14) Oguz, C.; Unal, S.; Long, T. E.; Gallivan, M. A. *Macromolecules* **2007**, *40*, 6529.
(15) Voit, B. *J. Polym. Sci. Part A: Polym. Chem.* **2005**, *43*, 2679.
(16) Voit, B. I.; Lederer, A. *Chem. Rev.* **2009**, *109*, 5924.
(17) Zhou, Y.; Yan, D. *Chem. Commun.* **2009**, 1172.
(18) Kricheldorf, H. R. *Polym. Adv. Technol.* **2002**, *13*, 969.
(19) Kricheldorf, H. R. *Macromol. Rapid Commun.* **2007**, *28*, 1839.
(20) Kricheldorf, H. R. *Acc. Chem. Res.* **2009**, *42*, 981.

(21) Qin, A.; Lam, J. W. Y.; Tang, B. Z. *Chem. Soc. Rev.* **2010**, *39*, 2522.
(22) Rostovtsev, V. V.; Green, L. G.; Fokin, V. V.; Sharpless, K. B. *Angew. Chem. Int. Ed.* **2002**, *41*, 2596.
(23) Kolb, H. C.; Finn, M. G.; Sharpless, K. B. *Angew. Chem. Int. Ed.* **2001**, *40*, 2004.
(24) Himo, F.; Lovell, T.; Hilgraf, R.; Rostovtsev, V. V.; Noodleman, L.; Sharpless, K. B.; Fokin, V. V. *J. Am. Chem. Soc.* **2004**, *127*, 210.
(25) Bernardin, A.; Cazet, A. l.; Guyon, L.; Delannoy, P.; Vinet, F. O.; Bonnaffé, D.; Texier, I. *Bioconjugate Chem.* **2010**, *21*, 583.
(26) Fournier, D.; Hoogenboom, R.; Schubert, U. S. *Chem. Soc. Rev.* **2007**, *36*, 1369.
(27) Franc, G.; Kakkar, A. K. *Chem. Soc. Rev.* **2010**, *39*, 1536.
(28) Gandini, A.; Coelho, D.; Silvestre, A. J. D. *Eur. Polym. J.* **2008**, *44*, 4029.
(29) Gandini, A.; Silvestre, A. J. D.; Coelho, D. *J. Polym. Sci. Part A: Polym. Chem.* **2010**, *48*, 2053.
(30) Golas, P. L.; Matyjaszewski, K. *Chem. Soc. Rev.* **2010**, *39*, 1338.
(31) Johnson, J.; Koberstein, J. T.; Turro, N. J.; US41270, 2008, p 53
(32) Johnson, J. A.; Baskin, J. M.; Bertozzi, C. R.; Koberstein, J. T.; Turro, N. J. *Chem. Commun.* **2008**, 3064.
(33) Johnson, J. A.; Finn, M. G.; Koberstein, J. T.; Turro, N. J. *Macromolecules* **2007**, *40*, 3589.
(34) Kappe, C. O.; Van der Eycken, E. *Chem. Soc. Rev.* **2010**, *39*, 1280.
(35) Nagao, Y.; Takasu, A. *Macromol. Rapid Commun.* **2009**, *30*, 199.
(36) Polaske, N. W.; McGrath, D. V.; McElhanon, J. R. *Macromolecules* **2009**, *43*, 1270.
(37) Sumerlin, B. S.; Vogt, A. P. *Macromolecules* **2009**, *43*, 1.
(38) van Dijk, M.; Rijkers, D. T. S.; Liskamp, R. M. J.; van Nostrum, C. F.; Hennink, W. E. *Bioconjugate Chem.* **2009**, *20*, 2001.
(39) Scheel, A. J.; Komber, H.; Voit, B. I. *Macromol. Rapid Commun.* **2004**, *25*, 1175.
(40) van Steenis, D. J. V. C.; David, O. R. P.; van Strijdonck, G. P. F.; van Maarseveen, J. H.; Reek, J. N. H. *Chem. Commun.* **2005**, 4333.
(41) Xie, J.; Hu, L.; Shi, W.; Deng, X.; Cao, Z.; Shen, Q. *J. Polym. Sci., Part B: Polym. Phys.* **2008**, *46*, 1140.
(42) Xie, J.; Hu, L.; Shi, W.; Deng, X.; Cao, Z.; Shen, Q. *Polym. Int.* **2008**, *57*, 965.
(43) Qin, A.; Lam, J. W. Y.; Jim, C. K. W.; Zhang, L.; Yan, J.; Häussler, M.; Liu, J.; Dong, Y.; Liang, D.; Chen, E.; Jia, G.; Tang, B. Z. *Macromolecules* **2008**, *41*, 3808.
(44) Wu, P.; Feldman, A. K.; Nugent, A. K.; Hawker, C. J.; Scheel, A.; Voit, B.; Pyun, J.; Fréchet, J. M. J.; Sharpless, K. B.; Fokin, V. V. *Angew. Chem. Int. Ed.* **2004**, *43*, 3928.
(45) Joralemon, M. J.; O'Reilly, R. K.; Matson, J. B.; Nugent, A. K.; Hawker, C. J.; Wooley, K. L. *Macromolecules* **2005**, *38*, 5436.
(46) Nagao, Y.; Takasu, A. *J. Polym. Sci. Part A: Polym. Chem.* **2010**, *48*, 4207.
(47) Chae, K. J.; Choi, M.; Ajayi, F. F.; Park, W.; Chang, I. S.; Kim, I. S. *Energy Fuels* **2008**, *22*, 169.
(48) Li, Q.; He, R.; Jensen, J.; Bjerrum, N. *Fuel Cells* **2004**, *4*, 147.
(49) Li, Q.; Jensen, J. O.; Savinell, R. F.; Bjerrum, N. J. *Prog. Polym. Sci.* **2009**, *34*, 449.
(50) Logan, B. E.; Hamelers, B.; Rozendal, R.; Schroder, U.; Keller, J.; Freguia, S.; Aelterman, P.; Verstraete, W.; Rabaey, K. *Environ. Sci. Technol.* **2006**, *40*, 5181.
(51) Minteer, S. D.; Liaw, B. Y.; Cooney, M. J. *Curr. Opin. Biotechnol.* **2007**, *18*, 228.
(52) Oh, S. E.; Logan, B. E. *Appl. Microbiol. Biotechnol.* **2006**, *70*, 162.

(53) Varcoe, J. R.; Slade, R. C. T. *Fuel Cells* **2005**, *5*, 187.
(54) Xiao, L.; Zhang, H.; Scanlon, E.; Ramanathan, L. S.; Choe, E.-W.; Rogers, D.; Apple, T.; Benicewicz, B. C. *Chem. Mater.* **2005**, *17*, 5328.
(55) Yu, S.; Benicewicz, B. C. *Macromolecules* **2009**, *42*, 8640.
(56) Narita, T.; Ohtakeyama, R.; Nishino, M.; Gong, J. P.; Osada, Y. *Colloid. Polym. Sci.* **2000**, *278*, 884.
(57) Wahlund, P. O.; Izumrudov, V. A.; Gustavsson, P. E.; Larsson, P. O.; Galaev, I. Y. *Macromol. Biosci.* **2003**, *3*, 404.
(58) Zelikin, A. N.; Akritskaya, N. I.; Izumrudov, V. A. *Macromol. Chem. Phys.* **2001**, *202*, 3018.
(59) Zelikin, A. N.; Litmanovich, A. A.; Paraschuk, V. V.; Sybatchin, A. V.; Izumrudov, V. A. *Macromolecules* **2003**, *36*, 2066.
(60) Zelikin, A. N.; Putnam, D.; Shastri, P.; Langer, R.; Izumrudov, V. A. *Bioconjugate Chem.* **2002**, *13*, 548.
(61) Williams, S. R.; Long, T. E. *Prog. Polym. Sci.* **2009**, *34*, 762.
(62) Layman, J. M.; Borgerding, E. M.; Williams, S. R.; Heath, W. H.; Long, T. E. *Macromolecules* **2008**, *41*, 4635.
(63) Williams, S. R.; Barta, Z.; Ramirez, S. M.; Long, T. E. *Macromol. Chem. Phys.* **2009**, *210*, 555.
(64) Williams, S. R.; Borgerding, E. M.; Layman, J. M.; Wang, W.; Winey, K. I.; Long, T. E. *Macromolecules* **2008**, *41*, 5216.
(65) Williams, S. R.; Salas-de la Cruz, D.; Winey, K. I.; Long, T. E. *Polymer* **2010**, *51*, 1252.
(66) Gibbs, C. F.; Littmann, E. R.; Marvel, C. S. *J. Am. Chem. Soc.***1933**, *55*, 753.
(67) Tant, M. R.; Mauritz, K. A.; Wilkes, G. L.; Editors *Ionomers: Synthesis, Structure, Properties and Applications*, 1997.
(68) Mather, B. D.; Miller, K. M.; Long, T. E. *Macromol. Chem. Phys.* **2006**, *207*, 1324.
(69) Mather, B. D.; Williams, S. R.; Long, T. E. *Macromol. Chem. Phys.* **2007**, *208*, 1949.
(70) Ozturk, G.; Long, T. E. *J. Polym. Sci. Part A: Polym. Chem.* **2009**, *47*, 5437.
(71) Williams, S. R.; Lepene, B. S.; Thatcher, C. D.; Long, T. E. *Biomacromolecules* **2009**, *10*, 155.
(72) Williams, S. R.; Mather, B. D.; Miller, K. M.; Long, T. E. *J. Polym. Sci. Part A: Polym. Chem.* **2007**, *45*, 4118.
(73) Williams, S. R.; Miller, K. M.; Long, T. E. *Prog. React. Kinet.***2007**, *32*, 165.
(74) Yamauchi, K.; Lizotte, J. R.; Long, T. E. *Macromolecules* **2002**, *35*, 8745.
(75) June, S. M.; Long, T. E. *Unpublished Results* **2010**.
(76) Goussé, C.; Gandini, A. *Polym. Bull.***1998**, *40*, 389.
(77) Laita, H.; Boufi, S.; Gandini, A. *Eur. Polym. J.***1997**, *33*, 1203.
(78) Murphy, E. B.; Bolanos, E.; Schaffner-Hamann, C.; Wudl, F.; Nutt, S. R.; Auad, M. L. *Macromolecules* **2008**, *41*, 5203.
(79) Veldman, B.; Kaully, T.; Feller, R. K.; Falcao, E.; Wudl, F. *Macromolecules* **2009**, *42*, 6848.
(80) Harrison, W. L.; Hickner, M. A.; Kim, Y. S.; McGrath, J. E. *Fuel Cells* **2005**, *5*, 201.

Chapter 3: Light-induced Building Blocks: Photocoupling and Photodegradation to Assemble and Disassemble Macromolecules

Stephen M. June and Timothy E. Long
Department of Chemistry
Virginia Tech
Blacksburg, VA 24060

(From: Manuscript in preparation)

3.1 Abstract

Within polymer science, an increasing trend towards the synthesis of photoactive polymers exists. Many photoactive polymers undergo photocleavages or rearrangements, often pendant to the polymer chain, resulting in smart properties. Furthermore, utilization of photopolymerization of chain-growth monomers commonly allows for the preparation of thin films. A much smaller branch of photoactive macromolecules includes assembly or disassembly of macromolecules upon exposure to UV-light, particularly either in the backbone of the polymer, or the formation of cross-links using methods other than free-radical addition. This review primarily focuses primarily on these photoactive polymers. Although many chromophores exist for the assembly and disassembly of macromolecules, a select few comprise the bulk of the literature: cyclobutane diimides, coumarins, cinnamates, thymines, and *o*-nitro benzyl esters. The synthesis of these compounds and their derivatives occurs easily, and they exhibit good control over the extent of photoreaction, either based on wavelength, total UV exposure, or chromophore concentration. Therefore, this review focuses on these chromophores and their utility.

3.2 Introduction

There is an increasing interest in stimuli-responsive or smart polymers, with these materials finding utility in a variety of fields, such as drug-delivery,[1,2] sensors,[3] lithography,[4-13] and self-assembly.[14-25] Smart polymers undergo a dramatic property change with a small change in environment,[26-33] such as the variation of pH, temperature, solvent polarity, solvent ionic strength, and exposure to UV.[4,26-33] This review focuses on smart polymers that respond to UV exposure in a dramatic manner.

There are several types of photoactive smart polymers. For the purposes of this review, three primary classifications of photoactive polymers exist: smart polymers where the chromophore, and as such the photocleavage or assembly is pendant to the polymer chain, and not between macromolecules,[34] smart polymers where free-radical chain-addition across an olefinic double bond results in the photoassembly,[4,35,36] and smart polymers where the chromophore assembly or disassembly either forms or cleaves within the backbone of a macromolecule, or forms or cleaves a cross-link between polymer chains. The first two classes are well established in the literature and extensive reviews exist elsewhere. For this reason, the third classification provides the focus of this review.

The primary discussion of this review will focus on several common photolinkers: coumarin derivatives,[2,24,37-42] cinnamate derivatives,[36,43,44] thymine derivatives,[1,45-47] and *o*-nitro benzyl esters, amides, and ethers.[6-11,13,21,34,48-62] With the notable exception of the *o*-nitro benzyl compounds, these photolinkers exhibit reversibility based on the wavelength of UV exposure. These chromophores routinely find utility either within the backbone of polymers, or as pendant groups for photocrosslinking.

3.3 Utilization of coumarin functionality for assembly and disassembly of polymers

The first synthesis and isolation of coumarin occurred in the 1820's. Coumarin also possesses over 800 natural derivatives.[42] It undergoes a photoaddition at ca. 280 nm and will photocleave back to the original coumarin moiety at ca. 250 nm of UV irradiation. The dimer formed from the photocoupling has four possible isomers, shown in **Figure 3.1**.[42] The majority of coumarin derivatives possess a hydroxyl functional group at one of the carbon positions. In particular, a vast majority of these derivatives are directly linked to a hydroxyl group at the 7 position. For this reason, 7-hydroxycoumarin is a common starting material for the formation of coumarin-functionalized photoreactive macromolecules.[42] Trenor and Long published excellent review of coumarins in polymers in 2004,[42] and thus the discussion here is limited to work performed in the Long group and others published since 2004.

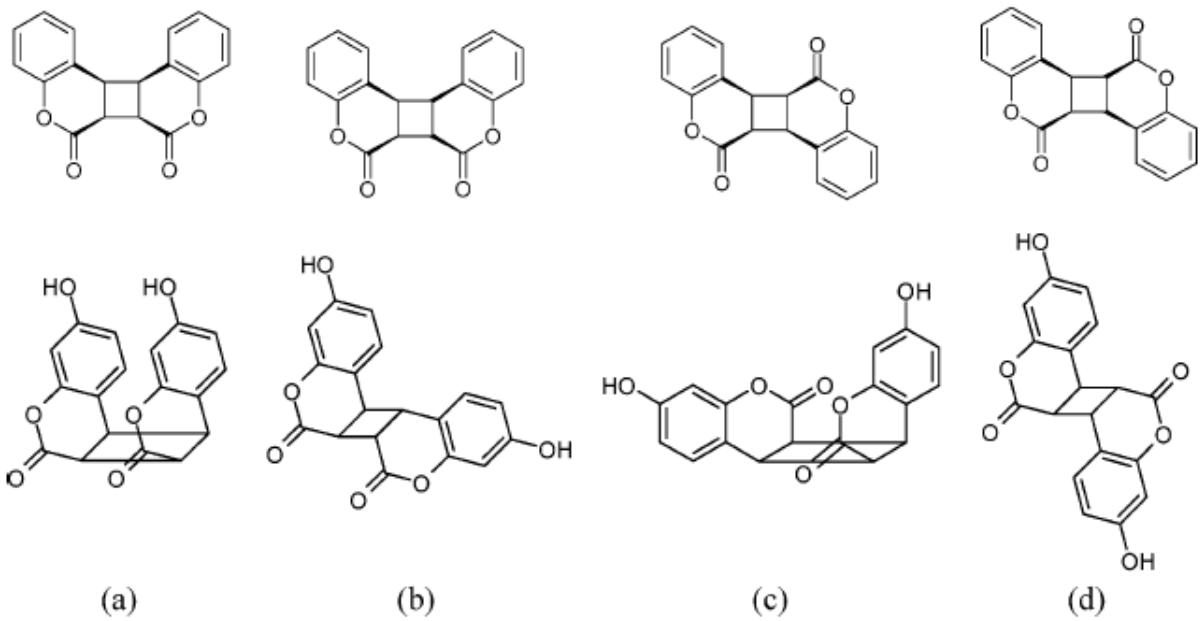

Figure 3.1 Isomers of the coumarin dimer, with a) representing the head-to-head syn addition, b) representing the head-to-head anti addition, c) representing the head-to-tail syn addition, and d) representing the head-to-tail anti addition.[42] (Reprinted with permission from Trenor, S. R.; Shultz, A. R.; Love, B. J.; Long, T. E. *Chem. Rev*. **2004**, 104, 3059. Copyright(2004) American Chemical Society.)

There has been a significant amount of research performed in our group on coumarin-containing polymers. In particular; Trenor, Long and coworkers published the synthesis and characterization of a photoreversible adhesive utilizing coumarin functionality.[40] The authors synthesized a pressure sensitive adhesive (PSA) copolymer containing 2-ethyl hexyl acrylate and hydroxyethyl acrylate. Further partial functionalization with an acyl chloride derivative of 7-hydroxycoumarin yielded polyacrylates with pendant coumarin functional groups as a reversibly crosslinkable PSA.[40]

UV-visible spectroscopy, gel-fraction analysis, and peel testing provided a method for characterization of this reversible PSA after UV exposure. **Scheme 3.1** demonstrates functionalization of the PSA copolymer with coumarin functionality and the subsequent photoreversible coupling of these polymers with UV light. **Figure 3.2** illustrates the peel strength loss as a function of UVA (cross-linking) and some regeneration of peel strength with exposure to UVC (photocleavage) on the left, and a plot of coumarin consumption as determined with UV-visible spectroscopy, gel fraction data as obtained with a soxhlet extraction, and peel strength, all as a function of UVA exposure.[40]

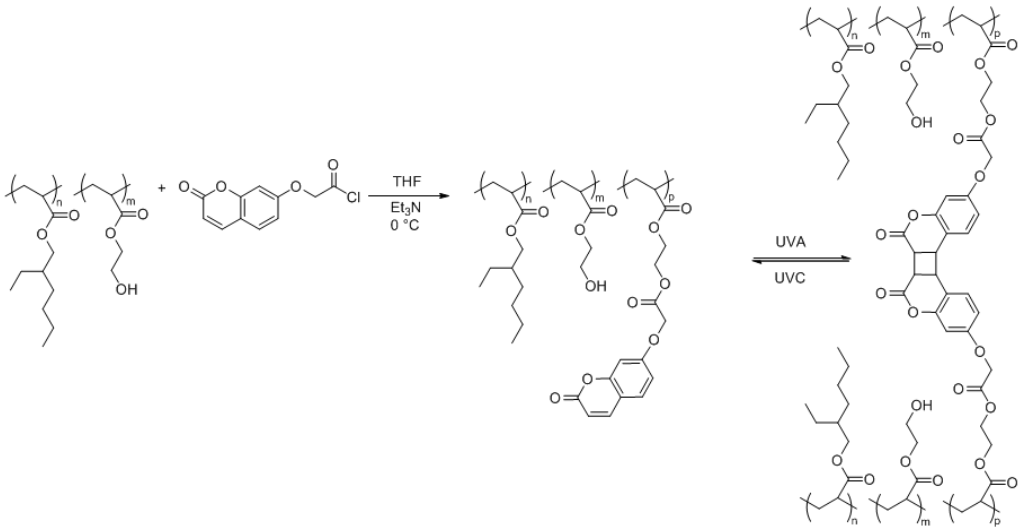

Scheme 3.1 Functionalization of PSA copolymer with acyl halide functionalized 7-hydroxy coumarin and subsequent reversible photocrosslinking of the obtained terpolymer.[40] (Reprinted

from "Trenor, S. R.; Long, T. E.; Love, B. J. *J. Adhes.* **2005**, 81, 213." with permission from Taylor and Francis publishing company.)

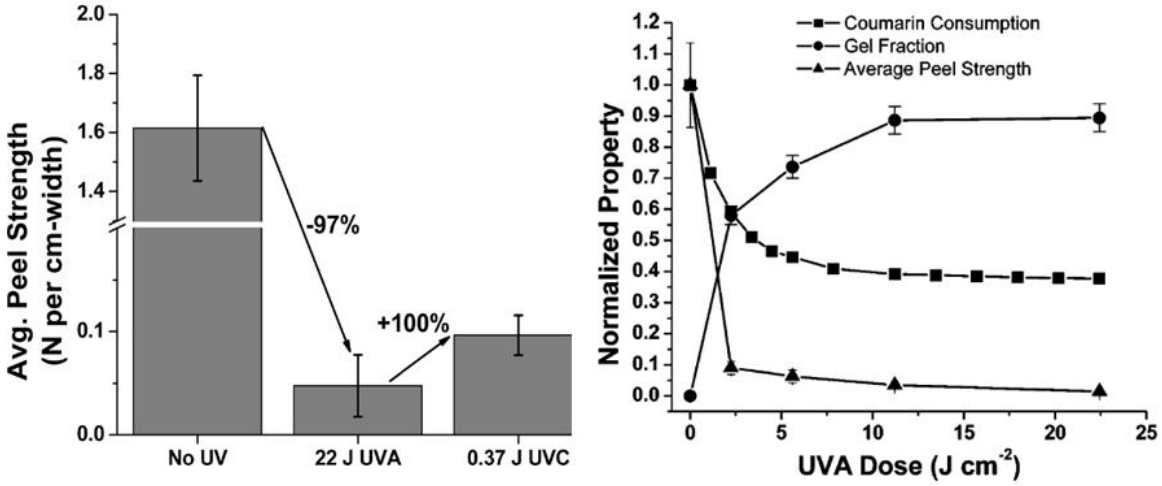

Figure 3.2 (On left) Plot of decrease in peel strength of coumarin functionalized PSA with exposure to UVA. Upon exposure of the photocrosslinked terpolymer to UVC light, the polymer regenerates some of its adhesive properties. (On right) Plot of coumarin consumption, gel fraction, and peel strength as a function of UVA dose.[40] (Reprinted from "Trenor, S. R.; Long, T. E.; Love, B. J. *J. Adhes*. **2005**, 81, 213." with permission from Taylor and Francis publishing company.)

In a paper similar to the photoreversible PSA paper referenced above, Trenor, Long, and coworkers also demonstrated the synthesis and characterization of a photoreversible chain extension of poly(ethylene glycol) (PEG). In this paper, the authors end-capped hydroxy-terminated poly(ethylene glycol) with the same acyl halide functionalized 7-hydroxy coumarin from the PSA manuscript.[40] Casting the coumarin functionalized PEG from either THF or $CHCl_3$ and drawing to controlled thickness using a doctor blade yielded films suitable for UV exposure. Upon irradiation, the coumarin-terminated macromonomer polymerized further to form chain-extended PEG polymers.[39]

Figure 3.3 demonstrates the synthesis of the photochain extended PEG and a plot of coumarin UV absorbance (which correlates to coumarin consumption, and thus PEG chain-extended molecular weight) as a function of UV irradiation. Three cycles of reversible chain extension, with chain-extension accomplished with UVA and photocleavage of the coumarin dimer units accomplished with UVC further confirmed the potential for photoreversible adhesive properties suggested in the PSA paper referenced earlier.[39]

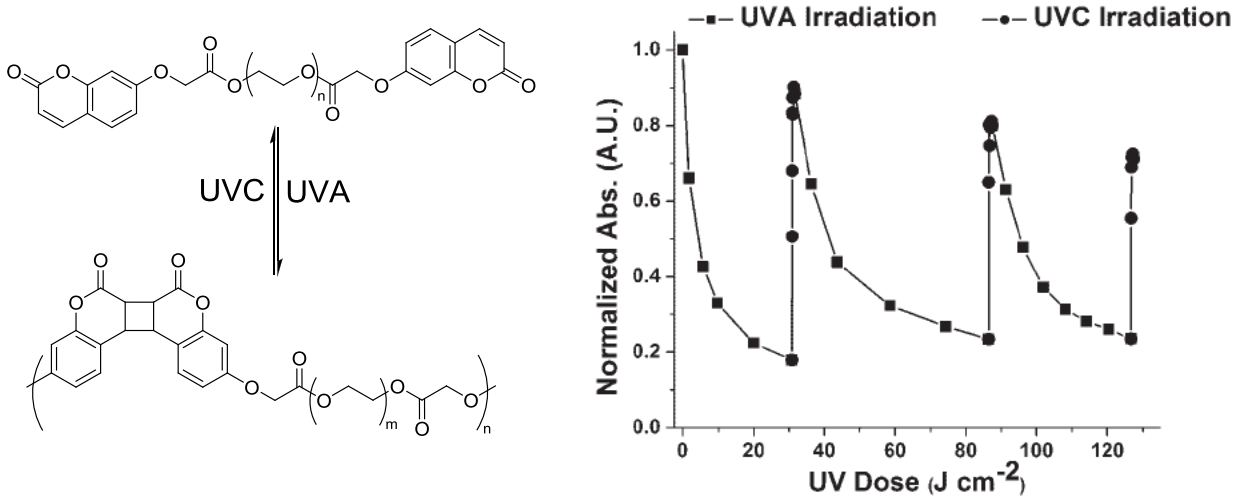

Figure 3.3 Scheme of photochain extension of coumarin-terminated PEG and plot demonstrating coumarin absorbance as a function of UV dose demonstrating photoreversibility of coumarin dimerization.[39] (Reprinted with permission from Trenor, S. R.; Long, T. E.; Love, B. J. *Macromol. Chem. Phys.* **2004**, *205*, 715.)

Huyck, Long, and coworkers published a paper detailing the synthesis of a series of photocross linkable coumarin-containing polymers utilizing methods similar to the Trenor papers referenced above.[38] This study analyzed of the effect of differing polymer compositions. In particular, copolymerization of hydroxy ethyl acrylate with varying alkyl acrylates and methacrylates and subsequent functionalization with coumarin resulted in a series of polymers with varying thermomechanical properties. All resulting polymers were exposed to UV light and in many cases high gel fractions resulted from exposure to UVA. However, those polymers with

higher glass transitions temperatures did not exhibit sufficient mobility to obtain efficient conversion of the coumarin monomer to form the coumarin dimer and yield high crosslink density.[38]

Figure 3.4 demonstrates UV/visible spectra of coumarin-containing alkyl acrylate copolymers with arrows indicating increasing UVA exposure. The peak at ca. 320 nm that decreases with UV exposure indicates coumarin monomer consumption with exposure to UV. The peak at ca. 250 nm represents formation of the coumarin dimer with UV exposure. This method for the synthesis of photocrosslinked polymers offered many advantages as there was no observed dependence of UV intensity towards coumarin consumption. Restated, this system demonstrated no difference between low intensity light for an extended time period relative to high intensity light for a shorter time period, assuming total exposure was the same. This is not the case for typical acrylics cured with a photoinitiator, as these systems often exhibit a dependence on UV intensity.[38]

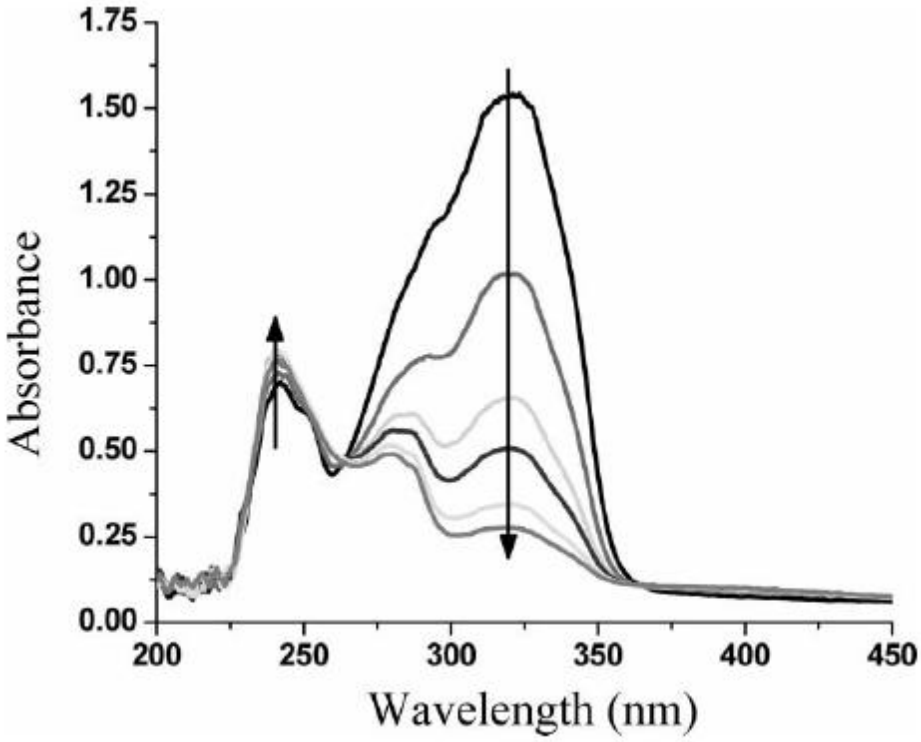

Figure 3.4 UV/visible spectra of coumarin containing alkyl acrylate copolymer. Arrow direction indicates increasing UV exposure.[38] (Reprinted from "Huyck, R. H.; Trenor, S. R.; Love, B. J.; Long, T. E. *J. Macromol. Sci., Part A: Pure Appl. Chem.* **2008**, 45, 9." with permission from Taylor and Francis publishing company.)

In 2008, Kim, Hampp, and coworkers published the synthesis and characterization of a coumarin dimer diol for utility as a photocleavable linker in drug-delivery applications.[2] One of the primary concerns addressed within this paper was the fear that ambient light may cause cleavage of the coumarin dimer and subsequent delivery of the drug prior to the desired timeframe. Based on two simultaneous studies with a single photon and dual photon absorption photocleavage of the coumarin dimer, the authors concluded that undesired photocleavage of the coumarin dimer required ca. 16 years of uninterrupted sunlight. However, upon exposure to high intensity UV light, rapid and nearly quantitative photocleavage occured.[2]

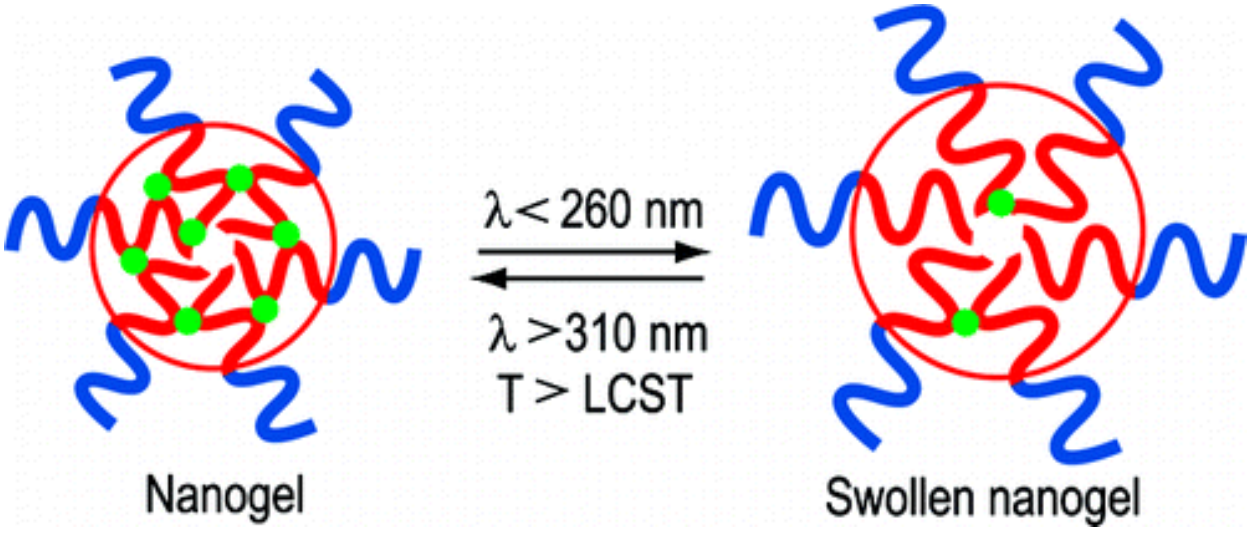

Figure 3.5 Phototailorable cross-link density and swellability of a coumarin containing cross-linked micelle.[37] (Reprinted with permission from He, J.; Tong, X.; Zhao, Y. *Macromolecules* **2009**, 42, 4845. Copyright(2009) American Chemical Society.)

Zhao and coworkers recently published several papers on the synthesis of photocrosslinkable micelles and nanogels utilizing coumarin functionality.[24,37,63] The authors synthesized an amphiphilic block copolymer comprising of one hydrophobic block and one

hydrophilic block. The hydrophobic block contained the coumarin functionality. Upon micelle formation, the solution was exposed to UV light, such that the coumarin units dimerized, thus stabilizing the micelle, and crosslinking it. By tailoring light intensity and dosage, the authors were able to tailor the crosslink density, and thus the swellability of the nanogel. **Figure 3.5** demonstrates this concept.[37]

3.4 Cyclobutane diimide-containing photoreactive polymers

As early as the late 1980's, cyclobutane diimide functionality within a polyimide backbone found utilization in photoreactive polymers.[12,64,65] In most cases, the primary monomer utilized for the formation of the chromophore within the polymer is 1,2,3,4-cyclobutane tetracarboxylic dianhydride (CBDA). The photodimerization of maleic anhydride at ca. 280 nm of UV exposure allows for the simple preparation of this monomer. Although this photocycloadditon results in two potential isomers, the primary isomer obtained is the trans-anti addition monomer, forming a nearly planar cyclobutane unit.

Moore and coworkers first reported the synthesis of polyimides using CBDA and their subsequent photodegradation in 1988.[12] The authors synthesized the homopolymer of CBDA and oxydianiline using standard polyimide reaction techniques. Solution casting the intermediate poly(amic acid) into a film, and subsequent thermal curing yielded the corresponding polyimide. The polyimide was then exposed to UV light with a SiO_2 masking agent covering portions of the film at a wavelength of 254 nm. After every exposure, the sample was washed with organic solvents such as DMAc and carefully dried. **Figure 3.6** includes a plot of the weight % of remaining polyimide film as a functionalization of UV dose. It is clear that photocleavage of the cyclobutane diimide unit left behind soluble residues which were then washed off of the surface

of the film. **Figure 3.6** also includes a micrograph of the masked sample after photodegradation, providing visual confirmation of degradation.[12]

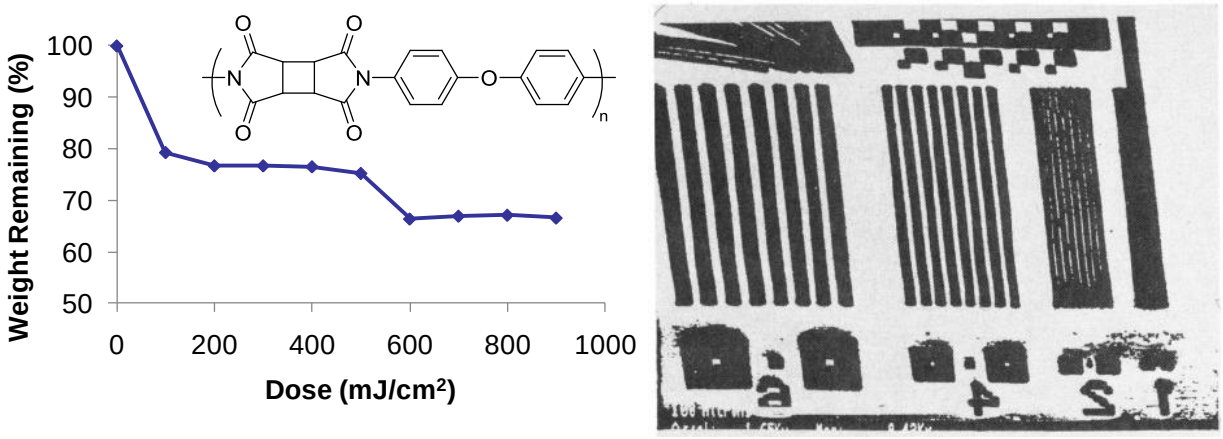

Figure 3.6 Weight remaining of photoactive polyimide as a function of UVC dose and micrograph of masked sample after UV exposure.[12] (Reprinted with permission from Moore, J. A.; Dasheff, A. N. *Chem. Mater.* **1989**, 1, 163. Copyright(1989) American Chemical Society.)

Utilizing techniques such as those described in Moore's work, as well as McGrath and coworkers' work describing the synthesis of dispersible poly(siloxane imides),[66-72] Long and coworkers developed a dispersible photoactive CBDA-containing poly(siloxane imide).[65] This polymer exhibited dispersibility in organic solvents and displayed elastomeric properties. AFM confirmed micro-phase separation of the resulting polymer, and ^{1}H NMR confirmed growth of the maleimide proton resonance, suggesting photodegradation of the cyclobutane diimide functionality in the backbone of the polymer upon exposure to narrow 254 nm UV irradiation.[65]

An observed spontaneous photopolymerization of maleimides when exposed to UVB and UVA irradiation required utilization of narrow-band UV light at 254 nm. This photopolymerization of the formed bismaleimides (f=4) upon photocleavage of the CBDA units resulted in crosslinked films. Decker and coworkers demonstrated similar spontaneous photoinduced homopolymerization of bismaleimides, confirming this conclusion. Fortunately, maleimides do not absorb at 254 nm, and thus, effective photocleavage in the absence of crosslinking occurred at 254 nm. **Scheme 3.2** demonstrates the synthesis of these photoactive

poly(siloxane imides) and **Figure 3.7** demonstrates the formation of peaks corresponding to maleimide functionality with increasing exposure of the CBDA-containing poly(siloxane imides) to UV light, suggesting the photodegradation of these poly(siloxane imides).[65]

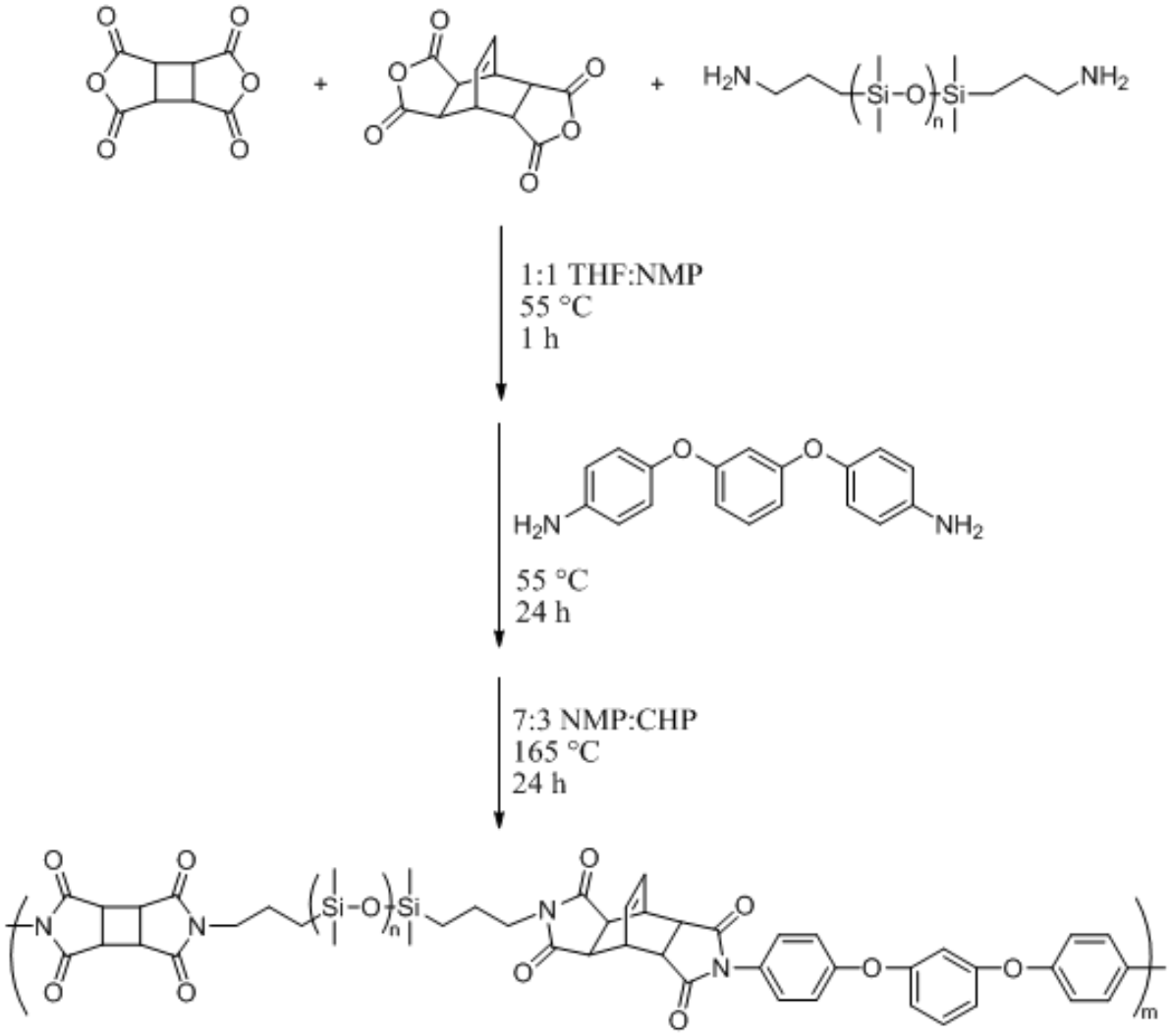

Scheme 3.2 Synthesis of photoactive CBDA-containing poly(siloxane imides) by thermal solution imidization.[65] (Reprinted from "June, S. M.; Suga, T.; Heath, W. H.; Long, T. E.; Lin, Q.; Puligadda, R. *The Journal of Adhesion* **2010,** 86, (10), 1012 – 1028" with permission from Taylor and Francis publishing company.)

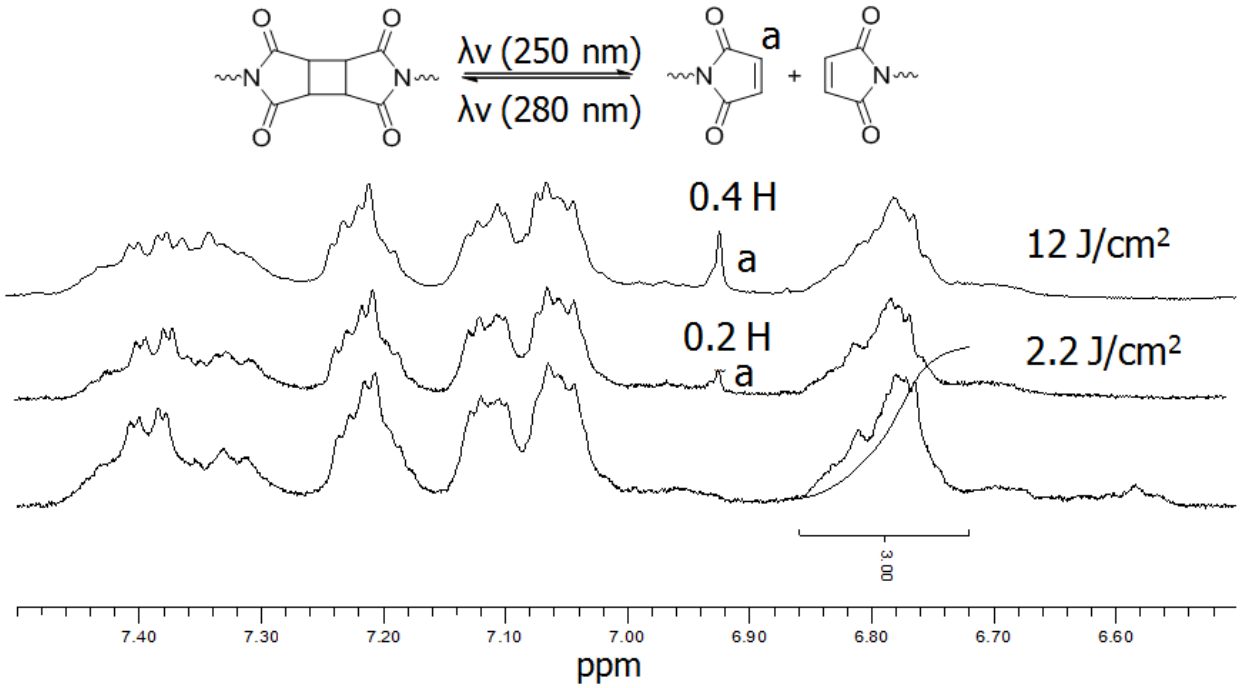

Figure 3.7 ^{1}H NMR confirming the formation of maleimide functionality in photoreactive CBDA-containing poly(siloxane imides) which suggests photodegradation of the cyclobutane diimide unit with UVC exposure.[65] (Reprinted from "June, S. M.; Suga, T.; Heath, W. H.; Long, T. E.; Lin, Q.; Puligadda, R. *The Journal of Adhesion* **2010,** 86, (10), 1012 – 1028" with permission from Taylor and Francis publishing company.)

3.5 Photoreactive polymers containing cinnamate functionality for polymeric assembly and disassembly

Another chromophore that received recent attention in the literature is the cinnimate functional group,[36,43,44] although reports dating back to the mid-1950's detail the photocyclicization of cinnamic acid derivatives.[76] Cinnamic acid and corresponding cinnamates, cinnamaldehydes, and other cinnamic acid derivatives are well known in organic chemistry for their ability to dimerize in a [2 + 2] cycloaddition. Several papers discuss the employment of this dimerization towards the formation and disassociation of macromolecules.

Our group recently published several papers utilizing esters and amides of cinnamic acid. Cashion, Long, and coworkers demonstrated the effective synthesis of PSAs containing cinnamate functionality.[43] This study analyzed the influence of hydrogen bonding on UV-

curable acrylic PSAs. The authors synthesized a copolymer of hydroxyethyl acrylate and 2-ethyl hexyl acrylate. Partial functionalization with hexane isocyanate to form the corresponding urethane linkage, followed with subsequent functionalization with cinnamoyl chloride yielded UV-curable PSAs. The synthesis of PSAs where the functionalization with cinnamoyl chloride matched the urethane polymers, but the remaining hydroxy ethyl acrylate units were unfunctionalized (instead of functionalized with hexane isocyanate) yielded suitable controls.[43] The authors confirmed a synergistic relationship between hydrogen bonding functionality and photocurable functionality. As with the Trenor PSA coumarin paper, an increase in chromophore consumption, and thus crosslink density decreased the peel strength of the PSA. However, those samples which possessed urethane hydrogen-bonding capabilities retained more peel strength than those that possessed only hydroxyethyl acrylate units.[43]

Williams, Long, and coworkers also developed photochain extendable and photocrosslinkable ammonium ionenes.[36] The reaction of 11-bromundecanol with cinnamoyl chloride yielded 11-bromundecyl cinnamate which was used as an end-capping reagent for the formation of cinnamate terminated 12,12-ammonium ionenes. Solution casting yielded ionomer films suitable for UV-exposure experiments. The authors observed a dramatic increase in glass transition, as well as enhanced tensile properties in comparison to the non-chain extended ammonium ionenes. SEC traces demonstrated peak broadening and a shift to lower elution volumes, indicating an increase in molecular weight.[36]

Figure 3.8 demonstrates the synthesis of a photocrosslinkable ammonium ionene using the reaction of tert-butyl bis(3-(dimethylamino)propyl)carbamate (bocDMPC) and N,N-bis(3-(dimethylamino)propyl) cinnamamide (cinDMPC) with 1,12-dibromododecane in a 9:1:10 ratio. Spin-coating onto a quartz slide and subsequent irradiation with UV light resulted in crosslinked

ionene networks. UV/visible spectroscopy demonstrated a decrease in the cinnamate absorbance with increasing UV exposure, indicating efficient crosslinking. Furthermore, soxhlet extraction of the resulting film confirmed high gel fractions up UV irradiation.[36]

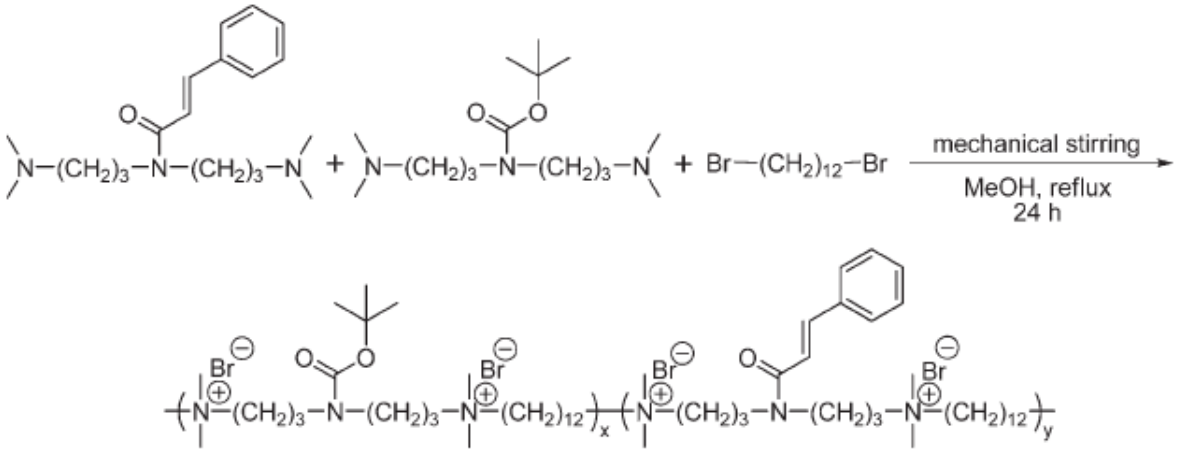

Figure 3.8 Synthesis of a photocrosslinkable ammonium ionene containing cinnamate units pendant to the backbone of the polymer.[36] (Reprinted with permission from Williams, S. R.; Barta, Z.; Ramirez, S. M.; Long, T. E. *Macromol. Chem. Phys.* **2009**, 210, 555.)

Leblanc and coworkers also published a paper using nitro-cinnamate functionality for reversible crosslinking.[44] The authors demonstrated the functionalization of polymeric gelatin with cinnamate for utilization as a synthetic scaffold. This method proved advantageous due to the ability to include a biodegradable site within the cross-link site, allowing for eventual solubility of the polymeric gelatin and subsequent removal from the body. ^{1}H NMR and UV/visible spectroscopy confirmed the photoreaction and extent of conversion. Swellability of the cross-linked structure was dependent on ionic strength, cross-link density due to varying UV exposures, and cross-link density due to varying extents of nitro-cinnamate functionality. **Figure 3.9** outlines the synthesis and subsequent cross-linking of the nitro-cinnamate functionalized gelatin.[44]

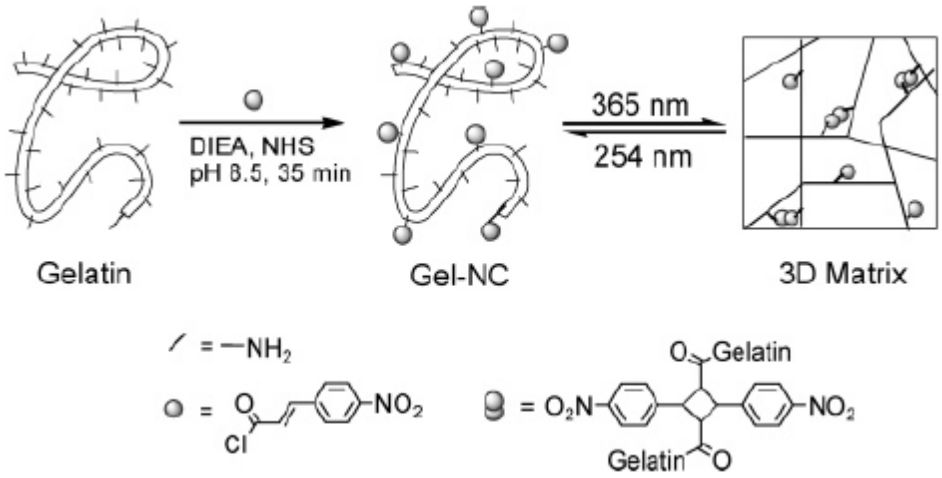

Figure 3.9 Synthesis and subsequent cross-linking of nitro-cinnamate functionalized gelatin.[44] (Reprinted with permission from Gattas-Asfura, K. M.; Weisman, E.; Andreopoulos, F. M.; Micic, M.; Muller, B.; Sirpal, S.; Pham, S. M.; Leblanc, R. M. *Biomacromolecules* **2005**, *6*, 1503. Copyright(2005) American Chemical Society.)

Other photoreactive structural analogues of cinnamic acid also exist. In particular, urocanic acid differs from cinnamic acid only in that the aromatic ring attached to the olefinic double bond is an imidazole (attached at the 4 position) rather than a phenyl group. Urocanic acid and its esters will also undergo reversible [2+2] photodimerization when exposed to UV light. It is of potential future interest to investigate the differences in structure-property relationships between cinnamate functionalized polymers and urocanate functionalized polymers.

3.6 Thymine functionalized photoreversible polymers

One of the primary photoinduced damages to DNA involves the dimerization of thymine units within the backbone of DNA. The body contains several repair mechanisms for this UV-induced dimerization, as DNA cannot replicate when in the dimerized state.[1] Many manuscripts established this topic in the literature, and adequately covered it in many published papers. Therefore, for the purposes of this review, only a brief overview on thymine dimerization occurs.

As with cyclobutane diimide, cinnamic acid derivatives, and coumarin derivatives, the photodimerization of thymine is a [2+2] cycloaddition, and is therefore thermally not allowed, but only photoallowed. Zinth, Kohler, and coworkers recently investigated the kinetics of the thymine dimerization using femptosecond time-resolved infrared spectroscopy. The study focused on poly(deoxynucleotide) where the thymine units acted as the nucleobase on every repeat unit, allowing for maximum association of thymine, and faster reaction times.[1]

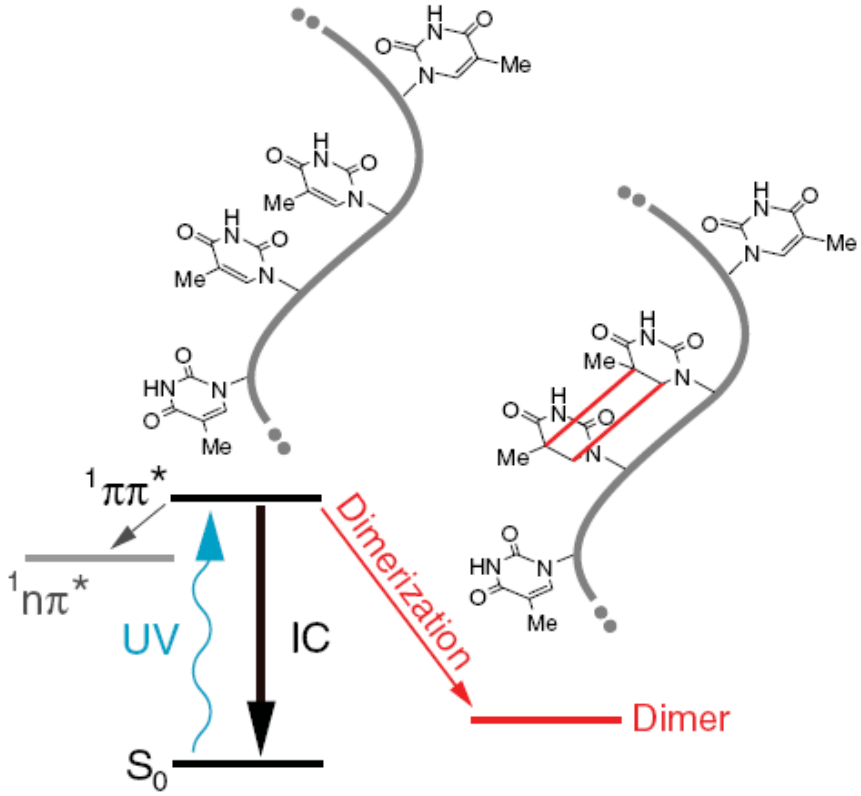

Figure 3.10 Ultrafast dimerization of thymine on an all-thymine deoxy oligonucleotide.[1] (From Schreier, W. J.; Schrader, T. E.; Koller, F. O.; Gilch, P.; Crespo-Hernandez, C. E.; Swaminathan, V. N.; Carell, T.; Zinth, W.; Kohler, B. *Science* **2007**, *315*, 625. Reprinted with permission from AAAS.)

The authors determined that upon exposure to UV light, the dimerization of thymine occurs as quickly as ca. 1 picosecond. The conditions utilized within this manuscript, where thymine is on every unit, allowed for a maximum number of favorable confirmations for

dimerization, likely increasing the reaction rate. The thymine dimerization typically exhibits a low quantum yield, but the authors suggest that the low concentration of thymine and therefore the lack of thymine-thymine conformations acceptable for the formation of the dimer explains these results. **Figure 3.10** outlines the formation of the thymine-thymine dimer upon exposure to UV light.[1]

Saito, Warner, and coworkers recently published the synthesis of core-bound polymer micelles based on the photodimerization of thymine.[47] The authors synthesized a diblock copolymer of sulfonated polystyrene and vinylbenzyl thymine using nitroxide mediated polymerization. This amphiphilic block copolymer formed micelles in solution, and subsequently photocrosslinked the thymine units to form stable micelles. Spectroscopic measurments, as well as transmission electron microscopy and atomic force microscopy confirmed these results. **Figure 3.11** is a schematic representation of the synthesis of the core-bound micelles.[47]

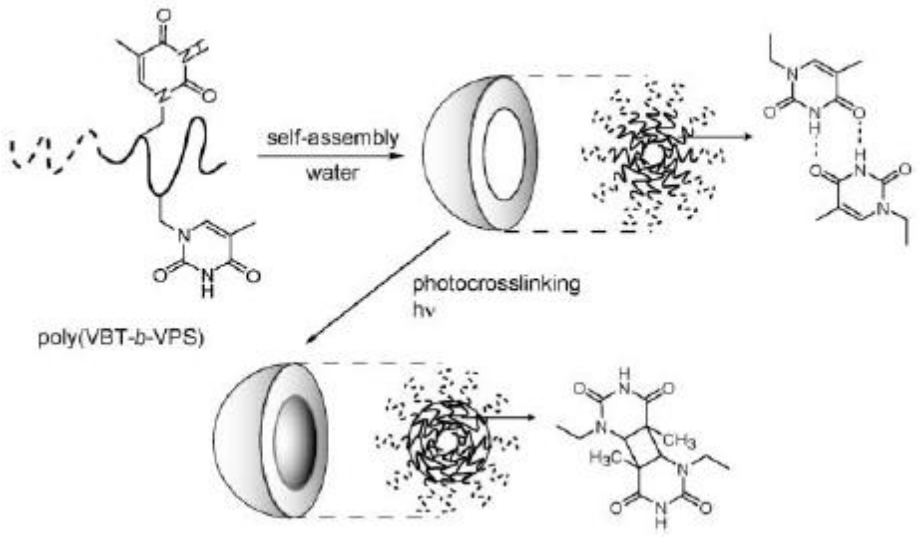

Figure 3.11 Core bound micellar particles stabilized with thymine dimerization-driven crosslinking.[47] (Fair use)

3.7 Synthesis of photoreactive polymers containing o-nitro benzyl units in the polymer mainchain

Protection and subsequent deprotection of alcohols, acids, amines, and amides is a crucial technique utilized in organic chemistry when functional groups may interfere with the formation of a desired product. Protecting groups that deprotect under UV irradiation exhibit significant usefulness, as chemical protecting groups often require extensive purification upon deprotection. For these reasons, the *o*-nitro benzyl (ONB) protecting group features prominently as a photoreactive protecting group in organic chemistry.[56,73] In particular *o*-nitro benzyl esters are especially reactive upon UV irradiation. The mechanism for this reaction is shown as **Figure 3.12**.[56,73] This simple deprotection finds common utility in polymer science towards the formation of stimuli responsive polymers, but most often deprotection of hydrophilic, hydrogen bonding, or polar sites occur, rather than actual photocleavage of a polymer backbone. However, many examples do exist of *o*-nitro benzyl esters within the backbone of polymers for photoresponsive applications.

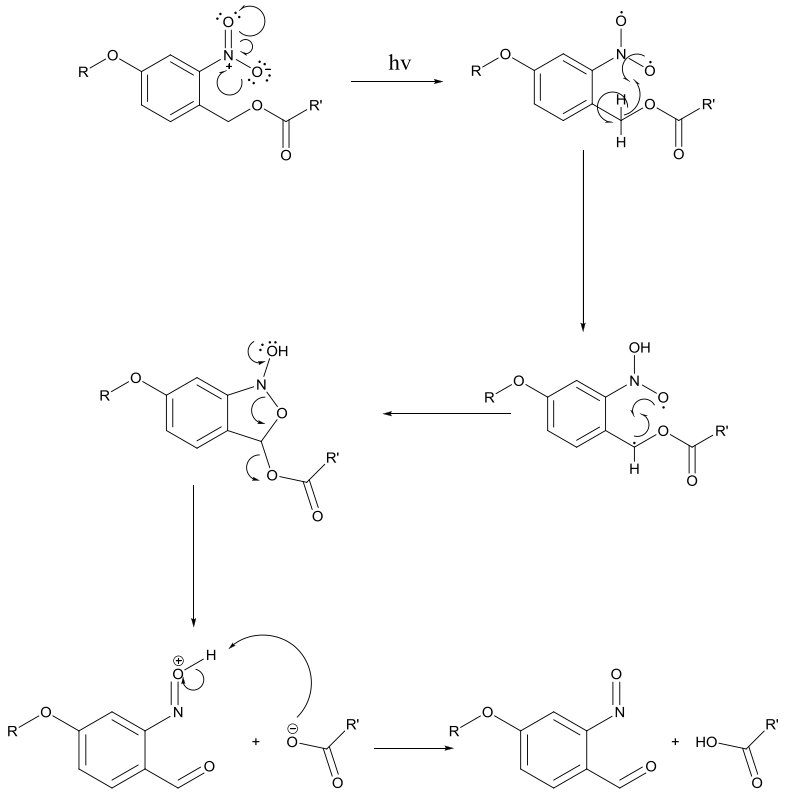

Figure 3.12 Mechanism for UV-induced photodegradation of o-nitro benzyl ester compounds.[56,73]

Kang and Moon published a paper in 2009 detailing the synthesis of a diblock copolymer linked with an *o*-nitro benzyl ester photocleavable unit.[19] Reaction of a mono-hydroxy terminated PEG at the 5 position of a 2-nitro benzyl alcohol and subsequent conversion into a benzyl ester suitable for usage as an ATRP initiator resulted in a photoactive macroinitiator. Utilization of the photoactive macroinitiator in the ATRP polymerization of styrene resulted in a photoactive diblock copolymer containing ONB functionality between the blocks. Styrene-PEO regularly forms lamellar structures, and the cast film of the authors' diblock copolymer did form lamellar morphology. Photocleavage with UV light and subsequent washing with polar solvents removed the cleaved PEO block, leaving behind nano-porous thin films. **Figure 3.13** demonstrates a TEM of the nano-porous thin film, as well as ^{1}H NMR spectroscopic and chromatographic confirmation of photocleavage.[19]

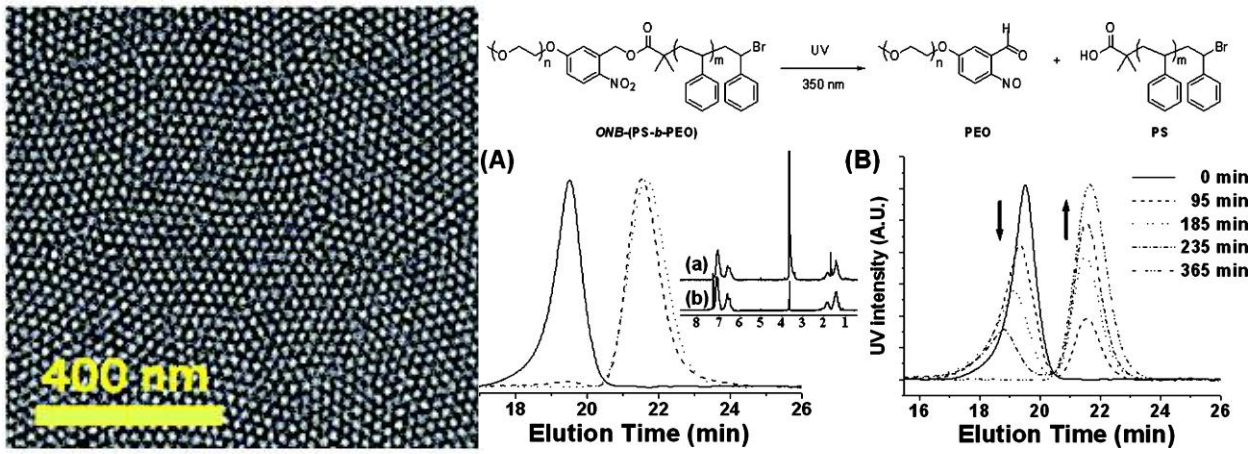

Figure 3.13 From left to right; TEM of obtained nano-porous thin film upon PS-PEO lamellar formation followed by UV photocleavage and removal of PEO by washing; SEC before and after photoirradiation of the ONB ester-linked PEO-PS and 1H NMR confirmation of ONB ester cleavage; SEC as a function of irradiation dosage.[19] (Reprinted with permission from Kang, M.; Moon, B. *Macromolecules* **2009**, 42, 455. Copyright(2009) American Chemical Society.)

Johnson, Turro, and coworkers published a series of papers in 2007 and 2008 detailing the synthesis of cross-linked polymers which provided routes using photocleavage of ONB esters towards well-defined morphologies.[57,58,74] In particular, the authors started with a ONB chromophore difunctionalized with an ATRP initiator, and subsequent polymerization prior to S_N2 with NaN_3 to convert the bis-bromo macromonomer into a bis-azide macromoner, and further reaction with a tetra-alkyne, formation of cross-linked networks occured. Since the ONB units were evenly spaced between cross-link points, photocleavage of these ONB units yielded monodisperse 4-arm star polymers.[58]

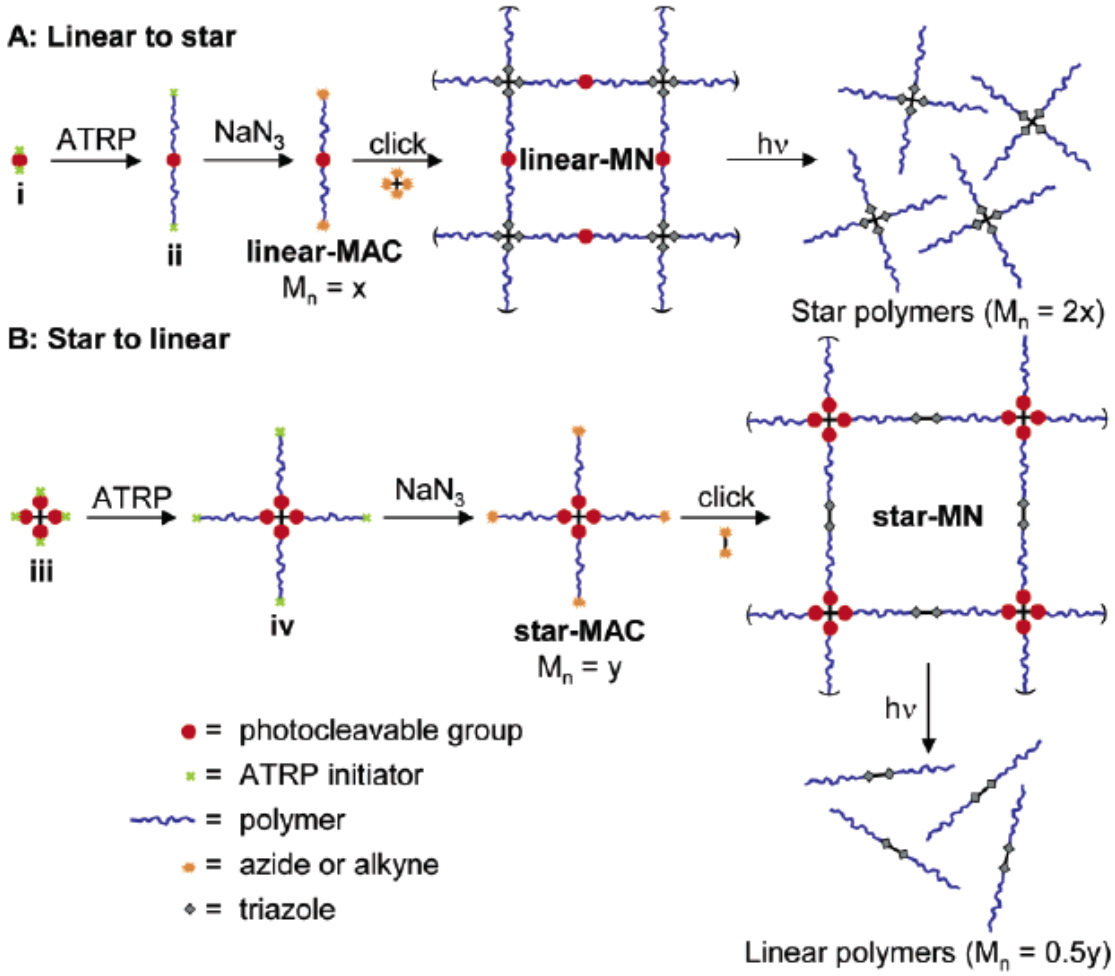

Figure 3.14 Utilization of "click" chemistry and ONB photocleavable functionality towards the synthesis of well-defined cross-linked networks and subsequent 4-arm star polymers and linear polymers.[58] (Reprinted with permission from Johnson, J. A.; Finn, M. G.; Koberstein, J. T.; Turro, N. J. *Macromolecules* **2007**, 40, 3589. Copyright(2009) American Chemical Society.)

Conversely, when the authors started with a 4-arm branched tetra-photocleavable ATRP tetra-initiator, they obtained a 4-arm star tetra-bromide end-capped polymer. Analogous S_N2 with NaN_3 resulted in the formation of the tetra-azide end-capped four-arm star polymer. Reaction of this star copolymer with a bisalkyne again yielded a regularly crosslinked network. However, in this case, upon photocleavage of the ONB unit, the authors isolated linear polymers. **Figure 3.14** represents this strategy schematically.[58]

Schumers and Fustin published a communication in 2009[75] that combined the ideas of Turro and coworkers, and Moon and coworkers. They synthesized an ONB-containing linker that possessed functionality on one side for ATRP, and alkyne functionality on the other side. Thus, upon exposure of this linking unit to a mono-azido terminated PEG under "click" chemistry conditions and styrene under ATRP conditions in one pot, the synthesis with simple synthetic conditions of a PEO-PS diblock copolymer occured. The authors anticipated that this copolymer would form similar morphologies to that which Moon and coworkers reported. **Figure 3.15** demonstrates the synthesis of this diblock copolymer.[75]

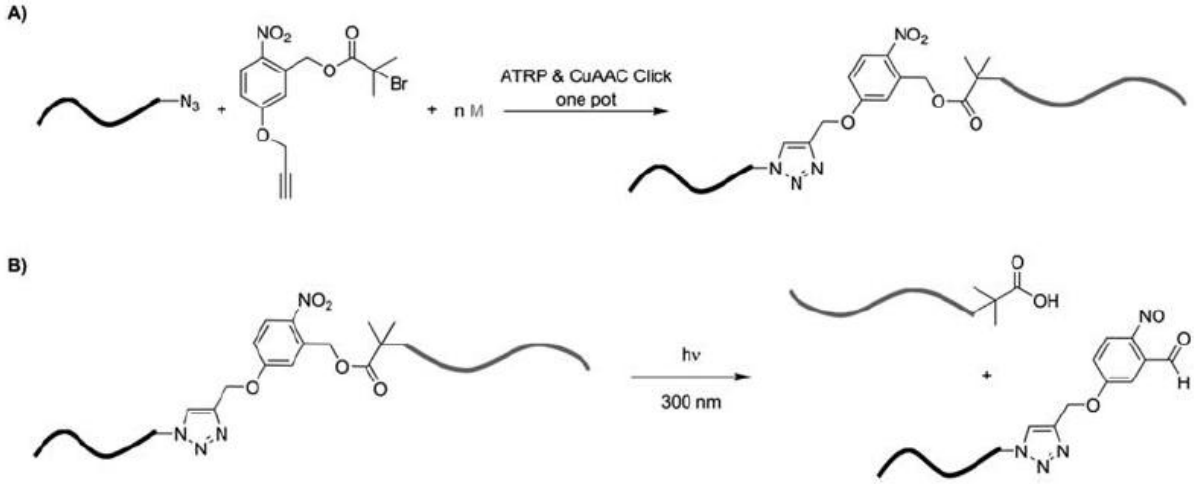

Figure 3.15 One-pot synthesis of diblock PEG-PS copolymer bearing ONB-functionality for a photocleavable linkage.[75] (Fair Use)

ONB-linkages also offer potential utility in the controlled synthesis of protein structures. Piggot and Karuso published a short communication in 2005 detailing the synthesis of a long, hydrophilic ONB-containing linker for utilization in solid-state synthesis of proteins.[62] The long, hydrophilic nature of these ONB-containing linker possessed several distinct advantages, as most common linkers for solid-state synthesis of proteins have short lengths and hydrophobic structures, limiting their utility for biological systems. The authors demonstrated successful

synthesis of the linker, as well as nearly 100% photocleavage after exposure to UV light at 356 nm. **Figure 3.16** demonstrates the synthesis of the ONB-containing linker for proteonomics.

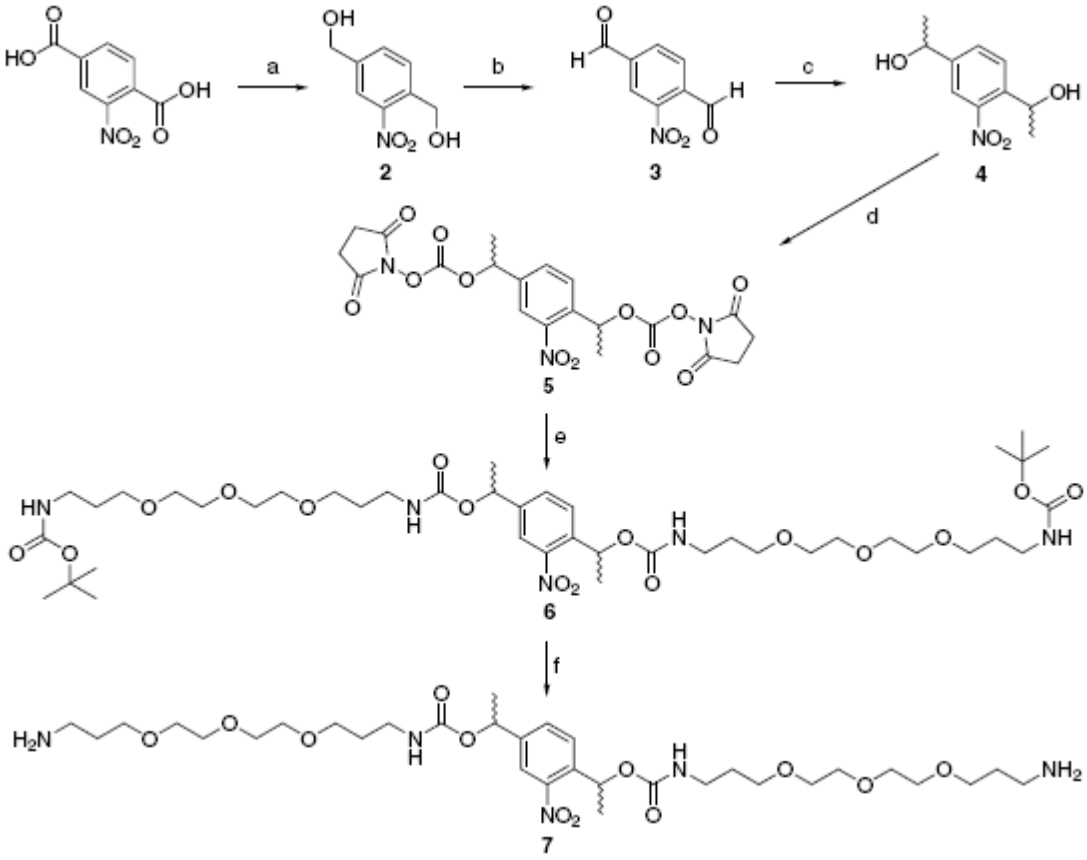

Figure 3.16 Synthesis of long, hydrophilic, photocleavable linker for proteonomics.[62] (Reprinted from Piggott, A. M.; Karuso, P. *Tetrahedron Lett.* **2005**, *46*, 8241. with permission from Elsevier.)

Although many of the examples presented so far included ONB functional groups only as a linker, with 1 unit per polymer chain; or at most as a highly regular linker between crosslink points, there are a few examples in the literature of ONB functionality within a monomer for utilization in a subsequent polymerization. In particular, Feng, Matsumoto, and coworkers published a series of papers detailing the synthesis of an *o*-nitro benzyl oxyamine and its use towards the synthesis of polyimides containing ONB functionality.[6,7] Copolymerization of this monomer with *p*-xylylene oxyamine and various dianhydrides yielded the corresponding

polyimides. Polymers synthesized from aliphatic alicyclic dianhydrides demonstrated significantly enhanced photocleavage, relative to aromatic analogs, as aromaticity distorted or masked the ONB group from UV-exposure.[6,7]

3.8 Outlook

Although photochemistry exhibits a high degree of efficacy in polymer science, the utilization of light for the assembly or disassembly of macromolecules may result in further advancements. "Smart" polymers offer the potential to tune properties with small adjustments in stimuli, and such property changes often result in marked differences in solubility, swellability, mechanical strength, and morphology. Although there is little prominence in the use of light for these assembly and disassembly processes, a constant increase in the depth and breadth of the field exists. Increasing the level of understanding of the effects of intensity, wavelength, and UV exposure time may lead to a further viability for photoactive materials. In spite of the current hurdles surrounding this field, it continues to exhibit a remarkable trend towards expansion with increasing technological demands.

3.9 References

(1) Schreier, W. J.; Schrader, T. E.; Koller, F. O.; Gilch, P.; Crespo-Hernandez, C. E.; Swaminathan, V. N.; Carell, T.; Zinth, W.; Kohler, B. *Science* **2007**, *315*, 625.
(2) Kim, H. C.; Haertner, S.; Hampp, N. *J. Photochem. Photobiol., A* **2008**, *197*, 239.
(3) McEwen, J. J.; Wallace, K. J. *Chem. Commun.* **2009**, 6339.
(4) Yagci, Y.; Jockusch, S.; Turro, N. J. *Macromolecules* **2010**, *43*, 6245.
(5) Awaji, H.; Kamikita, M.; Mizunuma, S.; JP 89-281135, 1991, p 18
(6) Feng, K.; Matsumoto, T.; Kurosaki, T. *J. Photopolym. Sci. Technol.* **1996**, *9*, 347.
(7) Feng, K.; Matsumoto, T.; Kurosaki, T. *Chem. Mater.* **1997**, *9*, 1362.
(8) Frechet, J. M. J.; Leung, M.-k.; Urankar, E. J.; Willson, C. G.; Cameron, J. F.; MacDonald, S. A.; Niesert, C. P. *Chem. Mater.* **1997**, *9*, 2887.
(9) Hayase, S.; Horiguchi, R.; Onishi, K.; JP 86-292488, 1988, p 4
(10) Hayase, S.; Onishi, Y.; Horiguchi, R. *J. Electrochem. Soc.* **1987**, *134*, 2275.
(11) Matsubara, S.; Nakai, H.; Urano, T.; Murakami, S.; JP 87-81375, 1988, p 7
(12) Moore, J. A.; Dasheff, A. N. *Chem. Mater.* **1989**, *1*, 163.
(13) Onishi, K.; Hayase, S.; Hirao, A.; Horiguchi, R.; JP 85-293182, 1987, p 4
(14) Ambade, A. V.; Burd, C.; Higley, M. N.; Nair, K. P.; Weck, M. *Eur. J. Chem.* **2009**, *15*, 11904.
(15) Berl, V.; Schmutz, M.; Krische, M. J.; Khoury, R. G.; Lehn, J.-M. *Eur. J. Chem.* **2002**, *8*, 1227.
(16) Blanco, V.; Gutierrez, A.; Platas-Iglesias, C.; Peinador, C.; Quintela, J. M. *J. Org. Chem.* **2009**, *74*, 6577.
(17) Cheng, C. C.; Yen, Y. C.; Ye, Y. S.; Chang, F. C. *J. Polym. Sci., Part A: Polym. Chem.* **2009**, *47*, 6388.
18) Huang, F.; Gibson, H. W.; Bryant, W. S.; Nagvekar, D. S.; Fronczek, F. R. *J. Am. Chem. Soc.* **2003**, *125*, 9367.
(19) Kang, M.; Moon, B. *Macromolecules* **2009**, *42*, 455.
(20) Karikari, A. S.; Williams, S. R.; Heisey, C. L.; Rawlett, A. M.; Long, T. E. *Langmuir* **2006**, *22*, 9687.
(21) Loewik, D. W. P. M.; Meijer, J. T.; Minten, I. J.; Van Kalkeren, H.; Heckenmueller, L.; Schulten, I.; Sliepen, K.; Smittenaar, P.; Van Hest, J. C. M. *J. Pept. Sci.* **2008**, *14*, 127.
(22) Meijer, J. T.; Henckens, M. J. A. G.; Minten, I. J.; Loewik, D. W. P. M.; van Hest, J. C. M. *Soft Matter* **2007**, *3*, 1135.
(23) Williams, S. R.; Lepene, B. S.; Thatcher, C. D.; Long, T. E. *Biomacromolecules* **2009**, *10*, 155.
(24) Zhao, Y.; Bertrand, J.; Tong, X.; Zhao, Y. *Langmuir* **2009**, *25*, 13151.
(25) Zhou, Y.; Yan, D. *Chem. Commun.* **2009**, 1172.
(26) Ayres, N.; Boyes, S. G.; Brittain, W. J. *Langmuir* **2006**, *23*, 182.
(27) Chen, X.; Gao, J.; Song, B.; Smet, M.; Zhang, X. *Langmuir* **2009**, *26*, 104.
(28) Koylu, D.; Carter, K. R. *Macromolecules* **2009**, *42*, 8655.
(29) Lowe, A. B.; McCormick, C. L. *Prog. Polym. Sci.* **2007**, *32*, 283.
(30) Mendes, P. M. *Chem. Soc. Rev.* **2008**, *37*, 2512.
(31) Murphy, E. B.; Wudl, F. *Prog. Polym. Sci.* **2010**, *35*, 223.
(32) Rowe, M. D.; Hammer, B. A. G.; Boyes, S. G. *Macromolecules* **2008**, *41*, 4147.
(33) Sanjuan, S.; Tran, Y. *Macromolecules* **2008**, *41*, 8721.

(34) Jiang, X.; Lavender, C. A.; Woodcock, J. W.; Zhao, B. *Macromolecules* **2008**, *41*, 2632.
(35) Decker, C.; Bianchi, C.; Jönsson, S. *Polymer* **2004**, *45*, 5803.
(36) Williams, S. R.; Barta, Z.; Ramirez, S. M.; Long, T. E. *Macromol. Chem. Phys.* **2009**, *210*, 555.
(37) He, J.; Tong, X.; Zhao, Y. *Macromolecules* **2009**, *42*, 4845.
(38) Huyck, R. H.; Trenor, S. R.; Love, B. J.; Long, T. E. *J. Macromol. Sci., Part A: Pure Appl. Chem.* **2008**, *45*, 9.
(39) Trenor, S. R.; Long, T. E.; Love, B. J. *Macromol. Chem. Phys.* **2004**, *205*, 715.
(40) Trenor, S. R.; Long, T. E.; Love, B. J. *J. Adhes.* **2005**, *81*, 213.
(41) Trenor, S. R.; Long, T. E.; Love, B. J. *Eur. Polym. J.* **2005**, *41*, 219.
(42) Trenor, S. R.; Shultz, A. R.; Love, B. J.; Long, T. E. *Chem. Rev.* **2004**, *104*, 3059.
(43) Cashion, M. P.; Park, T.; Long, T. E. *J. Adhes.* **2009**, *85*, 1.
(44) Gattas-Asfura, K. M.; Weisman, E.; Andreopoulos, F. M.; Micic, M.; Muller, B.; Sirpal, S.; Pham, S. M.; Leblanc, R. M. *Biomacromolecules* **2005**, *6*, 1503.
(45) Casis, N.; Luciani, C. V.; Berlanga, J. V.; Estenoz, D. A.; Martino, D. M.; Meira, G. R. *Green Chem. Lett. Rev.***2007**, *1*, 65
(46) Rahn, R. O. *Science* **1966**, *154*, 503.
(47) Saito, K.; Ingalss, L. R.; Lee, J.; Warner, J. C. *Chem. Commun.* **2007**, 2503.
(48) Afzali-Ardakani, A.; Kagan, C. R.; Kosbar, L. L.; Swanson, S. A.; Srinivasan, C.; US 2006-445326, 2007, p 11
(49) Awaji, H.; Kamikita, M.; Mizunuma, S. JP 89-281135, 1991, p 20
(50) Cameron, J. F.; Frechet, J. M. J. *J. Am. Chem. Soc.* **1991**, *113*, 4303.
(51) Case, F. H. *J. Am. Chem. Soc.* **1925**, *47*, 3005.
(52) de la Torre, B. G.; Albericio, F. *e-EROS Encycl. Reagents Org. Synth.* **2001**, No pp given.
(53) de la Torre, B. G.; Eritja, R.; Albericio, F. *e-EROS Encycl. Reagents Org. Synth.* **2001**, No pp given.
(54) Goldbach, J. T.; Russell, T. P.; Penelle, J. *Polym. Prepr.* **2002**, *43*, 470.
(55) Hanson, J. E.; Reichmanis, E.; Houlihan, F. M.; Neenan, T. X. *Chem. Mater.* **1992**, *4*, 837.
(56) Il'ichev, Y. V.; Schworer, M. A.; Wirz, J. *J. Am. Chem. Soc.* **2004**, *126*, 4581.
(57) Johnson, J.; Koberstein, J. T.; Turro, N. J.; WO 2006-US41270, 2008, p 53
(58) Johnson, J. A.; Finn, M. G.; Koberstein, J. T.; Turro, N. J. *Macromolecules* **2007**, *40*, 3589.
(59) Natt, F. J.-C.; Hunziker, J.; WO 2007-EP337, 2007, p 38pp.
(60) Nicolas, E.; Clemente, J.; Perello, M.; Albericio, F.; Pedroso, E.; Giralt, E. *Tetrahedron Lett.* **1992**, *33*, 2183.
(61) Nishi, T.; Onodera, J.; Abe, Y.; Sakai, K.; Yui, T. *Yamagata Daigaku Kiyo Kogaku* **1968**, *10*, 9.
(62) Piggott, A. M.; Karuso, P. *Tetrahedron Lett.* **2005**, *46*, 8241.
(63) Zhao, Y. *J. Mater. Chem.* **2009**, *19*, 4887.
(64) Suzuki, H.; Abe, T.; Takaishi, K.; Narita, M.; Hamada, F. *J. Polym. Sci., Part A: Polym. Chem.* **2000**, *38*, 108.
(65) June, S. M.; Suga, T.; Heath, W. H.; Lin, Q.; Puligadda, R.; Long, T. E. *J. Adhes.* **2010**, *In Press*.

(66) Arnold, C. A.; Summers, J. D.; Chen, Y. P.; Bott, R. H.; Chen, D.; McGrath, J. E. *Polymer* **1989**, *30*, 986.
(67) Bott, R. H.; Summers, J. D.; Arnold, C. A.; Blankenship, C. P., Jr.; Taylor, L. T.; Ward, T. C.; McGrath, J. E. *Sampe J.* **1988**, *24*, 7.
(68) Bott, R. H.; Summers, J. D.; Arnold, C. A.; Taylor, L. T.; Ward, T. C.; McGrath, J. E. *J. Adhes.* **1987**, *23*, 67
(69) Kaltenecker-Commercon, J. M.; Ward, T. C.; Gungor, A.; McGrath, J. E. *J. Adhes.* **1994**, *44*, 85.
(70) McGrath, J. E.; Dunson, D. L.; Mecham, S. J.; Hedrick, J. L. In *Progress in Polyimide Chemistry I* 1999; Vol. 140, p 61.
(71) Yoon, T. H.; Arnold-McKenna, C. A.; McGrath, J. E. *J. Adhes.* **1992**, *39*, 15.
(72) Yoon, T. H.; McGrath, J. E. *High Perform. Polym.* **1992**, *4*, 203.
(73) Patchornik, A.; Amit, B.; Woodward, R. B. *J. Am. Chem. Soc.* **2002**, *92*, 6333.
(74) Johnson, J. A.; Baskin, J. M.; Bertozzi, C. R.; Koberstein, J. T.; Turro, N. J. *Chem. Commun.* **2008**, 3064.
(75) Schumers, J.M.; Gohy, J.F.; Fustin, C.A. *Polym. Chem.* **2010**, *1*, 161.
(76) Minsk, L. M.; Van, D. W. P.; Robertson, E. M. US2670287, 1954.

Chapter 4: Photo-reactive Polyimides and Poly(siloxane imide)s as Reversible Polymeric Interfaces

Stephen M. June[1], Takeo Suga[1], William H. Heath[1], Qin Lin[2], Rama Puligadda[2], and Timothy E. Long[1]

1 – Department of Chemistry (0212), Virginia Tech, Blacksburg, VA 24061

2 – Brewer Science, Inc., 2401 Brewer Dr., Rolla, MO 65401

(Reprinted from "June, S. M.; Suga, T.; Heath, W. H.; Long, T. E.; Lin, Q.; Puligadda, R. *The Journal of Adhesion* **2010,** 86, (10), 1012 – 1028" with permission from Taylor and Francis publishing company.)

4.1 Abstract

Polyimides and poly(siloxane imide)s containing photo-active cyclobutane diimide units were developed as reversible adhesives for temporary bonding in micro-fabrication processes. Poly(amic acid) formation and in dipolar aprotic solvents and subsequent chemical or thermal solution imidization yielded the corresponding organic dispersible polyimides. Incorporation of nonplanar (alicyclic or bicyclic) structures and poly(dimethyl siloxane) blocks into the main chain improved the dispersibility. The synthesized poly(siloxane imide)s afforded tough and ductile films, which exhibited a rubbery plateau in the storage modulus, as observed using dynamic mechanical analysis. This plateau was attributed to the microphase-separation of the poly(dimethyl siloxane) segments and the polyimide segments. Spin-coated thin films on silicon substrates were photo-degraded with ultraviolet-C (UVC) light (254 nm). Nuclear magnetic resonance (NMR) spectroscopy demonstrated a growth in the proton resonance corresponding to the formation of maleimide functionality upon photo-cleavage. This observed photo-cleavage suggests possible applications as temporary structural adhesives.

4.2 Introduction

As electronic devices become increasingly advanced and miniaturized, the need has arisen for a temporarily-bound support substrate during the fabrication process. Utilization of a support substrate allows for device stability throughout a relatively rigorous fabrication process such as backside grinding, lithography, or deposition.[1]

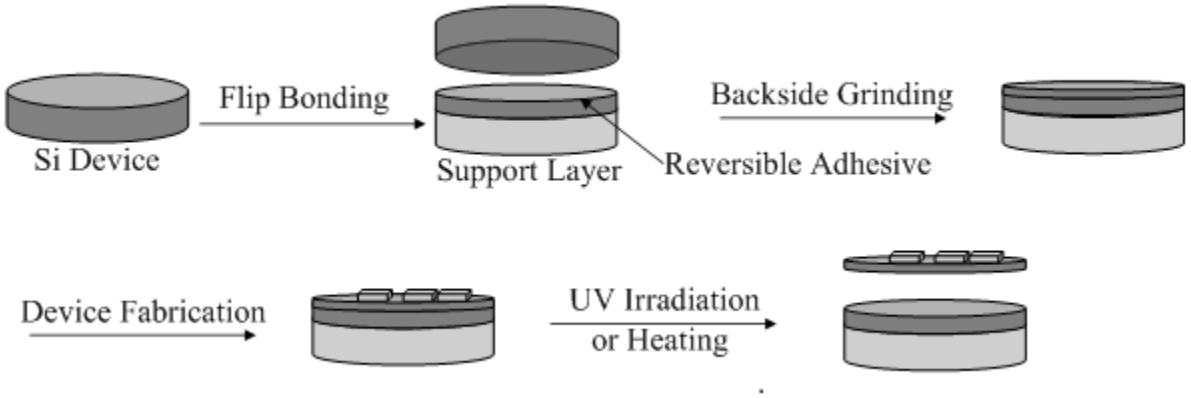

Figure 4.1 Scheme demonstrating temporary bonding for fabrication of electronic devices.

Figure 4.1 demonstrates a scheme for the fabrication of an electronic device utilizing temporary-bonding. A device substrate, such as a silicon wafer, is bonded to a support substrate with an adhesive. This allows for grinding, machining, and other fabrication of the device substrate without any risk of damaging the device itself. Thermal softening or degradation of the adhesive permits removal of the device from the support substrate upon completion of device fabrication. However, the thermal process is less controlled and requires extremely high temperatures, thus increasing the difficulty of handling and process complexity. Furthermore, repeated heating and cooling of thin and ultrathin wafers leads to deformation, cracking, warping, and folding.[2,3] For this reason, we have developed a model for an alternative photo-degradable structural adhesive, in lieu of an adhesive which is releasable upon thermal softening

or degradation. Our model compound is photolytically degraded, thus potentially allowing for a diminishment of adhesive properties, upon exposure to ultraviolet light. This will potentially allow for the facile removal of the device from the support substrate without the need for heating.

As structural adhesives, polyimides are promising materials for device applications and are widely utilized as low static permittivity materials in microelectronic devices, such as integrated circuits, due to their high thermal stability, chemical resistance, and dielectric properties. A wealth of research exists towards the development of photo-reactive polymers as photo-resists for the microelectronics industry.[4-16] For instance, *o*-nitro benzyl (ONB) esters, alcohols, and amides, have demonstrated utility as photo-cleavable linkers in polymers.[6,8] Photo-reversible groups such as the photodimer of maleic anhydride, 1,2,3,4-cyclobutane-tetracarboxylic dianhydride (CBDA), have proven effective as positive photoresist materials in the mid-1980s.[7] Such photo-reversible [2+2] cycloaddition/cleavage units have also shown utility as photo-crosslinking, photo-chain extension, or photo–cleavable sites in polymers and polymeric materials.[10-12,15-18] Our group has significant experience in developing thermally and photolytically reversible adhesives.[11-13,17,19,20] In particular, our group has developed the coumarin-functionalized poly(2-ethylhexyl acrylate-*co*-hydroxyethyl acrylate) and demonstrated a photo-reversible pressure-sensitive adhesive system.[11]

Requirements for the backbone polymer matrix for an adhesive as described include thermal and photolytic stability, dispersibility, and adequate adhesive performance. Other requirements include formation of uniform films and effective adherence to a variety of substrates.[3] It is for this reason that poly(siloxane imides) were utilized. McGrath and others previously demonstrated enhanced solubility and adhesive performance, relative to the

corresponding polyimide homopolymer.[4,21-29] Furthermore, incorporation of poly(dimethyl siloxane) blocks into polyimides does not decrease the thermal, oxidative, or UV stability of the polymer.[25-29] In addition, incorporation of oligo(dimethyl siloxane) blocks allow for microphase separation, and elastomeric mechanical properties.[27,28,30]

4.3 Experimental

4.3.1 Materials. Aminopropyl-terminated poly(dimethylsiloxane) (Gelest DMS-A12, M_n = 1,600, T_g = -122 °C) was purchased from Gelest, Inc. (Morrisville, PA) and used without further purification. Bicyclo[2.2.2]oct-7-ene-2-exo,3-exo,5-exo,6-exo-tetracarboxylic-2,3:5,6-dianhydride (BOEDA) and 4,4'-(1,3-phenylenedioxy)dianiline (PDDA) were purchased from TCI America (Portland, OR) and repeatedly recrystallized prior to use from acetonitrile and toluene, respectively. Purity upon recrystallization was confirmed using ^{1}H NMR spectroscopy and TLC. Anhydrous *N*-methyl-2-pyrrolidinone (NMP) equipped with an AcroSeal™ was purchased from Acros (Geel, Belgium) and was used as received. 1-Cyclohexyl-2-pyrrolidinone (CHP) and maleic anhydride were purchased from Aldrich (St. Louis, MO) and used as received. Tetrahydrofuran (THF), *N*,*N*'-dimethyl formamide (DMF), and toluene were purchased from Fisher Scientific (Pittsburg, PA) and purified using an MBraun (Garching, Germany) MB-SPS solvent purification system. All other solvents and reagents were purchased commercially and used as received.

4.3.2 Instrumentation. ^{1}H NMR spectroscopy was performed in THF-d_8, DMSO-d_6, DMF-d_7 or $CDCl_3$ at 23 °C with a Varian (Palo Alto, CA) 400 MHz INOVA, UNITY, or MR400 spectrometer. Thermogravimetric analysis (TGA) was performed using a TA Instruments (New

Castle, DE) Hi-Res TGA 2950 in a platinum pan under a constant nitrogen purge of 50 mL/min and a ramp rate of 10 °C/min. Differential scanning calorimetry (DSC) was conducted in a TA Instruments (New Castle, DE) Q1000 DSC at a heating rate of 10 °C/min and a cooling rate of 50 °C/min under a constant nitrogen purge of 50 mL/min. Glass transition temperatures (T_g) were reported as mid-point temperatures from the second heat. Dynamic mechanical analysis (DMA) data was obtained using a TA Instruments (New Castle, DE) Q800 dynamic mechanical analyzer in tension mode at a frequency of 1 Hz and temperature ramp of 3 °C/min. Tensile experiments were performed on an Instron (Norwood, MA) 4411 universal testing instrument utilizing sample strips and a crosshead speed of 2 mm/min with manual grips at ambient temperature.

Size-exclusion chromatography (SEC) was performed at 40 °C in THF (HPLC grade) at 1 mL/min using polystyrene standards on a Waters 707 autosampler equipped with three in-line PLgel 5 mm MIXED-C columns (Polymer Laboratories, Amberst, MA, USA), a Waters 410 refractive index detector (Waters Co. Milford, MA, USA), and an in-line Wyatt Technology Corp. mini-DAWN multiple-angle laser light scattering (MALLS) detector (Wyatt Technology, Santa Barbara, CA, USA). Reported number-average and weight-average molecular weights are relative to polystyrene standards.

Atomic force microscopy (AFM) was performed using a Veeco (Plainview, NY) MultiMode AFM equipped with a low modulus tip. Sample films were solution-cast from THF into a PTFE mold, and annealed at 80 °C *in vacuo* for 18 h prior to testing. UV/Visible spectra were obtained using an Analytical Instrument Systems Inc. spectrometer (Flemington, NJ) equipped with fiber-optic light guides, a DT1000CE light source, and an Ocean Optics (Drenedin, FL) USB2000 UV-Vis detector.

UV irradiation was performed using either a ThermoOriel (Newport Stratford Inc, Stratford, CT) mercury arc lamp, a Fusion UV Systems, Inc (Gaithersburg, MD) F300s series microwave powered electrodeless lamp source coupled with a LC-6B bench top conveyer at an intensity of 0.211 W/cm^2 in the UVC region, 1.513 W/cm^2 in the UVB region, and 2.044 W/cm^2 in the UVA region, or a R-52 Mineralight® Grid Lamp obtained from UVP (Upland, CA) irradiating at 254 nm with an intensity of 0.814 mW/cm^2. Gel fraction studies were performed utilizing a soxhlet extraction apparatus, with THF as a solvent and a 10 h exposure.

4.3.3 Synthesis

Cyclobutane-1,2,3,4-tetracarboxylic dianhydride (CBDA). The synthesis of CBDA was performed according to literature procedure [9]. Briefly, maleic anhydride (40 g, 408 mmol) was dissolved in 400 mL ethyl acetate and placed inside a photo-reactor. Photo-dimerization was carried out in a Pyrex photo-reactor system equipped with a 450 W high-pressure mercury lamp (180-450 nm), and a Pyrex water jacket for cooling. The utilization of Pyrex for the reactor was beneficial, as Pyrex effectively filters out light wavelengths below 280 nm, diminishing the effects of the reverse reaction. CBDA precipitated out of solution as it was formed. After 24 h, the product was filtered, dried at 50 °C at reduced pressure, and recrystallized from acetic anhydride with an isolated yield of 50%. ^{1}H NMR (400 MHz, DMSO-d_6, ppm): 3.86 (s, 4H, CH); ^{13}C-NMR (100 MHz, DMSO-d_6, ppm) : 170.9, 41.9. mp > 300 °C.

Polymerization of CBDA and 4,4'-oxydianiline (thermal bulk imidization method). Step-growth polymerization of CBDA and 4,4'-oxydianiline was performed according to the literature.[7] CBDA and oxydianiline were dissolved in a 1:1 molar ratio in *N*,*N*'-dimethyl acetamide (DMAc) (30 wt%) in a three-necked, round bottomed flask equipped with mechanical

stirring under nitrogen. The reaction solution was allowed to stir at ambient temperature, under nitrogen for 18 h to give the corresponding poly(amic acid). The resulting poly(amic acid) was solution cast from DMAc into a Teflon® mold. The film was clear and colorless, and uniform in thickness. Bulk thermal imidization was performed first at 150 °C for 3 h, and subsequently at 220 °C for 18 h *in vacuo*. As expected, the resulting film was nondispersible in organic solvents such as DMAc, DMF, NMP, THF, or $CHCl_3$. Furthermore, upon imidization the film had yellowed significantly, shrunk, and warped. These results confirmed the findings that Moore et al. had demonstrated previously.[7]

Polymerization of CBDA, BOEDA, and PDDA (chemical imidization method). CBDA, BOEDA, and PDDA (0.1/0.9/1.0) were dissolved in DMAc (30 wt%) in a three-necked round-bottomed flask equipped with mechanical stirring under nitrogen. The reaction solution was allowed to stir at 85 °C for 24 h. Chemical solution imidization was utilized to perform imidization on the corresponding poly(amic acid). Triphenyl phosphate (0.8 equivalents; relative to diamine) of triphenyl phosphite and 1.26 equivalents of pyridine were added to the reaction flask. The reaction was allowed to stir for 24 h at 85 °C. Finally, six equivalents each of acetic anhydride and triethylamine were added to the reaction solution and the solution was allowed to stir for an additional 24 h at 85 °C. The polymer was precipitated into methanol and the precipitate was collected. The collected polymer was dried at 85 °C *in vacuo* (yield 94%). M_n = 47,000; M_w/M_n = 2.33. ^{1}H NMR (400 MHz, DMSO-d_6, ppm): 7.41 (t, 8.4 Hz, 1H, Ph), 7.14 (m, 8H, Ph), 6.80 (d, 8.4 Hz, 2H, Ph), 6.75 (s, 1H, Ph), 6.27 (s, 1.8H, BOEDA olefin), 3.67 (s, 0.3H, CBDA methine), 3.49 (s, 1.8H, BOEDA bridgehead), 3.42 (s, 3.6H, BOEDA methine). The composition (CBDA/BOEDA) was 0.08/0.92. Similar methods were utilized to synthesize polymers containing 0 and 20% CBDA, relative to BOEDA.

Cyclobutane diimide-containing poly(siloxane arylene imide)s (thermal solution imidization method). CBDA and BOEDA were dissolved in a NMP/THF (1/1, 30 wt% solids) co-solvent system in a 0.7:0.3 ratio and stirred under nitrogen at 55 °C. Aminopropyl-terminated poly(dimethylsiloxane) (M_n = 1,600) was added drop-wise in a 0.5 molar equivalent (respective to anhydride functional group). A solution of 0.5 molar equivalents of PDDA in the reaction solvent was added to the reaction solution. The reaction was stirred under nitrogen for 24 h at 55 °C. After 24 h, the temperature was increased to 160 °C, removing the THF, cyclohexyl pyrrolidinone (CHP) was added as an azeoptrope agent (25%, relative to NMP) in order to perform thermal solution imidization. The imidization was allowed to take place for 24 h. The product was precipitated into methanol, vacuum-filtered, and dried at 50 °C at reduced pressure (yield 89%). ^{1}H-NMR (400 MHz, DMSO-d_8, ppm): 7.37 (br, 3H, Ph), 7.21 (br, 2H, Ph), 7.06 (br, 4H, Ph), 6.77 (br, 3H, Ph), 6.28 (s, 0.6H, BOEDA olefin), 6.14 (s, 0.4H, BOEDA olefin), 3.71 (br, 2H, PDMS endgroup methylene), 3.49 (br, 6H, CBDA methine), 3.28 (br, 4H, BOEDA methine), 3.07 (br, 1H, BOEDA bridgehead), 1.62 (br, 4H, PDMS endgroup methylene), 0.57 (br, 4H, PDMS endgroup methylene), 0.10 (s, 123H, PDMS methyl). Polymers containing 30 and 50 mol% CBDA, relative to BOEDA, were also synthesized as outlined above.

Poly(N-cyclohexyl maleimide). *N*-cyclohexyl maleimide (2.17 g, 12.1 mmol) was dissolved in degassed DMF (30 wt %). Azobisisobutyronitrile (AIBN) was added to the solution (20.5 mg, 0.5 mol %). The solution was allowed to stir (magnetic stirring) under inert atmosphere for 24 h at 60 °C. The solution was precipitated into ultrapure water and the precipitate was collected. The collected polymer was dried overnight *in vacuo* at 60 °C. ^{1}H-NMR (400 MHz, $CDCl_3$, ppm): 3.0-4.0 (br, 3H, backbone and cyclohexyl methine), 1.98 (br,

2H, cyclohexyl methylene), 174 (br, 3H, cyclohexyl methylene), 1.56 (br, 3H, cyclohexyl methylene), 1.19 (br, 3H, cyclohexyl methylene).

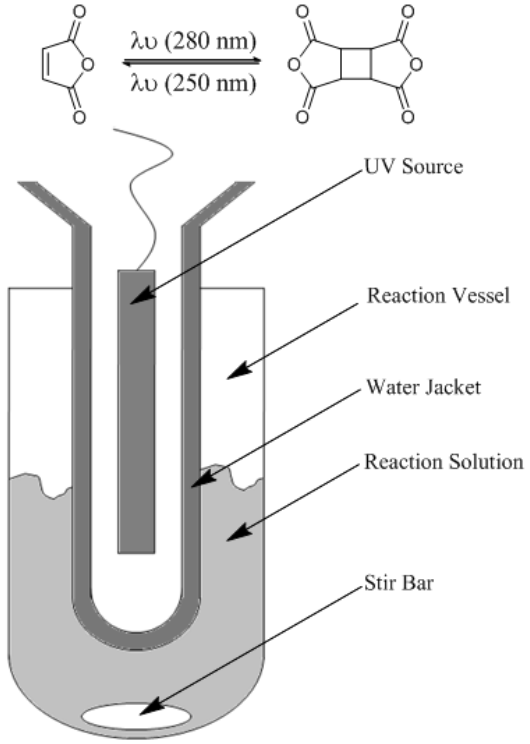

Figure 4.2 Reaction scheme and reactor setup for synthesis of CBDA.

4.4 Results and Discussion

4.4.1 Polymer Synthesis

Synthesis of Aromatic Polyimides Containing Cyclobutane Diimide. Synthesis of maleic anhydride dimer (CBDA) was perfomed using methods previously reported in the literature.[9] The obtained crude dimer was purified by recrystallization in acetic anhydride under nitrogen purge to afford pure product. The ^{1}H NMR of CBDA in DMSO-d_6 demonstrated a single resonance at 3.86 ppm, which was distinctly shifted from the olefin peak for maleic anhydride (7.45 ppm), confirming photo-dimerization. **Figure 4.2** demonstrates the reaction apparatus utilized for the synthesis of CBDA.[9] All dianhydrides were subjected to a thermal

treatment at 100 °C at reduced pressure prior to polymer synthesis in order to reverse any prior hydrolysis of anhydride functionality.

Initial attempts at incorporating cyclobutane diimide functionality into polyimides included only the use of CBDA and 4,4'-oxydianiline. However, as previously reported in the literature, the wholly aromatic polyimides obtained were not readily dispersible in any common organic solvent such as THF, $CHCl_3$, DMF, or NMP. In order to evaluate the effectiveness of this polymer for film or coating applications, the poly(amic acid) precursor was cast from the solution, and subsequent bulk thermal imidization yielded the corresponding polyimide film. However, bulk imidization induced a significant shrinkage and warping of the film. This was not appropriate to ensure uniform bonding, because film homogeneity is a crucial requirement for adhesives.[2,3]

Dispersible Alicyclic Polyimides Containing Cyclobutane Diimide. For improved dispersibility of the polyimides, the combination of dianhydrides and diamine were investigated. Previous literature studies have shown that incorporation of alicyclic dianhydrides such as bicyclo[2.2.2]oct-7-ene-2-exo,3-exo,5-exo,6-exo-tetracarboxylic-2,3:5,6-dianhydride (BOEDA), enhances dispersibility without significant loss of mechanical properties relative to aromatic dianhydrides.[31,32] Incorporation of *m*-linked aromatic diamines also increases dispersibility. Therefore, 4,4'-(1,3-phenylenedioxy)dianiline (PDDA) was selected as a co-monomer.[32-34]

Table 4.1 Polymerization of dispersible polyimides containing CBDA and BOEDA.

Molar Feed ratio CBDA:BOEDA	Composition CBDA:BOEDA	M_n [a]	M_w/M_n	$T_{d5\%}$ [b] (°C)	T_g [c] (°C)	Yield (%)
0.2:0.8	0.15:0.85	12,300	2.08	406	268	95
0.1:0.9	0.08:0.92	47,000	2.33	404	281	94
0:1.0	0:1.0	147,000	1.63	416	293	97

a) SEC - DRI, MALLS, NMP, 50 °C, 1 mL/min;
b) TGA - TA Instruments 2950 TGA, 10 °C/min, N_2 purge 50 mL/min
c) DSC - TA Instruments Q1000 DSC, 10 °C/min, N_2 purge 50 mL/min, 2nd heat

Syntheses of polyimides containing CBDA, BOEDA, and PDDA were performed using chemical solution imidization (**Table 4.1**). Chemical imidization with acetic anhydride in presence of triphenylphosphite and pyridine yielded the colorless and highly transparent polyimides, which is favorable for efficient photo-irradiation of cyclobutane diimide units. Thermo-gravimetric analysis (TGA) of the obtained polyimides exhibited high thermal stability with a 5% weight loss occuring at approximately 400 °C. The retro-Diels Alder degradation of BOEDA does not occur until approximately 360 °C, well beyond the required debonding temperature for our photo-releasable adhesives.[31]

The obtained polymers were slightly dispersible in NMP, DMSO, and DMF with a low loading of CBDA, but as chromophore (CBDA) loading increased, the dispersibility decreased markedly. The observed dispersibility of the polyimides effectively limited the usable chromophore loading into the mainchain of the polymer. Thus, it was evident that further dispersibility enhancements were necessary.

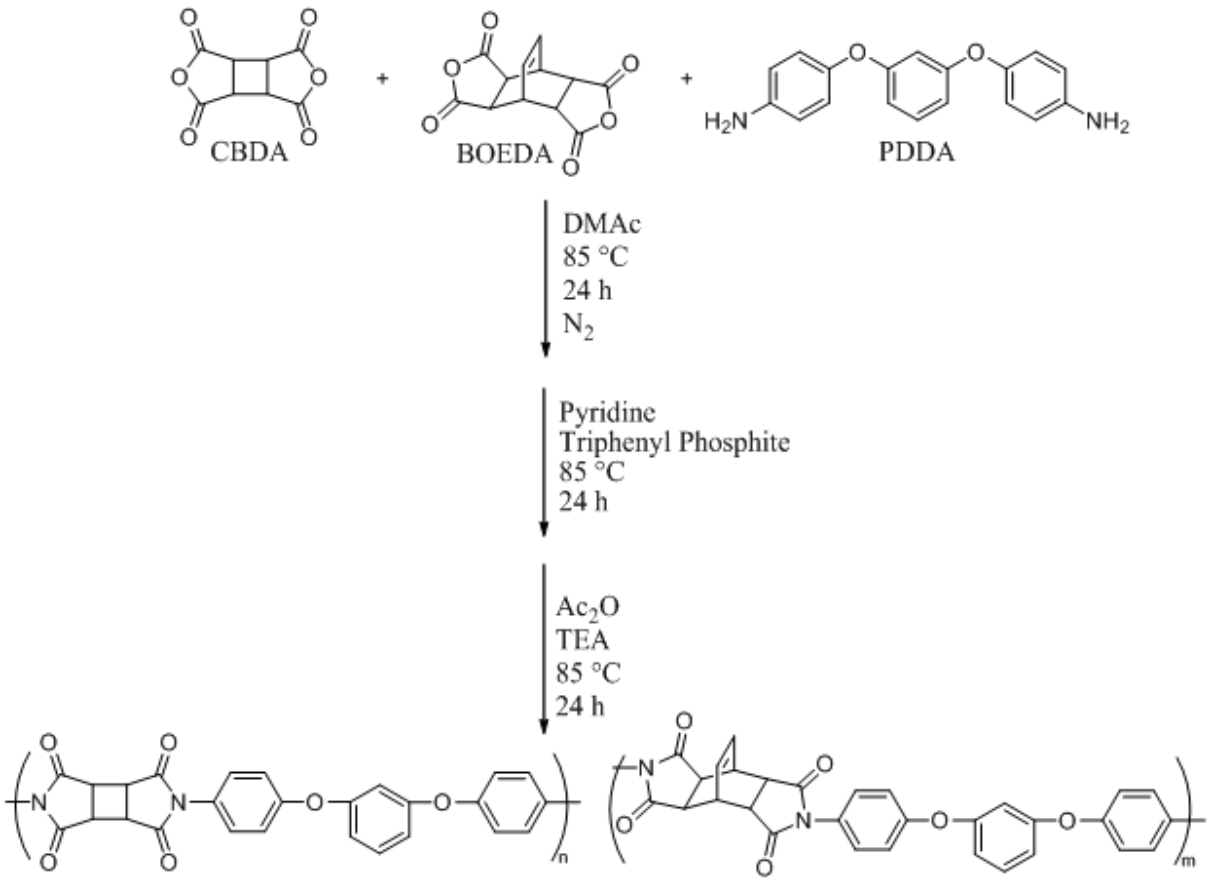

Scheme 4.1 Synthesis of dispersible polyimides containing CBDA and BOEDA via chemical imidization.

Poly(siloxane imide) Containing Cyclobutane Diimide

Subsequent efforts included the use of aminopropyl-terminated PDMS as a dispersibility enhancer, and as an enhancer of adhesive properties. McGrath et al. previously demonstrated that it is possible to dramatically increase the dispersibility of polyimides through incorporation of PDMS blocks in the polyimide mainchain.[25-29,35] Furthermore, several literature sources document that segmented poly(siloxane imides) will microphase separate into domains containing the polyimide blocks and domains containing the PDMS blocks, leading to favorable elastomeric properties.[21,23,24,30] Initially, chemical imidization was utilized in an attempt to yield

dispersible materials, as was the case with polyimides without PDMS blocks. However, this proved unsuccessful due to poor solubility of PDMS oligomers in dipolar, aprotic solvents. Therefore, another synthetic route was necessary.

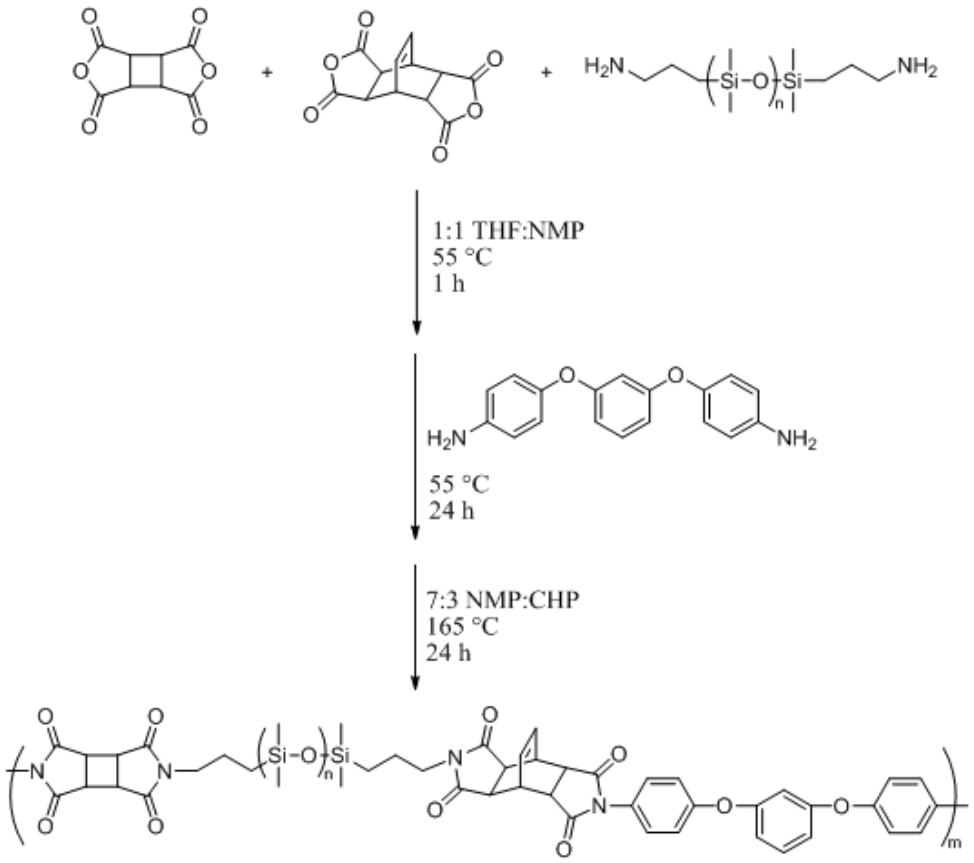

Scheme 4.2 Synthesis of poly(siloxane imides) containing cyclobutane diimide functionality.

McGrath et al. demonstrated the use of thermal solution imidization in a mixed solvent system that included an azeoptrope such as CHP.[4,21-30] This method proved successful and was utilized for the synthesis of a series of poly(siloxane imides) containing cyclobutane diimide units. **Scheme 4.2** demonstrates the synthesis of poly(siloxane imides) containing cyclobutane diimide functionality. The subsequent polymers were readily dispersible in THF, NMP, cyclopentanone, and DMF.

Table 4.2 Molecular weight and thermal analysis data for cyclobutane diimide-containing poly(siloxane imides).

Molar Feed Ratio							
PDMS	PDDA	CBDA	BOEDA	M_n[a] (g/mol)	M_w[a] (g/mol)	T_g[b] (°C)	$T_{d5\%}$[c] (°C)
0.5	0.5	0.7	0.3	17,000	47,000	-119	406
0.5	0.5	0.5	0.5	11,000	27,000	-121	420
0.5	0.5	0.3	0.7	13,000	30,000	-120	411

a) SEC - DRI, MALLS, THF, 40 °C, 1 mL/min; values relative to polystyrene standards
b) DSC - TA Instruments Q1000 DSC, 10 °C/min, N_2 purge 50 mL/min, 2nd heat
c) TGA - TA Instruments 2950 TGA, 10 °C/min, N_2 purge 50 mL/min

4.4.2 Characterization

Table 4.2 demonstrates compositions and molecular weight data for the series of synthesized cyclobutane diimide-containing poly(siloxane imides), as well as TGA and DSC analysis of the synthesized cyclobutane diimide-containing poly(siloxane imides). Molecular weights of the polymers obtained ranged from M_w of 27,000 to 47,000 with molecular weight distributions ranging from 2.3 to 2.7, and the polymers formed good films when solution cast from THF. The resulting films were tough, creaseable, and relatively transparent, albeit slightly colored. ^{1}H NMR confirmed in all cases that the feed composition closely matched the final composition of the polymer.

TGA and DSC were utilized to study the effects of composition on thermal properties of the synthesized polymers, as well as to evaluate thermal stability. TGA indicates that all polymers exhibit insignificant weight loss below 400 °C, suggesting thermal stability sufficient for flip bonding. The observed T_g of the poly(siloxane imide) was identical to that of the poly(dimethyl siloxane) macromonomer (T_g = -122 °C). This suggests microphase separation of the material into a polyimide domain (hard segment) and a PDMS domain (soft segment).

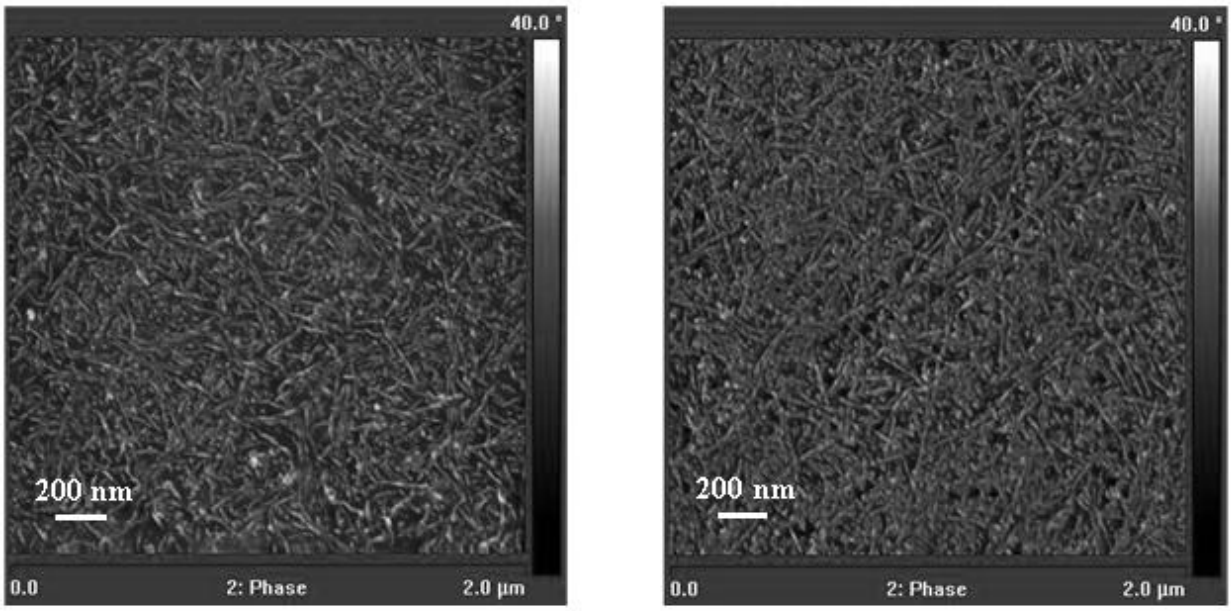

Figure 4.3 Atomic force micrographs showing phase images of cyclobutane diimide-containing poly(siloxane imides), which confirm microphase separation.

Atomic force microscopy (AFM) was utilized in order to confirm microphase separation of the poly(siloxane imides). The polymers were spin-coated from THF onto thin silicon wafers, and annealed under reduced pressure at 80 °C. The obtained micrographs of two CBDA:BOEDA compositions are shown in **Figure 4.3**, with lighter portions being the polyimide domain (hard segment), and the darker portions being the PDMS domain (soft segment). Although only one scale is shown, the surface properties do scale with variations in magnification. As expected, the surface morphology is microphase separated.

Table 4.3 Tensile data for cyclobutane diimide-containing poly(siloxane imides).

CBDA:BOEDA	Tensile stress at break (MPa)	Tensile strain at break (%)	Tensile stress at yield (MPa)	E Modulus (MPa)
7:3	4.6 +/- 0.5	55 +/- 11	5.4 +/- 0.6	49.6 +/- 9.9
5:5	6.2 +/- 0.4	114 +/- 9	6.5 +/- 0.7	46.0 +/- 5.0
3:7	6.5 +/- 2.4	234 +/- 67	7.6 +/- 1.4	38.2 +/- 3.3

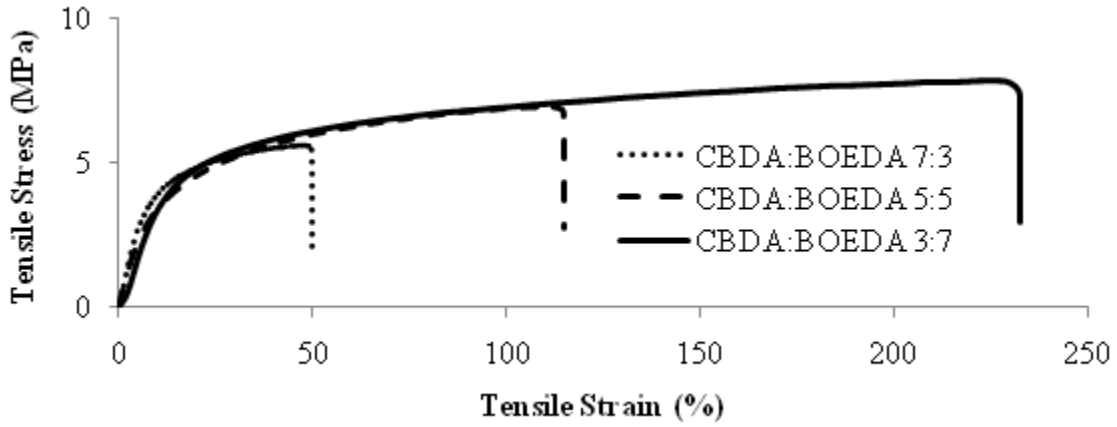

Figure 4.4 Tensile analysis of cyclobutane diimide-containing poly(siloxane imides).

Tensile testing (**Figure 4.4** and **Table 4.3**) and dynamic mechanical analysis (DMA) confirmed that the synthesized poly(siloxane imides) exhibited elastomeric properties. Representative DMA data is shown in **Figure 4.5**. As expected with elastomers, the DMA storage modulus demonstrated a marked decrease at approximately -110 °C. After the decrease, the storage modulus leveled off into a "rubbery plateau" which suggested elastomeric properties. This plateau is maintained until approximately 100 °C, giving these polymers an extremely wide temperature range during which the mechanical properties do not change significantly. From -50 °C to 100 °C the storage modulus diminished less than 100 MPa. This may prove exceptionally useful for adhesive applications that require little change in adhesive properties over a wide temperature range, such as flip bonding.

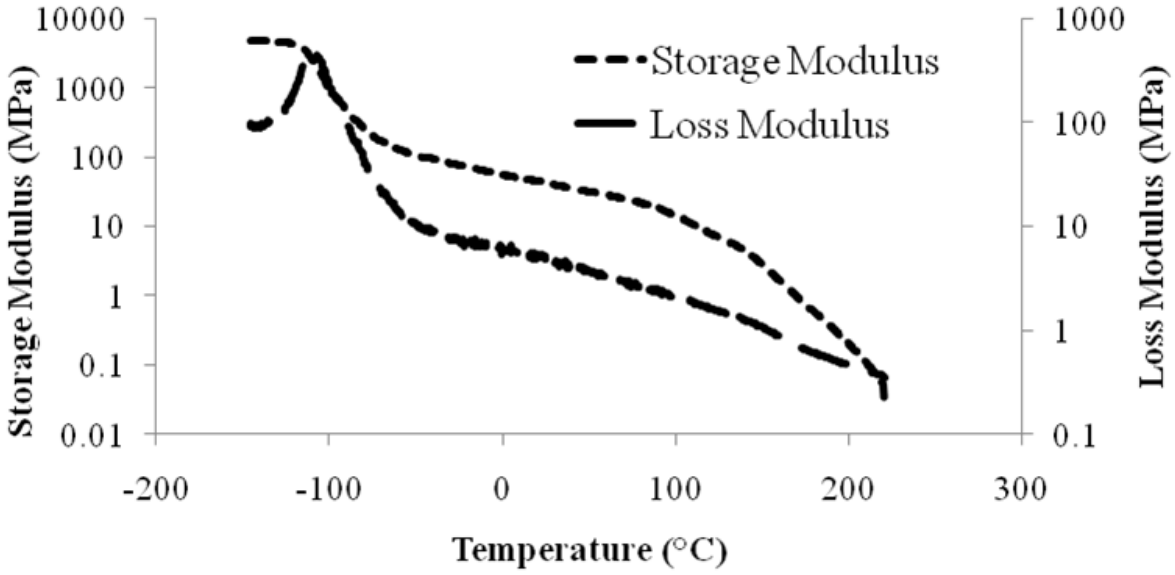

Figure 4.5 DMA of a representative cyclobutane diimide-containing poly(siloxane imide) demonstrates a rubbery plateau.

4.4.3 UV Irradiation Studies and Analysis

Decker et al. have previously demonstrated that bis-maleimides such as those formed upon the expected photo-degradation of cyclobutane diimide containing polyimides crosslink upon UV irradiation in the absence of a photo-initiator.[5] In order to ensure photo-cleavage in the absence of crosslinking, a model study was undertaken utilizing *N*-cyclohexyl maleimide (CyMI) (light tan powder), and the AIBN initiated homopolymer of the same (poly(CyMI)). Qualitative UV-visible spectroscopy of CyMI and poly(CyMI) is shown in **Figure 4.6**. Based upon this data, it is clear that imide and anhydride absorbances are distinctly different from those of maleimides. In order to efficiently photo-cleave the cyclobutane diimide units within the poly(siloxane imide) mainchain and prevent subsequent crosslinking of the formed maleimide residues, it is important to irradiate with a narrow bandwidth UV light centered in the region in which the anhydride and imide residues absorb but maleimides demonstrate no absorbance. For this purpose, all subsequent experiments were performed utilizing a lamp which provides a narrow source of UV light at 254 nm.

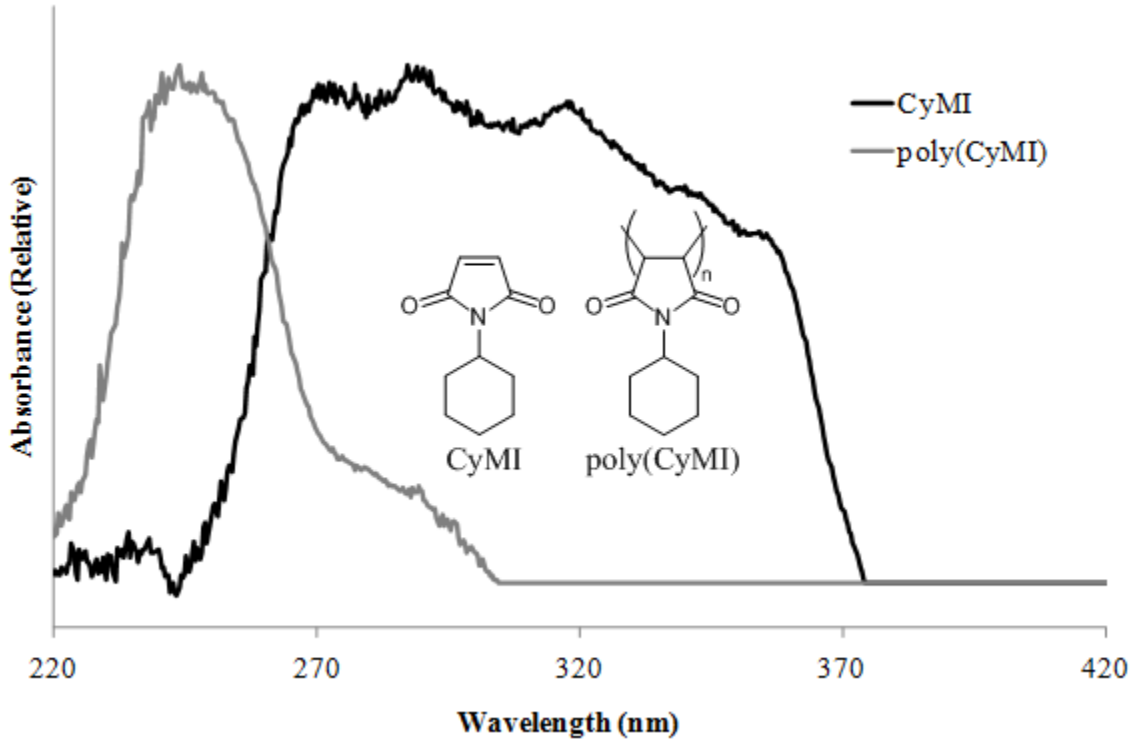

Figure 4.6 UV/Vis spectra of CyMI and poly(CyMI).

In order to obtain photo-cleavage in the absence of crosslinking, a narrow band UV source was utilized. CBDA-containing poly(siloxane imides) (0.7:0.3 CBDA:BOEDA) were exposed to UVC light at 254 +/- 10 nm in dosages ranging from 2.2-26 J/cm^2 UVC. The resulting films were entirely dispersible in THF and indicated no evidence of cross-linking. This finding confirmed the hypothesis obtained from the UV/Vis data as discussed above. **Figure 4.7** demonstrates a dramatic growth as a function of irradiation dosage in the peak corresponding to the formation of maleimide functionality in the ^{1}H NMR. As indicated in **Figure 4.7**, maleimide functionality forms as a function of irradiation dosage, confirming cleavage of the CBDA units in the polymer mainchain.

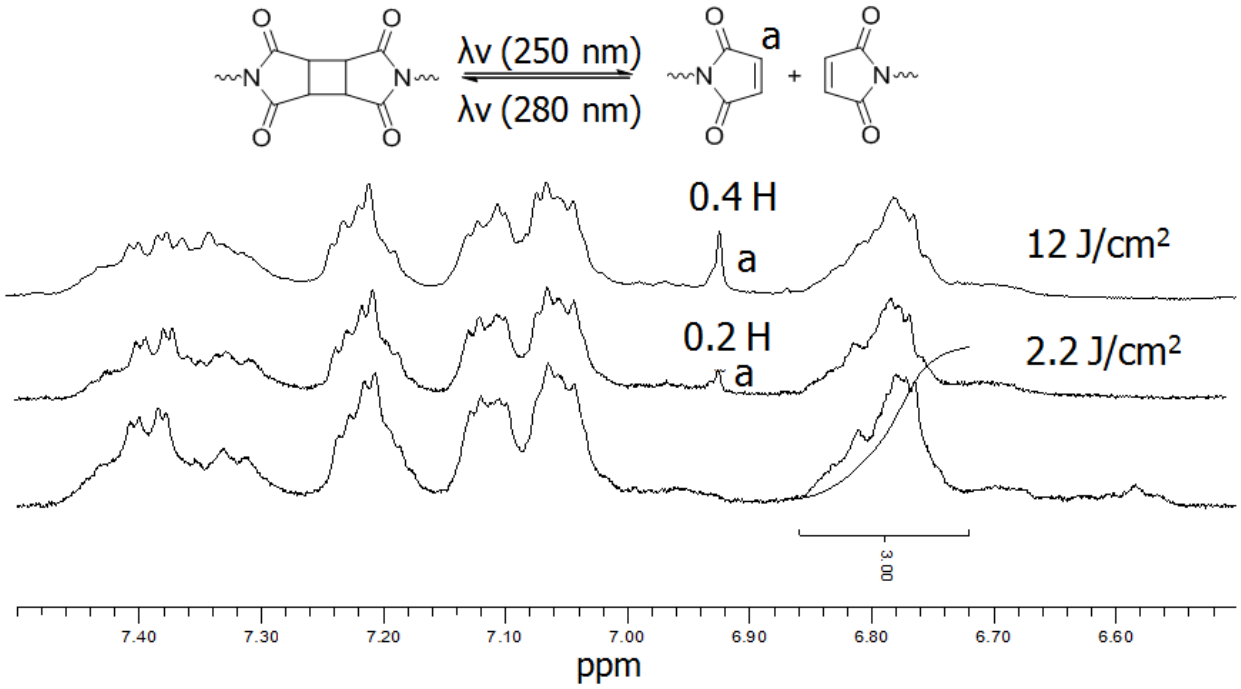

Figure 4.7 ^{1}H NMR spectroscopy demonstrates growth in peak corresponding to maleimide functionality as a function of UVC dose.

4.5 Conclusions

Photo-cleavable reversible structural adhesive poly(siloxane imides) containing photo-active cyclobutane diimide units within the mainchain were prepared *via* thermal solution imidization step-growth polymerization of CBDA, BOEDA, PDDA, and aminopropyl-terminated poly(dimethyl siloxane). Polymers were synthesized with varying compositions of CBDA, relative to BOEDA. Incorporation of PDMS blocks within the polyimide mainchain was necessary for dispersibility, adequate adhesion, and homogeneous film formability. Thermal and morphological testing indicated micro-phase separation, lending to the observation of elastomeric properties. Upon broad-spectrum UV irradiation, some crosslinking was observed. Model compound studies demonstrated the necessity for irradiation with a narrow UV band, centered at approximately 250 nm. Photo-cleavage in the absence of crosslinking was obtained

from the use of a narrow-spectrum UV source. Upon irradiation, ^{1}H NMR demonstrated an increase in the resonance corresponding to the formation of maleimide functionality, confirming cleavage of cyclobutane diimide functionality. These findings indicate that this system may provide a highly effective route for photo-reversible adhesion.

4.6 Acknowledgements

This material is based upon work supported in part by the U.S. Army Research Laboratory and the U.S. Army Research Office under the Army Materials Center of Excellence Program, contract W911NF-06-2-0014; in part by the Macromolecular Interfaces with Life Sciences (MILES) Integrative Graduate Education and Research Traineeship (IGERT) of the National Science Foundation grant under agreement No. DGE-0333378; and in part by Brewer Science, Inc. under contract # N00014-07-C-0797.

4.7 References

(1) Niklaus, F.; Stemme, G.; Lu, J. Q.; Gutmann, R. J. *J. Appl. Phys.* **2006**, *99*, 031101.
(2) Pillalamarri, S.; Puligadda, R.; Brubaker, C.; Wimplinger, M.; Pargfrieder, S. *J. Microelectron. Electron. Packag.* **2007**, *4*, 105.
(3) Puligadda, R.; Pillalamarri, S.; Hong, W.; Brubaker, C.; Wimplinger, M.; Pargfrieder, S. *Mater. Res. Soc. Symp. Proc.* **2007**, *970*, 239.
(4) Moyer, E. S.; Mohanty, D. K.; Shaw, J.; McGrath, J. E. *Int. SAMPE Electron. Conf.* **1989**, *3*, 894.
(5) Decker, C.; Bianchi, C.; Jönsson, S. *Polymer* **2004**, *45*, 5803.
(6) Kang, M.; Moon, B. *Macromolecules* **2009**, *42*, 455.
(7) Moore, J. A.; Dasheff, A. N. *Chem. Mater.***1989**, *1*, 163.
(8) Piggott, A. M.; Karuso, P. *Tetrahedron Lett.* **2005**, *46*, 8241.
(9) Suzuki, H.; Abe, T.; Takaishi, K.; Narita, M.; Hamada, F. *J. Polym. Sci., Part A: Polym. Chem.* **2000**, *38*, 108.
(10) Trenor, S. R.; Long, T. E.; Love, B. J. *Macromol. Chem. Phys.* **2004**, *205*, 715.
(11) Trenor, S. R.; Long, T. E.; Love, B. J. *J. Adhes.* **2005**, *81*, 213.
(12) Cashion, M. P.; Park, T.; Long, T. E. *J. Adhes.* **2009**, *85*, 1.
(13) Karikari, A. S.; Edwards, W. F.; Mecham, J. B.; Long, T. E. *Biomacromolecules* **2005**, *6*, 2866.
(14) Karikari, A. S.; Williams, S. R.; Heisey, C. L.; Rawlett, A. M.; Long, T. E. *Langmuir* **2006**, *22*, 9687.
(15) Trenor, S. R.; Long, T. E.; Love, B. J. *Eur. Polym. J.* **2005**, *41*, 219.
(16) Williams, S. R.; Barta, Z.; Ramirez, S. M.; Long, T. E. *Macromol. Chem. Phys.* **2009**, *210*, 555.
(17) Huyck, R. H.; Trenor, S. R.; Love, B. J.; Long, T. E. *J. Macromol. Sci., Part A: Pure Appl. Chem.* **2008**, *45*, 9.
(18) Saito, K.; Ingalss, L. R.; Lee, J.; Warner, J. C. *Chem. Commun.* **2007**, 2503.
(19) Viswanathan, K.; Ozhalici, H.; Elkins, C. L.; Heisey, C.; Ward, T. C.; Long, T. E. *Langmuir* **2005**, *22*, 1099.
(20) Yamauchi, K.; Lizotte, J. R.; Long, T. E. *Macromolecules* **2003**, *36*, 1083.
(21) Mahoney, C. M.; Gardella, J. A.; Rosenfeld, J. C. *Macromolecules* **2002**, *35*, 5256.
(22) Arnold, C. A.; Chen, Y. P.; Rogers, M. E.; Graybeal, J. D.; McGrath, J. E. *Int. SAMPE Electron. Conf.* **1989**, *3*, 198.
(23) Bott, R. H.; Summers, J. D.; Arnold, C. A.; Blankenship, C. P., Jr.; Taylor, L. T.; Ward, T. C.; McGrath, J. E. *Sampe J.* **1988**, *24*, 7.
(24) Bott, R. H.; Summers, J. D.; Arnold, C. A.; Taylor, L. T.; Ward, T. C.; McGrath, J. E. *J. Adhes.* **1987**, *23*, 67
(25) Arnold, C. A.; Summers, J. D.; Chen, Y. P.; Bott, R. H.; Chen, D.; McGrath, J. E. *Polymer* **1989**, *30*, 986.
(26) Yoon, T. H.; Arnold-McKenna, C. A.; McGrath, J. E. *J. Adhes.* **1992**, *39*, 15.
(27) Yoon, T. H.; McGrath, J. E. *High Perform. Polym.* **1992**, *4*, 203.
(28) McGrath, J. E.; Dunson, D. L.; Mecham, S. J.; Hedrick, J. L. In *Progress in Polyimide Chemistry I* 1999; Vol. 140, p 61.
(29) Kaltenecker-Commercon, J. M.; Ward, T. C.; Gungor, A.; McGrath, J. E. *J. Adhes.* **1994**, *44*, 85.

(30) Novák, I.; Sysel, P.; Zemek, J.; Spírková, M.; Velic, D.; Aranyosiová, M.; Florián, S.; Pollák, V.; Kleinová, A.; Lednický, F.; Janigová, I. *Eur. Polym. J.* **2009**, *45*, 57.
(31) Itamura, S.; Yamada, M.; Tamura, S.; Matsumoto, T.; Kurosaki, T. *Macromolecules* **1993**, *26*, 3490.
(32) Matsumoto, T.; Kurosaki, T. *Macromolecules* **1997**, *30*, 993.
(33) Gupta, N.; Varma, I. K. *J. Appl. Polym. Sci.* **1998**, *68*, 1759.
(34) Hsiao, S.-H.; Yang, C.-P.; Chen, Y.-C.; Wang, H.-M.; Guo, W. *J. Appl. Polym. Sci.* **2009**, *113*, 3993.
(35) Rogers, M. E.; Glass, T. E.; Mecham, S. J.; Rodrigues, D.; Wilkes, G. L.; McGrath, J. E. *J. Polym. Sci., Part A: Polym. Chem.* **1994**, *32*, 2663.

Chapter 5: Photo-Active Polyesters Containing *o*-Nitro Benzyl Ester Functionality for Photo-Deactivatable Adhesion

Stephen M. June[1], Takeo Suga[1], William H. Heath[1], Qin Lin[2], Rama Puligadda[2], Lei Yan[3], David Dillard[3], and Timothy E. Long[1*]

Department of Chemistry, Virginia Tech, Blacksburg, Virginia 24061-03, Brewer Science, Inc., 2401 Brewer Dr., Rolla, MO 65401, and Department of Engineering Science and Mechanics, Virginia Tech, Blacksburg, Virginia 24061-03

(From: Manuscript submitted to *The Journal of Adhesion*)

5.1 Abstract

The fabrication of modern microelectronic silicon devices mechanically challenges these thin silicon substrates during manufacturing operations. Melt and solution polyesterification enabled the synthesis of polyesters containing photoreactive *o*-nitro benzyl ester units for use as a potential photocleavable adhesive. Melt transesterification provided a solvent-free method for synthesis of 2-nitro-*p*-xylylene glycol (NXG) containing polyesters of controlled molecular weights. ^{1}H NMR spectroscopy confirmed the chemical composition of the photoactive polyesters. Size exclusion chromatography (SEC) determined the number-average molecular weights (M_n) of the polyesters synthesized in the range of 6000 g/mol to 12000 g/mol. ^{1}H NMR spectroscopy confirmed increasing levels of photocleavage of the *o*-nitro benzyl ester functionality with increasing exposure to broad wavelength UV irradiation, and exposure levels ranged from 0-187 J/cm^2 UVA. Photocleaveage of approximately 90% of the *o*-nitro benzyl ester (ONB) units within the backbone of the polymer occurred at maximum dosage. Wedge fracture testing revealed approximately a twofold decrease in fracture energy upon UV irradiation, suggesting that these structural adhesives offer potential for commercial "flip bonding" applications.

5.2 Introduction

There remains a sustained trend towards smaller and more advanced electronic components[1-5] in the microelectronics industry, which demands advancement of manufacturing techniques. Devices manufactured from mechanically brittle substrates, such as silicon wafers, often require advanced fabrication techniques such as "flip bonding" in order to prevent product damage and subsequent waste. This is due in part to the rigorous grinding and etching that occurs during manufacturing processes.[2] Thus, adhesion of the device wafer to a supporting substrate with a hot melt adhesives typically provides sufficient mechanical reinforcement to ensure device survival through the grinding and lithographic processes.[1-5]

The device must undergo a stressful removal process upon completion of the "flip bonding" production. In order to remove the device from the support substrate, the device and support substrate are commonly heated to soften or melt the adhesive and subsequently remove the product from the support. However, the repeated heating and cooling of the device leads to further product damage.[5] Due to thermal expansion and the differences in thermal expansion coefficients between silicon devices and support substrates, the heating and cooling cycles can lead to cracking, bending, folding, and warping.[6] An adhesive that withstands the production processes and allows for substrate removal at room temperature is a remaining challenge. It is desirable that this room-temperature debondable adhesive also operate without chemical debonding agents, (such as acid- or base-cleavable polymers or solvents). Chemical debonding agents for product removal are impractical due to lengthy time requirements for adhesive penetration and solvation.[1,2] However, an adhesive that contains a photo-cleavable unit within the backbone of the polymer in combination with a transparent support substrate may quickly decrease the adhesive properties without significant heating.[1-3] **Figure 5.1** shows a cartoon

representation of light-induced wafer debonding. In this cartoon, the blocks represent photocleavable chromophores within the backbone of a polymer chain. The chromophores photochemically cleave upon UV exposure, decreasing polymer molecular weight, and influencing the thermomechanical and adhesive properties.

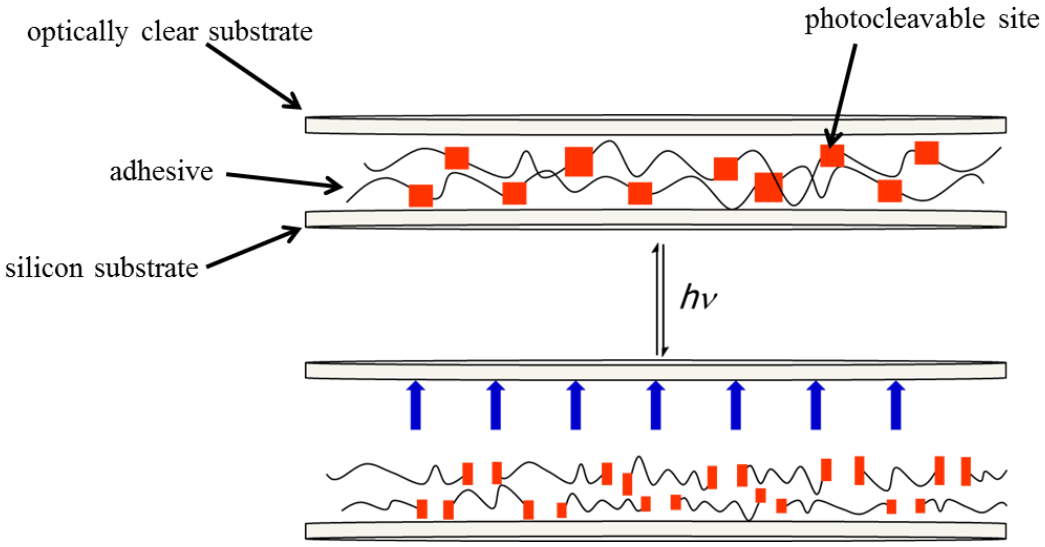

Figure 5.1 Light-induced product removal through photocleavage of the adhesive.

Several recent literature references cited the development of stimuli-responsive polymers for lithography,[7-11] tuning of hydrophobicity,[12-14] and reversible linkages of block copolymers.[15-22] Long et al. recently developed polymers containing photo-degradable units and photo-reversible adhesives. In particular, we demonstrated the utilization of cinnamate,[23,24] coumarin,[25-28] and cyclobutane diimide functionalities,[3] towards the development of photo-reactive coatings and adhesives. In addition, our group published research detailing the synthesis of star-shaped acrylic polymers with an acid labile core.[6] The literature richly describes the incorporation of photoactive sites in polymers either on pendant photo-reactive functionalities or linkages at the junction point of block copolymers.[13,15,17-19,22,25,29-36] Few investigations detailed

the synthesis of polymers with regular photoreactive units in the mainchain of a step-growth polymer.[3,9-11]

There are many literature examples disclosing *o*-nitro benzyl ester, amide, and ether functionalities as a photo-active protecting group for alcohols.[9,10,12,14,16,18,21,22,37-45] Several investigations also used *o*-nitro benzyl esters for photo-degradable units within the mainchain of polymers.[9,10,13,17-19,42] These units were typically linkers between segments or blocks rather than incorporated randomly within the polymer backbone, and the formation of the *o*-nitro benzyl ester in the principle polymerization step is absent from the literature. However, a main chain photoresponsive polyester adhesive requires that a photodegradable unit form during the polymerization process. For this purpose, we describe the utilization of 2-nitro-*p*-xylylene glycol for the synthesis of polyesters. This diol allowed for random placement of a photoresponsive functionality within a structural adhesive.

5.3 Experimental

5.3.1 Materials and Methods

2-nitro-p-xylylene glycol (NXG) was purchased from TCI and purified with repeated recrystallizations from chloroform. Isophthaloyl chloride (IPC) and 1,4-cyclohexane dimethanol (70:30 trans:cis – confirmed by ^{1}H NMR spectroscopy) (CHDM) were purchased from Aldrich and Alfa Aesar, respectively, and purified using vacuum distillation. Dimethyl isophthalate (DMIP), tetrabutylammonium iodide (TBAI), tetraethylammonium iodide (TEAI), sodium hydroxide, and titanium tetraisopropoxide were obtained from Aldrich and used without further purification. Purified water was obtained from a Millipore Milli-Q water purification system. Chloroform was purchased from Fischer and distilled from sodium and benzophenone.

Triethylamine (TEA) was purchased from Aldrich and distilled from calcium hydride. Tetrahydrofuran (THF), N,N'-dimethyl formamide (DMF), toluene, methanol, and dichloromethane (DCM) were purchased from Fischer and purified using an MBraun MB-SPS solvent purification system. All other chemicals were purchased from Aldrich and used as received.

^{1}H NMR was performed in THF-d_8, DMSO-d_6, or $CDCl_3$ at 23 °C with a Varian 400 MHz MR400 spectrometer. Thermogravimetric analysis (TGA) was performed with a TA Instruments Hi-Res TGA 2950 in a platinum pan under a nitrogen purge of 50 mL/min and a ramp rate of 10 °C/min. Dynamic scanning calorimetry was conducted with a TA Instruments Q1000 DSC at a heating rate of 10 °C/min and a cooling rate of 50 °C/min under a constant nitrogen purge of 50 mL/min. Glass transition temperatures (T_g's) were reported as mid-point temperatures from the second heat.

Size exclusion chromatography (SEC) was performed at 40 °C in THF or $CHCl_3$ (HPLC grade) at 1 mL/min on a Waters 707 Autosampler equipped with 3 in-line PLgel 5 mm MIXED-C columns, a Waters 410 refractive index detector, and an in-line Wyatt Technology Corp. mini-DAWN multiple angle laser light scattering (MALLS) detector. Reported number-average and weight-average molecular weights (M_n and M_w, respectively) are relative to polystyrene standards. UV irradiation was carried out using a Fusion UV Systems, Inc F300s series microwave powered, electrodeless, lamp source coupled with a LC-6B bench top conveyer at an intensity of 0.211 W/cm^2 in the UVC region, 1.513 W/cm^2 in the UVB region, and 2.044 W/cm^2 in the UVA region or using a Karl Suss Mask Aligner, model MA/BA6. The peak wavelength of the spectrum of the UV source was 365 nm and the UV intensity was 6.3 mW/cm^2. All photoactive samples were irradiated prior to mechanical tests for 1 and 10 minutes.

Wedge tests were performed to conform to ASTM D3762-03 standards. An adhesive sample was melt-pressed between two substrates, typically glass slides. Typical adhesive thickness was ~500 um. A wedge (typically a razor blade) was inserted between the slides in order to stress the adhesive. The length of the crack in the adhesive was measured using an electronic caliper. The glass-adhesive-glass substrate was then subjected to external stimuli, such as heat or UV exposure. Upon stimulus, the crack length increased, and was measured. Equation 1 was utilized to calculate the fracture energy.

5.3.2 Synthesis

Synthesis of o-nitro-dibenzyl ester containing poly(esters) in solution - In a representative synthesis, 0.58 g (3.2 mmols) NXG was dissolved in DMF in a 50-mL round-bottomed flask under argon. CHDM (0.60 g, 4.1 mmols), and IPC (1.34 g, 7.3 mmols) were added to the reaction solution separately as solutions in DMF. The solution was cooled to 0 °C, and TEA (1.48 g, 14.6 mmols) was added drop-wise. The reaction was stirred with magnetic stirring, allowed to rise to room temperature over 1 h and react for 18 h. The polymer was precipitated into methanol, collected upon vacuum filtration, washed 3x with water and methanol, and finally allowed to dry overnight at 60 °C at reduced pressure to yield a light brown powder.

Synthesis of o-nitro-dibenzyl ester containing poly(esters) in the melt - In a representative synthesis, 1.0 eq NXG, 1.5 eq CHDM, and 2.0 eq DMIP (1.25 excess of –OH functionality relative to $–COOCH_3$ functionality, excess diol subsequently removed under reduced pressure) were added to a 50-mL flask equipped with a nitrogen purge. 100 ppm of titanium tetraisopropoxide transesterification catalyst in butanol was added to the flask. The mixture was heated with mechanical stirring at 170 °C for 1 h, temperature was raised to 185 °C, and reaction

continued for another 2 h. The reaction was subsequently placed under reduced pressure (100 mTorr) and allowed to react for an additional 18 h. The flask was removed from the heat source and allowed to cool. The reddish-brown solid product was then removed from the flask and used without further treatment.

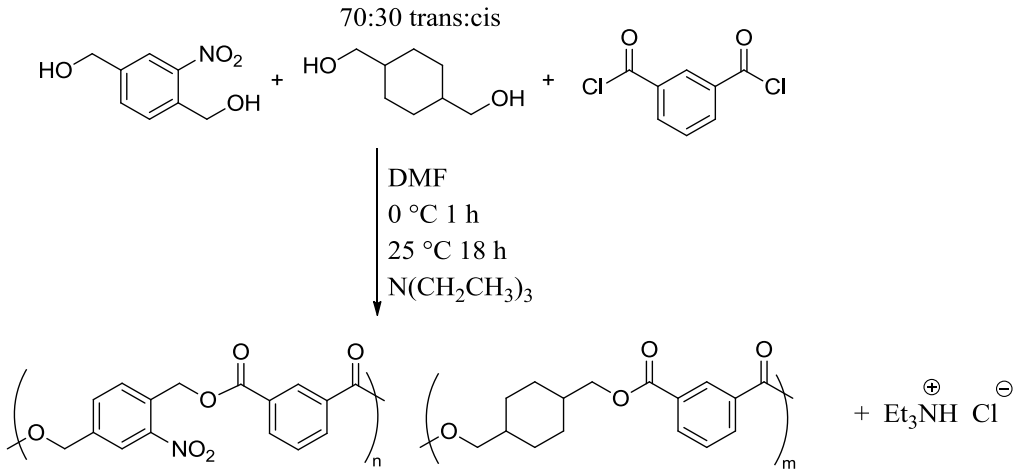

Scheme 5.1 Synthesis of *o*-nitro benzyl ester-containing polyesters in solution.

5.4 Results and Discussion

Solution polyesterification allowed for the synthesis of NXG-based polyesters containing *o*-nitro benzyl ester functionality. **Scheme 5.1** shows the synthesis of NXG-containing polyesters in solution. SEC revealed that the resulting polymers were oligomeric (M_n ~2,000 – 5,000), and as expected, formed brittle films when cast from chloroform. Melt transesterification provided an ideal alternative to solution polyesterification due to elimination of solvent and acid scavenger. An additional advantage of melt transesterification is the lack of stringent 1:1 stoichiometry requirements typical of most step-growth polymerizations, given a sufficiently volatile diol. This is due to the equilibrium nature of the transesterification reaction and the reduced pressures. Melt transesterifications are often performed at reaction temperatures approaching 300 °C with relatively short reaction times (~6 h). However, due to the low thermal stability of NXG, polyesterifications of NXG, CHDM, and DMIP were performed at 185 °C for

longer reaction times. A 70:30 trans:cis mixture of CHDM allowed for decreased crystallinity, which was also necessary due to the lower reaction temperatures.

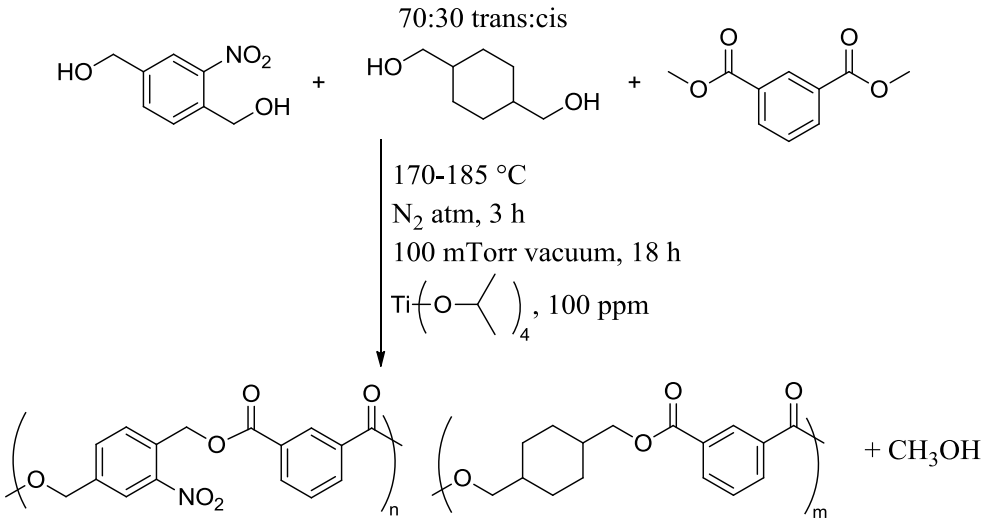

Scheme 5.2 Synthesis of *o*-nitro benzyl ester-containing polyesters using melt transesterification.

Melt transesterification as shown in **Scheme 5.2** successfully yielded polyesters containing *o*-nitro benzyl ester (ONB) units. **Table 5.1** details thermal transitions, thermal stabilities, and molecular weights of the NXG-containing polyesters synthesized using melt-transesterification. All obtained samples exhibited $T_{d5\%}$ above 275 °C, and DSC exhibited T_g's ranging from 68 and 84 °C. SEC demonstrated that the number-average molecular weights (M_n) of these samples varied from 6,000 g/mol to 12,000 g/mol. Upon high conversion, observed melt viscosities of the reaction mixtures containing NXG were very high. This observation offers a potential explanation for the abnormally high PDI values in these samples. The high viscosities likely limited the mobility of end-groups, which prevented typical reaction kinetics, and accordingly typical PDI values. The obtained polyesters formed free-standing films upon melt pressing.

Table 5.1 Comparison of thermal properties and molecular weights of *o*-nitro benzyl ester-containing polyesters.

Molar eq. NXG	Molar eq. CHDM	Molar eq. DMIP	T_g (°C)	$T_{d5\%}$ (°C)	M_n (g/mol)	M_w (g/mol)	M_w/M_n
0.5	0.75	1	84	296	6000	17000	2.8
0.2	1.0	1	83	290	9000	37000	4.1
0	2.25	1	68	383	12000	22000	1.8

After obtaining a series of ONB-containing polyesters, confirmation of the photocleavability of the photoactive polyesters remained critical. Spin-coating from chloroform onto either silicon or quartz wafers yielded films suitable for subsequent high intensity UV exposure experiments. Spin-coating was necessary in order to obtain films sufficiently thin for UV transmittance through the thickness of the film, ensuring that the entire bulk of the film received UV exposure. After spin coating, repeated passages under a UV Fusion® lamp equipped with a conveyor belt exposed the samples to high intensity UV light. Variation in the number of passes under the lamp provided differing UV doses. Doses ranged from 0 to 187 J/cm^2 of UVA exposure.

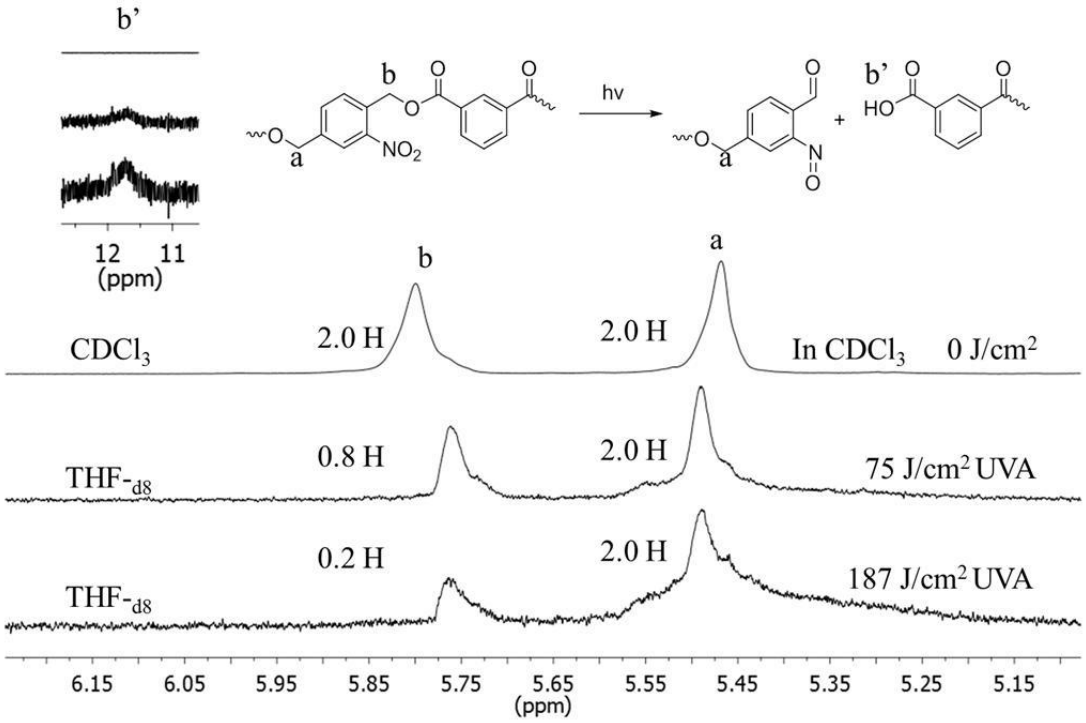

Figure 5.2 ^{1}H NMR spectroscopy demonstrates diminished integration as a function of UV exposure for the resonances corresponding to the *o*-nitro benzyl ester relative to the non-photoactive benzyl ester.

^{1}H NMR spectroscopy confirmed a significant decrease in the resonance corresponding to the *o*-nitro benzyl ester relative to the non-photo reactive *m*-nitro benzyl ester resonance with increasing UV exposure. These results confirmed the photo-degradation of the polyester. **Figure 5.2** demonstrates the ^{1}H NMR of ONB-containing polyesters as a function of UV exposure. These results suggest that the molecular weight, and thereby the adhesive and thermomechanical properties of these materials are significantly diminished upon UV exposure.

Wedge fracture tests allowed for confirmation of the photoinduced debonding of the adhesive properties of ONB-containing polyesters. Either the ONB-containing (25 % ONB functionality) melt polyester or WaferBOND® HT-10.10, a commercial adhesive for flip bonding from Brewer Scientific, was melt-pressed between two glass slides. Insertion of a thin

wedge between the two slides stressed the adhesive. Typical adhesive layer thickness was ~500 um. After external stimuli (UV exposure or temperature), a crack formed in the adhesive. The length of this crack directly related to the fracture energy of the adhesive where the fracture energy, G_c equals

$$G_c = \frac{3Et^3\Delta^2}{16a^4} \qquad \text{Equation 1}$$

where E is the Young's modulus of the material, t is the thickness of the glass slides, Δ is the thickness of the wedge, and a is the crack length. **Figure 5.3** is a cartoon representation of this wedge test.

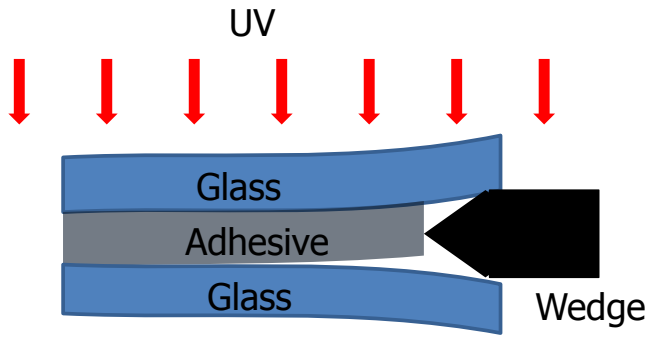

Figure 5.3 Cartoon demonstrating ASTM D3762-03 wedge testing to determine fracture energy.

The results of the wedge testing are shown in **Figure 5.4** as fracture energy as a function of UV exposure time for the synthesized CHDM:NXG polyester and temperature for Brewer Scientific's WaferBOND® HT-10.10. Prior to UV exposure, the synthesized ONB-containing polyester demonstrated a fracture energy of ~3.4 J/cm^2. After a UV dose of 378 mJ/cm^2, the fracture energy dropped ca. 5%. After maximum UV dosage of 3780 mJ/cm^2, the fracture energy was significantly diminished to ~1.6 J/cm^2. Errors were smaller than the size of the plot points in **Figure 5.4.** Brewer Scientific's WaferBOND® HT-10.10 provided utility as a control. Prior to heating, WaferBOND® HT-10.10 exhibited a fracture energy of ~2.6 J/cm^2. After heating to the recommended debonding temperature for "flip bonding", the fracture energy

decreased to ~0.6 J/cm^2. Both the ONB-containing polyester and the WaferBOND® HT-10.10 control exhibited approximately a 2 J/cm^2 loss in fracture energy upon external stimuli (UV exposure and temperature, respectively). This indicated that these adhesives may successfully act as photo-induced removable adhesives for flip bonding.

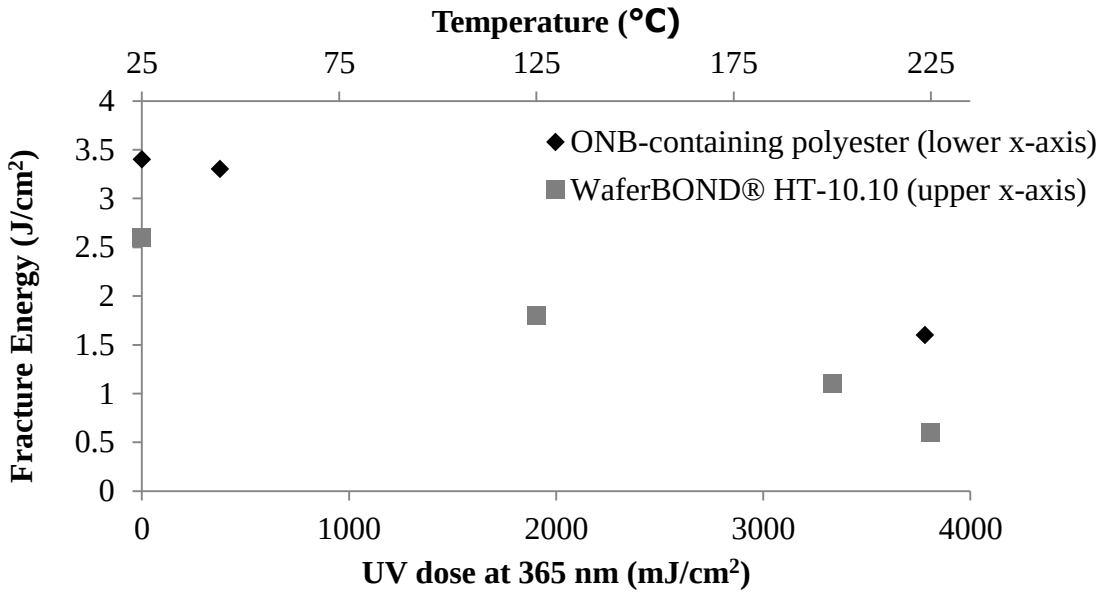

Figure 5.4 ASTM testing demonstrates diminished fracture energy upon UV irradiation for CHDM melt polyester which contain *o*-nitro benzyl ester units in the polymer mainchain.

5.5 Conclusions

Melt transesterification allowed for the successful synthesis of a series of photo-reactive polyester adhesives which contain *o*-nitro benzyl ester units in the polymer mainchain. SEC determined that the synthesized polyesters exhibited moderate molecular weights with M_n's ranging between 6,000 and 12,000 g/mol. TGA confirmed that the ONB-containing polyesters exhibited reasonable thermal stability. DSC demonstrated that the T_g's of the synthesized polymers ranged between 68 and 83 °C. ^{1}H NMR provided spectroscopic confirmation of the photo-reactivity of the synthesized adhesives. ASTM testing demonstrated the ability of these adhesive to undergo a photo-induced debonding. The resulting decrease in fracture energy of the photoactive polyester was similar to the decrease in fracture energy of WaferBOND® HT-10.10

upon an increase in temperature. These results indicate that the synthesized adhesives may possess utility for photoinduced room temperature removable adhesives for flip bonding applications without the requirement of temperature induced debonding.

5.6 Acknowledgements

This research was supported by Brewer Science, Inc. under contract # N00014-07-C-0797.

5.7 References

(1) Pillalamarri, S.; Puligadda, R.; Brubaker, C.; Wimplinger, M.; Pargfrieder, S. *J. Microelectron. Electron. Packag.* **2007**, *4*, 105.
(2) Puligadda, R.; Pillalamarri, S.; Hong, W.; Brubaker, C.; Wimplinger, M.; Pargfrieder, S. *Mater. Res. Soc. Symp. Proc.* **2007**, *970*, 239.
(3) June, S. M.; Suga, T.; Heath, W. H.; Long, T. E.; Lin, Q.; Puligadda, R. *J. Adhes.* **2010**, *86*, 1012
(4) Niklaus, F.; Stemme, G.; Lu, J. Q.; Gutmann, R. J. *J. Appl. Phys.* **2006**, *99*, 031101.
(5) Ma, Y.; Chan, Y. C. *J. Mater. Sci.* **2007**, *42*, 6658.
(6) Kilian, L.; Wang, Z.-H.; Long, T. E. *J. Polym. Sci., Part A: Polym. Chem.* **2003**, *41*, 3083.
(7) Maekawa, Y.; Kato, J.; Katakai, M.; Ishihara, M.; Enomoto, K.; Hagiwara, T.; Ishii, T.; Itoh, K.; Koshikawa, H.; Yoshida, M. *Macromol. Chem. Phys.* **2008**, *209*, 625.
(8) Yagci, Y.; Jockusch, S.; Turro, N. J. *Macromolecules* **2010**, *43*, 6245.
(9) Feng, K.; Matsumoto, T.; Kurosaki, T. *J. Photopolym. Sci. Technol.* **1996**, *9*, 347.
(10) Feng, K.; Matsumoto, T.; Kurosaki, T. *Chem. Mater.* **1997**, *9*, 1362.
(11) Moore, J. A.; Dasheff, A. N. *Chem. Mater.* **1989**, *1*, 163.
(12) Awaji, H.; Kamikita, M.; Mizunuma, S.; JP 89-281135, 1991, p 20
(13) Goldbach, J. T.; Russell, T. P.; Penelle, J. *Polym. Prepr.* **2002**, *43*, 470.
(14) Hanson, J. E.; Reichmanis, E.; Houlihan, F. M.; Neenan, T. X. *Chem. Mater.* **1992**, *4*, 837.
(15) Gattas-Asfura, K. M.; Weisman, E.; Andreopoulos, F. M.; Micic, M.; Muller, B.; Sirpal, S.; Pham, S. M.; Leblanc, R. M. *Biomacromolecules* **2005**, *6*, 1503.
(16) Johnson, J.; Koberstein, J. T.; Turro, N. J.; WO US41270, 2008, p 53
(17) Johnson, J. A.; Baskin, J. M.; Bertozzi, C. R.; Koberstein, J. T.; Turro, N. J. *Chem. Commun.* **2008**, 3064.
(18) Johnson, J. A.; Finn, M. G.; Koberstein, J. T.; Turro, N. J. *Macromolecules* **2007**, *40*, 3589.
(19) Kang, M.; Moon, B. *Macromolecules* **2009**, *42*, 455.
(20) Karikari, A. S.; Williams, S. R.; Heisey, C. L.; Rawlett, A. M.; Long, T. E. *Langmuir* **2006**, *22*, 9687.
(21) Natt, F. J.-C.; Hunziker, J.; WO 2007-EP337, 2007, p 38
(22) Piggott, A. M.; Karuso, P. *Tetrahedron Lett.* **2005**, *46*, 8241.
(23) Cashion, M. P.; Park, T.; Long, T. E. *J. Adhes.* **2009**, *85*, 1.
(24) Williams, S. R.; Barta, Z.; Ramirez, S. M.; Long, T. E. *Macromol. Chem. Phys.* **2009**, *210*, 555.
(25) Huyck, R. H.; Trenor, S. R.; Love, B. J.; Long, T. E. *J. Macromol. Sci., Part A: Pure Appl. Chem.* **2008**, *45*, 9.
(26) Trenor, S. R.; Long, T. E.; Love, B. J. *Macromol. Chem. Phys.* **2004**, *205*, 715.
(27) Trenor, S. R.; Long, T. E.; Love, B. J. *J. Adhes.* **2005**, *81*, 213.
(28) Trenor, S. R.; Long, T. E.; Love, B. J. *Eur. Polym. J.* **2005**, *41*, 219.
(29) Decker, C.; Bianchi, C.; Jönsson, S. *Polymer* **2004**, *45*, 5803.
(30) Gumbley, P.; Koylu, D.; Thomas, S. W. *Macromolecules* **2011**.
(31) He, J.; Tong, X.; Zhao, Y. *Macromolecules* **2009**, *42*, 4845.

(32) Hirota, S.; Fujimoto, Y.; Choi, J.; Baden, N.; Katagiri, N.; Akiyama, M.; Hulsker, R.; Ubbink, M.; Okajima, T.; Takabe, T.; Funasaki, N.; Watanabe, Y.; Terazima, M. *J. Am. Chem. Soc.* **2006**, *128*, 7551.
(33) Koylu, D.; Carter, K. R. *Macromolecules* **2009**, *42*, 8655.
(34) Schumers, J.-M.; Gohy, J.-F.; Fustin, C.-A. *Polym. Chem.* **2010**, *1*, 161.
(35) Zhao, Y. *J. Mater. Chem.* **2009**, *19*, 4887.
(36) Zhao, Y.; Bertrand, J.; Tong, X.; Zhao, Y. *Langmuir* **2009**, *25*, 13151.
(37) Cameron, J. F.; Frechet, J. M. J. *J. Am. Chem. Soc.* **1991**, *113*, 4303.
(38) Case, F. H. *J. Am. Chem. Soc.* **1925**, *47*, 3005.
(39) de la Torre, B. G.; Albericio, F. *e-EROS Encycl. Reagents Org. Synth.* **2001**, No pp given.
(40) de la Torre, B. G.; Eritja, R.; Albericio, F. *e-EROS Encycl. Reagents Org. Synth.* **2001**, No pp given.
(41) Frechet, J. M. J.; Leung, M.-k.; Urankar, E. J.; Willson, C. G.; Cameron, J. F.; MacDonald, S. A.; Niesert, C. P. *Chem. Mater.* **1997**, *9*, 2887.
(42) Hayase, S.; Onishi, Y.; Horiguchi, R. *J. Electrochem. Soc.* **1987**, *134*, 2275.
(43) Il'ichev, Y. V.; Schworer, M. A.; Wirz, J. *J. Am. Chem. Soc.* **2004**, *126*, 4581.
(44) Matsubara, S.; Nakai, H.; Urano, T.; Murakami, S.; JP 87-81375, 1988, p 7
(45) Nishi, T.; Onodera, J.; Abe, Y.; Sakai, K.; Yui, T. *Yamagata Daigaku Kiyo Kogaku* **1968**, *10*, 9.

Chapter 6: Segmented Block Copolyesters Using Click Chemistry

Stephen M. June, Philippe Bissel, and Timothy E. Long*

Department of Chemistry, Macromolecules and Interfaces Institute, Virginia Tech, Blacksburg, Virginia 24061-0344

(From: Manuscript Submitted to *Journal of Polymer Science Part A; Polymer Chemistry*)

6.1 Abstract

Copper(I) catalyzed azide-alkyne 1,3-Huisgen cycloaddition (click) chemistry was used for the synthesis of triazole-containing polyesters and segmented block copolyesters at moderate temperatures. Triazole-containing homopolyesters exhibited significantly increased (~40 °C) glass transition temperatures (T_g) relative to conventionally synthesized polyesters with analogous structures. Synthesis of azido-terminated poly(propylene glycol) (PPG) allowed for the preparation of segmented polyesters, which exhibited increased dispersibility and film flexibility relative to triazole-containing homopolyesters. Differential scanning calorimetry (DSC) demonstrated a soft segment (SS) T_g near -60 °C for the segmented polyesters, consistent with microphase separation. Tensile testing revealed Young's moduli ranging from 7 to 133 MPa as a function of hard segment (HS) content, and stress at break values approached 10 MPa for 50 wt % HS segmented click polyesters. Dynamic mechanical analysis demonstrated an increased rubbery plateau modulus with increased HS content, and the T_g's of both the SS and HS did not vary with composition, suggesting microphase separation. Atomic force microscopy (AFM) confirmed microphase separated and semicrystalline morphologies for the obtained segmented click polyesters. This is the first report detailing the preparation of segmented copolyesters using click chemistry.

6.2 Introduction

Polyesters, which Wallace Carothers pioneered in the 1930s,[1] possess a wide range of uses, including fibers, beverage bottles, liquid crystalline materials, and coatings. The primary method for synthesis of polyesters involves the polycondensation of a glycol and either a dicarboxylic acid or a dimethyl ester. These reactions, typically performed in the melt, require extremely high temperatures and metal catalysts to obtain high conversion and molecular weight. In addition, most common polyesters exhibit glass transition temperatures (T_g's) below 110 °C.[2] Utilization of a lower temperature polyaddition which does not require expensive metal catalysts may offer advantages over traditional polyesterification. Segmented block copolymers offer many advantages over classical thermoplastic high performance polymers. Addition of a flexible soft segment (SS) often offers increased dispersibility compared to the homopolymer of a rigid hard segment (HS). In addition, segmented block copolymers typically exhibit microphase separation, leading to elastomeric properties. Classical examples of segmented block copolymers include segmented polyurethanes, poly(siloxane imides), and poly(urethane ureas). Our research group recently published several papers on the synthesis of segmented block copolymers.[3-8] In addition, our group maintains a significant interest in polyester synthesis,[9-15] and the synthesis of high performance materials using step-growth polymerization.[16-21]

Copper(I) catalyzed azide-alkyne 1,3-Huisgen cycloaddition (CuAAC) exhibits a wide variety of advantages in the synthesis of polymeric materials. Sharpless and coworkers first coined the term click chemistry to describe CuAAC in the early 2000s.[22] This reaction proceeds at relatively low reaction temperatures, in a wide variety of solvents, and exhibits a remarkable tolerance to the presence of other functional groups. In addition, the reaction proceeds quantitatively, with no reaction byproducts. [23-25] For these reasons, click chemistry featured

prominently in many polymer publications in recent years as a convenient route towards polymer coupling,[26-30] post-polymerization pendant functionalization,[27,31,32] and the synthesis of star and graft copolymers.[30,33] Relatively few examples exist where azido-alkyne coupling provides the principle polymerization step, however some examples do exist. In particular, due to its quantitative nature, azido-alkyne coupling regularly finds utility in the synthesis of dendrimers.[25,33-38] Voit and coworkers first reported step-growth polyaddition using click chemistry in the synthesis of hyperbranched polymers, although the product exhibited insignificant solubility.[39] In 2008, Shi and coworkers described the first soluble, hyperbranched triazole-containing polymer.[40,41]

The literature presents fewer examples of utilization of click chemistry as the principle polymerization step towards linear polymers; however, some key examples do exist.[33,42] Only two reports describe the synthesis of "click polyesters", or polyesters where click chemistry acts as the principle polymerization step. Takasu and coworkers reported in 2009,[43] and again in 2010,[44] the synthesis of thermally stable linear polyesters using click chemistry. However, Takasu also reported limited solubility without thermomechanical properties, and most monomers utilized exhibited linear, aliphatic structures. The synthesis of aromatic or alicyclic click polyesters and determination of their mechanical properties remains unprecedented.

In this manuscript, we present the synthesis of polyesters and segmented copolyesters using click chemistry. Comparison of analagous polyesters which did not contain triazole units in the backbone with triazole-containing polyesters revealed a dramatic increase in glass transition temperature (T_g) upon triazole incorporation; however, the click polyesters exhibited brittleness and poor dispersibility. Utilization of azido-terminated poly(propylene glycol) macromonomers allowed for the synthesis of segmented click polyesters. The segmented click

polyesters exhibited dispersibility in a variety of solvents and formed mechanically robust films. Thermal and mechanical testing confirmed the microphase separated and elastomeric nature of these materials, and atomic force microscopy (AFM) further revealed microphase separated and semicrystalline morphologies.

6.3 Experimental

6.3.1 Methods and Materials. Terephthaloyl chloride, dimethyl isophthalate, titanium(IV) tetraisopropoxide, 2-bromoethanol, sodium azide, 1,4-butanediol, tetrabutylammonium bromide (TBAB) and diethylene glycol were purchased from Aldrich, isophthaloyl chloride, 6-bromohexanoyl chloride, propiolic acid, and cyclohexane dimethanol (70:30 trans:cis) from Alfa Aesar, and *p*-toluenesulfonic acid (pTsA) from Fluka and were used without further purification. Eastman Chemical, Inc generously donated cyclohexane dimethanol (99% trans) and Bayer MaterialScience kindly provided PPG 4200, 2200 (Aclaim) and 1000 (Arcol). Chloroform, N,N-dimethylformamide, N-methylpyrrolidone, dimethylsulfoxide, and tetrahydrofuran were purchased from Fisher Scientific and used as received. Dichloromethane and triethylamine were purchased from Fisher Scientific and distilled from calcium hydride. ^{1}H and ^{13}C NMR spectra were recorded on a 400-MHz Varian Inova spectrometer. Chemical shifts are reported in ppm downfield from the internal standard tetramethylsilane (TMS). Spin multiplicities are reported as s (singlet), d (doublet), t (triplet) or m (multiplet).

Thermogravimetric analysis (TGA) was conducted on a TA Instruments Hi-Res TGA 2950 at a temperature ramp rate of 10 °C/min under a N_2 atmosphere. Glass transition temperatures (T_g) were reported from the 2^{nd} heat of a heat/cool cycle (0°C to 150°C) at a heating rate of 10 °C/min and a cooling rate of 50 °C/min on a TA Instrument DSC Q1000 under

N_2. Compression molding provided films for mechanical testing and all samples were melt pressed at 200 °C for approximately 2 min at ~15,000 psi. All samples were annealed at 150 °C for a minimum of 18 h prior to use. Dynamic mechanical analysis (DMA) was performed on a TA Instruments DMA Q800 under an N_2 atmosphere in tension mode with strains of 15 um, frequencies of 1 Hz, and a ramp rate of 3 °C/min. Tensile testing was performed using sample strips on an Instron 5500R tensile frame with a crosshead speed of 50 mm/min. Atomic force microscopy (AFM) was performed in tapping mode on a Veeco Multimode AFM using a low force constant (5 N/m) tip.

6.3.2 Synthesis

Synthesis of Bis(2-bromoethyl)terephthalate (BrTP) (1). The dropwise addition of 2-bromoethanol (14 mL, 200 mmol) in CH_2Cl_2 (50 mL) to a solution of terephthaloyl chloride (10 g, 49 mmol), and $N(Et)_3$ (28 mL, 200 mmol) in CH_2Cl_2 (100 mL) at 0 °C followed by subsequent stirring at 23 °C for 20 h and washing with 5% aqueous solution of K_2CO_3 (3 x 50 mL), water (2 x 50 mL) and drying over $MgSO_4$ yielded **1** as a yellow solid. The crude product was recrystallized from ethyl acetate to give pure **1** (13.05 g, 70%) as white crystals; ^{1}H NMR ($CDCl_3$, 500 MHz) δ 3.26 (t, 4H), 4.26 (t, 4H), 7.45 (s, 4H).

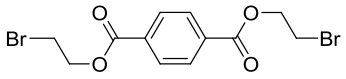

1

Synthesis of Bis(2-azidoethyl)terephthalate (BATP) (2). A mixture of **1** (10 g, 34 mmol), NaN_3 (17.6 g, 270 mmol), and TBAB (0.55 g, 1.7 mmol) in DMF (50 mL) was heated at 80 °C for 48 h. After cooling, a saturated aqueous solution of LiBr (50 mL) was added and the mixture was extracted with ethyl acetate (3 × 50 mL). The combined organic phases were

washed with water (3 × 50 mL), brine (50 mL), dried over $MgSO_4$ and the solvent removed under rotary evaporation. The crude was recrystallized from ethyl acetate to give **2** (mp 81 – 83 °C) (7.62 g, 59%) as white crystals; ^1H NMR ($CDCl_3$, 500 MHz) δ 3.62 (t, 4H), 4.52 (t, 4H), 8.14 (s, 4H).

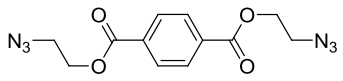

2

Synthesis of Bis(2-bromoethyl)isophthalate (BrIP) (3). A mixture of isophthaloyl chloride (27.3 g, 0.13 mol), $N(Et)_3$ (75 mL, 0.54 mol) in CH_2Cl_2 (400 mL), 2-bromoethanol (38 mL, 0.54 mol) in CH_2Cl_2 (50 mL) was added dropwise at 0 °C. The mixture was stirred at room temperature for 20 h. The mixture was washed with 5% aqueous solution of K_2CO_3 (3 x 150 mL), water (2 x 150 mL) and dried over $MgSO_4$. The crude was purified by SiO_2 chromatography ($CHCl_3$/hexanes 7:3) to give **3** (35.3 g, 72%) as white crystals; ^1H NMR ($CDCl_3$, 500 MHz) δ

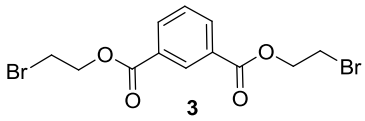

3

Synthesis of Bis(2-azidoethyl)isophthalate (BAIP) (4). A mixture of **3** (19.5 g, 52 mmol), NaN_3 (26.8 g, 410 mmol), and TBAB (0.84 g, 2.6 mmol) in DMF (100 mL) was heated at 80 °C for 48 h. After cooling, a saturated aqueous solution of LiBr (100 mL) was added and the mixture was extracted with ethyl acetate (3 × 100 mL). The combined organic phases were washed with water (3 × 100 mL), brine (100 mL), dried over $MgSO_4$ and the solvent removed under rotary evaporation. The crude was purified by SiO_2 chromatography ($CHCl_3$/hexanes 8:2)

to give **4** (13.0 g, 66%) as white crystals; (mp 73 – 75 °C) ^{1}H NMR ($CDCl_3$, 500 MHz) δ 3.63 (t, 4H), 4.53 (t, 4H), 7.59 (t, 1H), 8.28 (d, 2H), 8.75 (m, 1H).

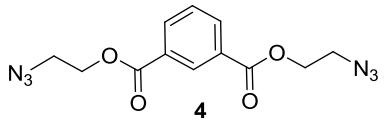

4

Synthesis of *trans*-1,4-Cyclohexyl Dimethylene Dipropiolate (T-CHDMDP) (5). A solution of *trans-1*,4-cyclohexyl dimethanol (5g, 35 mmol), pTsA (14.6 g, 77 mmol) and propiolic acid (8.6 mL, 143 mmol) in benzene (100 mL) was heated under reflux for 20 h. The mixture was washed with water (3 x 100 mL), brine (100 mL) and dried over $MgSO_4$. The solvent was removed under rotary evaporation. The crude was purified using SiO_2 chromatography ($CHCl_3$/Hex 7:3) to give **5** (5.65 g, 65%) as white crystals; (mp 119 – 121 °C) ^{1}HNMR ($CDCl_3$, 500 MHz) δ 1.04 (m, 4H), 1.68 (m, 2H), 1.85 (m, 4H), 2.89 (s, 2H), 4.03 (d, 4H);

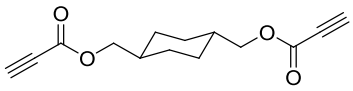

5

Synthesis of *cis/trans*-1,4-Cyclohexyl Dimethylene Dipropiolate (70:30-CHDMDP) (6). A solution of *cis/trans*-1,4-cyclohexyl dimethanol (70:30 trans:cis) (5.5 g, 38 mmol), pTsA (15.9 g, 84 mmol) and propiolic acid (9.3 mL, 155 mmol) in benzene (100 mL) was heated under reflux for 20 h. The mixture was washed with water (3 x 100 mL), brine (100 mL) and dried over $MgSO_4$. The solvent was removed under rotary evaporation and the crude was recrystallized from hexanes/ethyl acetate to give **6** (4.43 g, 47%) as white crystals; (mp 109 – 113 °C) ^{1}HNMR ($CDCl_3$, 500 MHz) δ 1.04 (m, 4H), 1.68 (m, 2H), 1.85 (m, 4H), 2.89 (s, 2H), 4.03 (d, 4H)

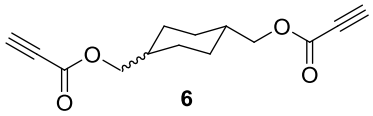

6

Synthesis of 1,4-Butanedipropiolate (8). To a solution of 1,4-butanediol (4.3 g, 48 mmol) in $CHCl_3$ (100 mL), pTsA (106 mmol) and propiolic acid (192 mmol) were added at 23 °C. The solution was heated under reflux for 18 h. After cooling, the solution was washed with an aqueous saturated $NaHCO_3$ solution (50 mL), water (3 x 50 mL), brine (50 mL) and dried over $MgSO_4$. The solvent was removed under rotary evaporation and the crude was recrystallized from hexanes/ethyl acetate to give compound **8** as pale yellow crystals. (mp 56 – 58 °C) (6.02 g, 65%); ^{1}H NMR ($CDCl_3$, 500 MHz) δ 1.79 (m, 4H), 2.88 (s, 2H), 4.23 (m, 4H)

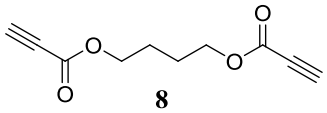

8

Synthesis of Diethylene Glycol Dipropiolate (9). To a solution of diethylene glycol (6.2 g, 58 mmol) in $CHCl_3$ (100 mL), pTsA (128 mmol) and propiolic acid (232 mmol) were added at 23 °C. The solution was heated under reflux for 18 h. After cooling, the solution was washed with an aqueous saturated $NaHCO_3$ solution (50 mL), water (3 x 50 mL), brine (50 mL) and dried over $MgSO_4$. The solvent was removed under rotary evaporation and the crude was purified by SiO_2 chromatography compound **9** as a yellow oil. (7.31 g, 60%); ^{1}H NMR ($CDCl_3$, 500 MHz) δ 2.91 (s, 2H), 3.73 (t, 4H), 4.33 (t, 4H);

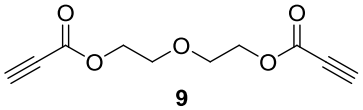

9

Synthesis of Poly(propylene glycol) Bis-6-bromohexanoate (10). To a solution of poly(propylene glycol) (PPG) (^{1}H NMR M_n = 1932, 19.8 g 9.0 mmol) in 100 mL of anhydrous dichloromethane, 2.76 mL (19.8 mmols – 2.2 molar excess) of triethylamine was added by syringe and the reaction was cooled to 0 °C. 3.02 mL (19.8 mmols – 2.2 molar excess) of 6-bromohexanoyl chloride was added dropwise, and the reaction was allowed to equilibrate at room temperature and stirred overnight. The produced triethylammonium chloride was filtered from the solution, and the solution was washed with saturated sodium bicarbonate (1x), deionized water (3x), and brine (1x). The solution was dried over $MgSO_4$, and the solvent was removed under rotary evaporation to yield **10** as a clear oil (14.36g, 72%). **10** was used without further purification. The structure was confirmed using ^{1}H NMR spectroscopy.

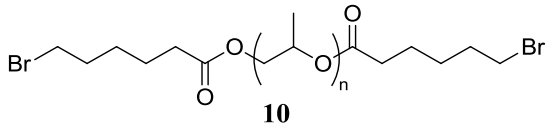

10

Synthesis of Poly(propylene glycol) Bis-6-azidohexanoate (11). To a solution of **10** (^{1}H NMR M_n = 2289, 14.36 g, 6.4 mmol) in 100 mL DMF, 2.92 g (44.9 mmol) of sodium azide (7 molar excess) was added. The mixture was allowed to react for 48 h at 65 °C. After cooling, a saturated aqueous solution of NaCl (100 mL) was added and the mixture was extracted with ethyl acetate (3 × 100 mL). The combined organic phases were washed with water (3 × 100 mL), brine (100 mL), dried over $MgSO_4$ and the solvent removed under rotary evaporation to yield **11** as a clear oil. The crude product was purified by passing over SiO_2 with chloroform as an eluent (68 % isolated yield). The structure was confirmed using ^{1}H NMR spectroscopy.

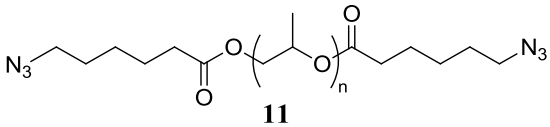

11

Polymer Synthesis. In a representative synthesis, an equimolar amount of bisazide and bispropiolate were dissolved in DMF or DMSO. The reaction solution was sparged for at least 10 min with Ar or N_2 to remove any dissolved oxygen. A small amount (~100 ppm) of both CuI and Cu powder were added to the reaction mixture. The solution was heated to 60 °C and stirred overnight under an inert atmosphere. The resulting mixture was precipitated into an aqueous solution of N,N,N',N',N''-pentamethyldiethylene triamine and vacuum filtration yielded the polymer in powder form. The resulting polymer was dried overnight at reduced pressure and 50 °C to afford the dry product. Segmented click polyesters were synthesized using a similar method.

6.4 Results and Discussion

The synthesis of several bisazide and bispropiolate monomers allowed for the utilization of click chemistry towards the synthesis of novel segmented polyesters. The reaction of 2-bromoethanol with both terephthaloyl dichloride and isophthaloyl dichloride yielded the corresponding dibromides for utilization in the synthesis of bisazide monomers. Reaction of the dibromides with sodium azide resulted in the formation of the corresponding bisazides. ^{1}H NMR spectroscopy confirmed the structures of the synthesized bisazides. **Scheme 6.1** details the synthesis of these bisazides. Reaction of an excess of propiolic acid with 1,4-butane diol (BD), diethylene glycol (DEG), *trans*-1,4-cyclohexane dimethanol (CHDM), or a mixture of *trans*- and *cis*-CHDM (the *trans:cis* ratio was 70:30) in refluxing chloroform or benzene at 80 °C for 18 h with an excess of *p*-toluene sulfonic acid yielded monomers with bispropiolate functionality, as depicted in **Scheme 6.2**. ^{1}H NMR spectroscopy confirmed the structures and purity of the bispropiolates.

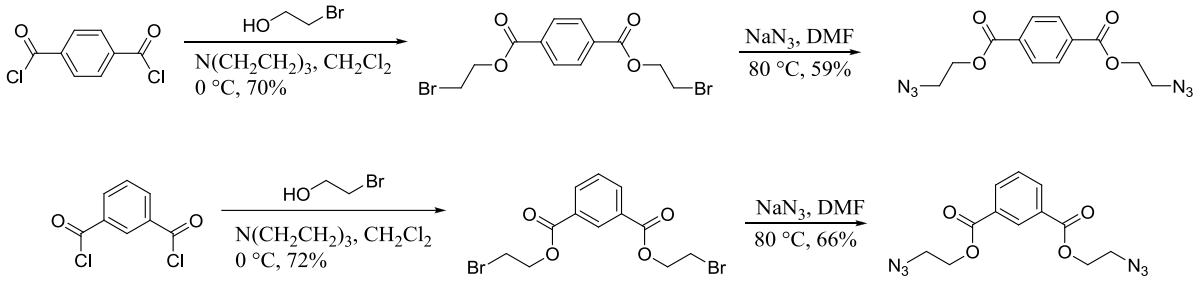

Scheme 6.1 Synthesis of bis-2-bromoethyl terephthalate and isophthalate and subsequent conversion into the corresponding bis-azide for utility in Cu(I) catalyzed 1,3-Huisgen cycloaddition.

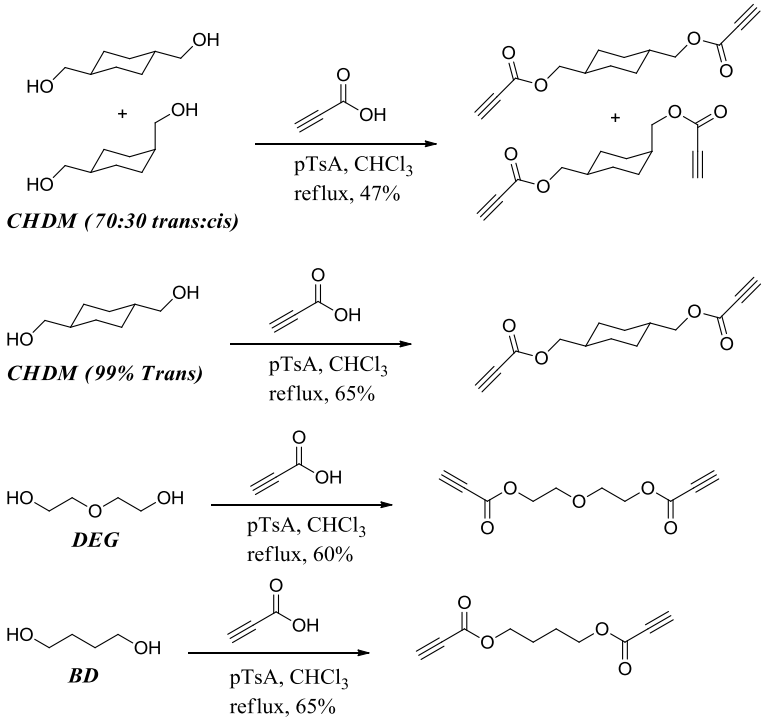

Scheme 6.2 Conversion of various diols into the corresponding propiolates for subsequent synthesis of polyesters using Cu(I) catalyzed 1,3-Huisgen cycloaddition.

The utilization of click chemistry resulted in a diverse series of triazole-containing polyesters. Preliminary syntheses with bisazidoterephthalates yielded polymers that exhibited

insignificant dispersibility in most organic solvents. However, when isophthalate-derived bisazides were used for the synthesis of polyesters, they demonstrated dispersibility in DMSO and NMP upon heating. These polymers also melt-pressed into free-standing, albeit brittle films. The polymers exhibited remarkably high glass transition temperatures (T_g) and demonstrated good thermal stability. **Scheme 6.3** illustrates the synthesis of polyesters using 1,3 Huisgen CuAAC click chemistry.

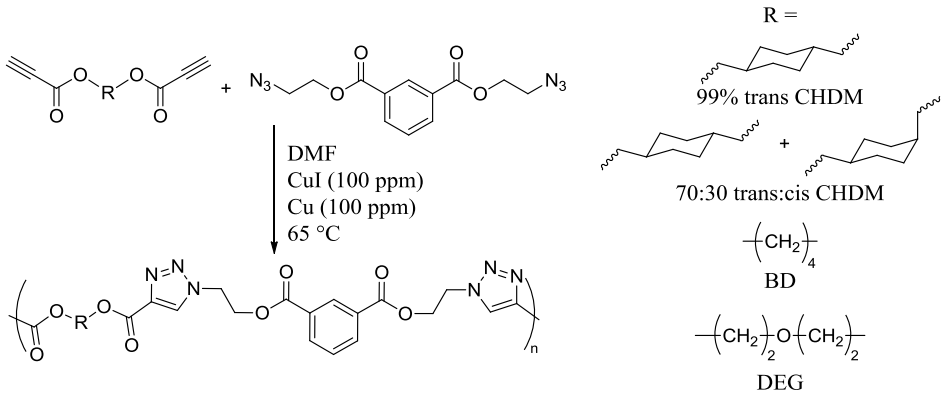

Scheme 6.3 1,3-Huisgen CuAAC as a synthetic route for polyesters containing 1,2,3-triazole units.

Synthesis of non-click polyester analogs using melt transesterification offered a control series to elucidate the effects of the triazole ring on the physical and chemical properties of the polymers and to compare the glass transitions of the click polyesters to structurally similar polyesters. The resulting polyesters exhibited good dispersibility in chloroform and melt-pressed into mechanically robust films. **Scheme 6.4** compares the structures and synthetic conditions of the click polyesters and the melt transesterification polyesters.

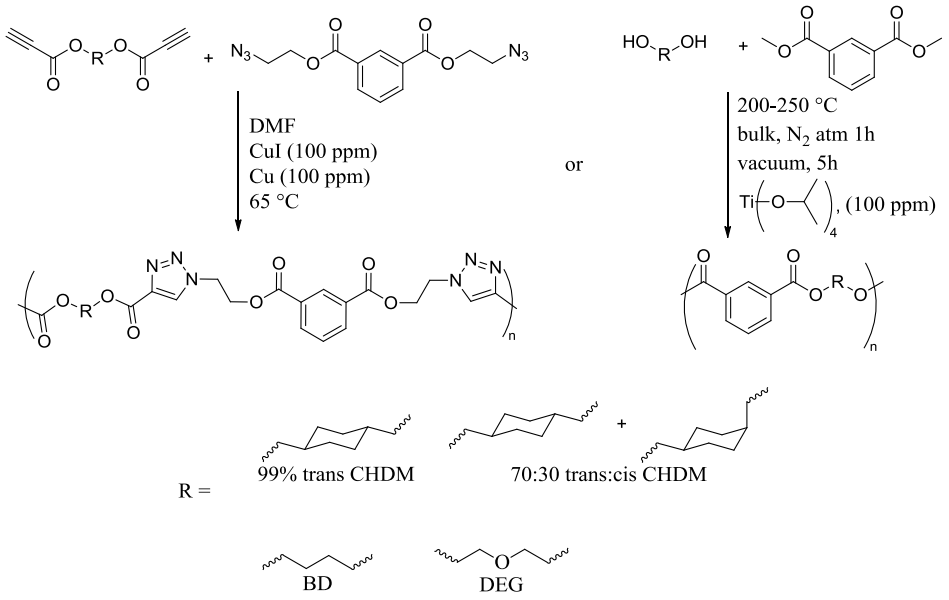

Scheme 6.4 Synthesis of triazole-containing polyesters and their structurally analogous melt transesterification polyesters for comparison of thermal properties.

Differential scanning calorimetry allowed for a determination of T_g's of the click polyesters as well as the melt polyesters in order to compare the thermal properties of the triazole-containing polyesters with structurally analogous melt polyesters, and **Table 6.1** illustrates these results. Polyesters synthesized using click chemistry in all cases exhibited at least a 40 °C higher T_g than their structural analogues, and in most cases demonstrated a crystalline T_m, which required a high degree of structural regularity for polyesters that did not contain triazoles in the backbone. In addition, some triazole-containing polyesters exhibited T_g's near 125 °C, approaching bisphenol-A polycarbonate.

Table 6.1 Comparison of thermal transitions of triazole-containing polyesters and structurally analogous melt transesterification polyesters.

	Triazole-Containing Polyesters		Melt Polyesters	
HO-R-OH	T_g (°C)	T_m (°C)	T_g (°C)	T_m (°C)
cyclohexane dimethanol 99% trans	121	201	80	214
cyclohexane dimethanol trans:cis	117	182	72	-
butane diol	95	178	25	142
diethylene glycol	77	-	25	-

Due to the high glass transition temperatures of the synthesized triazole-containing polyesters, they were potentially useful as a hard segment in segmented polyesters. Preparation of segmented polyesters required the synthesis of an azide-functionalized "soft segment". Poly(propylene glycol) (PPG) offered good dispersibility in many solvents, a low T_g, and commercial availability in good purity at a variety of molecular weights. Each of these properties allowed for PPG to serve as the basis for the soft segment in the synthesis of segmented polyesters. The typical acyl-chloride reaction of 6-bromohexanoyl chloride and PPG (M_n – 1932) yielded bromine-terminated PPG segments (PPG-dibromide) in ~70% yield. Subsequent reaction with an excess of sodium azide yielded the azide-functionalized PPG oligomer (PPG-bisazide) in ~60% yield. ^{1}H NMR spectroscopy confirmed the purity, functionality, and molecular weight of this difunctional oligomer. **Scheme 6.5** illustrates the synthesis of PPG-dibromide and subsequent conversion into PPG-bisazide.

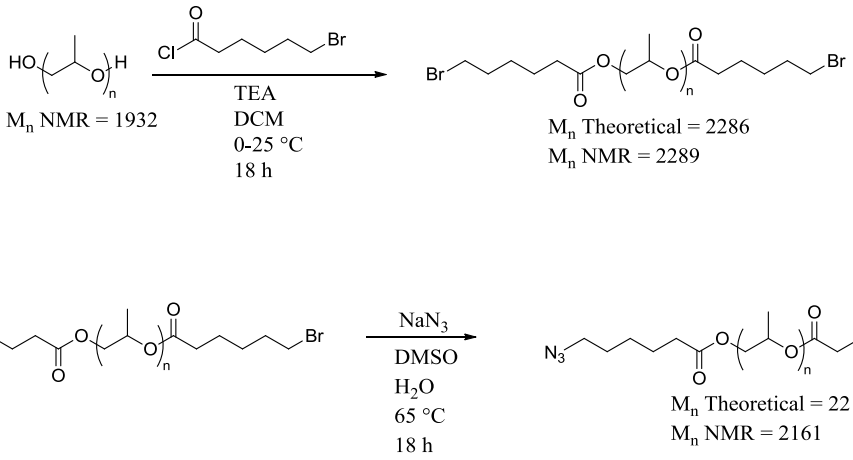

Scheme 6.5 Synthesis of azide-terminated PPG for preparation of segmented polyesters using Cu(I) catalyzed 1,3-Huisgen cycloaddition.

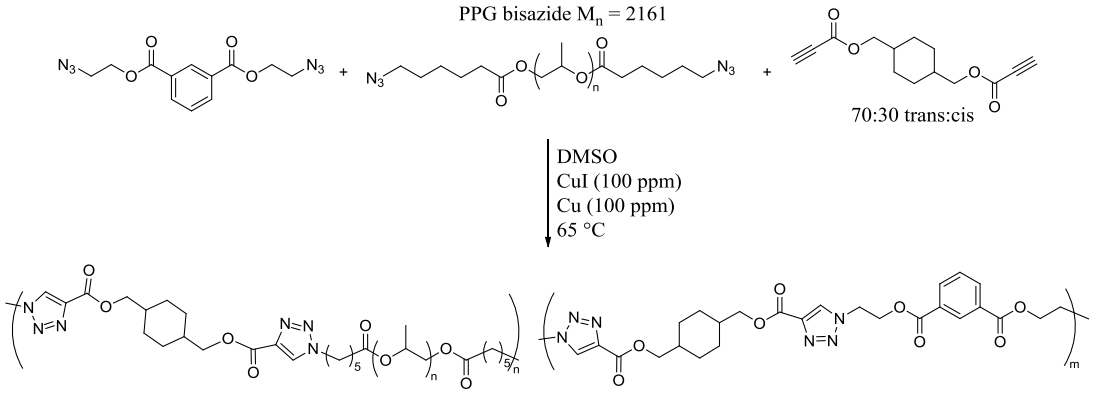

Scheme 6.6 Synthesis of segmented polyesters using Cu(I) catalyzed 1,3-Huisgen cycloaddition.

Upon the synthesis of PPG-bisazide, it, along with *cis/trans*-1,4-cyclohexyl dimethylene dipropiolate (70:30-CHDMDP), and bis(2-azidoethyl)isophthalate (BAIP were used to synthesize segmented polyesters) in DMSO with catalytic Cu and CuI with hard segment (HS) contents of 30, 40, and 50 wt %, shown as **Scheme 6.6**. Equation 6.1 demonstrates the calculations utilized to determine HS content. The obtained polyesters were tan, elastomeric, and dispersible in DMF, DMSO, and NMP. However, the polymers were not fully soluble in any suitable SEC solvent, so molecular weight data was unattainable. (Appendix A) Melt pressing yielded light tan, free-standing films that exhibited flexibility and creaseability. Differential scanning calorimetry (DSC) and thermogravimetric analysis (TGA) provided

analysis of the thermal transitions of the segmented polyesters, and **Table 6.2** illustrates these results. Soft segment T_g's near -60 °C indicated microphase separation, while 1st heat T_m's illustrated the semicrystalline nature of these polyesters, signifying the likelihood of elastomeric properties. In addition, TGA demonstrated that these polyesters exhibited $T_{d(onset)}$ temperatures above 300 °C, suggesting excellent thermal stability.

$$\text{Hard segment content} = \frac{CHDMBP + BAIP}{CHDMBP + BAIP + PPG{-}bisazide} * 100 \qquad \text{(Equation 6.1)}$$

Table 6.2 Thermal characterization of segmented click polyesters.

Hard Segment Content	**T_g (°C)**	**T_m (°C)**	**$T_{d\ (onset)}$ (°C)**
30 wt %	-61	114	313
40 wt %	-61	168	329
50 wt %	-	171	321

In situ FTIR spectroscopy offered a method for evaluation of the reaction rates of the click reaction towards segmented click polyesters. **Figure 6.1** illustrates the FTIR spectrum at 2106 cm^{-1} as a function of time. This wavenumber corresponded to the azide stretching frequency. Initially, the absorbance at 2106 cm^{-1} decreased linearly with time. After approximately 2 h, the peak reached a plateau, indicating a lowered reaction rate due to a decreasing concentration of azide and alkyne functional groups within the solution. After ~8 h, complete azide consumption occurred, indicating high conversion and reaction completion.

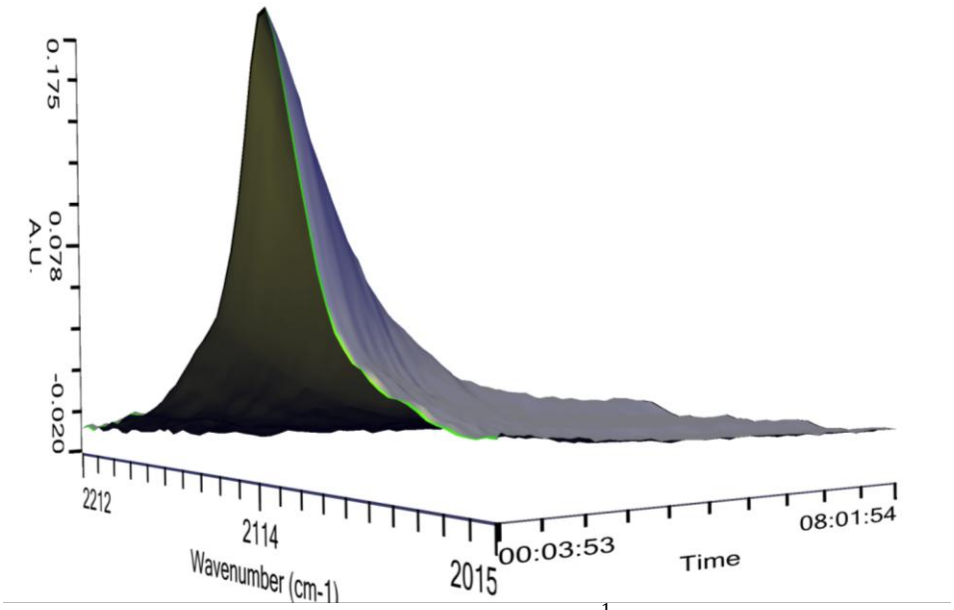

Figure 6.1 *In situ* FTIR spectrum at 2106 cm^{-1} demonstrating complete azide consumption at ~8 h.

Tensile testing offered an efficient method to evaluate the moduli of these segmented click polyesters; **Figure 6.2** shows representative traces for each HS content. Tensile testing of melt pressed films revealed Young's moduli of 7, 22, and 133 MPa for the 30, 40, and 50 wt % HS segmented polyesters, respectively. As expected, the moduli increased with increasing wt % HS, consistent with microphase separated thermoplastic elastomers. Stress at break also increased as a function of HS content, with values ranging from 1.4 to 9.2 MPa. Strain at break did not exhibit a dependence on HS content, with values in all cases near 35%. **Table 6.3** illustrates these results.

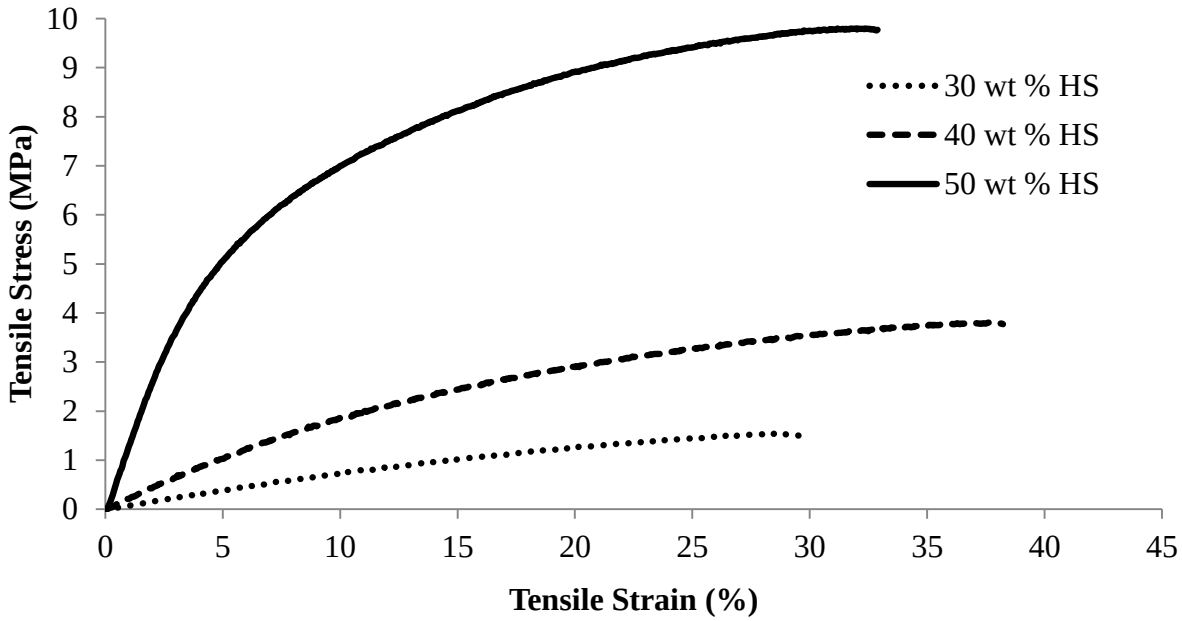

Figure 6.2 Representative tensile traces for segmented click polyesters with varying hard segment content.

Table 6.3 Tensile data for segmented click polyesters with varying hard segment content

HS Content	Stress at Break (MPa)	Strain at Break (%)	E Modulus (MPa)
30 wt %	1.4 +/- 0.1	32 +/- 3	7 +/- 1
40 wt %	3.5 +/- 0.3	38 +/- 2	22 +/- 4
50 wt %	9.2 +/- 0.6	35 +/- 4	133 +/- 7

Dynamic mechanical analysis (DMA) provided an efficient means to further probe this microphase separation, as well as the mechanical properties as a function of temperature. **Figure 6.3** illustrates DMA traces of storage modulus as a function of temperature for each HS content segmented click polyester. **Table 6.4** shows the values of the soft segment (SS) T_g, the HS T_g, and the HS T_m. Only minor variation occurred among the SS T_g values, as well as among the HS T_g values, in good agreement with the SS T_g values shown in **Table 6.2**. The T_m of the HS increased with increasing HS content, also consistent with DSC results, perhaps suggesting a lower level of crystallinity in lower HS content segmented click polyesters. The observed glassy storage modulus did not substantially change with hard segment content; however the rubbery

plateau modulus exhibited a significant increase as a function of increasing HS content. These results show good agreement with the tensile data, and are consistent with literature precedence on semicrystalline segmented block copolymers with varying HS content.[45,46]

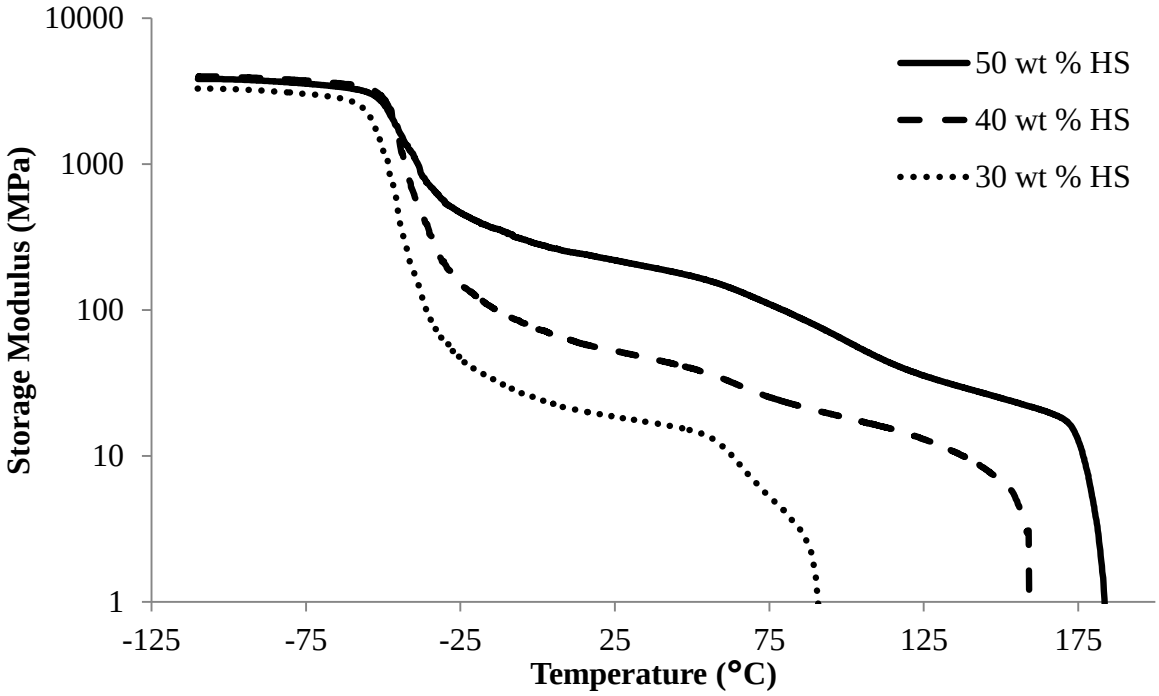

Figure 6.3 Dynamic mechanical analysis of segmented click polyesters with varying hard segment content.

Table 6.4 Thermal transitions of segmented click polyesters with varying hard segment content obtained from dynamic mechanical analysis.

Hard Segment Content	Sample	$T_{g,1}$ (°C)	$T_{g,2}$ (°C)	T_m (°C)
30 wt %	30 wt % HS	-48	57	87
40 wt %	40 wt % HS	-52	55	154
50 wt %	50 wt % HS	-52	62	175

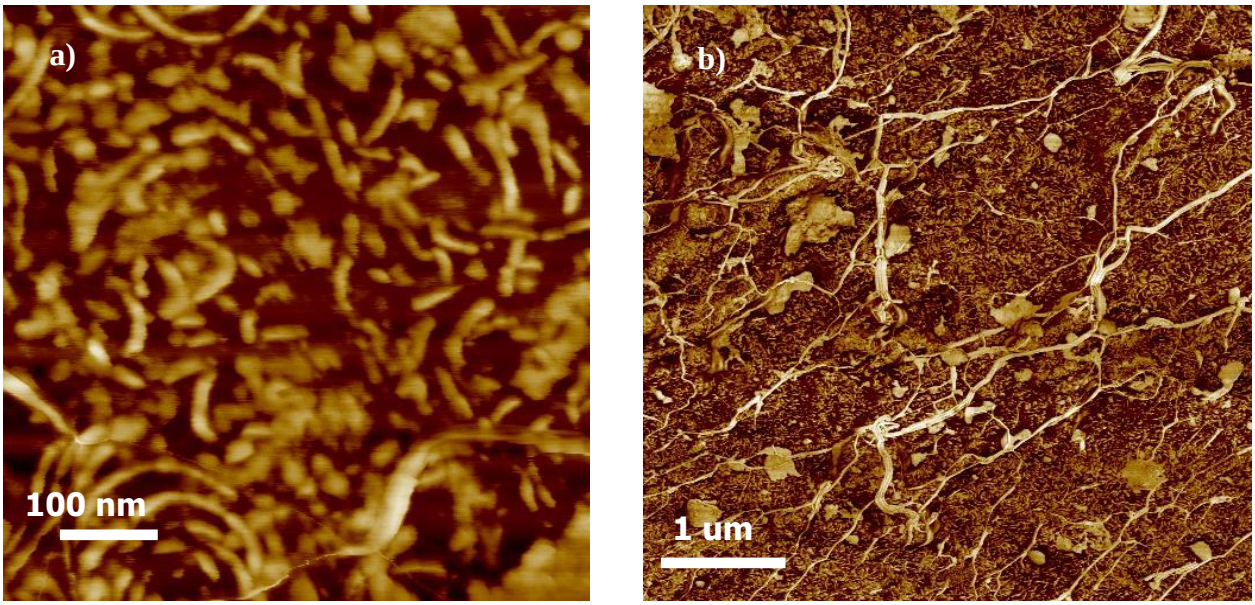

Figure 6.4 Atomic force microscopy images of 40 wt % HS segmented click polyester demonstrated microphase separated morphology and crystalline domains.

Atomic force microscopy (AFM) provided a method to further confirm the microphase separated nature of the segmented click polyesters. Melt-pressing and subsequent annealing at 140 °C provided films suitable for AFM. **Figure 6.4a** shows a 1x1 um image of the 40% HS polyester. In this image, the lighter features represent the HS, whereas the darker features represent the SS. **Figure 6.4b** shows a 5x5 um image of the same sample. At this magnification, the microphase separated domains are also visible; however, the brighter, ribbon-like features represent the semicrystalline domains. These results further confirm the microphase separated and semicrystalline nature of these segmented click polyesters. Literature precedence exists for AFM observation of short-range ribbon microstructures in semicrystalline segmented block copolymers, similar to those in **Figure 6.4a**, and transmission electron microscopy commonly depicts long-range ribbon microstructures in semicrystalline segmented block copolymers similar to those in **Figure 6.4b**.[46]

6.5 Conclusions

This manuscript is the first reported synthesis of segmented copolyesters using copper(I) catalyzed azide-alkyne 1,3-Huisgen cycloaddition. Click chemistry offered an efficient, low-temperature method towards the synthesis of polyesters and segmented block copolyesters. DSC confirmed a significant increase (~40 °C) in T_g of the triazole-containing homopolyesters relative to structurally analogous polyesters synthesized using melt transesterification. Utilization of azido-functionalized PPG macromonomers for the synthesis of a series of segmented click polyesters with varying HS content resulted in a marked increase in polymer dispersibility and film flexibility. DSC demonstrated microphase separation of the segmented click polyesters, suggesting the potential for elastomeric properties. Tensile testing revealed an increase in Young's modulus from 7 to 133 MPa and stress at break from 1.5 to 9 MPa as HS content increased from 30 to 50 wt %, and DMA displayed microphase separation and an increase in rubbery plateau modulus and crystalline T_m with increasing HS content. AFM confirmed the existence of microphase separated and semicrystalline morphological domains. These results suggest a high degree of utility of click chemistry towards the synthesis of high performance polyesters and segmented block copolyesters.

6.6 Acknowledgements. The authors would like to thank Dr. Qin Lin and Dr. Rama Puligadda for insightful discussions during the conception of this research. This research was supported by Brewer Science, Inc. under contract # N00014-07-C-0797.

6.7 References

(1) Carothers, W. H. *Trans. Faraday Soc.* **1936**, *32*, 39.
(2) Rogers, M. E.; Long, T. E.; Turner, S. R. *Synthetic Methods in Step-Growth Polymers* **2003**, 1.
(3) Williams, S. R.; Lepene, B. S.; Thatcher, C. D.; Long, T. E. *Biomacromolecules* **2009**, *10*, 155.
(4) Unal, S.; Ozturk, G.; Sisson, K.; Long, T. E. *J. Polym. Sci., Part A: Polym. Chem.* **2008**, *46*, 6285.
(5) June, S. M.; Suga, T.; Heath, W. H.; Long, T. E.; Lin, Q.; Puligadda, R. *J. Adhes.* **2010**, *86*, 1012
(6) Williams, S. R.; Wang, W.; Winey, K. I.; Long, T. E. *Macromolecules* **2008**, *41*, 9072.
(7) Williams, S. R.; Salas-de la Cruz, D.; Winey, K. I.; Long, T. E. *Polymer* **2010**, *51*, 1252.
(8) Tamami, M.; Williams, S. R.; Park, J. K.; Moore, R. B.; Long, T. E. *J. Polym. Sci., Part A: Polym. Chem.* **2010**, *48*, 4159.
(9) Kang, H.; Long, T. E. *Polym. Mater. Sci. Eng.* **2001**, *84*, 909.
(10) Karikari, A. S.; Williams, S. R.; Heisey, C. L.; Rawlett, A. M.; Long, T. E. *Langmuir* **2006**, *22*, 9687.
(11) Lin, Q.; Pasatta, J.; Long, T. E. *J. Polym. Sci., Part A: Polym. Chem.* **2003**, *41*, 2512.
(12) Lin, Q.; Pasatta, J.; Wang, Z.-H.; Ratta, V.; Wilkes, G. L.; Long, T. E. *Polym. Int.* **2002**, *51*, 540.
(13) Lin, Q.; Unal, S.; Fornof, A. R.; Armentrout, R. S.; Long, T. E. *Polymer* **2006**, *47*, 4085.
(14) Ozturk, G. I.; Pasquale, A. J.; Long, T. E. *J. Adhes.* **2010**, *86*, 395.
(15) Unal, S.; Long, T. E. *Macromolecules* **2006**, *39*, 2788.
(16) Cashion, M. P.; Park, T.; Long, T. E. *J. Adhes.* **2009**, *85*, 1.
(17) Huyck, R. H.; Trenor, S. R.; Love, B. J.; Long, T. E. *J. Macromol. Sci., Part A: Pure Appl. Chem.* **2008**, *45*, 9.
(18) Karikari, A. S.; Edwards, W. F.; Mecham, J. B.; Long, T. E. *Biomacromolecules* **2005**, *6*, 2866.
(19) Layman, J. M.; Borgerding, E. M.; Williams, S. R.; Heath, W. H.; Long, T. E. *Macromolecules* **2008**, *41*, 4635.
(20) Mather, B. D.; Baker, M. B.; Beyer, F. L.; Berg, M. A. G.; Green, M. D.; Long, T. E. *Macromolecules* **2007**, *40*, 6834.
(21) Cheng, S.; Zhang, M.; Dixit, N.; Moore, R. B.; Long, T. E. *Macromolecules* **2012**, *45*, 805.
(22) Kolb, H. C.; Finn, M. G.; Sharpless, K. B. *Angew. Chem. Int. Ed.* **2001**, *40*, 2004.
(23) Himo, F.; Lovell, T.; Hilgraf, R.; Rostovtsev, V. V.; Noodleman, L.; Sharpless, K. B.; Fokin, V. V. *J. Am. Chem. Soc.* **2004**, *127*, 210.
(24) Rostovtsev, V. V.; Green, L. G.; Fokin, V. V.; Sharpless, K. B. *Angew. Chem. Int. Ed.* **2002**, *41*, 2596.
(25) Wu, P.; Feldman, A. K.; Nugent, A. K.; Hawker, C. J.; Scheel, A.; Voit, B.; Pyun, J.; Fréchet, J. M. J.; Sharpless, K. B.; Fokin, V. V. *Angew. Chem. Int. Ed.* **2004**, *43*, 3928.
(26) Golas, P. L.; Tsarevsky, N. V.; Sumerlin, B. S.; Walker, L. M.; Matyjaszewski, K. Aust. J. Chem. **2007**, *60*, 400.
(27) Golas, P. L.; Matyjaszewski, K. *Chem. Soc. Rev.* **2010**, *39*, 1338.
(28) Johnson, J. A.; Baskin, J. M.; Bertozzi, C. R.; Koberstein, J. T.; Turro, N. J. *Chem. Commun.* **2008**, 3064.

(29) Johnson, J. A.; Finn, M. G.; Koberstein, J. T.; Turro, N. J. *Macromolecules* **2007**, *40*, 3589.
(30) Qin, A.; Lam, J. W. Y.; Tang, B. Z. *Chem. Soc. Rev.* **2010**, *39*, 2522.
(31) Bernardin, A.; Cazet, A. l.; Guyon, L.; Delannoy, P.; Vinet, F. o.; Bonnaffé, D.; Texier, I. *Bioconjugate Chem.* **2010**, *21*, 583.
(32) Schumers, J. M.; Gohy, J.-F.; Fustin, C.A. *Polym. Chem.* **2010**, *1*, 161.
(33) Fournier, D.; Hoogenboom, R.; Schubert, U. S. *Chem. Soc. Rev.* **2007**, *36*, 1369.
(34) Voit, B. I.; Lederer, A. *Chem. Rev.* **2009**, *109*, 5924.
(35) Franc, G.; Kakkar, A. K. *Chem. Soc. Rev.* **2010**, *39*, 1536.
(36) Joralemon, M. J.; O'Reilly, R. K.; Matson, J. B.; Nugent, A. K.; Hawker, C. J.; Wooley, K. L. *Macromolecules* **2005**, *38*, 5436.
(37) Polaske, N. W.; McGrath, D. V.; McElhanon, J. R. *Macromolecules* **2009**, *43*, 1270.
(38) Sumerlin, B. S.; Vogt, A. P. *Macromolecules* **2009**, *43*, 1.
(39) Scheel, A. J.; Komber, H.; Voit, B. I. *Macromol. Rapid Commun.* **2004**, *25*, 1175.
(40) Xie, J.; Hu, L.; Shi, W.; Deng, X.; Cao, Z.; Shen, Q. *J. Polym. Sci., Part B: Polym. Phys.* **2008**, *46*, 1140.
(41) Xie, J.; Hu, L.; Shi, W.; Deng, X.; Cao, Z.; Shen, Q. *Polym. Int.***2008**, *57*, 965.
(42) Gao, Y.; Chen, L.; Zhang, Z.; Gu, W.; Li, Y. *Biomacromolecules* **2010**, *11*, 3102.
(43) Nagao, Y.; Takasu, A. *Macromol. Rapid Commun.* **2009**, *30*, 199.
(44) Nagao, Y.; Takasu, A. *J. Polym. Sci., Part A: Polym. Chem.* **2010**, *48*, 4207.
(45) Eisenbach, C. D.; Baumgartner, M.; Plenum: 1986, p 51.
(46) Reinoud J, G. *Prog. Polym. Sci.* **2011**, *36*, 713.

Chapter 7: Click Chemistry as an Efficient Route towards Novel Photodegradable Polyesters

Stephen M. June, Philippe Bissel, and Timothy E. Long*

Department of Chemistry, Macromolecules and Interfaces Institute, Virginia Tech, Blacksburg, Virginia 24061-0344

(From – Manuscript in Progress)

7.1 Abstract

Development of polyesters containing photoactive *o*-nitro benzyl ester functionalities offered good potential for adhesives with reversible bonding capabilities. Utilization of click chemistry provided a novel route towards photoactive polyesters. These polymerizations required the synthesis of novel bisalkynes, including photoactive bisalkynes, and bisazides. Copper(I) catalyzed azide-alkyne cycloaddition of these monomers yielded novel photoreactive polyesters which exhibited dispersibility in dipolar aprotic solvents. The synthesized polyesters melt-pressed into free-standing, albiet brittle films. Exposure to high-intensity, broad wavelength ultraviolet light in dimethyl sulfoxide-$_{d6}$ resulted in photodegradation of the photoactive polyesters. Nuclear magnetic resonance (NMR) spectroscopy demonstrated decreased intensity in the proton resonance corresponding to the *o*-nitro benzyl ester methylene unit in the polymer backbone and a growth in the proton resonance corresponding to the formation of the carboxylic acid product of the photodegradation. Synthesis of azide functionalized PPG oligomers enabled the preparation of segmented triazole-containing polyesters which demonstrated dispersibility in a variety of solvents and pressed into free-standing and flexible films. Photodegradation experiments with narrow wavelength (365 nm)

lamp and subsequent ^{1}H NMR spectroscopy provided confirmation of photoreactivity of the segmented photoreactive polyester. These results suggest potential utility of the polymers as photoreversible structural adhesives.

7.2 Introduction

With the advancement of microelectronics and microfabrication techniques, a continued concern exists relating to device fragility relative to the level of rigor required for fabrication.[1,2] Emerging techniques for manufacture of thin and ultrathin silicon-based microelectronic devices require support substrates in order to afford sufficient mechanical integrity to allow for rigorous production methods. These devices must withstand many manufacturing stresses including lithography, surface deposition, and backside grinding.[1,2] The thin and ultrathin silicon wafers cannot withstand these stresses without the aid of a temporary support substrate. Temporary binding of a silicon wafer to a substrate, such as aluminum, glass, or quartz provides sufficient support and integrity such that the wafer can withstand some of the rigorous stresses associated with manufacture as discussed above. Typically a hot-melt thermoplastic adhesive provides this temporary bond. After the successful device production, heating of the support and device above the melt temperature of the adhesive, and subsequent removal of the support allows for device isolation.[1-3]

The thermal shock due to repeated heating and cooling of the thin and ultrathin silicon devices often leads to folding, warping, expansion, contraction, and cracking, which subsequently results in discarded product. In order to prevent this, we developed herein a photoreactive polymer which may act as a model for the creation of a temporary photoreleasable adhesive. Upon exposure to high intensity UV light *in situ*, the photoreactive units within the

mainchain underwent photocleavage, significantly diminishing the molecular weight, and accordingly the mechanical and adhesive properties of the polymer. This photodegradation resulted in a polymer product which likely no longer exhibited adhesive properties, thus facilitating potential device removal from the support substrate.[1-3]

A significant amount of literature relating to photoreactive polymers exists. As far back as the mid-1980's research groups utilized cyclobutane dianhydride for the formation of photoreactive polyimides.[4] Photoinitiators often find utility for commercial coatings applications. Our group recently published several papers on photoreactive polymers, as well as polymers which undergo controlled degradations.[5-10] We also performed some work on photoreversible adhesion. In particular our group developed photoreversible pressure sensitive adhesives using coumarin[6-9] and cinnamate functionality,[5,10] and poly(siloxane imides) containing cyclobutane diimide functionality as models for a potential photoreversible adhesive.[3]

Since Sharpless and coworkers developed the copper(I)-catalyzed alkyne-azide cycloaddition (CuAAC) in 2001, otherwise known as click chemistry, it has featured prominently in many research publications.[11,12] This reaction takes place under relatively mild conditions, and exhibits remarkable tolerance to solvents, functional groups, and pH. This tolerance of CuAAC to other functional groups generated extensive utility of the CuAAC reaction in the synthesis of block copolymers using ATRP, graft copolymers, and other functional polymers.

Although CuAAC found some recent utility towards the synthesis of step-growth polymers, only in the last few years have publications arisen detailing the utilization of CuAAC for the synthesis of polyesters.[11,12] A typical synthesis of polyester requires either the use of direct melt condensation of a diol and diacid or melt transesterification of a diol and a diester.

However, both of these methods require high temperatures (>200 °C) and reduced pressure (100 mTorr), as well as organometallic catalysts such as titanium tetraisopropoxide.[13-26] As mentioned above, click reactions operate at relatively mild conditions, without expensive metal catalysts. These advantages give CuAAC click reactions high potential for utility as the major reaction mechanism towards synthesis of polyesters, in particular polyesters where thermal stabilities of monomers or functional groups require lower reaction temperatures.

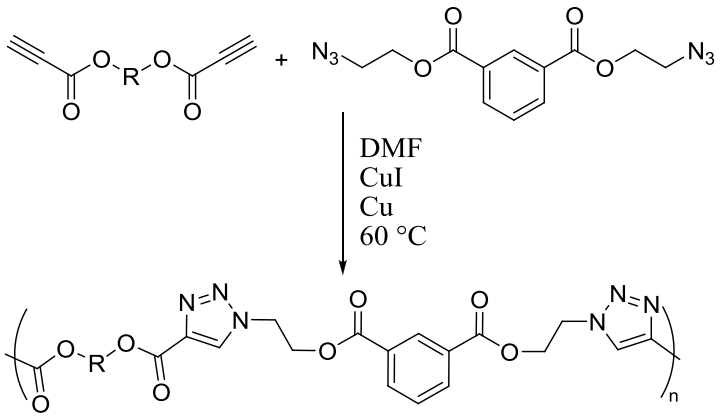

Scheme 7.1 Click chemistry as a synthetic route for polyesters containing 1,2,3 triazole units.

The literature well establishes the photocleavage reaction of *o*-nitro benzyl esters at approximately 356 nm to yield the corresponding nitroso and carboxylic acid compounds.[27-43] In our work towards utilizing melt transesterification toward the synthesis of *o*-nitro benzyl (ONB) ester containing polyesters (to be published elsewhere), we observed that 2-nitro-*p*-xylylene glycol (NXG) exhibited insignificant thermal stability above 185 °C, complicating melt transesterification of this compound. Therefore, utilization of click chemistry offered an effective method for the synthesis of polyesters containing ONB units. **Scheme 7.1** demonstrates a synthetic scheme for synthesis of these polyesters.

7.3 Experimental

7.3.1 Methods and Materials. Terephthaloyl chloride, 2-bromoethanol, 1,4-butane diol, sodium azide, 1,4-butanediol, and tetrabutylammonium bromide (TBAB) were purchased from Aldrich, isophthaloyl chloride, 6-bromohexanoyl chloride, propiolic acid, and cyclohexane dimethanol (70:30 trans:cis) from Alfa Aesar, and *p*-toluenesulfonic acid (pTsA) from Fluka and were used without further purification. Bayer MaterialScience kindly provided PPG 2200 (Aclaim). Chloroform, N,N-dimethylformamide, N-methylpyrrolidone, dimethylsulfoxide, and tetrahydrofuran were purchased from Fisher Scientific and used as received. Dichloromethane and triethylamine were purchased from Fisher Scientific and distilled from calcium hydride. ^{1}H and ^{13}C NMR spectra were recorded on a 400-MHz Varian Inova spectrometer. Chemical shifts are reported in ppm downfield from the internal standard tetramethylsilane (TMS). Spin multiplicities are reported as s (singlet), d (doublet), t (triplet) or m (multiplet).

Thermogravimetric analysis (TGA) was conducted on a TA Instruments Hi-Res TGA 2950 at a temperature ramp rate of 10 °C/min under a N_2 atmosphere. Glass transition temperatures (T_g) were reported from the 2nd heat of a heat/cool cycle (0°C to 150°C) at a heating rate of 10 °C/min and a cooling rate of 50 °C/min on a TA Instrument DSC Q1000 under N_2.

7.3.2 Synthesis

Synthesis of Bis(2-bromoethyl)terephthalate (BrTP) (1). To a solution of terephthaloyl chloride (10 g, 49 mmol), and $N(Et)_3$ (28 mL, 200 mmol) in CH_2Cl_2 (100 mL), 2-bromoethanol (14 mL, 200 mmol) in CH_2Cl_2 (50 mL) was added dropwise at 0 °C. The mixture was stirred at 23 °C for 20 h. The mixture was washed with 5% aqueous solution of K_2CO_3 (3 x 50 mL), water (2 x 50 mL) and dried over $MgSO_4$. The crude was recrystallized from ethyl acetate to give **1**

(13.05 g, 70%) as white crystals; ^{1}H NMR ($CDCl_3$, 500 MHz) δ 3.26 (t, 4H), 4.26 (t, 4H), 7.45 (s, 4H).

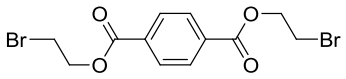

1

Synthesis of Bis(2-azidoethyl)terephthalate (BATP) (2). A mixture of **1** (10 g, 34 mmol), NaN_3 (17.6 g, 270 mmol), and TBAB (0.55 g, 1.7 mmol) in DMF (50 mL) was heated at 80 °C for 48 h. After cooling, a saturated aqueous solution of LiBr (50 mL) was added and the mixture was extracted with ethyl acetate (3 × 50 mL). The combined organic phases were washed with water (3 × 50 mL), brine (50 mL), dried over $MgSO_4$ and the solvent removed under rotary evaporation. The crude was recrystallized from ethyl acetate to give **2** (7.62 g, 59%) as white crystals; (mp 81-83 °C) ^{1}H NMR ($CDCl_3$, 500 MHz) δ 3.62 (t, 4H), 4.52 (t, 4H), 8.14 (s, 4H).

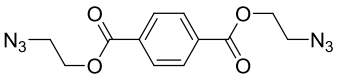

2

Synthesis of Bis(2-bromoethyl)isophthalate (BrIP) (3). A mixture of isophthaloyl chloride (27.3 g, 0.13 mol), $N(Et)_3$ (75 mL, 0.54 mol) in CH_2Cl_2 (400 mL), 2-bromoethanol (38 mL, 0.54 mol) in CH_2Cl_2 (50 mL) was added dropwise at 0 °C. The mixture was stirred at room temperature for 20 h. The mixture was washed with 5% aqueous solution of K_2CO_3 (3 x 150 mL), water (2 x 150 mL) and dried over $MgSO_4$. The crude was purified by SiO_2 chromatography ($CHCl_3$/hexanes 7:3) to give **3** (35.3 g, 72%) as white crystals; ^{1}H NMR ($CDCl_3$, 500 MHz) δ

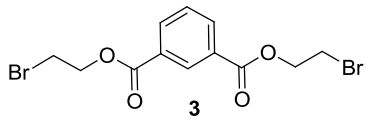

3

Synthesis of Bis(2-azidoethyl)isophthalate (BAIP) (4). A mixture of **3** (19.5 g, 52 mmol), NaN_3 (26.8 g, 410 mmol), and TBAB (0.84 g, 2.6 mmol) in DMF (100 mL) was heated at 80 °C for 48 h. After cooling, a saturated aqueous solution of LiBr (100 mL) was added and the mixture was extracted with ethyl acetate (3 × 100 mL). The combined organic phases were washed with water (3 × 100 mL), brine (100 mL), dried over $MgSO_4$ and the solvent removed under rotary evaporation. The crude was purified by SiO_2 chromatography ($CHCl_3$/hexanes 8:2) to give **4** (13.0 g, 66%) as white crystals; (mp 73-76 °C) ^{1}H NMR ($CDCl_3$, 500 MHz) δ 3.63 (t, 4H), 4.53 (t, 4H), 7.59 (t, 1H), 8.28 (d, 2H), 8.75 (m, 1H).

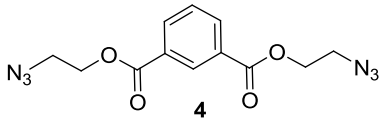

4

Synthesis of 2-Nitro-*p*-xylylene Glycol Dipropiolate (NXGDP) (6). A solution of 2-nitro-*p*-xylylene glycol (5g, 27 mmol), *p*-TsOH (11.3 g, 59 mmol) and propiolic acid (6.5 mL, 108 mmol) in benzene (100 mL) was heated under reflux for 20h. The mixture was washed with water (3 x 100 mL), brine (100 mL) and dried over $MgSO_4$. The solvent was removed under reduced pressure. The crude was purified by silicagel chromatography ($CHCl_3$) to give **7** (5.02 g, 65%) as a yellow liquid; ^{1}HNMR ($CDCl_3$, 500 MHz) δ 2.97 (s, 1H), 2.99 (s, 1H), 5.29 (s, 2H), 5.65 (s, 2H), 7.68 (d, 1H), 7.70 (d, 1H), 8.18 (d, 1H)

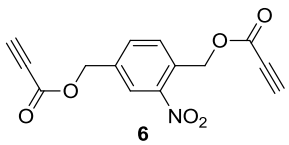

6

Synthesis of Neopentyl Propiolate (7). To a solution of neopentyl alcohol (5.0 g, 57 mmol) in $CHCl_3$ (100 mL), pTsOH (125 mmol) and propiolic acid (228 mmol) was added at room temperature. The solution was heated under reflux for 18h. After cooling, the solution was washed with an aqueous saturated $NaHCO_3$ solution (50 mL), water (3 x 50 mL), brine (50 mL) and dried over $MgSO_4$. The solvent was removed under rotary evaporation and the crude was purified by chromatography over silicagel (CH_2Cl_2/MeOH 95:5) to yield **10** as a pale yellow liquid. (4.33 g, 55%); ^{1}H NMR ($CDCl_3$, 500 MHz) δ 0.97 (s, 9H), 2.88 (s, 1H), 3.90 (s, 2H); ^{13}C NMR ($CDCl_3$, 128.5 MHz) δ 26.2, 31.3, 74.5, 74.7, 75.4, 152.9.

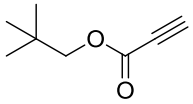

8

Synthesis of Poly(propylene glycol) Bis-6-bromohexanoate (9). To a solution of poly(propylene glycol) (PPG) (^{1}H NMR M_n = 1932, 19.8 g 9.0 mmol) in 100 mL of anhydrous dichloromethane, 2.76 mL (19.8 mmols – 2.2 molar excess) of triethylamine was added by syringe and the reaction was cooled to 0 °C. 3.02 mL (19.8 mmols – 2.2 molar excess) of 6-bromohexanoyl chloride was added dropwise, and the reaction was allowed to equilibrate at room temperature and stirred overnight. The produced triethylammonium chloride was filtered from the solution, and the solution was washed with saturated sodium bicarbonate (1x), deionized water (3x), and brine (1x). The solution was dried over $MgSO_4$, and the solvent was removed under rotary evaporation to yield **10** as a clear oil (14.36g, 72% yield). **10** was used without further purification. The structure was confirmed using ^{1}H NMR spectroscopy.

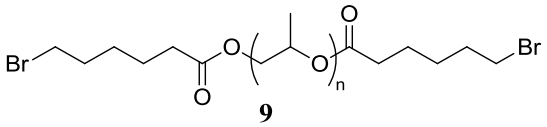

9

Synthesis of Poly(propylene glycol) Bis-6-azidohexanoate (11). To a solution of **10** (^{1}H NMR M_n = 2289, 14.36 g, 6.4 mmol) in 100 mL DMF, 2.92 g (44.9 mmol) of sodium azide (7 molar excess) was added. The mixture was allowed to react for 48 h at 65 °C. After cooling, a saturated aqueous solution of NaCl (100 mL) was added and the mixture was extracted with ethyl acetate (3 × 100 mL). The combined organic phases were washed with water (3 × 100 mL), brine (100 mL), dried over $MgSO_4$ and the solvent removed under rotary evaporation to yield **11** as a clear oil. The crude product was purified by passing over SiO_2 with chloroform as an eluent. The structure was confirmed using ^{1}H NMR spectroscopy.

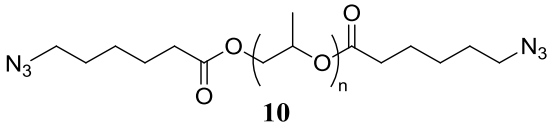

10

Polymer Synthesis. In a representative synthesis, an equimolar amount of bisazide and bispropiolate were dissolved in DMF or DMSO. The reaction solution was sparged for at least 10 min with Ar or N_2 to remove any dissolved oxygen. A small amount (~100 ppm) of both CuI and Cu powder were added to the reaction mixture. The solution was heated to 60 °C and stirred overnight under an inert atmosphere. The resulting mixture was precipitated into an aqueous solution of N,N,N',N',N''-pentamethyldiethylene triamine and vacuum filtration yielded the polymer in powder form. The resulting polymer was dried overnight at reduced pressure and 50 °C to afford the dry product. Segmented click polyesters were synthesized using a similar method.

7.4 Results and Discussion

The synthesis of several bis-azido and bis-propiolate esters resulted in monomers suitable for the utilization of click chemistry towards the synthesis of novel photoactive polyesters.

Reaction of 1-bromoethanol with both isophthaloyl dichloride and isophthaloyl dichloride afforded the corresponding dibromides and subsequent reaction of the dibromides with sodium azide resulted in the formation of the corresponding bisazides (**Scheme 7.2**). The reaction of an excess of propiolic acid reacted with 1,4-butane diol (BD) or 2-nitro-*p*-xylylene glycol (NXG) in refluxing chloroform or benzene at 80 °C for 18h with an excess of *p*-toluene sulfonic acid resulted in monomers, including a photoactive monomers, with bisalkyne functionality (**Scheme 7.3**). ^{1}H and ^{13}C NMR spectroscopy confirmed the structures of the corresponding monomers for utilization in click polyesters.

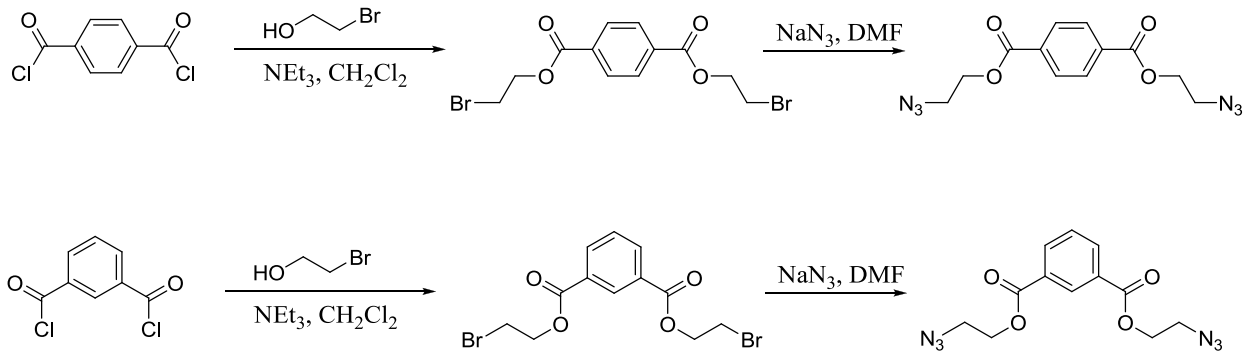

Scheme 7.2 Synthesis of bisazies for the synthesis of triazole-containing polyesters.

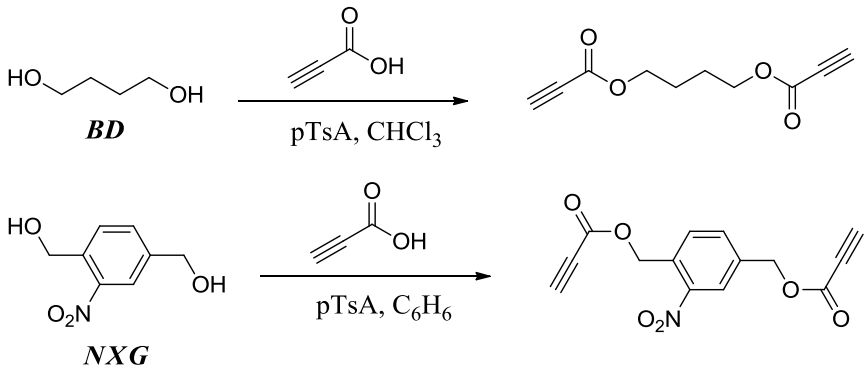

Scheme 7.3 Synthesis of bisalkynes for the synthesis of photoreactive triazole-containing polyesters.

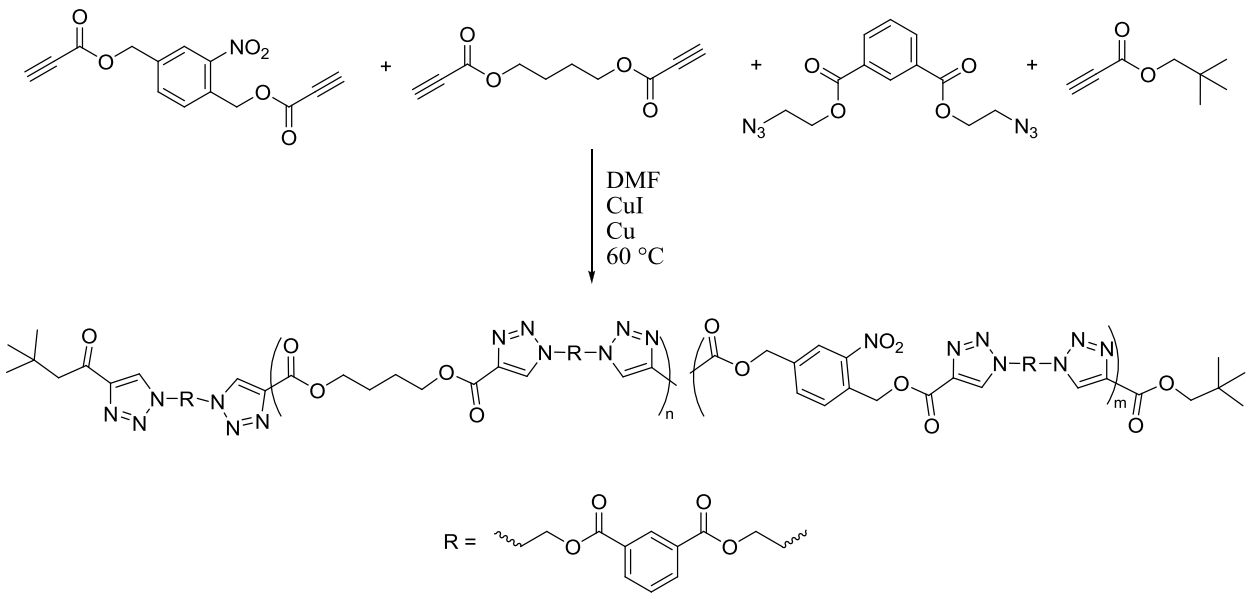

Scheme 7.4 Utilization of end-capping and varying offsets of stoichiometry to confirm control of molecular weight in *o*-nitro benzyl ester containing click polyesters.

Utilization of click chemistry allowed for the successful synthesis of photoactive polyesters. The reaction of an equimolar amount of bisazide and bisalkyne in DMSO with catalytic CuI and Cu powder and subsequent precipitation yielded triazole-containing polyesters as light tan powders which melt-pressed into free-standing, albeit brittle films. The polymers exhibited dispersibility in DMSO and NMP upon heating, but possessed poor dispersibility in other solvents, even with heating. The polymers exhibited relatively high glass transition temperatures (T_g) near 85 °C and demonstrated good thermal stability.

One of the primary drawbacks of the synthesized click polyesters was their lack of dispersibility in many solvents. In particular, they exhibited extremely poor dispersibility, even upon heating, in any common SEC solvent, suggesting the unsuitability of SEC to obtain molecular weights of these materials. Therefore, the reaction of neopentyl alcohol with an excess of propiolic acid was used to synthesize a monofunctional end-capping agent allowed for

a method to determine molecular weight of a series of samples utilizing ^{1}H NMR end-group analysis. The utilization of this end-capping agent in conjunction with offset stoichiometry allowed for the synthesis of a series of click copolyesters with varying degrees of polymerization. The reaction of a 1:1 ratio of NXG-bispropiolate and BD-bispropiolate with varying excesses of 1,3-bis-2-azidoethyl isophthalate and sufficient monofunctional end-capper to ensure 1:1 azide to propiolate functionality resulted in a series of photoreactive polyesters of three distinct controlled molecular weights. **Scheme 7.4** demonstrates the synthesis of the series of varying molecular weight polyesters. **Table 7.1** compares the molecular weights obtained as determined with a comparison of the integration of the *t*-butyl end-groups with an internal proton resonance. This comparison allowed for an effective absolute determination of the number-average molecular weight (M_n). These results demonstrated that the obtained molecular weights closely matched the targeted molecular weight. The level of control demonstrated in these samples suggested that those samples prepared with 1:1 bisazide and bispropiolate likely exhibited reasonable molecular weights.

Table 7.1 Targeted and experimentally determined M_n values for *o*-nitro benzyl ester containing click polyester.

Targeted M_n (g/mol)	**Obtained M_n (g/mol) (^{1}H NMR)**
3000	4000
5000	4900
8000	7900

Dissolving of the 7900 g/mol photoactive triazole-containing polyester and UV irradiation of the solution in standard Pyrex® NMR tubes and subsequent NMR spectroscopy allowed for confirmation of photocleavage of ONB functional groups. **Figure 7.1** demonstrates these spectra as a function of UV exposure. As shown in **Figure 7.1**, the integration of the resonance corresponding to the *o*-nitro benzyl protons diminishes in intensity relative to the *m*-

nitro benzyl protons. This evidence strongly suggests that the *o*-nitro benzyl ester undergoes photocleavage with exposure to UV light.

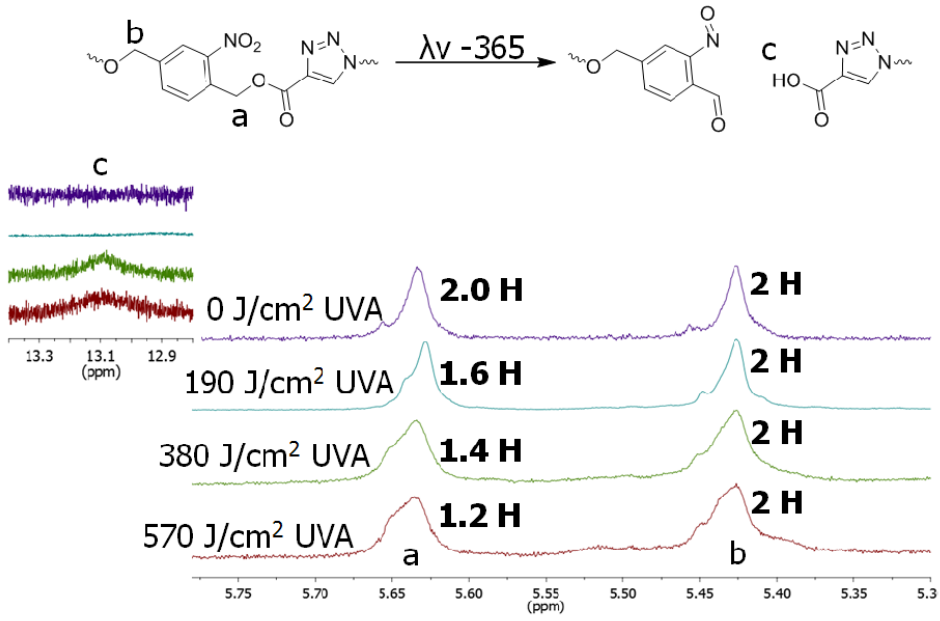

Figure 7.1 ^{1}H NMR demonstrating photodegradability of *o*-nitro benzyl ester containing click polyesters.

Segmented block copolymers often offer enhanced dispersibility relative to the homopolymer of the corresponding hard segment. Also, films of segmented block copolymers also typically exhibit good flexibility and elastomeric properties. Azide functionalized poly(propylene glycol) allowed for a method to obtain segmented block copolymers which contain triazole units within the polymer backbone. Reaction of PPG-2000 in a typical acyl-chloride reaction with 6-bromohexanoyl chloride and subsequent nucleophilic substitution with sodium azide resulted in bisazido-functionalized PPG difunctional oligomers. **Scheme 7.5** illustrates the synthesis of azide-functional PPG oligomers for the synthesis of segmented polyesters

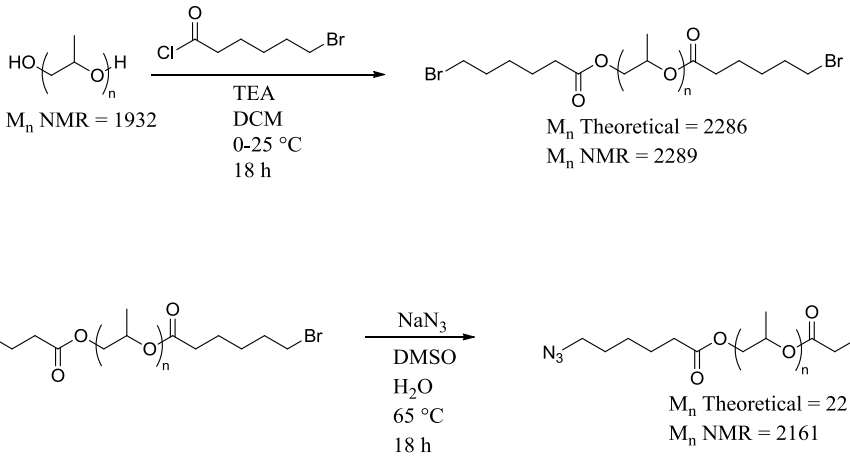

Scheme 7.5 Synthesis of azide-terminated PPG for preparation of segmented polyesters using Cu(I) catalyzed 1,3-Huisgen cycloaddition.

Photoreactive segmented polyesters were synthesized using the reaction of the PPG-bisazide with BAIP and NXGBP (30 wt % HS) in DMSO. The resulting polymers exhibited dispersibility in DMSO, NMP, and THF. DSC revealed a T_g of -67 °C, suggesting microphase separation and TGA revealed an onset of degradation above 350 °C. Melt-pressing resulted in films that demonstrated good flexibility, creasability and elastomeric properties and also provided films suitable (thickness <100 um) for subsequent photodegradation experiments.

Utilization of a UV lamp with a narrow exposure at 365 nm allowed for photodegradation experiments of the photoactive segmented polyester. **Figure 7.2** illustrates the ^{1}H NMR spectrum both before and after exposure to UVA. Comparison of the resonance at 5.42 ppm (the non-photoactive benzyl ester) with the resonance at 5.64 (the photoactive *o*-nitro benzyl ester) demonstrated a marked decrease in peak integration with exposure to UVA. These results confirmed the photodegradation of the ONB functional group within segmented triazole-containing polyesters, and are consistent with the results shown in **Figure 7.1.**

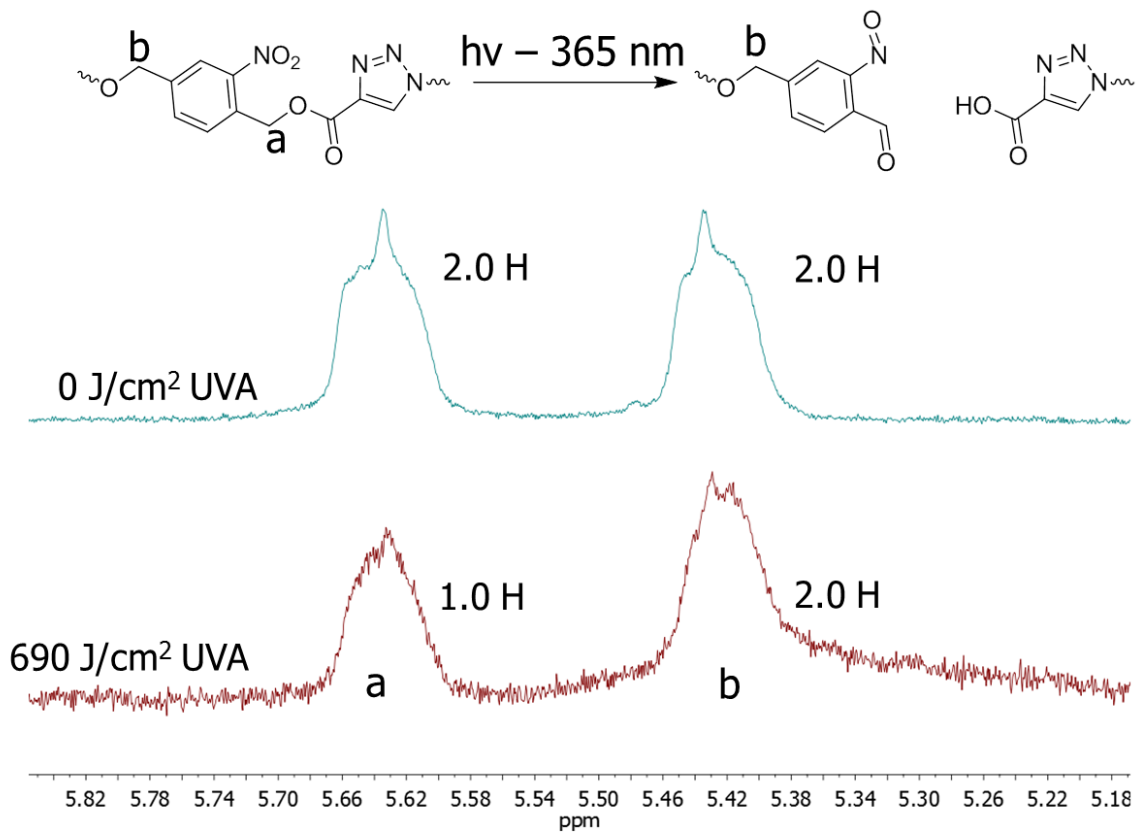

Figure 7.2 ^{1}H NMR spectroscopy confirming photodegradation of ONB functional groups within a segmented triazole-containing polyester.

7.5 Conclusions

Click chemistry allowed the synthesis of photoactive polyesters and segmented polyesters which contained triazole functional groups within the polymer backbone. The polyesters formed free-standing, brittle films whereas the segmented polyesters melt-pressed into free-standing, flexible films. ^{1}H NMR demonstrated good control of molecular weight relative to targeted molecular weights when utilizing offset stoichiometries and Carothers' equation in the synthesis of photoactive polyesters. Upon varying exposures to UV light, ^{1}H NMR demonstrated effective cleavage of the *o*-nitro benzyl ester units within the polymer mainchain, suggesting potential utility towards reversible adhesives.

7.6 Acknowledgements

This material is based upon work supported by Brewer Science, Inc. under contract # N00014-07-C-0797. The authors would like to acknowledge Dr. Rama Puligadda and Dr. Qin Lin for helpful discussions during the conception and execution of this research.

7.7 References

(1) Pillalamarri, S.; Puligadda, R.; Brubaker, C.; Wimplinger, M.; Pargfrieder, S. *J. Microelectron. Electron. Packag.* **2007**, *4*, 105.
(2) Puligadda, R.; Pillalamarri, S.; Hong, W.; Brubaker, C.; Wimplinger, M.; Pargfrieder, S. *Mater. Res. Soc. Symp. Proc.* **2007**, *970*, 239.
(3) June, S. M.; Suga, T.; Heath, W. H.; Long, T. E.; Lin, Q.; Puligadda, R. *J. Adhes.* **2010**, *86*, 1012
(4) Moore, J. A.; Dasheff, A. N. *Chem. Mater.* **1989**, *1*, 163.
(5) Cashion, M. P.; Park, T.; Long, T. E. *J. Adhes.* **2009**, *85*, 1.
(6) Huyck, R. H.; Trenor, S. R.; Love, B. J.; Long, T. E. *J. Macromol. Sci., Part A: Pure Appl. Chem.* **2008**, *45*, 9.
(7) Trenor, S. R.; Long, T. E.; Love, B. J. *Macromol. Chem. Phys.* **2004**, *205*, 715.
(8) Trenor, S. R.; Long, T. E.; Love, B. J. *J. Adhes.* **2005**, *81*, 213.
(9) Trenor, S. R.; Long, T. E.; Love, B. J. *Eur. Polym. J.* **2005**, *41*, 219.
(10) Williams, S. R.; Barta, Z.; Ramirez, S. M.; Long, T. E. *Macromol. Chem. Phys.* **2009**, *210*, 555.
(11) Nagao, Y.; Takasu, A. *Macromol. Rapid Commun.* **2009**, *30*, 199.
(12) Nagao, Y.; Takasu, A. *J. Polym. Sci., Part A: Polym. Chem.* **2010**, *48*, 4207.
(13) Kang, H.; Long, T. E. *Polym. Mater. Sci. Eng.* **2001**, *84*, 909.
(14) Lin, Q.; Long, T. E. *Macromolecules* **2003**, *36*, 9809.
(15) Lin, Q.; Pasatta, J.; Long, T. E. *J. Polym. Sci., Part A: Polym. Chem.* **2003**, *41*, 2512.
(16) Lin, Q.; Pasatta, J.; Wang, Z.-H.; Ratta, V.; Wilkes, G. L.; Long, T. E. *Polym. Int.* **2002**, *51*, 540.
(17) Lin, Q.; Unal, S.; Fornof, A. R.; Armentrout, R. S.; Long, T. E. *Polymer* **2006**, *47*, 4085.
(18) Lin, Q.; Unal, S.; Fornof, A. R.; Wei, Y.; Li, H.; Armentrout, R. S.; Long, T. E. *Macromol. Symp.* **2003**, *199*, 163.
(19) Long, T. E.; Turner, S. R., Step-growth polymerization. In Applied Polymer Science, 2000; pp 979-997
(20) McKee, M. G.; Unal, S.; Wilkes, G. L.; Long, T. E. *Prog. Polym. Sci.* **2005**, *30*, 507.
(21) Oguz, C.; Unal, S.; Long, T. E.; Gallivan, M. A. *Macromolecules* **2007**, *40*, 6529.
(22) Ozturk, G. I.; Pasquale, A. J.; Long, T. E. *J. Adhes.* **2010**, *86*, 395.
(23) Rogers, M. E.; Long, T. E.; Turner, S. R. *Synthetic Methods in Step-Growth Polymers* **2003**, 1.
(24) Unal, S.; Lin, Q.; Mourey, T. H.; Long, T. E. *Macromolecules* **2005**, *38*, 3246.
(25) Unal, S.; Long, T. E. *Macromolecules* **2006**, *39*, 2788.
(26) Unal, S.; Ozturk, G.; Sisson, K.; Long, T. E. *J. Polym. Sci., Part A: Polym. Chem.* **2008**, *46*, 6285.
(27) Awaji, H.; Kamikita, M.; Mizunuma, S.; JP 89-281135, 1991, p 20
(28) Cameron, J. F.; Frechet, J. M. J. *Journal of the American Chemical Society* **1991**, *113*, 4303.
(29) Feng, K.; Matsumoto, T.; Kurosaki, T. *J. Photopolym. Sci. Technol.* **1996**, *9*, 347.
(30) Feng, K.; Matsumoto, T.; Kurosaki, T. *Chem.Mater.* **1997**, *9*, 1362.
(31) Frechet, J. M. J.; Leung, M.-k.; Urankar, E. J.; Willson, C. G.; Cameron, J. F.; MacDonald, S. A.; Niesert, C. P. *Chem.Mater.* **1997**, *9*, 2887.
(32) Goldbach, J. T.; Russell, T. P.; Penelle, J. *Polym. Prepr.* **2002**, *43*, 470.

(33) Hanson, J. E.; Reichmanis, E.; Houlihan, F. M.; Neenan, T. X. *Chem.Mater.* **1992**, *4*, 837.
(34) Hayase, S.; Onishi, Y.; Horiguchi, R. *J. Electrochem. Soc.* **1987**, *134*, 2275.
(35) Il'ichev, Y. V.; Schworer, M. A.; Wirz, J. *J. Amer. Chem. Soc.* **2004**, *126*, 4581.
(36) Jiang, X.; Lavender, C. A.; Woodcock, J. W.; Zhao, B. *Macromolecules* **2008**, *41*, 2632.
(37) Johnson, J.; Koberstein, J. T.; Turro, N. J.; WO, 2008, p 53
(38) Johnson, J. A.; Finn, M. G.; Koberstein, J. T.; Turro, N. J. *Macromolecules* **2007**, *40*, 3589.
(39) Matsubara, S.; Nakai, H.; Urano, T.; Murakami, S.; JP 87-81375, 1988, p 7
(40) Meijer, J. T.; Henckens, M. J. A. G.; Minten, I. J.; Loewik, D. W. P. M.; van Hest, J. C. M. *Soft Matter* **2007**, *3*, 1135.
(41) Natt, F. J.-C.; Hunziker, J.; WO 2007-EP337, 2007, p 38
(42) Nishi, T.; Onodera, J.; Abe, Y.; Sakai, K.; Yui, T. *Yamagata Daigaku Kiyo Kogaku* **1968**, *10*, 9.
(43) Piggott, A. M.; Karuso, P. *Tetrahedron Lett.* **2005**, *46*, 8241.

Chapter 8: Bisphenol-A Free Epoxy Networks

Stephen M. June, Philippe Bissel, Evan Margaretta, and Timothy E. Long*
Department of Chemistry, Macromolecules and Interfaces Institute, Virginia Tech, Blacksburg VA 24061-0212

(From – Manuscript in preparation)

8.1 Abstract

Epoxy networks act as primary components in many composites, electronic materials, adhesives, coatings, and food and beverage can liners. Typically, bisphenol A (BPA) provides the primary structural component in these epoxy networks. BPA exhibits endocrine disrupting properties, and may potentially leach into foods or beverages packaged in containers lined with these networks; therefore, the replacement of BPA in these products may prove beneficial. Utilization of 2,2,4,4-tetramethyl-1,3-cyclobutanediol (CBDO) in recent years as a monomer yielded polymers that exhibit mechanical properties analogous with BPA-based polymers. Described herein is the synthesis of CBDO-diglycidyl ether (CBDO-GE) and its subsequent reaction with aminopropyl-terminated poly(propylene oxide)s (Jeffamine)s to yield epoxy networks. Comparison of these networks with analogous BPA-based epoxy networks served as an effective control experiment. Tensile testing and dynamic mechanical analysis demonstrated that CBDO-based epoxy networks perform similarly with BPA-based epoxy networks. Tensile testing revealed a Young's modulus of the epoxy network formed from the reaction of CBDO-GE and Jeffamine (molecular weight 230 g/mol) of 840 +/- 140 MPa. Utilization of melt rheology allowed for the determination of the gel time of CBDO-GE and Jeffamine (molecular weight 400 g/mol) and yielded a gel time of 150 m. These findings suggest that CBDO-based epoxy networks may serve as an effective replacement for BPA-epoxy networks.

8.2 Introduction

Epoxy networks and coatings play a significant role in many industries in today's markets. In particular, utilization of these materials as adhesives, composites, electronic materials, and coatings is prominent.[1-3] Additionally, these materials often find utility in the food packaging industry. Many beverage and food cans contain a coating of epoxy networks derived from bisphenol-A diglycidyl ether (BPA-GE) as a corrosion inhibitor, thereby increasing shelf-life of many canned consumer goods.[3-6] Epoxy networks cure with the addition of heat during the reaction of a diamine, such as aminopropyl-terminated polypropylene oxides (Jeffamines), with a diglycidyl ether, such as BPA-GE. BPA-GE is the product of the reaction of bisphenol-A (BPA) and epichlorohydrin. BPA-GE is one of the most commonly utilized diglycidyl ethers for the preparation of epoxy networks. Networks derived from BPA-GE exhibit excellent adhesion, high chemical and thermal resistance, increased mechanical strength, and excellent electrical insulating properties.[6]

In spite of the benefits of these epoxy networks, significant health concerns surround BPA. The first synthesis of BPA occurred in the 1890s and in the 1930s Dodds and coworkers investigated BPA as a potential synthetic estrogen mimic.[7] Although Dodds eventually generated a more effective estrogenic compound than BPA, it was clear that BPA exhibited estrogenic qualities.[7] Although BPA never found use as a drug, utilization of BPA in both epoxy networks and polycarbonates began in the 1950s.[6] In the last decade, concerns over the estrogenic properties of BPA led to a wealth of literature surrounding the negative endocrine-disrupting effects of BPA.[1,3,5,6,8-12] Several studies positively linked BPA exposure to diabetes,[8,10] cardiovascular disease,[8] an increased rate of miscarriages,[11] and other health complications.[6]

One of the primary utilizations of BPA-GE-derived epoxy networks is for coatings of food and beverage cans.[3,6,12,13] There exists concern regarding potential leaching of unreacted BPA and BPA-GE from these can liners into consumer products, and the eventual health risk associated with consumption of BPA and BPA-GE. In 2010, Lin and coworkers reported unreacted BPA-GE concentrations of up to 70.98 μg/6 dm^2 in canned food liner samples taken from various brands of canned meat, fish, and fruit.[4] In 2011, Michels and coworkers reported that individuals who consumed one can of canned soup per day, over a period of five days, exhibited a 1000% increase in urinary BPA levels.[14] Furthermore, in 2002 Soto-Valdez and coworkers reported BPA levels as high as 65.45 μg/kg in canned jalapeño samples.[5] While these values did not exceed legal limits (3 mg/kg), concerns continue regarding the health effects of even this small level of BPA.

There remains a recent trend towards development of BPA-free polymers to replace polymers such as BPA-polycarbonate. In particular, Eastman Chemical Company recently developed and released the Tritan® family of copolyesters for replacement of BPA-polycarbonate in food and beverage applications.[15-22] These polyesters exhibit mechanical and impact properties comparable with BPA-polycarbonate, and do not utilize BPA or BPA derivatives.[15-22] Additionally, Beall and coworkers demonstrated the synthesis of copolyterephthalates that possess ballistic properties greater than those of BPA-polycarbonate.[23] In both cases, the monomer responsible for these enhanced mechanical properties, relative to conventional polyesters is 2,2,4,4-tetramethylcyclobutane diol (CBDO), attributed to the cycloaliphatic, rigid structure of CBDO.

Based upon these observed properties of CBDO-containing polyesters, it is likely that the reaction of the diglycidyl ether of CBDO with diamines should provide mechanical properties

comparable to analogous BPA-based epoxy networks. Our research group has extensive experience in the synthesis and characterization of high performance step-growth polymers.[24-40] In particular we recently published several papers in efficiently cross-linked Michael networks and demonstrated high gel fractions and excellent mechanical properties.[41-48] Using this experience, we describe herein the synthesis of the diglycidyl ether of CBDO (CBDO-GE) and the subsequent synthesis of CBDO-containing epoxy networks. A comparison of these CBDO-derived epoxy networks with analogous epoxy networks synthesized from BPA-GE will determine the suitability of CBDO-GE as a potential replacement for BPA-GE.

8.3 Experimental

8.3.1 Materials and Methods. Eastman Chemical Co. (Kingsport, TN) provided 2,2,4,4-Tetramethyl-1,3-cyclobutanediol (CBDO) (50:50 trans:cis) which was used as received. Epibromohydrin, sodium hydride, BPA-diglycidyl ether and amino-propyl terminated poly(propylene oxide) were purchased from Aldrich (St. Louis, MO) and were used as received. Tetrahydrofuran was purchased from Fisher Scientific (Hampton, NH) and was purified on a PS-MD-3 PureSolv® solvent purification system purchased from Innovative Technology Inc. (Chantily, VA).

^{1}H NMR spectroscopy was performed in $CDCl_3$ at 23 °C with a Varian 400 MHz MR400 spectrometer (Varian, Palo Alto, CA, USA). Thermogravimetric analysis (TGA) was performed using a TA Instruments Hi-Res TGA 2950 (TA Instruments, New Castle, DE, USA) in a platinum pan under a constant nitrogen purge of 50 mL/min and a ramp rate of 10 °C/min. Differential scanning calorimetry (DSC) was conducted in a TA Instruments Q1000 DSC (TA Instruments, New Castle, DE, USA) at a heating rate of 10 °C/min and a cooling rate of

50 °C/min under a constant nitrogen purge of 50 mL/min. Glass transition temperatures (T_g) were reported as mid-point temperatures from the second heat. Dynamic mechanical analysis (DMA) data was obtained using a TA Instruments (New Castle, DE) Q800 dynamic mechanical analyzer in tension mode at a frequency of 1 Hz, 15 um strain, and temperature ramp of 3 °C/min. Tensile experiments were performed on an Instron (Norwood, MA) 4411 universal testing instrument utilizing sample strips and a crosshead speed of 2 mm/min with manual grips at ambient temperature. Melt rheology data was obtained using a TA Instruments AR2000 Rheometer equipped with a peltier plate. Experiments were performed isothermally at 80 °C using an oscillatory strain of 10 degrees. Gel times were taken at the crossover point between G' and G". Gel fractions were determined using soxhlet extraction. Typical extraction times were 24 h using THF as a solvent.

8.3.2 Synthesis

Synthesis of CBDO-diglycidyl ether. 1.54 g CBDO (10.65 mmols) and 100 mL of THF were added to a 2-necked round-bottomed flask equipped with a reflux condenser. After cooling in an ice bath, 0.56 g sodium hydride (23.45 mmols – 2.2 eq) was added to the flask. The mixture was then refluxed for 1 h. The flask was then cooled in an ice bath for 30 min. and 7.29 g epibromohydrin (53.25 mmols – 5 eq) was added to the flask. The mixture was allowed to react for 48 h from 0-25° C. Upon completion, THF was removed under reduced pressure. The resulting brown solid was dissolved in $CHCl_3$, washed 3x with H_2O and 1x with brine. The organic phase was dried with magnesium sulfate, filtered, and the solvent was removed under reduced pressure. The resulting orange oil was then purified using silica gel chromatography, and subsequently distilled for further purification. The resulting product was a clear oil, and ^{1}H and ^{13}C NMR confirmed the structure (isolated yield ~50 %).

Synthesis of CBDO- and BPA-containing epoxy networks. In a representative synthesis, 1 eq of aminopropyl-terminated PPO was mixed with 2 eq CBDO- or BPA-diglycidyl ether. The mixture was poured into an aluminum or Teflon® dish and heated at 80 °C overnight under atmospheric conditions. The resulting networks were used directly from the mold without further purification.

8.4 Results and Discussion

Synthesis of the diglycidyl ether of CBDO allowed for preparation of CBDO-containing epoxy networks. ^{1}H NMR confirmed the composition of CBDO as a 50:50 mixture of trans- and cis-CBDO. The reaction of CBDO and epibromohydrin, using NaH as a base to deprotonate CBDO, yielded the diglycidyl ether of CBDO (CBDO-GE) as shown in **Scheme 8.1**. The reactivity of CBDO to base accounted for low yields and the extensive purification required. Commercially available BPA-diglycidyl ether (BPA-GE) allowed for the synthesis of control networks which provided direct comparisons of the thermal and mechanical properties of CBDO-containing and classical BPA-containing epoxy networks.

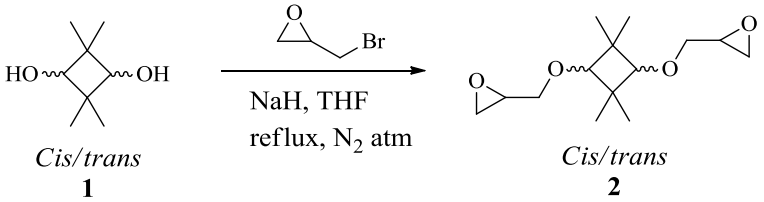

Scheme 8.1 Synthesis of CBDO-GE.

The reaction of CBDO- or BPA-diglycidyl ether and aminopropyl-terminated PPO of molecular weights of 230, 400, and 2000 (Jeffamine 230, 400, and 2000) successfully yielded CBDO- and BPA-containing epoxy networks. The resulting networks varied in flexibility, based on the PPO molecular weight. Gel fractions of all networks, as determined using soxhlet extraction from THF are shown as **Table 8.1**. All samples exhibited gel fractions above 90%,

demonstrating efficient crosslinking. **Scheme 8.2** demonstrates the synthesis of epoxy networks from CBDO and aminopropyl-terminated PPO.

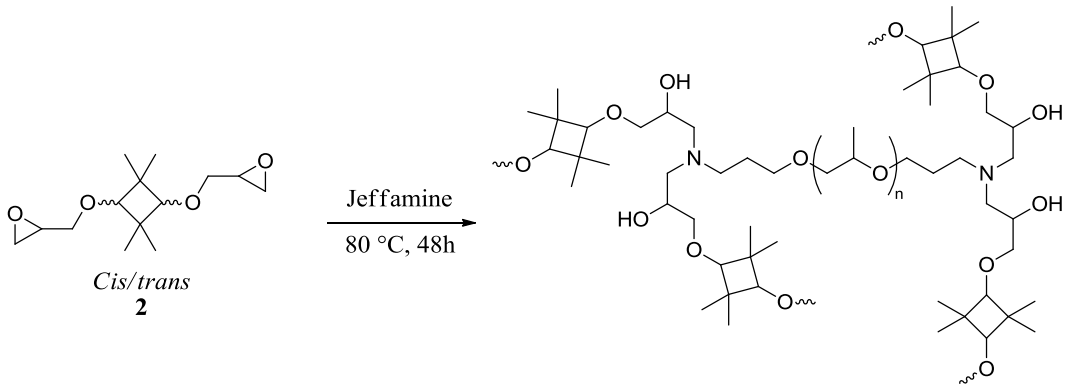

Scheme 8.2 Synthesis of CBDO-containing epoxy networks with aminopropyl-terminated PPO.

Table 8.1 Gel fractions of synthesized CBDO- and BPA-containing epoxy networks.

Glycidyl Ether	Jeffamine M_n (g/mol)	Gel Fraction (%)
CBDO-GE	2000	91
CBDO-GE	400	96
CBDO-GE	230	99
BPA-GE	2000	97
BPA-GE	400	99
BPA-GE	230	99

TGA and DSC provided thermal analysis of the CBDO- and BPA-containing epoxy networks. TGA demonstrated degradation temperatures above 300 °C in all cases. Glass transition temperatures (T_g) of the networks varied greatly based upon the molecular weight of the PPO and the structure of the diglycidyl ether. **Table 8.2** demonstrates the glass transition temperatures of the CBDO and BPA-containing epoxy networks. In all cases, for a given molecular weight of PPO, the T_g of the networks remains significantly higher for the BPA-containing networks than for the CBDO-containing networks; however, at low molecular weights of PPO, the CBDO networks exhibit a T_g above room temperature, an important parameter for many epoxy network applications, such as beverage can liners.

Table 8.2 Glass transition temperatures of CBDO- and BPA-containing epoxy networks.

Glycidyl Ether	Jeffamine M_n (g/mol)	T_g (°C)
CBDO-GE	2000	-57
CBDO-GE	400	6
CBDO-GE	230	42
BPA-GE	2000	-46
BPA-GE	400	51
BPA-GE	230	79

Tensile testing provided the Young's modulus of the synthesized epoxy networks. **Figures 8.1a-c** show representative tensile curves comparing BPA- and CBDO-containing epoxy networks synthesized with Jeffamine molecular weights of 2000, 400, and 230, respectively. **Table 8.2** demonstrates the Young's modulus, tensile stress at yield, and tensile strain at break for the epoxy networks. CBDO-containing networks synthesized using Jeffamine 2000 and Jeffamine 230 exhibit comparable moduli, stresses at yield, and strains at break to the analogous BPA-containing epoxy networks. The CBDO-containing network synthesized with Jeffamine 400 possesses a significantly lower modulus and stress at yield, although a much higher strain at break than the analogous BPA-containing network. These results are consistent with the T_g values of the corresponding networks. At ambient temperatures, both the BPA-containing and CBDO-containing networks synthesized with Jeffamine 2000 were above their T_g and both the BPA-containing and CBDO-containing networks synthesized with Jeffamine 230 were below their T_g. However, in the case of the samples synthesized using Jeffamine 400, the BPA-containing sample is below its T_g, while the CBDO-containing network is above its T_g, leading to dramatic differences in mechanical properties. This suggested that with careful diamine selection, these CBDO-containing networks may serve as an effective replacement for BPA-containing epoxy networks.

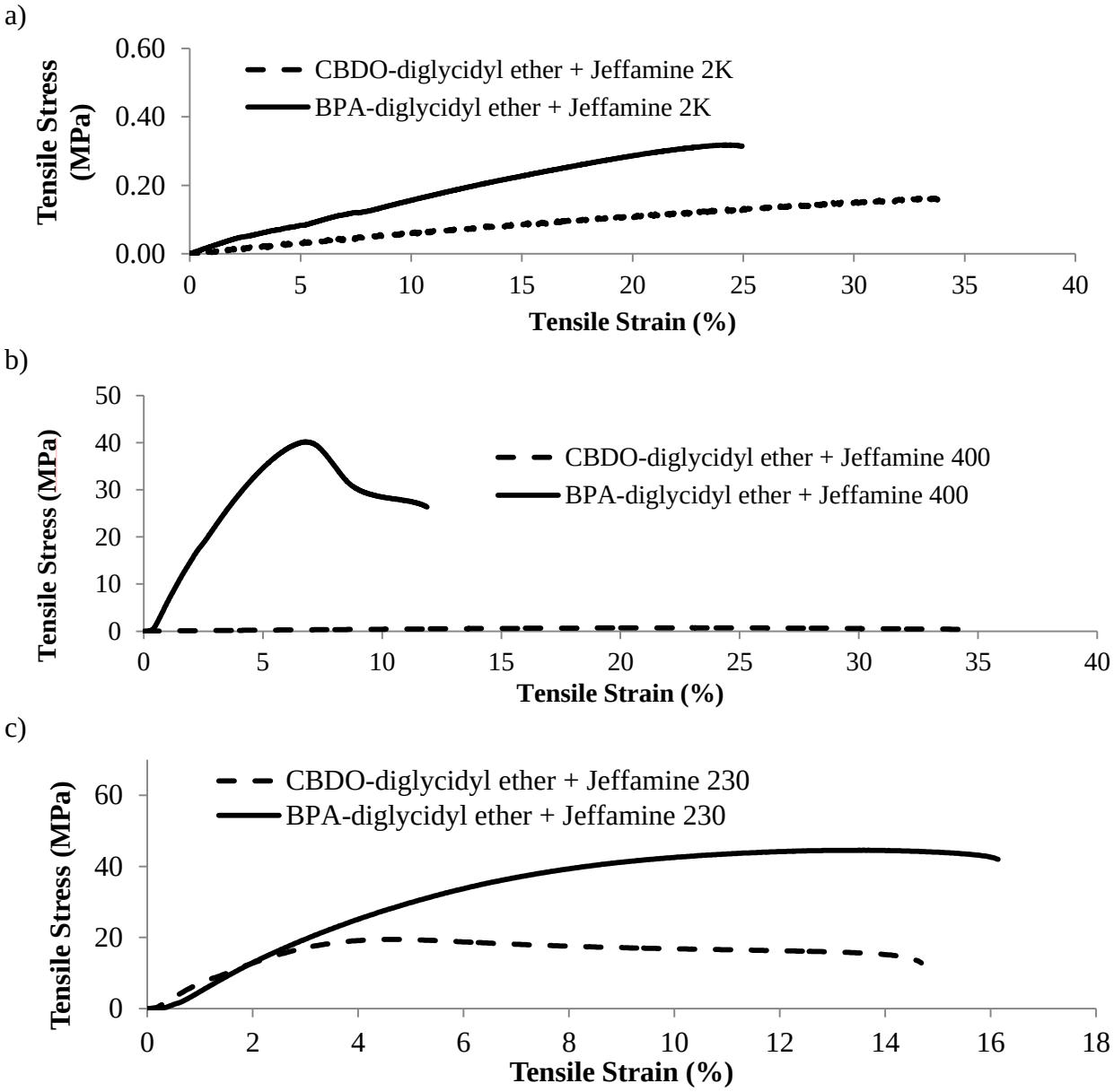

Figure 8.1 Representative tensile curves of CBDO- and BPA- containing epoxy networks synthesized with aminopropyl terminated PPO with a molecular weight of 2000 (a), 400 (b), and 230 (c).

Table 8.2 Tensile data for CBDO- and BPA-containing epoxy networks.

Glycidyl Ether	Jeffamine M_n	Young's Modulus (MPa)	Stress at Yield (%)	Strain at Break (%)
CBDO-GE	230	840 +/- 140	20 +/- 2	19 +/- 3
CBDO-GE	400	4.7 +/- 0.2	0.6 +/- 0.1	34 +/- 1
CBDO-GE	2000	0.6 +/- 0.1	0.2 +/- 0.1	46 +/- 14
BPA-GE	230	1080 +/- 240	47 +/- 2	16 +/- 4
BPA-GE	400	950 +/- 150	35 +/- 5	19 +/- 7
BPA-GE	2000	1.7 +/- 0.2	0.33 +/- 0.02	26 +/- 3

Dynamic mechanical analysis (DMA) further clarified the mechanical properties of the BPA- and CBDO-containing epoxy networks, as shown in **Figure 8.2**. As expected, the T_g's for the networks closely match those obtained using DSC. Furthermore, analysis of the sub-T_g moduli of the networks confirmed similar mechanical properties. In addition, rubbery moduli of these networks increased with decreasing Jeffamine molecular weight which corresponded to the decreased crosslink density associated with higher molecular weight Jeffamines. These results further demonstrated that with careful diamine selection, it proved possible to tailor the properties of the networks such that CBDO-based networks were mechanically equivalent to BPA-based epoxy networks.

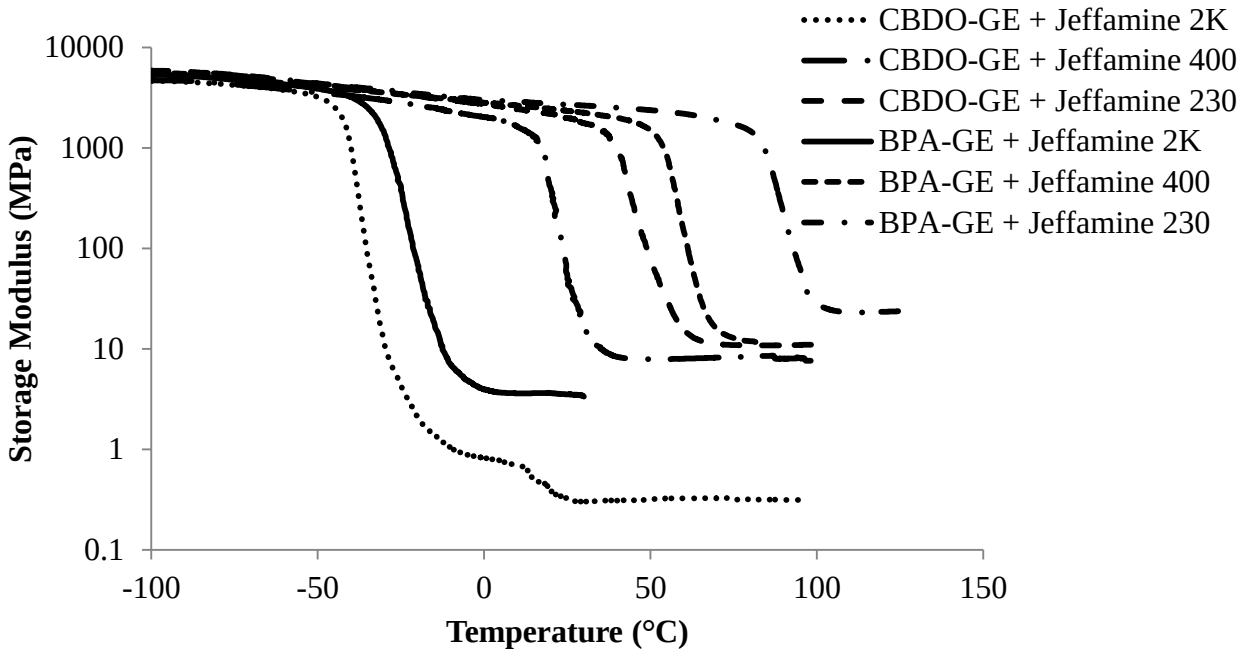

Figure 8.2 DMA curves comparing moduli vs. temperateure for BPA- and CBDO-containing epoxy networks.

In order to understand the relative rates of reaction of CBDO-GE and BPA-GE with diamines, melt rheology provided a measure of the gelation time for the reaction of Jeffamine 400 with both BPA-GE and CBDO-GE. **Figure 8.3** demonstrates G' and G" for the reaction of

PPO with CBDO-GE and BPA-GE at 80 °C as a function of time. When G' and G" were plotted on the same scale, the gel time occurred at the crossover point of the two curves. The reaction of Jeffamine 400 and BPA-GE exhibited a gel time of 78 minutes at 80 °C while the reaction of Jeffamine 400 and CBDO-GE resulted in a gel time of 150 minutes at 80 °C. Although CBDO-GE had a slower reaction rate, likely due to sterics from the pendant methyl groups, both reactions proceeded efficiently and relatively quickly.

a)

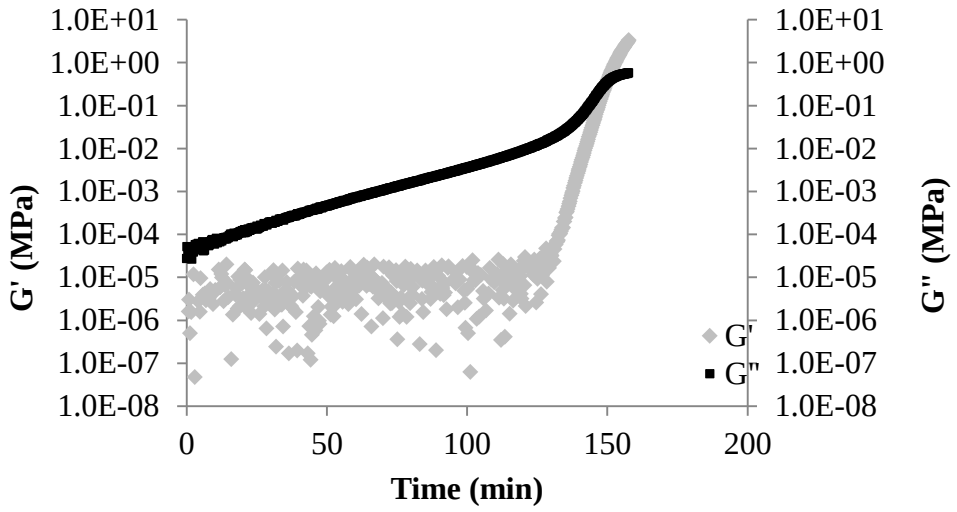

b)

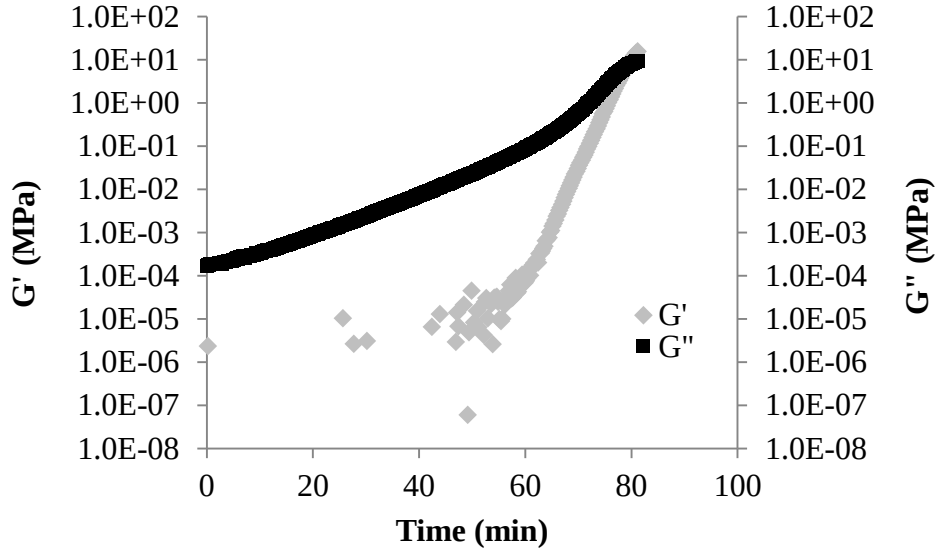

Figure 8.3 Melt rheology of epoxidation of (a) CBDO-GE and (b) BPA-GE and Jeffamine 400 indicating gel times of (a) 150 and (b) 78 min.

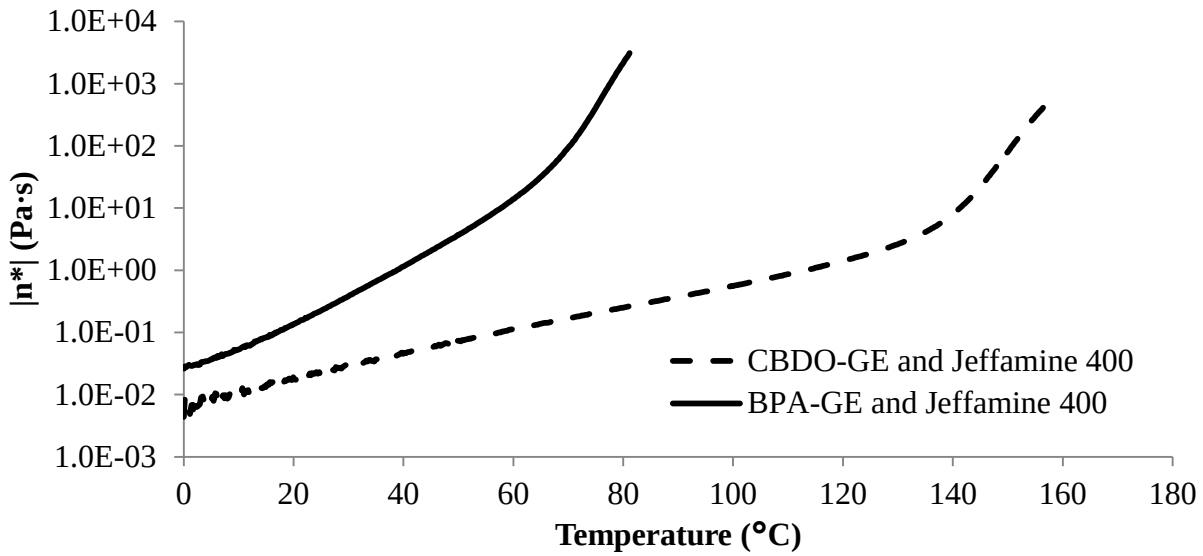

Figure 8.4 Melt viscosity as a function of temperature for the epoxidation of CBDO-GE or BPA-GE with Jeffamine 400.

Figure 8.4 demonstrates the complex viscosity of both reactions as a function of time. In both reactions, the viscosity increases linearly as a function of time time until approximately 10 minutes prior to the gel time. At this point, the reaction exhibited a dramatic upturn in viscosity as the sample began to cross-link. This indicated that CBDO-GE provides a 70 minute longer application window upon mixing with Jeffamine than BPA-GE.

8.5 Conclusions

Due to health concerns surrounding BPA and its derivatives, it may prove imperative to develop an effective replacement for food packaging applications. Towards this end, the reaction of CBDO with epibromohydrin successfully yielded CBDO-GE. Curing of CBDO-GE with various molecular weight Jeffamines resulted in the formation of epoxy networks with high gel content. Analogous control networks synthesized using BPA-GE provided an effective control. In both systems, T_g exhibited a strong dependence on the molecular weight of the Jeffamine. DMA demonstrated near identical sub-T_g storage moduli for all samples, suggesting

that at temperatures below the T_g, these materials exhibit similar stiffness regardless of diglycidyl ether utilized. Tensile testing indicated that samples below their T_g exhibited comparable Young's moduli, near 1 GPa. Samples above their T_g also exhibited similar Young's moduli, independent of diglycidyl ether. Melt rheology revealed a gel time for the reaction of BPA-GE and Jeffamine 400 of 78 min and the reaction of CBDO-GE and Jeffamine 400 exhibited a gel time of 150 min. These results suggested that, given appropriate diamine selection, CBDO-GE may serve as a suitable replacement for BPA-GE in applications where human exposure is a concern.

8.6 Acknowledgements

The authors would like to acknowledge Eastman Chemical Company for their generous donation of CBDO.

8.7 References

(1) Ben-Jonathan, N.; Steinmetz, R. *Trends Endocrinol. Metab.***1998**, *9*, 124.
(2) Beverly S, R. *J. Steroid Biochem. Mol. Biol.* **2011**, *127*, 27.
(3) Kamrin, M. A. *MedGenMed* **2004**, *6*, 7.
(4) Hong, Z.; Ming, X.; Yanyan, Z.; Zhiyuan, D.; Kunhui, L. *Anal. Bioanal.Chem.* **2010**, *398*, 3165.
(5) Munguia-Lopez, E. M.; Peralta, E.; Gonzalez-Leon, A.; Vargas-Requena, C.; Soto-Valdez, H. *J. Agric. Food. Chem.* **2002**, *50*, 7299.
(6) Rubin, B. S. *J. Steroid Biochem. Mol. Biol.* **2011**, *127*, 27.
(7) Dodds, E. C.; Lawson, W. *Nature* **1936**, *137*, 996.
(8) Lang, I. A.; Galloway, T. S.; Scarlett, A.; Henley, W. E.; Depledge, M.; Wallace, R. B.; Melzer, D. *JAMA* **2008**, *300*, 1303.
(9) Mariscal-Arcas, M.; Rivas, A.; Granada, A.; Monteagudo, C.; Murcia, M. A.; Olea-Serrano, F. *Food Chem. Toxicol.* **2009**, *47*, 506.
(10) Shankar, A.; Teppala, S. *J. Clin. Endocrinol. Metab.* **2011**, *96*, 3822.
(11) Sugiura-Ogasawara, M.; Ozaki, Y.; Sonta, S.-i.; Makino, T.; Suzumori, K. *Hum. Reprod.* **2005**, *20*, 2325.
(12) Vogel, S. A. *Am J Public Health* **2009**, *99 Suppl 3*, S559.
(13) Tanaka, Y.; US4722982A 1988, p 6 pp.
(14) Carwile, J. L.; Ye, X.; Zhou, X.; Calafat, A. M.; Michels, K. B. *JAMA* **2011**, *306*, 2218.
(15) Crawford, E. D.; McWilliams, D. S.; Porter, D. S.; Connell, G. W.; US7855267B2 2010, p 47
(16) Crawford, E. D.; McWilliams, D. S.; Porter, D. S.; Connell, G. W.; US7838620B2 2010, p 47.
(17) Crawford, E. D.; Pecorini, T. J.; Porter, D. S.; Connell, G. W.; Keegan, M. J.; US7915376B2 2011, p 63
(18) Crawford, E. D.; Pecorini, T. J.; Porter, D. S.; Connell, G. W.; Keegan, M. J.; US7893188B2 2011, p 50
(19) Crawford, E. D.; Porter, D. S.; Connell, G. W.; US7842776B2, p 46
(20) Crawford, E. D.; Porter, D. S.; Connell, G. W.; US20110144266A1, p 54
(21) Crawford, E. D.; Porter, D. S.; Connell, G. W.; US7906610B2, p 43
(22) Crawford, E. D.; Porter, D. S.; Connell, G. W.; US7893187B2, p 47
(23) Booth, C. J.; Kindinger, M.; McKenzie, H. R.; Handcock, J.; Bray, A. V.; Beall, G. W. *Polymer* **2006**, *47*, 6398.
(24) Cheng, S.; Ozturk, G. I.; Long, T. E. *Polym. Prepr.* **2009**, *50*, 209.
(25) June, S. M.; Suga, T.; Heath, W. H.; Long, T. E.; Lin, Q.; Puligadda, R. *J. Adhes.* **2010**, *86*, 1012
(26) Kang, H.; Long, T. E. *Polym. Mater. Sci. Eng.* **2001**, *84*, 909.
(27) Lin, Q.; Long, T. E. *Macromolecules* **2003**, *36*, 9809.
(28) Long, T. E.; Turner, S. R., Step-growth polymerization. In Applied Polymer Science, 2000; pp 979-997
(29) Oguz, C.; Unal, S.; Long, T. E.; Gallivan, M. A. *Macromolecules* **2007**, *40*, 6529.
(30) Ozturk, G. I.; Pasquale, A. J.; Long, T. E. *J. Adhes.* **2010**, *86*, 395.
(31) Rogers, M. E.; Long, T. E.; Turner, S. R. *Synthetic Methods in Step-Growth Polymers* **2003**, 1.
(32) Unal, S.; Lin, Q.; Mourey, T. H.; Long, T. E. *Macromolecules* **2005**, *38*, 3246.

(33) Unal, S.; Long, T. E. *Macromolecules* **2006**, *39*, 2788.
(34) Williams, S. R.; Barta, Z.; Ramirez, S. M.; Long, T. E. *Macromol. Chem. Phys.* **2009**, *210*, 555.
(35) Williams, S. R.; Borgerding, E. M.; Layman, J. M.; Wang, W.; Winey, K. I.; Long, T. E. *Macromolecules* **2008**, *41*, 5216.
(36) Williams, S. R.; Long, T. E. *Prog. Polym. Sci.* **2009**, *34*, 762.
(37) Williams, S. R.; Salas-de la Cruz, D.; Winey, K. I.; Long, T. E. *Polymer* **2010**, *51*, 1252.
(38) Williams, S. R.; Wang, W.; Winey, K. I.; Long, T. E. *Macromolecules* **2008**, *41*, 9072.
(39) Yamauchi, K.; Kanomata, A.; Inoue, T.; Long, T. E. *Macromolecules* **2004**, *37*, 3519.
(40) Zhang, M.; June, S. M.; Long, T. E. In *Comprehensive Polymer Science*; 2nd ed.; Moeller, M., Matyzaszewski, K., Eds.; Elsevier: In press; Vol. 5.
(41) Mather, B. D.; Baker, M. B.; Beyer, F. L.; Berg, M. A. G.; Green, M. D.; Long, T. E. *Macromolecules* **2007**, *40*, 6834.
(42) Mather, B. D.; Miller, K. M.; Long, T. E. *Macromol. Chem. Phys.* **2006**, *207*, 1324.
(43) Mather, B. D.; Viswanathan, K.; Miller, K. M.; Long, T. E. *Prog. Polym. Sci.* **2006**, *31*, 487.
(44) Mather, B. D.; Williams, S. R.; Long, T. E. *Macromol. Chem. Phys.* **2007**, *208*, 1949.
(45) Ozturk, G.; Long, T. E. *J. Polym. Sci., Part A: Polym. Chem.* **2009**, *47*, 5437.
(46) Williams, S. R.; Lepene, B. S.; Thatcher, C. D.; Long, T. E. *Biomacromolecules* **2009**, *10*, 155.
(47) Williams, S. R.; Mather, B. D.; Miller, K. M.; Long, T. E. *J. Polym. Sci., Part A: Polym. Chem.* **2007**, *45*, 4118.
(48) Williams, S. R.; Miller, K. M.; Long, T. E. *Prog. React. Kinet.* **2007**, *32*, 165.

Chapter 9: Overall Summary and Conclusions

Utilization of step-growth polymerization methods allowed for the synthesis of several different novel polymer structures. The novel structures included poly(siloxane imides), polyesters, poly(triazole esters), poly(triazole ether esters), and epoxy networks. Each of these polymers included either the incorporation of a photoactive unit within the polymer backbone or high-performance elastomeric properties.

Thermal solution imidization offered an optimal route for the preparation of photoactive poly(siloxane imides). Photoactive segmented poly(siloxane imides) were synthesized from from cyclobutane-1,2,3,4-tetracarboxylic dianhydride and other comonomers. Size exclusion chromatography confirmed high molecular weights and Gaussian molecular weight distributions for the photoactive polyimides. Differential scanning calorimetry confirmed a soft segment T_g of -122 °C, suggesting microphase separated morphologies. Atomic force microscopy confirmed microphase separation, demonstrating the presence of a hard segment and a soft segment. Dynamic mechanical analysis confirmed the presence of a rubbery plateau, further confirming elastomeric properties. ^{1}H NMR spectroscopy confirmed an increase in the integration of resonances corresponding to maleimide formation upon UV exposure, confirming effective photocleavage at wavelengths near 254 nm. These results indicated that these photoactive poly(siloxane imides) would effectively serve as reversible adhesives in flip bonding applications.

Melt transesterification provided a facile route towards the synthesis of photoactive polyesters. The synthesis of polyesters containing *o*-nitro benzyl ester functionality using melt transesterification afforded a thermoplastic photoreversible adhesive. Size exclusion

chromatography results suggested good molecular weights and polydispersities of the photoactive adhesive. ^{1}H NMR spectroscopy confirmed a decrease in the integration of the resonance corresponding to the photoactive *o*-nitro benzyl ester functionality, relative to the photostable *m*-nitro benzyl ester units after exposure to UV. ASTM wedge testing revealed a decrease in adhesive fracture energy of nearly 2 J/cm^2 upon UV exposure, comparable to the decrease in fracture energy of a hot melt adhesive upon exposure to increased temperatures. These results indicated the utility of these photoactive polyesters in commercial flip bonding applications.

Click chemistry allowed for the synthesis of triazole-containing polyesters and segmented block copolyesters at decreased temperatures, relative to melt transesterification. Triazole-containing homopolyesters exhibited remarkably increased (~40 °C) T_g's relative to structurally analogous classical polyesters. However, melt-pressed films of the homopolyesters exhibited low flexibility. The synthesis of azide-functionalized poly(propylene glycol) allowed for the preparation of segmented triazole-containing polyesters with varying hard segment contents. The segmented polyesters exhibited increased dispersibility and film flexibility relative to homopolymers of the corresponding hard segment. Differential scanning calorimetry determined a soft segment T_g of the segmented polyesters near -62 °C, indicating microphase separation, and a crystalline T_m ranging from 114-171 °C as a function of hard segment content, suggesting semicrystalline morphologies. Dynamic mechanical analysis confirmed the presence of a rubbery plateau, with increasing rubbery plateau moduli and flow temperatures as a function of hard segment content. Atomic force microscopy confirmed microphase separated morphologies as well as the existence of semicrystalline structures. These results suggested the potential utility of click chemistry towards high performance polyesters and segmented block copolyesters.

Click chemistry also was used for the synthesis of photoactive triazole-containing polyesters and segmented copolyesters. The obtained photoactive polyesters exhibited poor dispersibility and film flexibility, whereas the photoactive segmented polyesters exhibited enhanced dispersibility and film robustness. Utilization of Carothers's equation confirmed controllable molecular weights, determined using ^{1}H NMR spectroscopy. These results suggested stoichiometric balance likely produced high molecular weight triazole-containing polyesters. ^{1}H NMR spectroscopy confirmed photocleavage of *o*-nitro benzyl ester functional groups upon UV exposure in both segmented and non-segmented photoactive triazole-containing polyesters. These results indicated the potential utility of these systems in "smart" polymer applications.

Synthesis of the glycidyl ether of 2,2,4,4-tetramethyl-1,3-cyclobutane diol (CBDO-GE) provided the capability for the production of epoxy networks which did not contain bisphenol-A or bisphenol-A derivatives. Analogous epoxy networks, synthesized using bisphenol-A glycidyl ether (BPA-GE) acted as an effective control. All epoxy networks synthesized exhibited high gel fractions, suggesting effective crosslinking. Tensile testing revealed T_g dependent Young's moduli for the epoxy networks, although a comparison of samples both above and below T_g suggested an insignificant difference in the Young's moduli for samples prepared using CBDO-GE and BPA-GE. Dynamic mechanical analysis revealed a consistent glassy modulus, regardless of glycidyl ether utilized, and rubbery moduli dependent on diamine molecular weight. Melt rheology revealed gel times of 78 min for BPA-GE based networks, and 150 min for CBDO-GE based networks. These results indicated the potential utility of CBDO-GE as a replacement for BPA-GE in epoxy networks produced for food packaging applications.

Chapter 10: Suggested Future Directions

Future Work Directions:

10.1 Synthesize photo-active polyimides using "click" chemistry. Reaction of an excess of 3-aminophenylacetylene with CBDA under standard thermal solution imidization conditions may yield a photoactive bisalkyne. Reaction of this bis-alkyne with either small molecule bisazides or the bisazides proposed in part 1 will yield photo-active polyimides using "click" reaction conditions. Differential scanning calorimetry will likely confirm high T_g's of the synthesized poly(triazole imides). Size exclusion chromatography will provide molecular weights of the polymers, and should offer a method for analysis of the extent of photodegradation upon exposure to UV light with a wavelength of 254 nm. **Scheme 10.1** illustrates the synthesis of a photoactive bisalkyne subsequent reaction with a bisazide to yield poly(triazole imides).

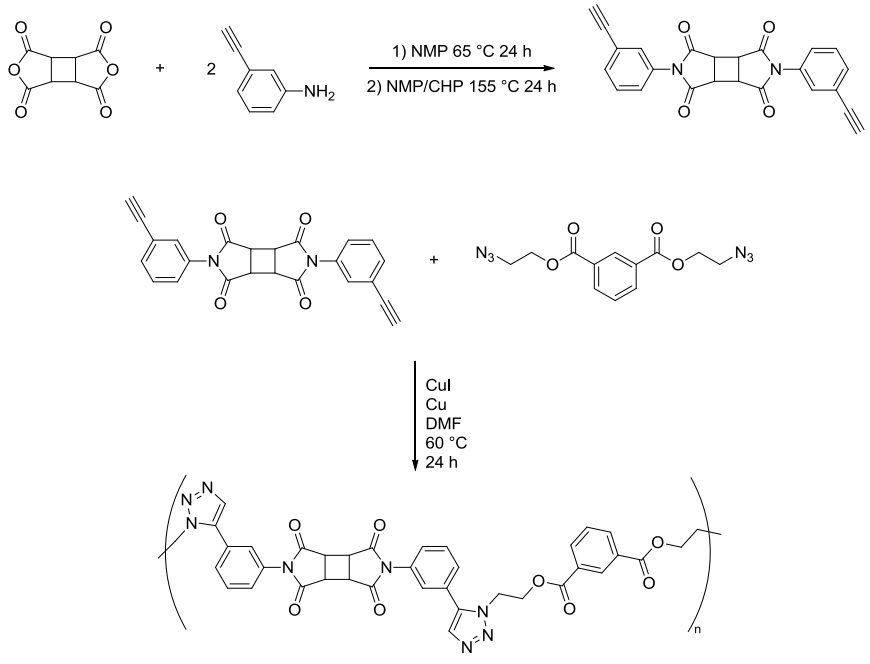

Scheme 10.1 Preparation of CBDA-bisalkyne and subsequent polymerization under click reaction conditions.

10.2 Investigate the potential for urocanic acid as a chromophore for use in photoactive polymers. In particular, the synthesis of urocanic acid-functionalized polyols, such as poly(tetramethylene oxide) (PTMO) should allow for a photochain extendable polyether under wavelengths near 320 nm. This photoreactive polyether should also undergo reversible photocleavage at 254 nm to afford the original poly(tetramethylene oxide) diurocanate. Differential scanning calorimetry will likely confirm an increase in T_g upon chain extension, and a subsequent decrease upon photocleavage. UV/visible spectroscopy and ^{1}H NMR spectroscopy will provide an effective means for the observation of these photoreactions. **Figure 10.1** illustrates an obtained UV/visible spectrum for methyl urocanate and **Scheme 10.2** outlines the synthesis of urocanate-functionalized PTMO.

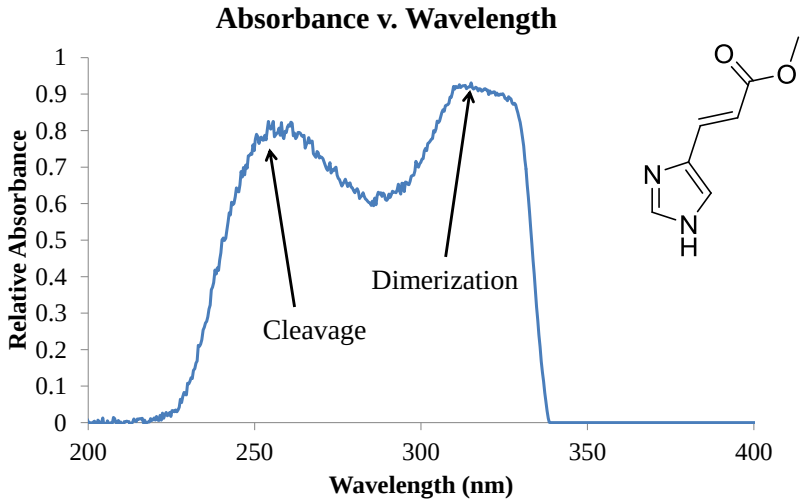

Figure 10.1 UV/visible spectrum of methyl urocanate indicating the wavelengths of photocleavage and photodimerization.

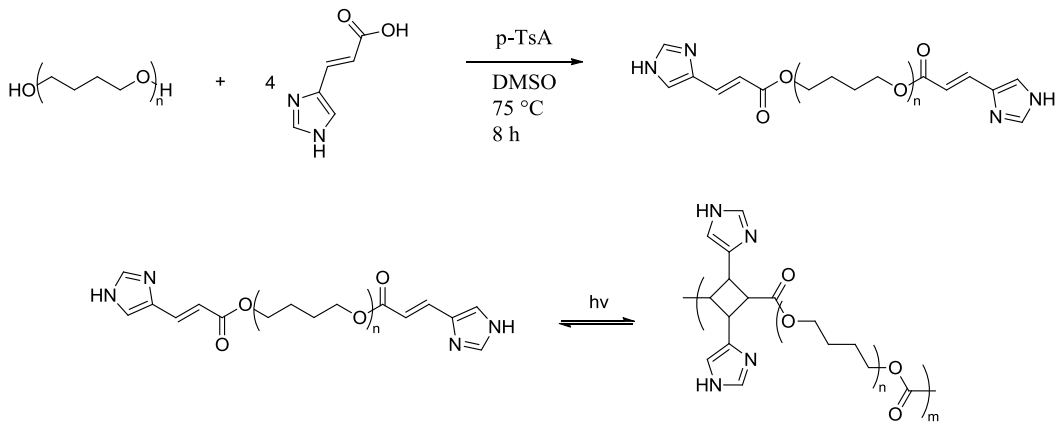

Scheme 10.2 Synthesis of poly(tetramethylene oxide) diurocanate and subsequent reversible photochain extension.

10.3 Synthesize polyurethanes using click chemistry. The reaction of 2-bromoethanol with hexamethylene diisocyanate and subsequent conversion of the bromide functional groups into azide groups provides a simple route towards a urethane-containing bisazide. Analogously, reaction of ethylene glycol with hexamethylene diisocyanate and subsequent reaction with propiolic acid will provide urethane-containing propiolates. Reaction of these two urethane-containing monomers under standard click reaction conditions will result in poly(urethane triazoles). The incorporation of PPG-bisazide, as described in **Chapter 6**, will afford segmented poly(urethane ether triazoles). The combination of hydrogen bonding and triazole association should yield polyurethanes with exceptional mechanical toughness. **Scheme 10.3** details the synthesis of urethane-containing propiolates for subsequent click polymerizations.

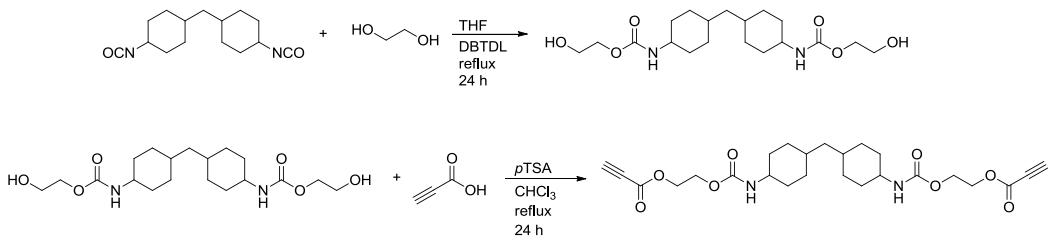

Scheme 10.3 Synthesis of urethane-containing propiolates for preparation of poly(triazole urethanes)

10.4 Synthesis of polyurethanes chain extended with 2,2,4,4-tetramethyl-1,3-cyclobutane diol (CBDO) should provide superior mechanical toughness and strength relative to conventional poly(ether urethanes). As discussed in **Chapter 8**, CBDO often provides enhanced mechanical properties, such as Young's modulus, tensile strength, and toughness when incorporated into polyesters and epoxy networks. It is likely that utilizing CBDO in lieu of traditional chain extenders for segmented polyurethanes may similarly offer enhanced mechanical properties. Synthesis of a series of varying hard segment content polyurethanes which utilize CBDO as a chain extender, and comparison with conventional 1,4-butane diol-chain extended polyurethanes will provide confirmation of this theory. **Scheme 10.4** illustrates the synthesis of a segmented poly(ether urethane) using CBDO.

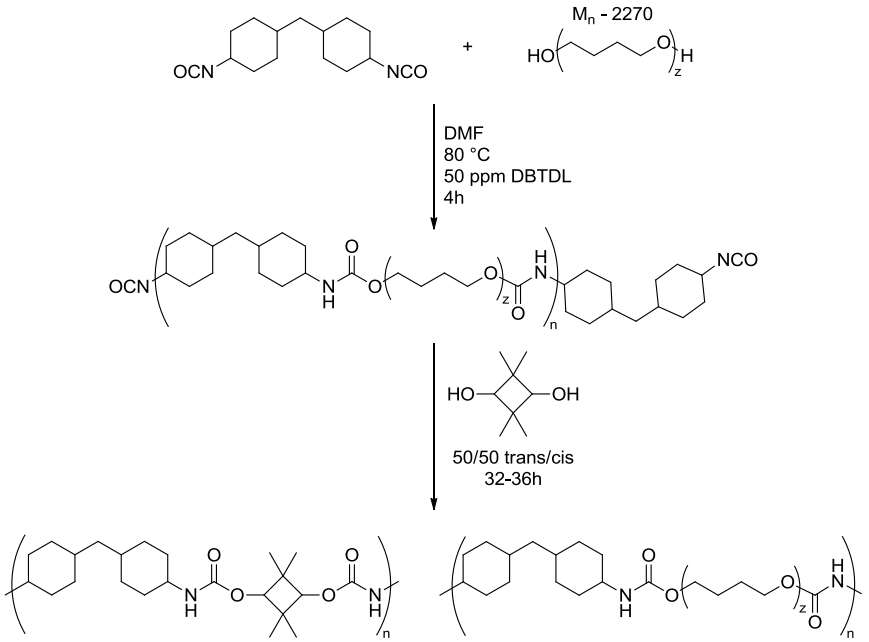

Scheme 10.4 Synthesis of segmented poly(ether urethanes) utilizing CBDO as a chain extender.

10.5 Synthesis of triazole-containing polyesters using melt-transesterification. In order to fully confirm the effects of triazole units on polyester thermal properties, structurally identical polyesters to those referenced in **Chapters 6 and 7** will be synthesized. Reaction of CHDMBP with 2-azidoethanol will yield a diol that, when polymerized with dimethyl isophthalate, will yield a polyester with the identical structure of the triazole-containing polyester synthesized in **Chapter 6** from CHDMBP and BAIP. The reaction will be performed under typical melt-transesterification conditions. **Scheme 10.5** details the synthesis of this polyester. It is expected that the thermal transitions of this polyester will be identical to those reported in **Chapter 6**, thereby confirming that the increased thermal transitions were a result of the triazole functionality, and not the synthetic method.

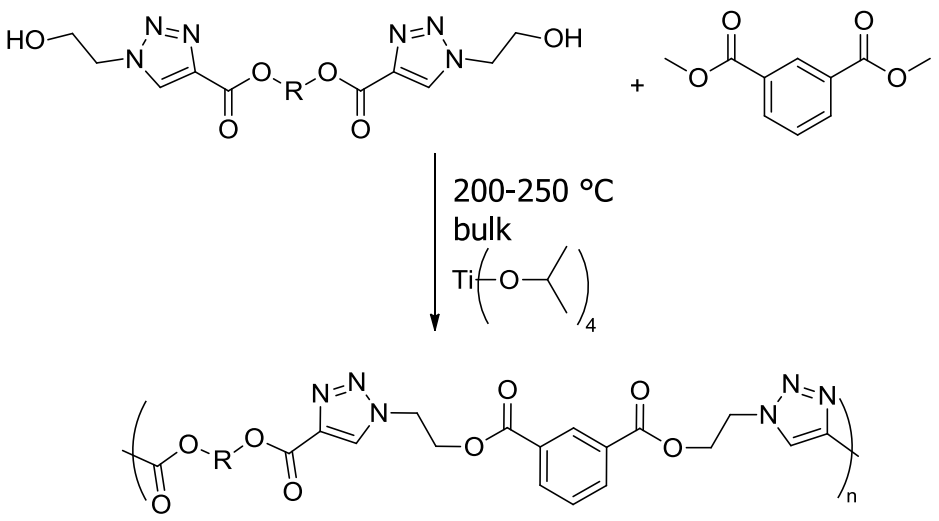

Scheme 10.5 Synthesis of triazole-containing polyesters using melt transesterification.

Appendix A: Supplemental Information

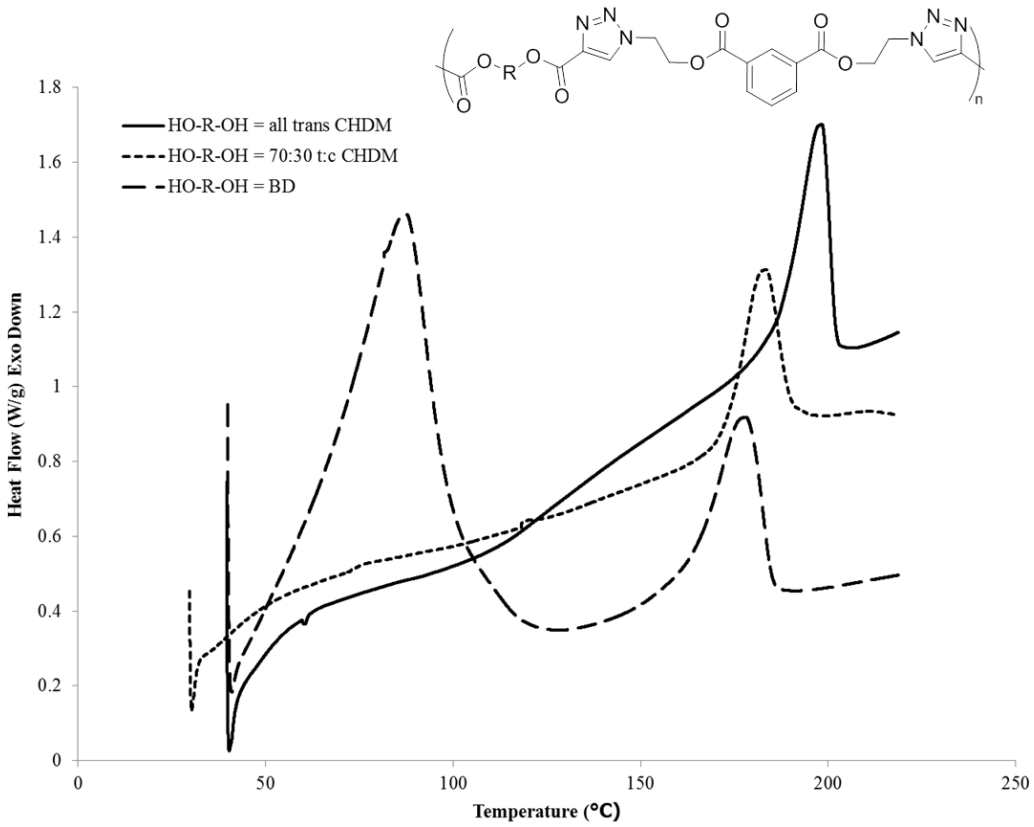

Figure A.1 1st heat DSC traces for homopolyesters prepared using click chemistry (**Chapters 6 and 7**).

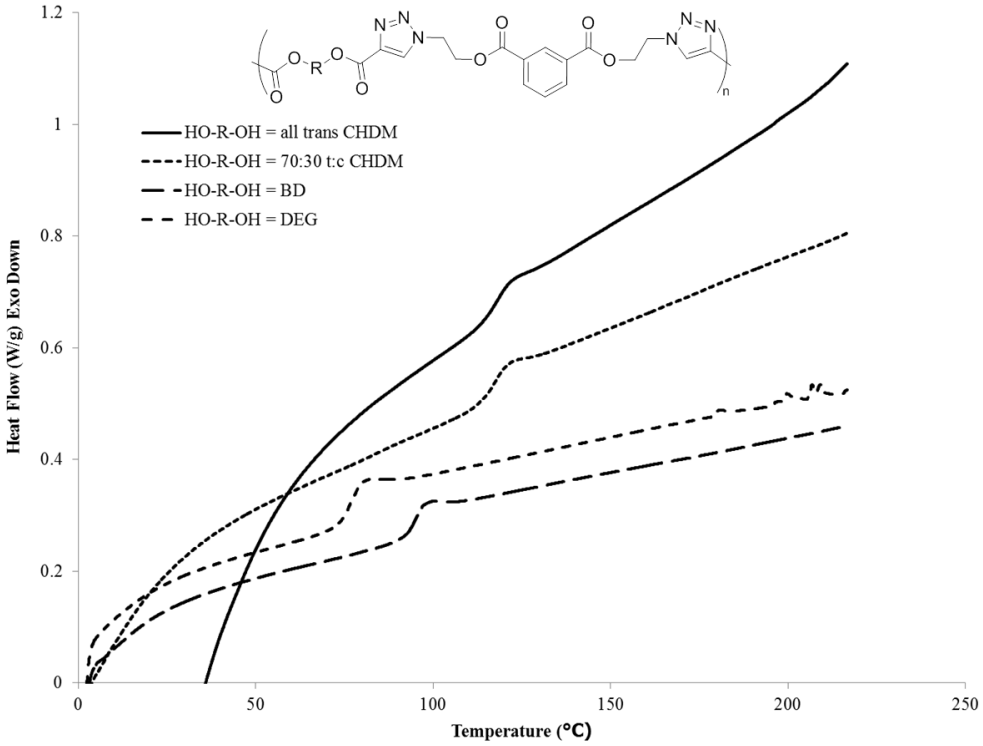

Figure A.2 2nd heat DSC traces for homopolyesters prepared using click chemistry (**Chapters 6 and 7**).

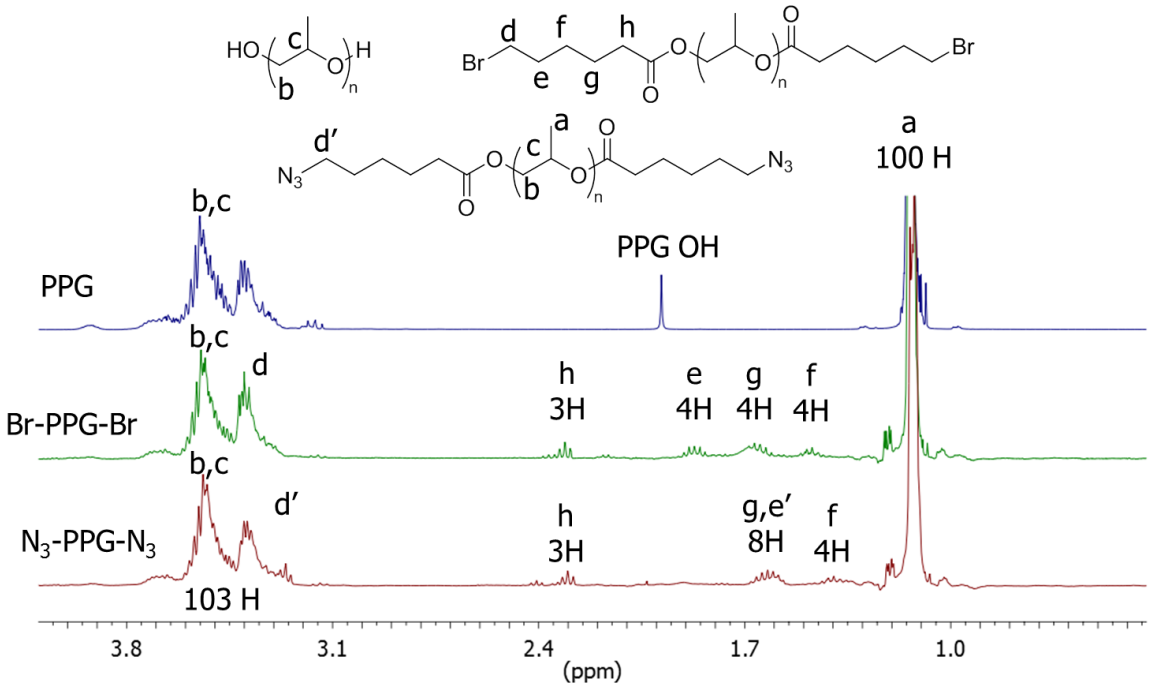

Figure A.3 1H NMR spectroscopy assigning all resonances and confirming structure, purity, and difunctionality of telechelic bromo- and azide-terminated PPG oligomers (**Chapters 6 and 7**).

Table A.1 Hydroxyl titration results for 2K PPG derivatives (**Chapters 6 and 7**).

Sample	OH Number	M_n
Blank	0	-
2K PPG	60.7	1850
2K PPG dibromide	0	-
2K PPG bisazide	0	-
2K PPG bistriazyl alcohol	48.7	2300

Table A.2 Comparison of M_n obtained from ^{1}H NMR spectroscopy and from hydroxyl titrations (**Chapters 6 and 7**). Theoretical M_ns of the PPG derivatives were calculated from the observed Mn of the 2K PPG for each technique.

PPG derivative	^{1}H NMR M_n (theoretical)	^{1}H NMR M_n (observed)	Titration M_n (theoretical)	Titration M_n (observed)
2K PPG	-	1932	-	1850
2K PPG-dibromide	2286	2289	2204	-
2K PPG-bisazide	2216	2161	2134	-
2K PPG-bistrazyl alcohol	2328	2273	2246	2300

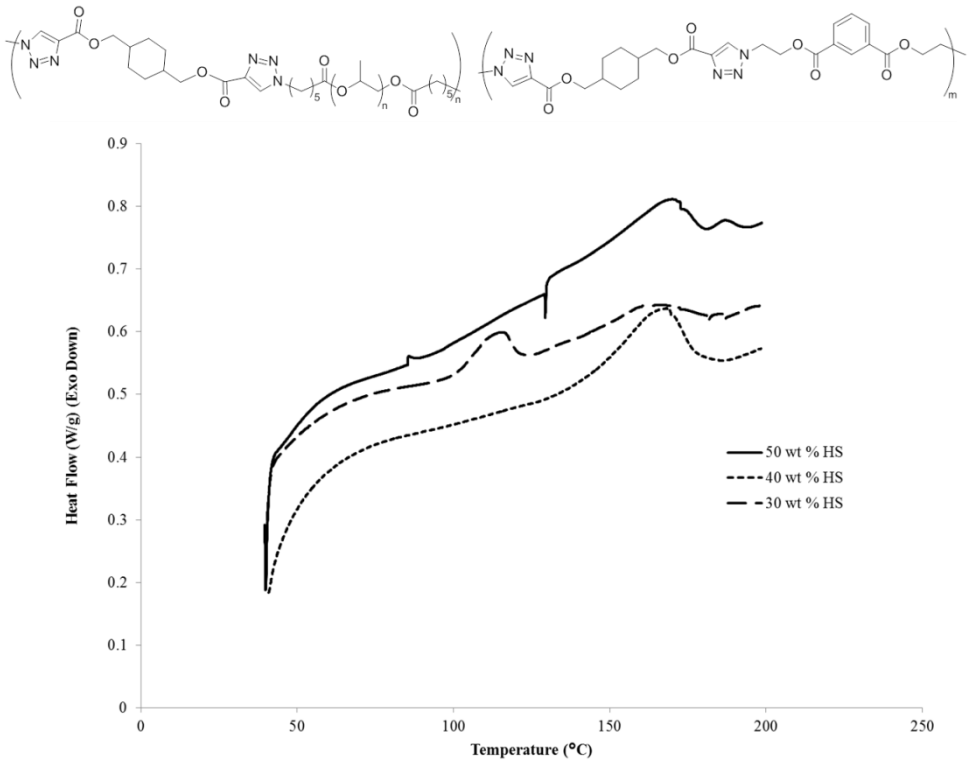

Figure A.4 1st heat DSC traces for segmented polyesters prepared using click chemistry (**Chapter 6**).

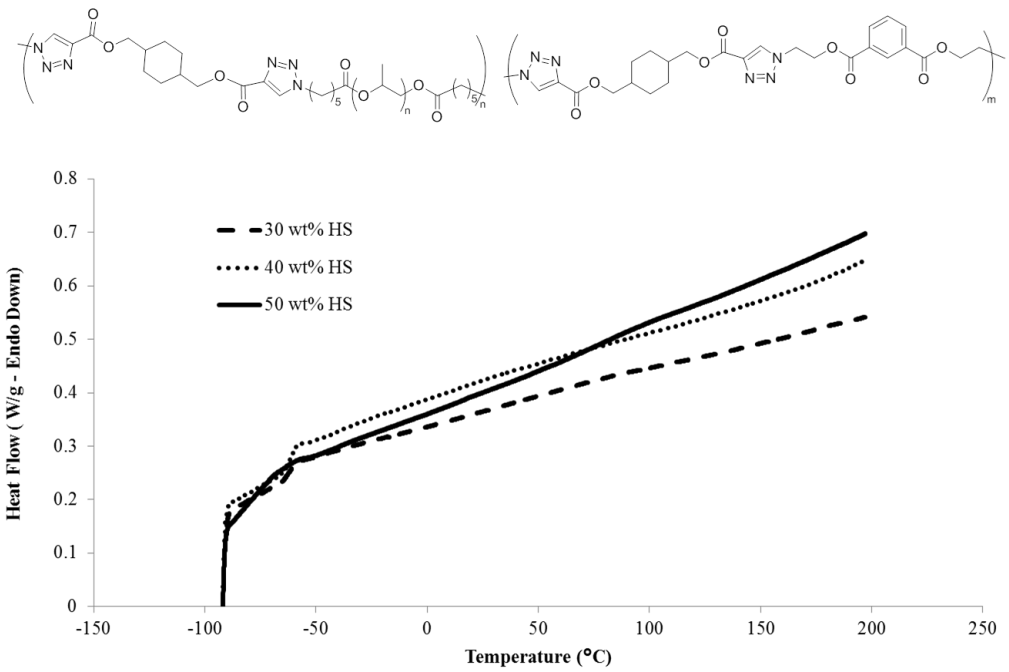

Figure A.5 2nd heat DSC traces for segmented polyesters prepared using click chemistry (**Chapter 6**).

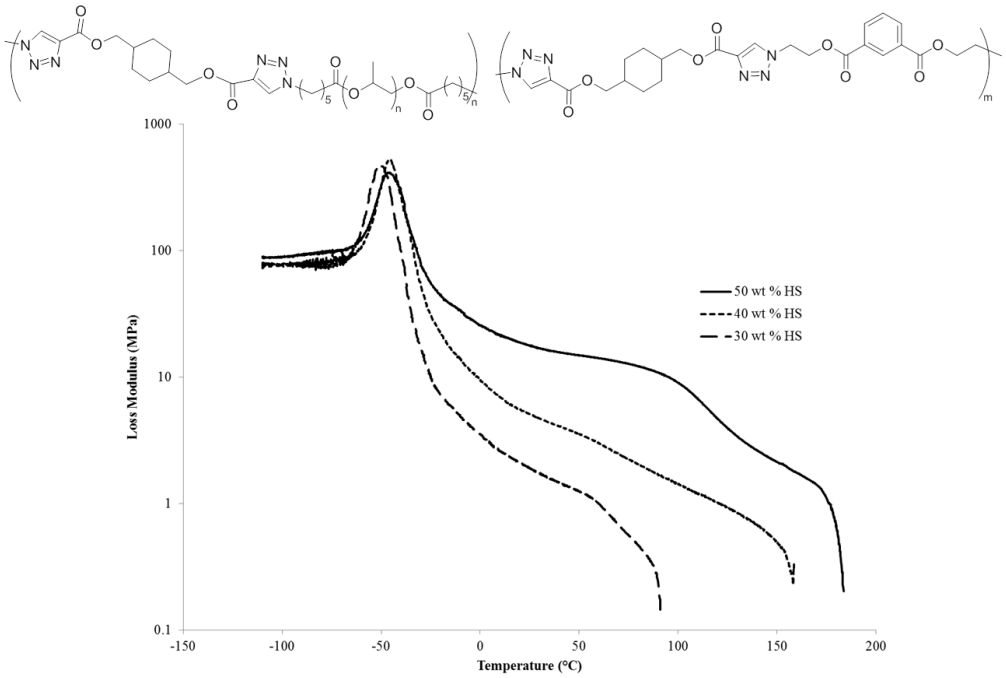

Figure A.6 Loss Modulus DMA traces for segmented polyesters prepared using click chemistry (**Chapter 6**).

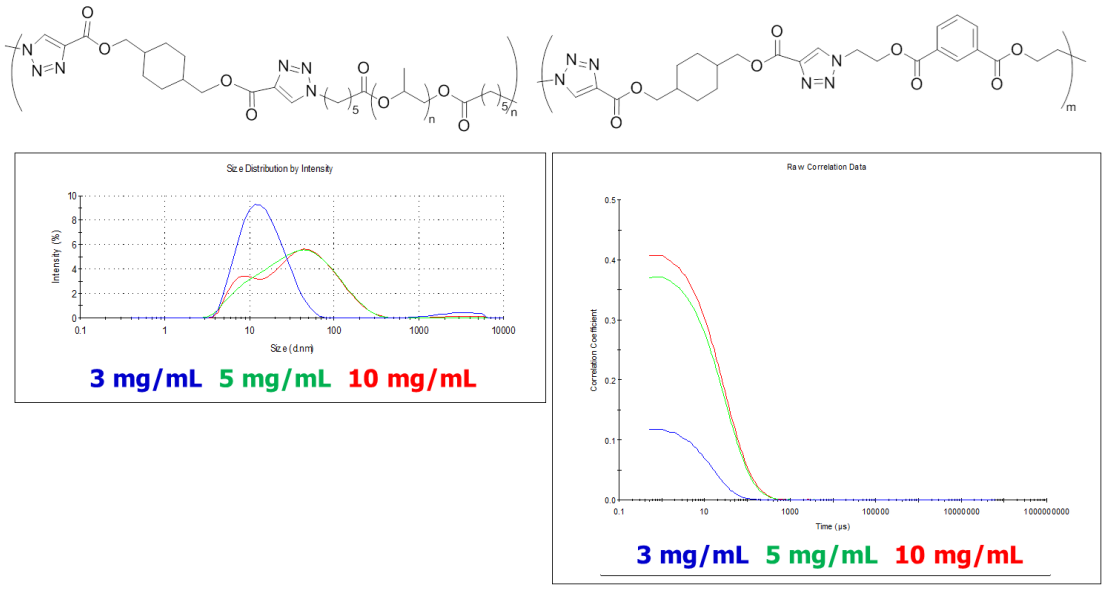

Figure A.7 DLS traces for 50 wt % HS segmented triazole-containing polyester showing poor correlation at low concentrations and aggregations at higher concentrations in DMF (**Chapter 6**).

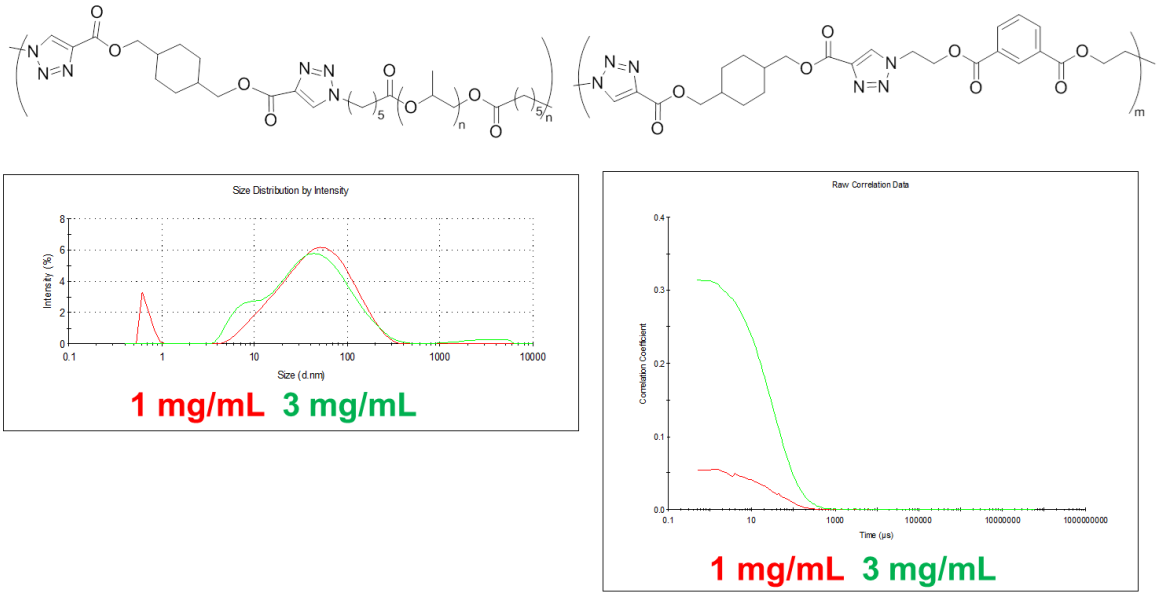

Figure A.8 DLS traces for 50 wt % HS segmented triazole-containing polyester showing poor correlation at low concentrations and aggregations at higher concentrations in DMF containing 0.05 M LiBr (**Chapter 6**).

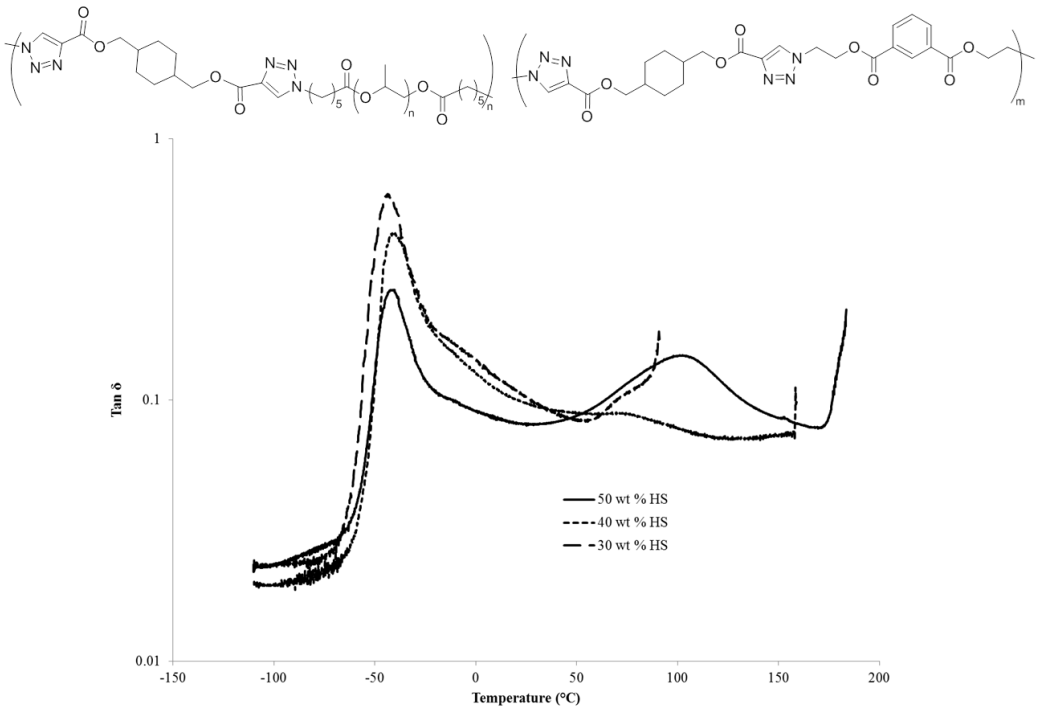

Figure A.9 Tan δ DMA traces for segmented polyesters prepared using click chemistry (**Chapter 6**).

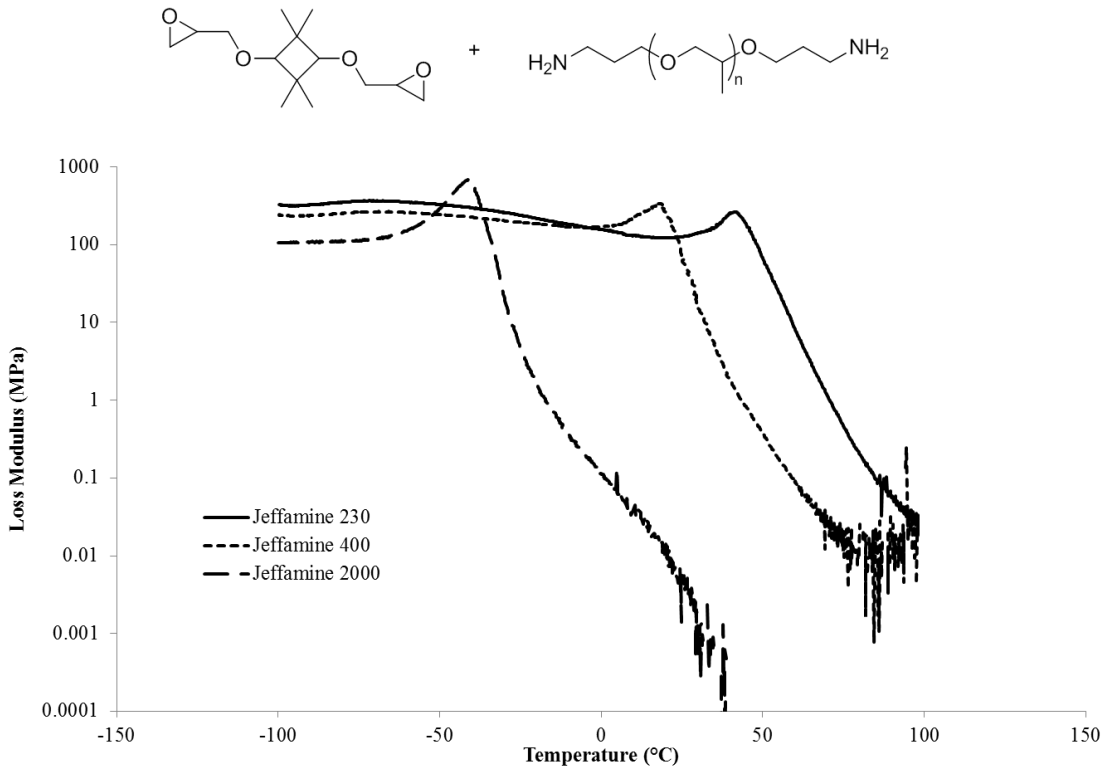

Figure A.10 Loss Modulus DMA traces for epoxy networks prepared from CBDOGE and Jeffamines of various M_n (**Chapter 8**).

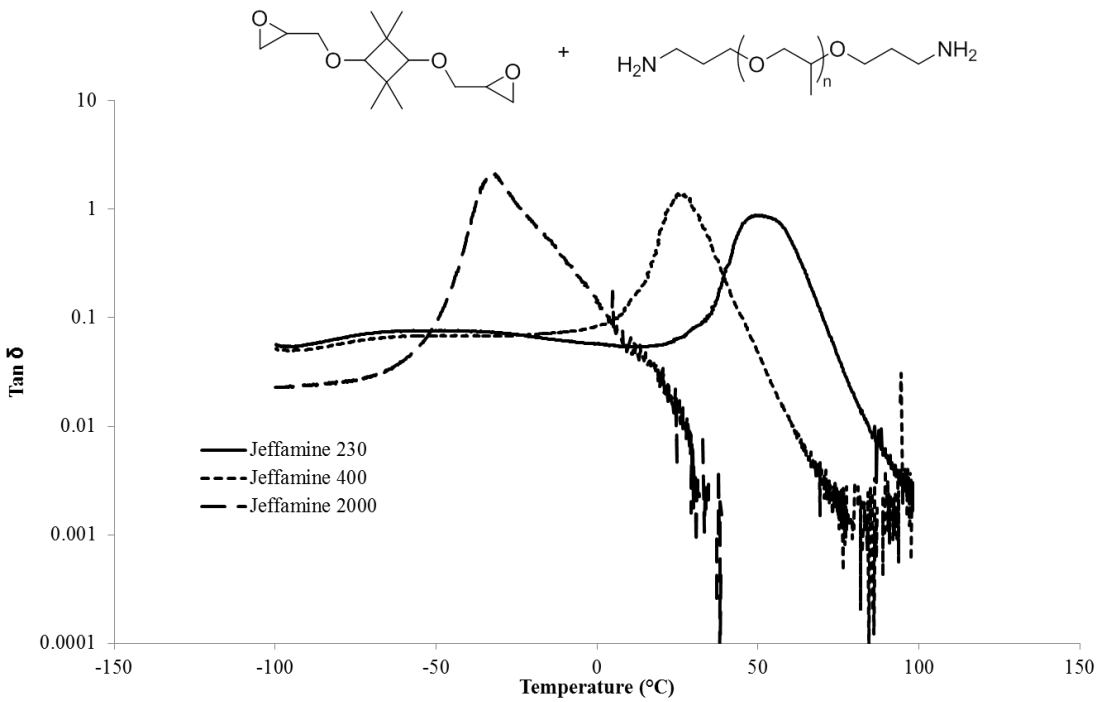

Figure A.11 Tan δ DMA traces for epoxy networks prepared from CBDOGE and Jeffamines of various M_n (**Chapter 8**).

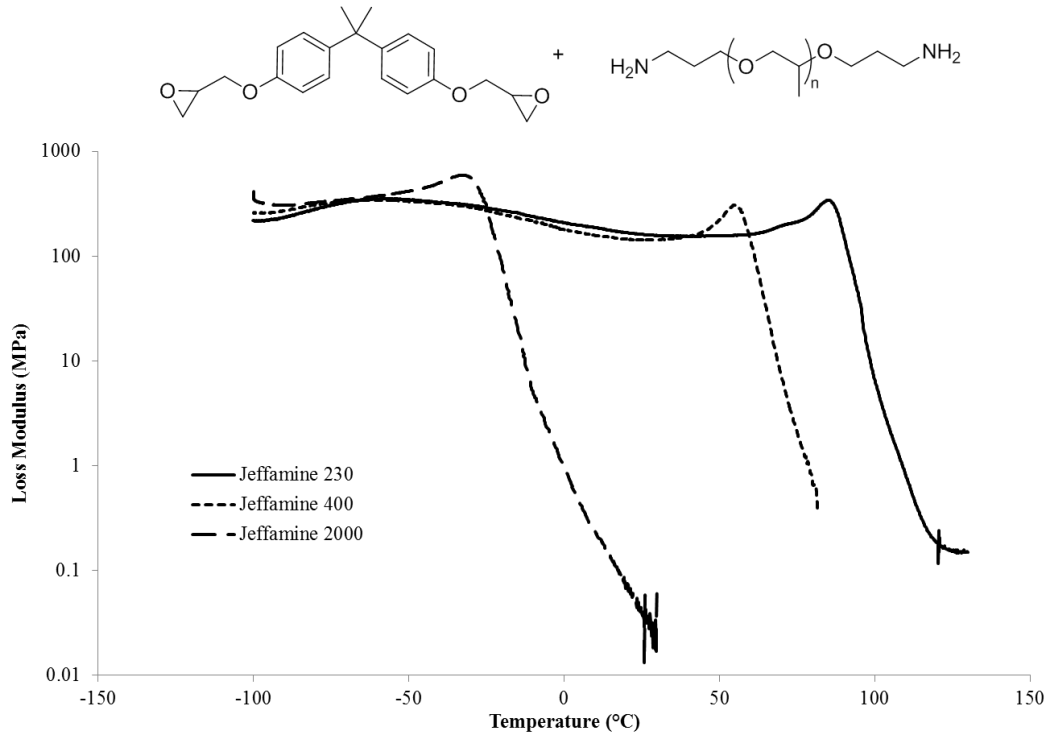

Figure A.12 Loss Modulus DMA traces for epoxy networks prepared from BPAGE and Jeffamines of various M_n (**Chapter 8**).

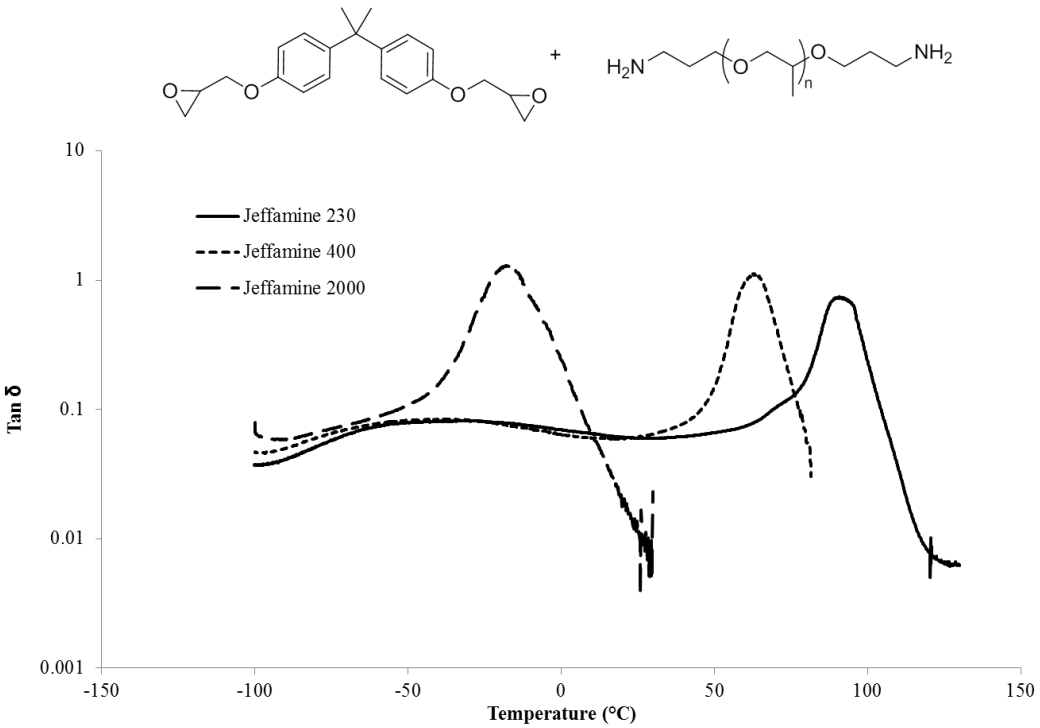

Figure A.13 Tan δ DMA traces for epoxy networks prepared from BPAGE and Jeffamines of various M_n (**Chapter 8**).